A Study of Neurodegeneration and Neuroprotection in *Nothobranchius guentheri*

by

Tyrone Genade

Thesis Presented for the Degree of Doctor of Philosophy (Anatomy & Cell Biology) in the Department of Human Biology at University of Cape Town.

January 2012

Promoter: **Prof. D. M. Lang**
Department of Human Biology

A Study of Neurodegeneration and Neuroprotection in *Nothobranchius guentheri*

Tyrone Genade

June 4, 2012

Abstract

This thesis details a study into aging-related neurodegeneration of *Nothobranchius guentheri* and the affect of resveratrol-treatment on this neurodegeneration. The goal of the study was to identify cytological probes by which to study neurodegeneration and use these to deliver novel findings pertaining to *Nothobranchius* aging and resveratrol induced neuroprotection.

The SMI31 (against phosphorylated neurofilamant protein), GA-5 anti-GFAP (against glial fibrillary acid protein in radial glia), DAKO Z0334 anti-GFAP, anti-TNR antibodies (against Tenascin-R on oligodendrocytes) and E587 antiserum (against goldfish L1 which is implicated in synaptic plasticity) were shown to react against *Nothobranchius* tissue with high fidelity. By western blot and immunofluorescent microscopy evidence is presented that these antibodies are identifying the corresponding epiptopes in *Nothobranchius* as other species. BS-I Isolectin was shown to bind to microglia in the optic nerve and retina but not the brain (where no microglia have thus far been detected).

Using the SMI31 antibody we demonstrate that neuronal density declines with age in the stratum griseum superficale of the optic tectum. Resveratrol-treatment did not decrease this neuron loss even though it extended lifespan of *N. guentheri*. Using the E587 antiserum it was shown that resveratrol-treated fish had more E587 immunoreactive neurons than age-matched controls. The E587 antiserum was used in conjunction with the GA-5 antibody to label and count radial glia in the stratum griseum superficiale. It was found that the density of radial glia declined with age but was rescued by resveratrol-treatment. Western Blots indicated that the ratios of the GFAP isoforms change with age and resveratrol-treatment maintains youthful GFAP isoform proportions. The density of perineuronal nets, using the anti-TNR antibody, was also observed to decline with age. Resveratrol-treatment protected against this decline.

Five antibodies and a lectin were tested against *Nothobranchius guentheri* tissue and found to be useful. Using these antibodies novel data was gathered suggesting that resveratrol lifespan extension is not strictly associated with the preservation of neurons into old age but is associated with the maintenance of synaptic plasticity.

Dedicated to my loving wife and parents who have supported me through everything, and helped me to this point; and with great thanks to GOD who provided me with such interesting research material.

Acknowledgments

My wife, Laura, for encouragement, support and lots of patience and love.

Prof. Dirk Lang for seeing the potential in the project and for all the support, technical and otherwise. Thanks for all the fish!

Dale Wilcox for endless proof reading and lending an ear in times of trouble.

Prof. Dirk Bellstedt for all the fish food and friendship.

Dr. Lester Davids and Prof. Susan Kidson for sharing their knowledge and thoughtful discussion. Doctors Liz van der Merwe and Kishor Bugarith and Professors Lauri Kelleway and Vivian Russell for sharing their experience and asking clever questions over tea.

Dr. Prince and the Prince lab for turning a blind eye to me looting their reagent cabinet with impunity.

Toni Wiggins, Barbara Mohr and Bruce Dando for making sure the lab was functional, the reagents arrived on time and always being ready to help. Ray and Charles for doing all the little jobs we take for granted but can't do without.

Britta, Vicki, Aisha, Rosa and Krishna for all the help in the lab. It was great having people around I could rely on to lend a helping hand.

Stefano Valdesalici, Alessandro Cellerino, Eva Terzibasi, Dario Valenzano, Nicola Origlia and Luciano Domenici for inviting me to Italy to work with them. It was in their nurturing environment that this project was born.

This thesis was typeset in LaTeX 2_ε. Kpfonts were used for the text body, Bera Sans for the headings and Lxfonts for diagrams. Diagrams and cartoons were generated using TpX (developed by Alexander Tsyplakov).

Abbreviations

Aβ	amyloid-β
AD	Alzheimer's Disease
ADAM	a-disintegrin-and-metalloproteinase
AMPK	AMP-activated protein kinase
ARE	anti-oxidant response element
ATF6	activating transcription factor 6
BiP	binding immunoglobulin protein
CAMKII	Ca^{2+}/calmodulin-dependent protein kinase II
CNS	central nervous system
CNX	calnexin
CREB	cAMP responsive element binding protein
CSPG	chondroitin sulfate proteoglycan
DAB	3,3'-diaminobenzidine
ECM	extracellular matrix
ER	endoplastic reticulum
ERK	extracellular signal-regulated kinase
FJB	FluoroJade-B
GFAP	glial fibrillary acid protein
GPx	glutathione peroxidase
GSK3β	glucose synthase kinase 3β
HO-1	hemeoxygenase-1
IHC	immunohistochemistry
IRE1	inositol requiring element-1
JNK	c-Jun N-terminal kinase
lSGI	lower stratum griseum intermediale
LTP	long term potentiation
MAPK	mitogen-activated protein kinases
MMP	matrix metalloproteinase
MnSOD	manganese superoxide dismutase
NCAM	neuronal cell adhesion molecule
NOS	nitric oxide synthase
NFT	neurofibrillary tangles
Nrf2	NF-E2-related factor 2
ON	optic nerve
OT	optic tectum
PDI	protein disulfide isomerase
PERK	PKR-like ER kinase
PKA	cAMP regulated protein kinase A
PKC	protein kinase C
PNN	perineuronal net
PP2A	protein phosphatase 2A
ROS	reactive oxygen specie(s)
sAβgal	senescent associated β-galactocidase
SAI	stratum album intermediale
SGI	stratum griseum intermediale
SGS	stratum griseum superficiale
SO	stratum opticum

SGPV	stratum griseum periventriculare
SP	senile plaque
SZ	stratum zonale
TNR	tenascin-R
UPR	unfolded protein response
uSGI	upper stratum griseum intermediale

Contents

List of Figures

List of Tables

Chapter 1

Introduction

> Bet your life there's something killing you,
> Its a shame we have to die my dear,
> No one's getting out of here alive.
>
> *DOA*, the Foo Fighters.

Alzheimer's Disease (AD) is a leading cause of death among people 65 years of age and older [1]. AD (as well as other forms of dementia), cancer and heart disease are most prevalent among individuals of the 60 to 80 year old demographic; and are thus considered aging-related diseases. In western society, on account of a declining birth rate and advances in medicine, this demographic is increasing disproportionately to the younger (economically active) populations [2]. This threatens severe social and economic problems for the future, particularly in countries where a large proportion of the population is dependent on state welfare in old age. These dire conditions call not just for more research in aging-related disease but *faster* research into alleviating the burden of aging-related diseases on society. That is, to ensure that the aging-population remains healthier and active for longer so the burden does not unnecessarily fall on the state. This dire situation calls for a shorter-lived model organism which is a vertebrate with comparative cell composition but which is also anatomically simple. Such an ideal organism must manifest a well defined aging process which includes, among other maladies, a neurodegenerative phenotype with age. Such an organism is found in the fish of the genus *Nothobranchius* [3].

1.1 *Nothobranchius* in review: 2006 to the present

Nothobranchius furzeri is an ideal model organism for aging research based on its extremely short lifespan, ease of culture and vertebrate nature [4]. Genade et al. [3] reviewed the body of knowledge concerning *Nothobranchius* and presented evidence that well established biomarkers of aging are present in *N. furzeri* as well as other *Nothobranchius* species. The retardation of these

biomarkers by resveratrol-treatment was reported by Valenzano et al. [5] one year later (in 2006).

Valenzano et al. [5] demonstrated that with age there was an increase in neurodegeneration as well as a decline in operant learning and muscle strength. Resveratrol-treatment reduced the level of neurodegeneration compared to age matched controls while operant learning ability and muscle strength improved relative to age matched controls. Resveratrol-treatment increased median lifespan from 8.5 weeks to 11 weeks. These results constituted the first evidence that resveratrol could modulate vertebrate lifespan and health. Furthermore, this body of research was completed in less than one year proving the claim that *Nothobranchius* provided an opportunity to accelerate aging research.

Since Valenzano et al. [5] *Nothobranchius* aging research has progressed rapidly in spite of the small number of researchers working with these fish. It has been demonstrated that a general reduction in chemical reaction rate through the maintenance of *N. furzeri* at lower temperatures prolonged their functional lifespan [6]. This phenomenon was also demonstrated by Podrabsky & Somero [7] and Liu et al. [8] for other annual fish species of the Cyprinodontidae family (*Austrofundulus* and *Austrolebias* respectively). Dietary restriction has been proven to extend lifespan in *N. furzeri* along with reducing the levels of lipofuscin accumulation and neurodegeneration in the short-lived Gonarezhou strains but reduced the median lifespan of the long-lived MZM-04/10P strain from Mozambique [9]. Maximum lifespan was increased for both the Gonarezhou and wild derived strains. Differences in lifespan and survival graph patterns have been published for the inbred Gonarezhou and wild derived strains [10] suggesting that differences at the genetic level may underpin the differences in dietary restriction response by the different strains.

A linkage map has been published making the genetic mapping of lifespan altering loci possible [11]. This linkage map has already revealed the presence of sex chromosomes in this species as well as the linking of tail color to these sex chromosomes. Reichwald et al. [12] report a high number of tandem repeats in the genome of *N. furzeri* and that the Gonarezhou strain is highly inbred. Studies of *N. furzeri* telomere length and telomerase activity revealed that there is a significant shortening of telomere length in the MZM-04/3 wild derived strain of *N. furzeri* but there was no significant shortening in the Gonarezhou strain. Furthermore, telomerase expression was seen to increase with age. Hsu et al. [13] report telomere shortening in *N. rachovii* as well as no significant change in telomerase activity with age. Interestingly, no change in telomerase activity was detected in the naked molerat, whose telomeres are abnormally short, suggesting that telomere length may have nothing to do with aging, though it may provide protection against cancer [14].

Hsu et al. [13], using *N. rachovii*, demonstrated the same increase in senescent associated β-galactosidase activity (sAβgal) as well as lipofuscin, as was reported by Genade et al. [3] using *N. furzeri*. In addition to these two biomarkers, the levels of lipid peroxidation and protein oxidation also increased with

age whereas the activities of catalase, glutathione peroxidase and superoxide dismutase decreased with age. Lipid peroxidation was also demonstrated in *N. korthausae* [15]. The studies on *N. korthausae* also revealed that its lifespan can be modulated by photoperiod and that this sensitivity to photoperiod differed between Mafia Island and mainland Tanzania populations[1] [17]. These observations in *N. korthausae* have since been elaborated on and aging-related changes in diurnal rhythm and morphology further analyzed [18].

di Cicco et al. [19] have published data indicating that the frequencies of neoplasias not only increases with age, as first shown in *N. guentheri* [20, 21], but that there are differences in neoplasmic frequency between the short and long-lived *N. furzeri* strains. In addition, mitochondrial function is observed to decline with age as in other species [22]. These advances support the assertion of Genade et al. [3] that *Nothobranchius* can serve as general models of aging.

1.2 The need for *Nothobranchius* specific CNS cellular markers

The study of neurodegeneration in *N. furzeri* employed both behavioral and histological markers of aging [5, 6, 9]. The behavioral assays consisted of an active avoidance assay of operant learning efficiency; and a spontaneous locomotion assay. Neurodegeneration could not be studied at a cellular level in the central nervous system (CNS). While the accumulation of lipofuscin [23] and FluoroJade-B (FJB) [24] signal is linked to neurodegeneration they do not label a particular cell type.

Valenzano et al. [5] (of which T.G. was a co-author), linked the increase in FJB signaling with neurofibrillary tangles (NFTs) on account of FJB staining degenerating neurons [24] and the presence of fine FJB stained fibers in the *N. furzeri* OT. Schmued, who developed FJB, did not see evidence to support this link (pers. comm). His skepticism was validated in 2007 when Damjanac et al. [25] published data showing that FJB labelled gliotic astrocytes and microglia and very few, if any, neurons or NFTs in a mouse model of AD. This emphasizes the need for cell-type and protein specific markers of neurodegeneration. In Terzibasi et al. [9], glial fibrillary acid protein (GFAP) levels were seen to increase in the course of normal aging in *N. furzeri*. An increase in GFAP expression is regarded as a sign of neurodegeneration [26]. In the course of dietary restriction experiments *N. furzeri* showed an increase in GFAP immunoreactivity compared to the age-matched controls. Terzibasi et al. [9] had used the 6F2 and GA-5 anti-GFAP antibodies for their study. This result in the dietary restriction fish was unexpected and needs to be further investigated. Additional cellular markers are needed to study neurodegeneration and neuroprotection in *N. furzeri*. What is more, it is important to have means to study

[1] The mainland populations have since been described as a distinct species, *Nothobranchius ruudwildekampi*, by Costa [16].

the morphology and structure-function relationship of specific cells within the CNS.

For this study we selected antibodies (Table 1.1) based on an interest in CNS injury as well as regeneration and antibody availability. BS-I isolectin was used in this study because of its success in labeling microglia in degenerating brain tissue by Kim et al. [27]. The role of microglia, astrocytes and proteins targeted by the successful antibodies are reported in Chapter 4 together with the evidence of their effectiveness within *Nothobranchius*.

1.3 Investigating neurodegeneration

Nothobranchius research to date, in particular with reference to resveratrol lifespan extension, leaves several critical questions unanswered. The questions addressed in this thesis are as follows:

1. Can cell-type specific markers be identified by which neurodegneration and protection can be studied in this fish?
2. What changes are there at the cellular level in the aging *Nothobranchius* CNS, and how does this relate to changes observed in other model organisms and humans?
3. With resveratrol-treatment, which of the above documented changes differ between treated and control animals?
4. How does the frequency of gliotic and/or atrophied astrocytes differ between young, aged and resveratrol-treated animals; and how does this correlate with the levels of GFAP among these groups?
5. Does resveratrol achieve neuroprotection in *Nothobranchius* by preventing neuron death or damage, or by preserving or promoting neurogenesis in aged fish?

These questions are, in turn, addressed in Chapters 5 through 6.

Aging-related neurodegeneration will be reviewed in Chapter 2 with the goal of drawing the reader's attention to the similarities in the aging processes between species and what one would expect to encounter in *Nothobranchius* as they aged. Senile Plaques (SPs) and NFTs are used as exemplary pathologies to the important topics of CNS protein and extracellular matrix (ECM) homeodynamics. The role of neurons and glia with respect to neurodegeneration are discussed with respect to these two central topics and referred back to the current state of *Nothobranchius* research.

The anti-aging and neuroprotective properties of polyphenols are extensively reviewed in Chapter 3. The chapter addresses theories of the mechanism of action of polyphenol compounds and only articles pertinent to forging links

Table 1.1: Table of antibodies (and lectins) used in this study as well as their prospective cellular targets.

Antibody	Cellular Target
E578 serum	L1 neuronal cell adhesion molecule on astrocytes, ependyma, endothelial cells and neural processes
GA-5 (monoclonal)	glial fibrillary acid protein in astrocytes
anti-GFAP (polyclonal)	glial fibrillary acid protein in astrocytes
SMI310	neurofilament protein in neurons and their processes
anti-TNR (monoclonal)	Tenascin-R on oligodendrocyes
BS-I isolectin	labels microglia and endothelial of blood vessels

between the competing theories or falsifying defective theories have been given much attention. A crucial question pertaining to polyphenol induced neuroprotection is "what dose?" An entire section addresses this subject within the theory of hormesis. These theories will be compared to the expected degenerative signs observed in *Nothobranchius* and what is expected to be observed based on neurodegeneration in other species. The role of resveratrol will not be reviewed in any great depth but will be discussed in the experimental chapters in relation to experimental observations.

Pertinent issues raised in these two review chapters will be highlighted briefly in the experimental chapters. The subjects of neurodegeneration and polyphenol bioactivity are vast, spanning many thousands of articles and hundreds of reviews. The two review chapters are, in this respect, brief and focused on the study direction of the Author which involves extensive use of antibodies for studying the ECM and protein homeodynamics; and the dosing of resveratrol to achieve a neuroprotective outcome.

In spite of great research effort, both the neuroprotective mechanism of resveratrol and the general causative mechanisms of neurodegeneration remain clouded in a mystery of contention and conflicting research outcomes. Results of in vitro and in situ experiments often contradict each other, with respect to both the experimental outcomes and resveratrol concentration, and there are large differences in results between model organisms used. Further complicating matters, there is still confusion as to what constitutes an age-dependent pathology and an age-related disease (such as AD). What is required is a model organism which ages rapidly and so allows for rapid experimentation, dissection of cause and effect relationships, and testing of hypotheses. This model organism must be so evolutionary disparate to other model organisms so that evolutionary conserved mechanisms of neurodegeneration and neuroprotection are more easily discerned through the framework of comparative biology.

Chapter 2

Neurodegenerative-Aging: molecular mechanisms and cellular interactions

> Well you asked me if I will forget my baby, I guess I will some day.
> I don't like it but I guess it happens that way.
>
> *Guess things happen that way*, Johnny Cash.

2.1 Introduction

Alzheimer's Disease (AD), Parkinson's Disease (PD) and Huntington's Disease are diseases characterized by massive neuronal loss in specific brain regions [28]. This is not the case with normal aging where there is more glial atrophy than neuron loss [28, 29]. Much of the research into neurodegeneration has focused on diseased as opposed to normal aging. The afore mentioned diseases are aging-associated, which is to say that with age the likelihood of developing the disease increases. The question is how can we make use of our knowledge of these diseases in the context of normal aging; and how can this be applied to *Nothobranchius* aging?

Aging manifests as the accumulation of biological changes over time that cause the organism progressively more likely to die [30]. The manifestation of this aging process, neurodegenerative-aging, is the topic of this thesis. Neurodegenerative-aging is characterized by the gradual decline in cognitive ability which could eventually give way to dementia [31]. Whether dementia is inevitable (a matter of the individual simply living long enough to manifest the disease) or a consequence of specific causes is not known.

The goal is to stave off death, that is to delay aging and the role of the CNS in aging appears to be critical. There is good evidence that neuroprotection in itself results in *both* longer lifespan and healthspan [32, 33]. It must be

emphasized that when it comes to anti-aging interventions what is sought is a *healthy* long life, not simply longer life. Understanding how the brain ages and how its cells and tissues malfunction is critical to ensuring a healthier and longer life.

The collective knowledge of neurodegeneration is now so vast that a single review cannot contain all the information pertaining to the subject in detail as well as frame it in a broader context. My goal is to frame this information within the context of normal aging. The starting point will be the etiology of the pathologies observed during the progression of AD (SPs and NFTs) which are also related to aging. SPs and NFTs are the two best studied pathologies and best correlated with cognitive decline (which serves as the best measure of neurodegenerative-aging). The etiology of these pathologies involves a disturbed homeostasis at the level of the intra-cellular systems as well as extracellular milieu in which the cell lives. This milieu is composed of both the extracellular matrix (ECM) and the other cells living in that matrix.

Little is known about *Nothobranchius* aging and neurodegeneration but there is enough data to forge links with current thinking regarding neurodegeneration. Whether the FJB used by Valenzano et al. [5] actually indicates an increase in NFTs[1] or some other manifestation of neurodegeneration is secondary to the observation that neurodegeneration is occurring in *Nothobranchius*. The nature of this neurodegeneration needs to be determined but it is safe to say that it will entail one or another form of protein aggregate [34].

Besides SPs and NFTs, which are the hallmarks of AD, there are many other pathologies pertaining to neurodegeneration, such as the Lewy bodies of Parkinson's Disease. The mechanisms of degeneration pertaining to these other diseases goes beyond the scope of this chapter. The next section will chiefly discuss the protein aggregates: SPs and NFTs.

When a neuron finally dies, due to SP or NFT formation, its remains have to be disposed of by means of the support cells of the CNS: the astrocytes and microglia. These will be the subject of Section 2.3. It is not only the neurons which begin to fail with age but the entire CNS milieu begins to malfunction. A critical constituent of this milieu is the ECM which is discussed Section 2.4. The ECM plays host to the interactions between glia and neurons and its integrity changes in the course of aging and neurodegeneration. The ECM is laid down by the glia and neurons at great cellular expense. Protein synthesis and export is an energetically expensive activity. Protein trafficking and the phenomenon of endoplasmic reticulum (ER) stress are the subject of Section 2.5. In Section 2.5 a general mechanism of neurodegenerative-aging, which affects all the cells of the CNS, will be presented.

Where information pertinent to *Nothobranchius* aging is available it will be interjected into the narrative. In the concluding section of this chapter the nature of neurodegenerative-aging will be reflected upon and the usefulness of *Nothobranchius* for aging research recapitulated with respect to this review.

[1] Verily, the FJB does stain neurons in aged fish as shown in Figure 7 of Terzibasi et al. [10] but mostly stains the glia limitans.

The blood brain barrier and vasculature have been excluded from this review. These subjects will be touched on in the next chapter. For the reader, the information presented in this chapter must be kept in mind in preparation for the next chapter. In the next chapter the various mechanisms of polyphenol neuroprotection will be discussed. As the experimental work is discussed the content of this and the next chapter must be kept in mind.

2.2 Protein aggregates: plaques and tangles

Old models of neurodegeneration put forward a degenerative cascade whereby misprocessing of amyloid precursor protein (APP) results in amyloidβ (Aβ) oligomerization. These oligomers aggregate and form SPs which poison neurons, causing the development of NFTs and ultimately killing the neuron [35]. This Amyloid Cascade Hypothesis has been contested and is now considered unsatisfactory as a general mechanism of neurodegeneration. From kokanee salmon [36] to humans [37] Aβ deposition has been observed as a downstream product of neurodegeneration and its abundance has neither correlated with NFT abundance nor cognitive decline. On the other hand Dani et al. [38] report that SP burden correlates with age. Armstrong [35] concludes that SPs and NFTs are independent lesions and are themselves products of degenerative processes rather than the cause. While correlation doesn't necessary imply causation an unavoidable link between SP pathology and NFT development remains [39]. SPs and NFTs remain the diagnostic hallmarks of AD. And, referring to the kokanee salmon [36], SP formation does correlate with age in fish as it does humans [38].

2.2.1 Senile plaques and amyloidβ

The development of SPs are reviewed by Haass [40] and Unger [41] and is outlined in Figure 2.1. The development of this pathology will be discussed in some depth as many of the enzymes involved are mentioned repeatedly in this and later chapters. As will be discussed in the next chapter, many polyphenols have been shown to affect the process of SP development.

Aβ is not in itself neurotoxic: both the 40 and 42 amino acid peptide fragments play roles in healthy brain function and in particular neural plasticity [42, 43]. Similarly, the other fragments of the APP also serve physiological functions. These functions and the processing of the fragments are reviewed by Zhang et al. [44]. Those parts of the process relevant to later discussion will be recapitulated here. The soluble alpha fragment (sAPPα) plays a role in plasticity as well as inhibiting cyclin dependent kinase 5 (Cdk5) which has been reported to play a role in NFT development [45]. APP is processed by a-disintegrin-and-metalloproteinase (ADAM) 9, 10 and 17. Many of these ADAMs are produced by astrocytes and other glia [46] and their dysregulation is implicated in neurodegeneration [47]. α-processing prevents the generation of the β-fragments. β-processing is executed by the BACE enzyme complex

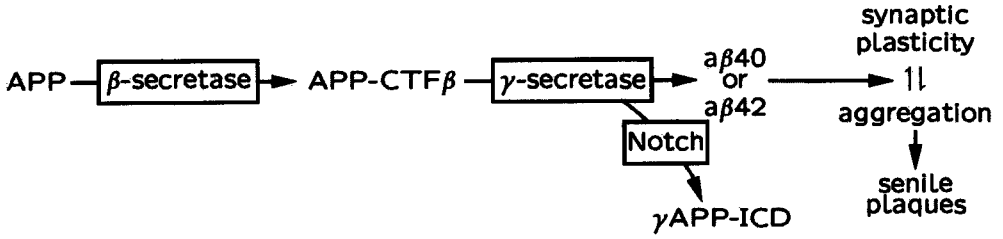

Figure 2.1: The development of senile plaques from amyloid precursor protein (APP) involves cleavage first by β-secretase to produce the APP C-terminal fragment β (APP-CTFβ) followed by cleavage of the presenilin/γ-secretase complex. This second cleavage yields either the 40 amino amyloidβ product (Aβ40) or the 42 amino acid product (Aβ42) which aggregate, forming senile plaques. The intracellular domain (ICD) is obtained by processing the remainder of the APP-CTFβ by Notch. This fragment partakes in intracellular signaling processes. Information obtained from Haass [40].

which catalyzes the β-secretase step. This yields the APP C-terminal fragment and soluble APPβ which plays a role in axon pruning and neuronal cell death. The C-terminal fragment is then processed by γ-secretase, a complex of four subunits: presenilin (PS, PS1 or PS2), nicastrin, anterior pharynx-defective-1, and presenilin enhancer-2; γ-secretase activity is believed to rest in presenilin. Mutation of PS1 or 2 has been identified in cases of familial AD. The γ-secretase complex resides mostly in the endoplasmic reticulum (ER) and Golgi with smaller amounts in the endocytic compartments and lipid rafts at the cell surface [48]. APP cleavage happens in the golgi. The cleavage of APPβ generates 40 or 42 amino acid Aβ peptides and intracellular domains which partake in cellular communication and play a role in the trafficking of APP. In the course of diseases the 40 and 42 amino acid Aβ oligomerize and aggregate to form insoluble fibrils which deposit on the cell surface, forming plaques [40]. No correlation has been found between Aβ concentration and dementia, but patients who later developed dementia did have a low Aβ42/Aβ40 ratio compared to controls [49] suggesting underlying problems in protein processing. The Aβ42 is less soluble than Aβ40, and Aβ40 fibrils recycle faster than Aβ42 fibrils [50], suggesting that it is the increase in Aβ42 incorporation in fibrils which spurs on SP formation. It will become clear from this and the next chapter that while SP formation may not in itself be neurodegenerative, this process is affected by and effects other processes implicated in neurodegeneration. Neuroprotective therapies also affect this process.

Zhang et al. [44] review the factors affecting APP trafficking and report that Aβ levels accumulate intracellularly long before they accumulate extracellularly. APP-CTFα participates in feed-forward signaling, regulating the cellular trafficking of APP to the cell surface where it is cleaved to generate sAPPα instead of Aβ. Retromer, which is involved in retrograde transport from the endosome to the Golgi, is also implicated in APP processing [51]. Deficiency of retromer caused an increase in the secretion of Aβ42, increas-

ing the Aβ42:Aβ40 ratio[2] which is linked to clinical outcomes of cognitive decline [49]. Slower retrograde transport could result in slower Golgi function meaning more time for APP to be processed in the Golgi and ER by BACE and γ-secretase. The spontaneous aggregation of Aβ in the Golgi apparatus, or the disproportionate recruitment of Heat Shock Protein 70 (Hsp70) to stabilize the Aβ would put tremendous pressure on the resources of the Golgi and ER to maintain order and put additional strain on the power supply of the cell. This subject is dealt with more extensively in Section 2.5, page 20.

2.2.2 Neurofibrillary tangles

NFTs are the hallmarks of AD and many other dementias. Even though high concentrations of amyloid-β may be present, dementia only develops in the presence of advanced NFTs [37]. NFTs have been found in all sampled brains of people over 75 years of age and in brains as young as 45 years. The hippocampal region of the human brain is especially vulnerable.

NFTs form as a consequence of hyper-phosphorylation of the protein tau [52, 53]. Properly phosphorylated tau (3 phosphates per molecule) is needed to organize and stabilize the microtubule network in the neuron and its processes. Hyperphosphorylated tau (6–12 phosphates per molecule) is unable to stabilize the microtubules, giving rise to the formation of paired helical filaments in axons (that form the aggregates referred to as NFTs) and neurophil threads found in dystrophic dendrites [52]. The development of NFTs is linked to the unregulated activity of kinases within the neuronal cells [52] as well as a decline in protein phosphatase 2A (PP2A) concentration and activity [45, 54]. A schematic summarizing the progression of functional tau to hyperphosphorylated tau is shown in Figure 2.2. A wide range of kinases can affect tau processing.

PP2A is the phosphatase responsible for dephosphorylating tau [54] as well as regulating cell signaling through dephosphorylating mitogen-activated protein kinases (MAPKs) [45]. The decline in PP2A activity is concomitant with the increase in glucose synthase kinase 3β (GSK3β) activity [45, 53] as well as an increase in the activities of MAPKs such as extracellular signal-regulated kinase 1 and 2 (ERK 1/2), Cdk5, p38, c-Jun N-terminal kinase (JNK) [55], S6 kinase (S6K) [56] and cyclic adenosine monophosphate (cAMP) regulated protein kinase A (PKA) [45]. All of these kinases have been reported to phosphorylate tau. The dysregulated activity of these kinases is viewed as causing the NFT pathology. PP2A is inactivated by S6K on activation by mTORC1 (mammalian target of rapamycin) [56]. The mTOR pathway is known to be dysregulated in degenerate neurons and can be activated by various means: growth factor receptor signaling, cytokines, hormones and calcium influx [57].

PKA and Protein Kinase C (PKC) have important roles in the response of the axon growth cone to extracellular cues [58] and are essential for memory

[2] A low serum Aβ42:Aβ40 ratio would imply that more Aβ42 is deposited in SPs, implying that there is more Aβ42 produced than Aβ40.

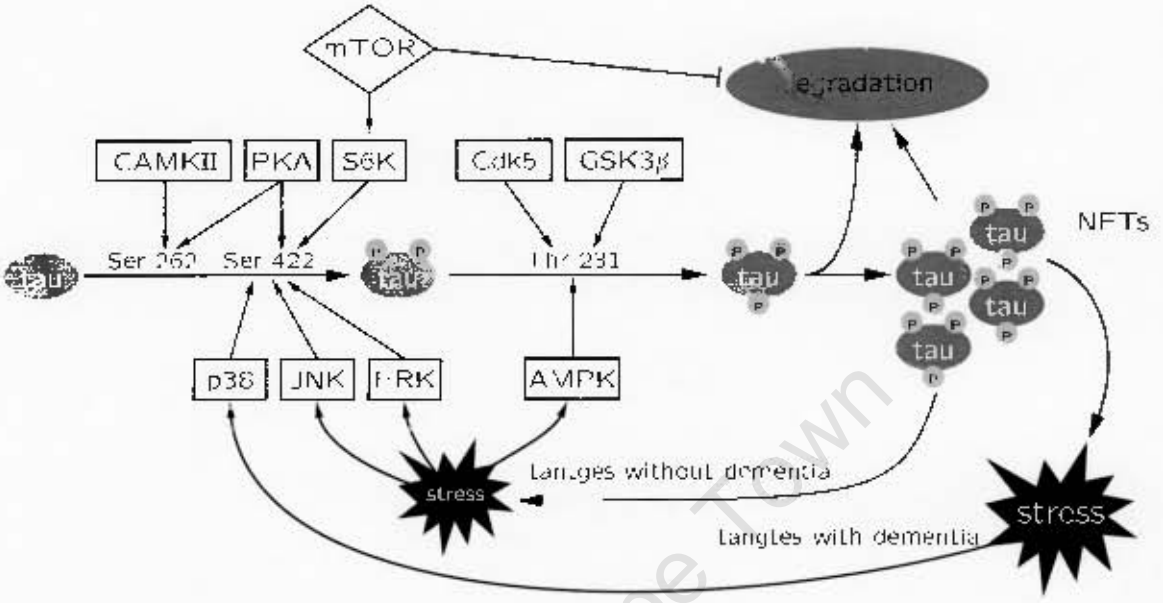

Figure 2.2: Tau hyperphosphorylate proceeds by priming at specific residues by PKA, CAMKII and S6K. Once primed, phosphorylated tau is phosphorylated at the critical Thr231 residue by Cdk5 or GSK3β to produce hyperphosphorylated tau which aggregates to form NFTs. This sets off a stress response, activating AMPK and JNK. ERK is also activated along with AMPK and JNK which primes more tau for hyperphosphorylation. At this stage dementia has not manifested. Abnormal p38 activation was only present in individuals who had developed dementia. S6K is activated by mTOR which also inhibits the cell's protein degradation machinery as well as PP2A which dephosphorylates tau. Figure based on [62].

formation and neural plasticity [1] along with calcium-calmodulin-dependent protein kinase II (CAMKII) [59]. PKA is primarily activated by cAMP generated by adenylate cyclase in response to receptor activation or calcium influx. CAMKII is activated directly by calcium influx. Both these kinases can phosphorylate tau at positions Ser-262 and -422 which are needed for NFT formation [52]. Long term potentiation (LTP) requires activation of the MAPKs [60]. This can occur via various mechanisms involving cross-talk between PKA and PKC converging on MEK via Raf-1 and B-Raf [60]. In aging this signaling cross-talk is known to be disrupted [61]. Many such signaling disruptions will be indicated in the sections which follow.

PKA and CAMKII are suspected of priming tau for hyperphosphorylation by GSK3β (Figure 2.2) [45, 52]. The phosphorylation of tau at Thr-231 is critical for the development of NFTs [45]. This can be accomplished by Cdk5 and GSK3β. Cdk5 plays a role in neuronal migration, cortical layering and synaptic plasticity [63] but the accumulation of Aβ leads to the activation of calpain which cleaves Cdk5's regulator, p35 specific activator, into a p25 fragment which causes Cdk5 to localize to the microtubules and phosphorylate tau. Hy-

perphosphorylated tau detaches from the microtubules and is free to associate with other tau, forming pair helical filaments and finally neurofibrillary tangles [64]. Free tau is ordinarily pumped out of the cell body by a retrograde barrier in the axon initial segment operating as cellular rectifier [65]. This barrier only allows antegrade movement of tau into the axon and dendrites, keeping it out of the cell body. Its function relies on tau being able to bind to the microtubule scaffold of the cell. This missorting of tau has been observed in cell culture [66] and AD model mice brains [67] using the SMI31 antibody. The SMI31 antibody reacts against abnormally phosphorylated neurofilament proteins which is found within NFTs generated by hyperphosphorylated tau [68–70]. But Cdk5 is not the kinase believed to be the culprit.

GSK3β is reported as the single most likely candidate kinase responsible for taupathies [52]. It and its roles in neurodegeneration are reviewed by Giese [71]. GSK3β expression in *Drosophila* was required to cause the development of advanced taupathies [72] though in vitro combination of PKA, Cdk5 and CAMKII was able to hyperphosphorylate tau and trigger its spontaneous assembly into tangles [45]. The activity of GSK3β is regulated by Akt [53]. Using confocal microscopy, activated Akt has been seen to co-localize with GSK3β in the vicinity of hyperphosphorylated tau. The PI3K/Akt/GSK3β pathway is, in part, regulated by APP and its products [73]. The sAPPα fragment, via neurotrophin receptors, activate PI3K, ultimately inactivating GSK3β. Conversely, The Aβ peptide inhibits neurotrophin activation of PI3K and the inactivation of GSK3β.

GSK3β is observed to be dysregulated in a myriad of pathologies [74] suggesting to the Author that it is more likely a symptom than the root cause of the pathology. That GSK3β knock-out *Drosophila* [72] or GSK3β inhibition by Li$C\ell$ prevent the development of taupathies is hardly convincing evidence for GSK3β being the prime suspect. Over expression of active GSK3β would cause NFTs as surely as excess Aβ peptide would inhibits GSK3β inactivation. GSK3β has multiple targets, not all of which have been identified or properly studied, and there is little understanding of how GSK3β, its activators and its substrates integrate in proper cellular function.

PKC is also a negative regulator of GSK3β activity [1]. In AD brains there is a decline in PKC activation that is linked to a decline in abundance of the scaffolding protein RACK1 that ferries activated PKC to cellular targets [1]. RACK1 has also been observed to decline with age [75] making its decline more relevant to the cognitive deficit associated with normal aging. RACK1 also ferries cAMP-specific phosphodiesterase-4D5, linking it to the regulation of cAMP levels and thus the suppression of PKA activity [76]. Another PKC chaperone, Hsp70, has been reported to decline with age [77]. Without Hsp70, PKC will interact randomly with the microtubule cytoskeleton [78]. PKA is also tethered to anchoring proteins which keep PKA in close proximity to S6K, its inhibitor [56]. PP2A, B and C are all associated with the microtuble network in the cell [79]. Kinase and phosphatase activity is carefully regulated on a spatial basis. The evidence of the aging and age-related dysfunction of

the individual signaling pathways, the crosstalk between them as well as signal integration is reviewed in Carlson et al. [61]. By simultaneously activating the priming kinases together with the inhibitors of the hyperphosphorylating kinases the cell instigates protective measures to prevent NFTs. In an abnormal cell these protective measures do not reach their target, be it because of a decline in RACK1 or some other cause.

ERK and JNK activity is linked to pre-dementia neurodegeneration [55]. In LTP ERK is activated, and with declining PP2A activity, its inactivation could become problematic. Activated ERK can reinforce the activation of both PKA and PKC by phosphorylating ion channels and receptors in the plasma membrane [80]; and in so doing reinforce its own activation in a dysregulated system. Similarly, Aβ can open ion channels linked to neurotrophin receptor channels allowing Ca^{2+} to enter the cell and activate kinases such as Cdk5 [63]. Calcium homeodynamics is known to be perturbed in degenerating brain tissue [81]. CAMKII activates Nitric Oxide Synthase (NOS) which produces nitric oxide (NO) [82]. NO causes mitochondrial uncoupling. Uncoupling results in the generation of reactive oxygen species (ROS). NO also causes S-nitrosylation of proteins and this nitrosylation denatures them [83]. The thioredoxin and glutaredoxin systems work to counter this [84]. These systems rely on an abundant supply of ATP equivalents from mitochondria. In this scenario the electron transport chain is now uncoupled causing a drop in ATP equivalent supply [85]. A relative increase in AMP (due to a decrease in ATP) would activate AMPK in order to restore the energy deficit but AMPK is also able to phosphorylate tau at the critical Thr-231 residue [86]. Without a functional microtubule network it is unlikely AMPK could fulfill its intended function. NADPH oxidase activation at the cell membrane via Rac/PI3K signaling also generates ROS [87]. Transient ROS is required for proper cellular signaling whereas chronic ROS has a detrimental effect. The activation of NOS and other ROS generating enzymes must be strictly controlled. With age the mTOR/S6K/NOS pathway is dysregulated [88, 89].

The kinase, p38, is dysregulated along with ERK and JNK in patients who have manifested dementia [55], and p38 can also prime tau for hyperphosphorylation. Increased ROS as well as cytokines can activate p38 via MEKK1-4/MKK3/6 pathway [90]. This pathway can also activate JNK and more space will be devoted to this subject in the next chapter.

Given the complex interplay between the kinases, phosphatases and second messengers, it is unlikely that any single kinase is responsible for NFT formation. In vitro experiments demonstrated that the application of PP2A alone was enough to not only dephosphorylate tau but to cause the disassembly of paired helical filaments [45]. The lack of dephosphorylation could be more important than the over activity of the kinases. In the catalytic site of tyrosine phosphatases is a cysteine residue which is particularly susceptible to oxidation [91] and is repaired by glutaredoxin using glutathione (GSH) [92]. These enzymes can only reduce oxidized cysteine that hasn't been oxidized beyond the sulfenic form. In a cellular environment containing excessive chronic

levels of ROS this oxidation beyond the sulfenic form is possible but as yet undemonstrated. Excessive ROS generation can permanently inactivate tyrosine phosphatases which could explain the observed decline in PP2A activity with age.

One of several mechanisms can lead to Ca^{2+} influx, kinase activation, ROS generation and PP2A deactivation causing MAPK activity to spiral out of control. If a culprit needs to be singled out then that culprit is mTOR. mTOR, as well as being activated by Akt, can also activate Akt [93, 94]. Akt activation inhibits FoxO activation which is needed for neuroprotection [32]. mTOR also activates S6K which, in addition to phosphorylating tau, inhibits autophagy and lysosomal degradation of protein and increasing tau expression. The role of mTOR in aging and neurodegeneration is discussed by Blagosklonny [94] and Garelick & Kennedy [57].

2.2.3 Protein aggregates: the cause of neurodegeneration?

Protein aggregates, such as NFTs and SPs, are typical of neuropathologies [34] and while they may be the intermediary cause of neurodegeneration in certain cases neither can be considered as the basis for a general mechanism of neurodegeneration. What should be clear from the previous section is that there are many means by which to *cause* the accumulation of SPs and NFTs. It could be a mutation in a gene causing a misprocessed protein, an external insult causing excessive signal transduction, a decline in one or another scaffolding protein or chaperone, or a chronic lack of ATP equivalents. Whatever the root cause the outcome is a misprocessed or misfolded protein which is a threat to cellular homeodynamics.

Ordinarily, misfolded protein is degraded in the proteosome or sequestered to the aggresome (a cellular compartment distinct from the lysosome) [95]. The aggresome is composed of a core of ubiquitinated protein enclosed in a vimentin cage. Disruption of microtubule networks[3] block the formation of a neat aggresome and the misfolded protein then becomes distributed out along the cell periphery. Experiments in *C. elegans* showed that protein aggregation increases with age and that the aggresome is enriched for proteins which can assemble into β-sheets [97] (such as Aβ). Hsp70 is critical to the maintenance of the aggresome machinery but is itself susceptible to protein aggregation. Mention has already been made to its role in regulating the kinases involved in tau phosphorylation. Additionally, it is well known that the ubiquitin-proteosome system is perturbed in Alzheimer's and other neurological diseases (reviewed by Riederer et al. [98]) where protein aggregation occurs, suggesting that the aggresome system may already be overloaded or impaired (perhaps by excessive mTOR signaling) before SP and NFT pathologies develop. Conversely, a more efficient cellular response to misfolded protein may allow the cells to accumulate NFTs and Aβ fibrils to the point where they are the diagnostic hallmarks of the disease even though they are merely a symptom of an

[3]The size of the microtubule network decreases with age [96].

underlying problem. This subject will be revisited in Section 2.5 after a look at other aspects of neurodegeneration.

Neurons are a small subset of the cells making up the CNS and the contribution of other cell types to neurodegeneration should be taken into account. It is worth mentioning, on the outset, that even astrocytes develop protein aggregates: Rosenthal fibers in Alexander's Disease [99]. NFTs also accumulate in glia, causing glial fibrillary tangles [100]. In addition to protein misfolding there are also problems with protein degradation in astrocytes as the CNS ages [101]. The glial contribution to neurodegeneration will be discussed in the next section before we return to protein processing.

2.3 The role of glia in neurodegeneration

In rats it has been observed that with advancing age there is an increase in activated astrocytes and microglia [27]. There are similar observations for humans with the exception that activation of astrocytes and microglia are only associated with SPs and NFTs [41]. In general, there is a priming for immune system hyperactivity while both the CNS [102] and whole-body immune system senesces [103]. The growing dysfunction of the human neuroimmune system is reviewed by von Bernhardi et al. [104].

Hyperactive microglia are a source of ROS [103, 105]. This is the Inflam-Aging hypothesis of aging where the dysregulation of the innate immune system (giving rise to unchecked inflammation) causes the pathologies associated with aging [106]. Experiments in aged rats have revealed that animals subjected to excitotoxic damage had more widespread microglial activation 12 hours postlesion, and greater microglial density three days postlesion [107]. Aged rats also had more cyclooxygenase-2 positive cells postlesion. Inducible NOS was also more abundant in the aged brains. Together, these seemingly disparate bits of data suggest a trend towards a much greater inflammatory response with age. But it has been found that senescent dystrophic microglia are associated with tau pathology and that their senescence precedes the onset of symptomatic AD [102]. This dystrophy of the microglia correlates with age indicating that the neuroimmune system senesces much like the rest of the organism. This research may settle the question as to whether microglia are neuroprotective or neurotoxic. The remaining activated microglia, insufficient in number to effectively respond to a CNS insult, remain active causing damage instead of rescuing the surrounding neurons.

The immune system is not the only source of ROS and free radicals. Protein aggregates, intra- and extracellularly, can also generate free radicals [108]. It would be these extracellular aggregates—the remains of dead neurons and astocytes—which the astrocytes and microglia would be required to clear from the ECM. Without active microglia these extracellular aggregates would cause damage to the surrounding ECM and cells where the endogenous antioxidant defenses cannot undo the damage.

Gliosis, the activation of astrocytes in response to CNS injury, is restricted

to specific regions of the AD brain while s100B and GFAP (as measured using GFAP antibodies against Western Blots and immunohistochemistry) increases in the course of normal aging without widespread neuronal death [41]. Gliotic astrocytes are believed to be pathological [109]. The gliotic astrocytes lay down dense scar tissue composed of GFAP which inhibits CNS regeneration but this belief is slowly changing. Neurons can subsist in glial scars indefinitely and remain functional. It is now believed that gliotic astrocytes fulfill a beneficial role in the CNS [26]. Following CNS insult the astrocytes react to nurture the surviving neurons and clear the debris. There is a stronger correlation between atrophic astrocytes and CNS dysfunction than gliotic astrocytes [101, 110]. As with microglia the problem may not be over-active astrocytes as much as an inadequate number of reactive astrocytes capable of meeting the challenge posed by the insult.

The protein s100B is tightly correlated with CNS injury [111] and its expression is up-regulated by activated astrocytes. S100B has been shown to activate GSK3β and JNK in neuronal precursor cells [112]. JNK (and p38) are also activated in response to cellular stress (such as caused by ROS) [55]. JNK can activate AP-1 (through phosphorylation of c-Jun or fos) [78, 113] as well as activate FoxO3a [114] while inhibiting survival signaling though the PI3K-Akt pathway [106]. The simultaneous activation of AP-1 and FoxO3a can lead to the activation of cell death programs, such as autophagy or apoptosis. These aspects of cellular signaling will be discussed in Chapter 3.3. While astrocytes exhibit many aging-related changes [115] a decline in antioxidant capacity is not one of them [116] suggesting that antioxidant capacity is not the problem. The greater problem is that they cannot respond to their surroundings.

With age astrocytes develop protein degradation problems [101], i.e. lysosomal disruption. This chronologically related astrocytic malfunction has been observed in many species [26]. Lysosomal disruption (caused by microtubule disruption) in the course of autophagy results in an increase in γ-secretase activity [117]. Whether the increase in presenilin-1 and γ-secretase activity also occurs during hyperphosphorylation of tau caused microtubule disruption is an unanswered question. Degenerate astrocytes could create the environment required for the pathological misprocessing of Aβ. As the NFTs inhibit apoptosis [118], the degenerate neurons persist, misprocessing APP and poisoning surrounding neurons and astrocytes.

The sequence of plaque formation described by Nagele et al. [119] involves a mechanism whereby Aβ accumulates in the ECM and on neurons. The neurons degenerate and the astrocytes attempt to clear the SPs by internalizing it. The aged astrocytes have no means of metabolizing these insoluble protein aggregates and are in turn poisoned and die. In the interim, the dying neuron as well as stressed astrocyte, have secreted cytokines to summon microglia for help. The microglia accumulate in the SPs and begin to clear the Aβ but they also cannot metabolize the Aβ. They accumulate aggregates in them and they secrete more cytokines. Ikeda et al. [120] who showed intimate contact between GFAP positive astrocytic processes and thioflavine-S dyed aggregates

in what are termed ghost tangles—the end stage of the plaque. Also, in experiments where astrocytes were exposed to Aβ, the resulting gliotic astrocytes were not only unable to support neurons, they appeared to secrete some sort of neurotoxin killing neurons which were not in immediate contact with the gliotic astrocyte [121]. In this scenario the development of SPs may appear to be the first cause of the degenerative cascade but the preceding sections must be recalled: SPs are already the product of an underlying problem in protein processing.

2.4 The role of the extra cellular matrix

Axon guidance and newborn neuron migration is facilitated by the surrounding tissue [58] which guides the neuron or cell process though repulsion and attraction signals received by the growth cone of axons or leading process of migrating neurons. These signals activate PKA, PKC, Ras-MAPK as well as Wnt signaling which employs GSK3β [53, 58, 59]. PKA is also activated in the process of fastening synaptic contact and LTP [59]. Brain areas such as the hippocampus of humans [122], and the optic tectum of fish are dynamic with new neurons and glia being generated and new connections being forged [123–127]. It may be no coincidence that it is in these dynamic brain areas, where PKA and CAMKII are persistently activated, that taupathies develop and why Aβ deposits can spread randomly through the rest of the brain with little consequence.

The expression of axon guidance receptors has been shown to change with age and developmental stage [58, 123, 128]. Furthermore, the integrity of the ECM has been shown to deteriorate with age [129, 130]. With age (in mice and humans) there is an increase in the abundance of fibrillar granules composed of laminin and heparan sulfate proteoglycan (and other proteins) around astrocytes [131]. The deposition of ECM proteins is an early event in the pathogensis of SPs and is reviewed in Jucker & Ingram [131]. As well as deterioration in the quality of the ECM there are also aging-associated changes in the volume of the extracellular space on account of both metabolic and structural changes by aged neurons and glia [132]. These changes can directly affect the ability of neurons to form and maintain synaptic contacts.

The role of matrix metalloproteinases (MMP) are reviewed by Romero et al. [130] and Ethell & Ethell [133]. Gliotic astrocytes cause a local increase in glutamate concentration[4] which leads to the activation of MMP-9 which is ordinarily involved in plasticity. The dysregulation of MMP-9 has neurotoxic consequences (one of which is the potential destruction of laminin). Similarly, microglia express MMP-7 which ordinarily is involved in tissue remodeling and wound repair. MMP-7 activates MMP-9. Healthy astrocytes produce tumor necrosis factor-α as well as inhibitors of MMP-9 (thrombospondins) which improve synaptic efficiency. As neurodegeneration is linked to prolonged

[4] Acting on the N-methyl-D-aspartic acid (NMDA) receptor, activating PKA to facilitate LTP.

microglial activation, the extended activation of MMP-7, and resulting over-activation of MMP-9, can explain why regeneration instead turns into degeneration. Astrocyte transplants restore plasticity [134] suggesting that it could be the intrinsic aging of astrocytes which initiate neurodegenerative-aging. If aged astrocytes are unable to maintain proper protein homeodynamics within themselves it is unlikely that they can maintain the ECM which they secrete.

Both microglial and astrocyte activation cause a local increase in ROS. The chondroitin sulfate proteoglycans (CSPGs) in perineuronal nets (PNNs) are hypothesized to provide an antioxidant defense for the neurons encased in the PNN [135]. PNNs also appear to protect the neurons they encase from tau pathology [136]. PNNs form around parvalbumin containing GABAergic[5] neurons in the brain [137]. Following pilocarpine excitotoxic insult these GABAergic neurons are lost even though there is an upregulation of TNR as the axons reorganize. PNNs serve a role in stabilizing synapses, striking a balance between plasticity and stability, as well as compartmentalization of the neuronal surface [138]—in essence: they anchor the cortical columns to their sensory inputs. They are also believed to play roles in neurite sprouting and synapse pruning [138]. The loss of these neurons and their PNN results in a loss of functional plasticity which occurs via top-down circuit modulation of the cortical column [139].

PNNs are laid down by neurons as well as glia: astrocytes and oligodendrocytes [138]. They consist of, in addition to CSPG: TNR, hyaluronan acid, neurocan, brevican, versican, aggrecan and phosphacan [140]. Brevican is produced by astrocytes while neurocan and aggrecan are produced by neurons; and versican and TNR by oligodendrocytes [140, 141]. Each cell type contributes to the formation of the PNNs implying careful cooperation between the cell types. Brevican is up-regulated during late brain development [142] and knock-out mutants display poorly defined PNNs and have severe impairment of LTP. Abnormal brevican processing was observed in AD model Tg2576 mice [143] while PNN staining differences were found between senescent-accelerated prone mouse strain 8 and senescent-accelerated resistant mouse strain 1 [144]. Similarly, TNR knock-outs also display reduced LTP [145, 146].

PNNs are reported to be lost in brain regions associated with age-related loss of function [147] and as *Nothobranchius* display both an increase in neurodegeneration and decrease in muscle control it is expected that PNNs would be lost in the course of *Nothobranchius* aging. If behavioral enrichment (i.e. exercise) rescued the loss of the PNNs in aged rats it will be interesting to see if resveratrol-treatment has any affect on PNN density in light of its other anti-aging effects in *Nothobranchius*. This question can be answered by using the TNR antibody to label the PNNs and then count them.

TNR is located in lipid rafts where it forms a scaffold for receptor/signaling networks [148]. γ-secretase activity is also associated with lipid rafts [48] where they are tethered to the Notch receptor which partners with tyrosine kinases and integrin receptors. The receptors of the Wnt pathway are fixed to

[5] γ-aminobutynic acid generating neurons.

lipid rafts in the cell membrane [149]. These lipid rafts are rich in highly unstaturated fatty acids which are particularly susceptible to lipid-peroxidation, in particular ω-6 fatty acids. The levels of ω-6 fatty acids, specifically docosahexaenoic acid, is observed to decrease with age [119]. The decline of ω-6 fatty acids is linked to various neurological disorders (including dementia).ω-6 fatty acids supplementation was able to remedy the disorder.

Lipofuscin is a well characterized lipid-peroxidation product and biomarker of aging [150]. It is probable that lipofuscin accumulation can lead to a change in membrane fluidity and permeability [151]. This can affect the activity and cooperation of the cell surface receptors that activate kinases within the axon and dendrites [152]. These signal transduction pathways regulate the cytoskeleton[6] and determine the pathway choices of axonal growth cones [154] as well as dendritic spine growth [155]. In addition, the disruption of the integrin receptors in the lipid rafts disrupts neurogenesis [112]. Changes in membrane permeability can affect depolarization of the cell and thus activation of CREB[7] (via PKA and PKC) that is ordinarily needed to sustain and guide the growing axons and establish synapses [58]. Young rats can clear lipid peroxides from their membranes while old rats cannot [156]. The lipid peroxides are cleared via autophagy to lysosomes where lipofuscin is then formed. This lipofuscin can then go on to disrupt proteosome autophagocytosis [23].

The L1 neuronal cell adhesion molecule (L1-NCAM, or L1 for short), which is also associated with lipid rafts where it interacts with integrin receptors, is crucial for synaptic plasticity [157, 158]. It is also modified by γ-secretase and two metalloproteinases, ADAM10 and 17 [159]. The serum levels of L1 were shown to be increased in the brains of patients with dementia and schizophrenia [47]. There was also a correlation between the levels of cleaved NCAM (neuronal cell adhesion molecule) fragments with both the age of the patients and whether or not they had AD. L1 and NCAM are involved in neuronal plasticity, neuronal cell adhesion, migration of neural progenitor cells and neurite outgrowth [159]. In particular, L1 has been observed to stabilize the axon-axon and axon-glia contacts [160, 161]. Its expression appears to be carefully restricted. In the hippocampus of the rat it is absent from spine synapses but present on those of mossy synapses [162]. Becker & Becker [163] have reported a role for L1 in spinal regeneration and Lang et al. [123], using the E587 antiserum, have reported its involvement in the regeneration of the optic nerve of fish. Developmentally, a lack of L1 has been shown to result in disorderly nerve fasicles [164].

NCAM is known to signal via phospholipase C and PKC. Both L1 and NCAM interact with integrins to signal via Raf, Rac1, PI3K and other partners in src tyrosine kinase signaling but only as long as the receptor complex is tethered to the cytoskeleton. Disruption of the L1 link to actin results in the inhibition of ERK. The inhibition of ERK directly and via PLCγ has been ob-

[6] These are also essential in regulating the cytoskeleton of astroctyes and are reviewed by Theodosis et al. [153].

[7] cAMP responsive element binding protein

served to reduce cell surface sialylation and fucosylation. This had a negative effect on neurite outgrowth and cell survival [165]. NCAM sialylation is crucial for plasticity and has been observed to be upregulated in response to dietary restriction in aged rats [166]. Disruption of L1 signaling has serious consequences: impaired cell survival, inability to make and retain synapses, and an impaired ability for neuronal progenitor cells to migrate through the ECM. The disruption of L1 signaling can culminate in neurodegeneration. One of the dysregulated kinases implicated in the hyperphosphorylation of tau, Cdk5 [45], is crucial in the migration of newborn neurons [167] and the regulation of Cdk5 involves proper integrin activation [168] which is in turn dependent on both L1 and TNR integrin interaction in lipid rafts.

γ-secretase processes a variety of ECM proteins, such as L1 [159] and GFAP [169]. While Aβ may accumulate in the course of neurodegeneration γ-secretase activity declines [170]. Competition for γ-secretase could be a mechanism of neurodegeneration which engages all participants in CNS tissue homeostasis. If this is the case then efforts to inhibit γ-secretase as a treatment for AD [171] may prove worse than a failure.

2.5 ER stress and catabolic malfunction

In the preceding sections the formation of protein aggregates was mentioned. Aβ oligomers may accumulate internally long before they manifest as plaques in the extracellular matrix [44] and NFTs may persist for decades without consequence [172]. Quality control mechanisms within the ER serve to suppress the formation of aggregates [173]. The propensity of proteins to aggregate is made clear by David et al. [97] who found that widespread protein aggregation was an inherent part of *C. elegans* aging. The protein aggregates retrieved from old worms were enriched with proteins which tend to self-organize into β-sheets and which contained polyglutamine repeats—a feature common to several neurodegenerative diseases such as Huntington's Disease. These aggregates were also enriched with chaperone proteins.

The processing of proteins in the ER and how this changes with advancing age are reviewed by Naidoo [174]. The process is outlined in Figure 2.3 (page 21).

The ER processing of protein requires an abundant supply of ATP equivalents and is a carefully orchestrated process. Including the investment of ATP equivalents in translating mRNA into a polypeptide, large amounts of ATP equivalents are used in folding the protein, setting the sulfide bridges and glycosylation as well as maintaining the appropriate ER environment. In order to set the disulfide bridges an optimized oxidative environment needs to be retained and to ensure correct glycosylation the calcium concentration is critical. Both maintaining the oxidative environment and calcium concentration of the ER requires a constant supply of ATP equivalents. Should a protein be processed correctly still more energy is needed to shunt it into the Golgi apparatus; or should the protein be misprocessed energy is needed to ferry it to

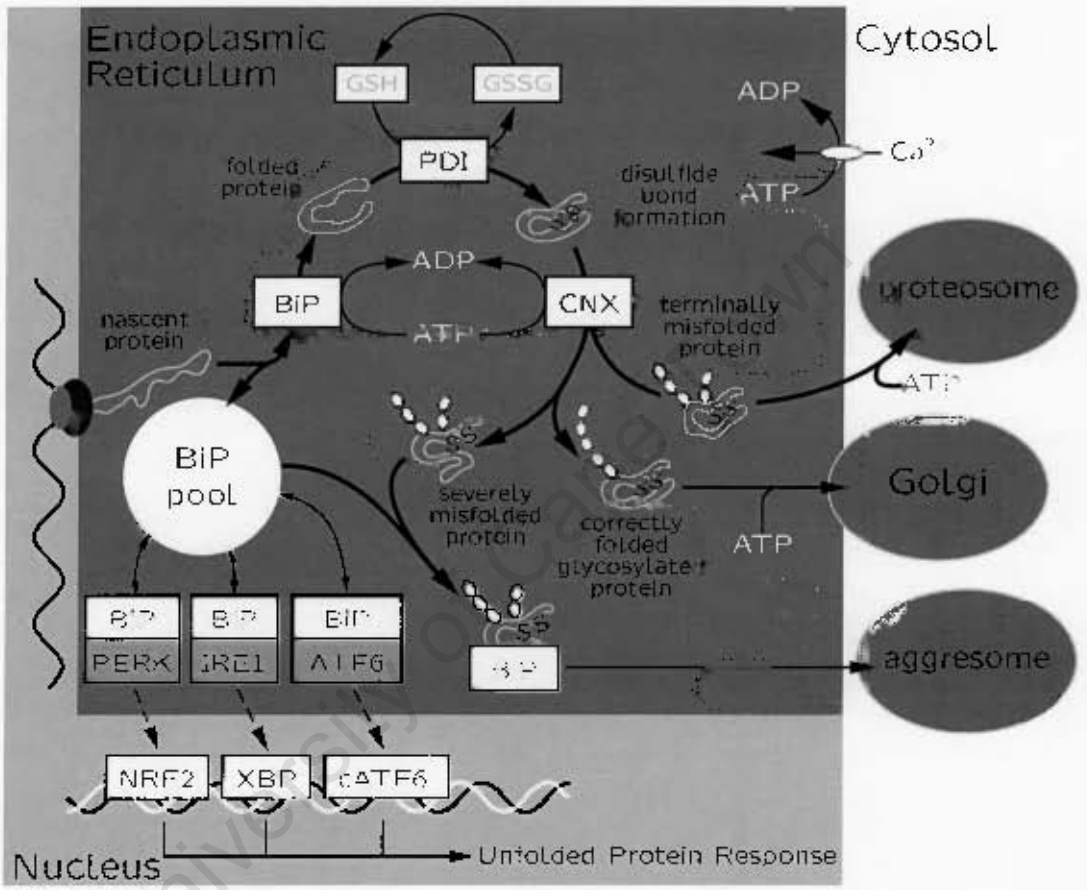

Figure 2.3: Schematic of protein processing in the endoplasmic reticulum. Polypeptides are chaperoned by BiP (which is recruited from a pool of cellular BiP) as they are translated from RNA and folded using ATP. Folded protein is processed by PDI which forms sulfide bridges using GSH. CNX then glycosylates the folded protein using up ATP. CNX function is dependent on the ER calcium concentration which is imported using ATP. Correctly processed protein is exported to the Golgi apparatus using ATP. Terminally misfolded proteins are shunted to the proteosome for degradation while severely misfolded proteins are chaperoned by BiP to the aggresome for degradation. Both processes use ATP. BiP also inhibits the activity of PERK, IRE1 and ATF6 by direct binding. Competitive inhibition of PERK/IRE1/ATF6 binding by unfolded or misfolded protein leads to activation of the unfolded protein response. PERK activates Nrf2 as well as inhibits further protein translation. ATF6 is cleaved and dimerizes into the active transcription protein. IRE1 activates the X-box binding protein 1 transcription factor (XBP). Cartoon modified from Naidoo [174].

the proteosome for digestion. Still more energy is needed to transport proteins via the Golgi to their end destination. Should a protein be misfolded in such a manner that the protein cannot be ferried to the proteosome it needs to be chaperoned by binding immunoglobulin protein (BiP), a chaperone of the Hsp70 family, for reprocessing or sequestering in the aggresome. Synthesizing more BiP is energetically expensive. Given the energy intensive nature of protein processing any disruption in ATP equivalent flux could be catastrophic. This section reviews a simple mechanism underlying ER catastrophe based neurodegeneration.

The first protein effecting quality control in the ER is BiP[8] [174]. As the RNA transcript is translated the nascent polypeptide is chaperoned and folded by BiP. Naidoo et al. [175] have reported that with age the basal expression of BiP in the mouse cortex declines and Paz Gavilan et al. [176] have reported the same for rat hippocampus. A similar decline has been observed in other brain regions of the rat as well as the lung, liver, heart, spleen and kidney [177] which suggests this is a phenomenon of intrinsic aging and not the consequence of a specific pathology. BiP has also been reported to show increased propensity to carbonylation in the course of oxidative damage [178, 179]. As BiP is intimately involved in protein processing and protein aggregates can generate ROS [108] the increase in BiP carbonylation with age could indicate an escalation in protein misprocessing with age.

BiP is also the means by which ER stress is sensed by the cell [174]. It binds to and inhibits the activities of three proteins: PKR-like ER kinase (PERK), inositol requiring element-1 (IRE1), and activating transcription factor 6 (ATF6). These proteins serve to execute the unfolded protein response (UPR). As can be seen in Figure 2.3 there is competition for BiP. Should the amount of nascent poplypeptide or misfolded protein increase there would be an increased demand for BiP which would come at the expense of the fraction of BiP binding the UPR proteins. The unbound UPR proteins would then signal the synthesis of more BiP and in so doing close the negative feedback loops to terminate the UPR.

Activation of the UPR proteins also triggers an antioxidant response through the NF-E2-related factor 2 (Nrf2) transcription factor (which is affected by polyphenols). Nrf2 is activated by PERK which also phosphorylates eukaryote initiation factor 2α which reduces translation—lessening the demand for BiP [180]. IRE1 activation enables it to execute endoribonuclease activity against the mRNA of X-box binding protein 1, producing a splice variant which can facilitate the transcription of genes involved in ER expansion and quality control [181–185]. X-box binding protein 1 transcription is regulated by ATF6 [185] along with that of the transcription of BiP and GRP94 [186], thus correcting the ER stress caused by a reduction in available BiP.

Redox dependent folding is mediated by protein disulfide isomerase (PDI) which is a member of the thioredoxin family. Its activity has been shown to decline with age [178], particularly in the rat hippocampus [176], and is sensi-

[8] Also called Glucose Response Protein 78—GRP78—or Hsp5A.

tive to oxidation [178, 179, 187]. PDI formation of disulfide bonds relies on the ratio of GSH to glutathione disulfide (GSSG) [188]. GSH levels are known to decline with age in several tissues [189]. This problem is all the more pressing given the need to maintain an oxidative environment in the ER to facilitate the formation of the disulfide bridges. The proteins of the ER are especially prone to oxidative damage [190].

Calnexin (CXN) is a calcium binding chaperone involved in glycoprotein folding and quality control and whose activity is dependent on calcium concentration in the ER. Like other ER proteins it is highly susceptible to oxidation [187] and its cellular levels decline with age [176, 191]. The loss of CNX also sensitizes cells to apoptosis [192]. As the protein is folded, glycosylated and redox modifications needed to assume the correct tertiary conformation are made, ERp57 and CXN keep the protein in the ER. ERp57 is also a member of the PDI family and it interacts with glycoproteins in the ER in association with CXN. Once correctly folded the immature folded glycoprotein is released into the Golgi for further processing and delivery [174]. If the protein is misfolded it is reglucosylated by uridine diphosphate glucose:glycoprotein glucosyl transferase which is able to recognize misfolded protein conformations. If the protein is released by CXN it is ignored by uridine diphosphate glucose:glycoprotein glucosyl transferase even if it is misfolded. Such terminally misfolded proteins are chaperoned by BiP. Unless the misfolded protein is reglucosylated it cannot be ferried to the proteosome for degradation and is instead sequestered to the aggresome [95].

It should be clear that protein homeostasis is dependent on a steady supply of ATP equivalents to synthesize and maintain proteins in their functional state. A decline in mitochondrial efficiency is associated with age in several species: humans [193], rats [85, 194] and *Nothobranchius furzeri* [22].

The Mitochondrial Cascade hypothesis of Swerdlow et al. [195] postulates that as one ages the mitochondria of quiescent cells, such as neurons which do not divide, deteriorate and the rate of deterioration is dependent on the quality of the mitochondria inherited through the maternal line. Their hypothesis stands in contrast to the received wisdom [196] which holds that mitochondrial dysfunction occurs during the late stages of neurodegeneration. This is not supported by the data indicating that there is significant mitochondrial dysfunction by 50 years of age [193], long before debilitating symptoms of neurodegeneration manifest. An alternative hypothesis is that of De Grey's Survival of the Slowest [197]. De Grey proposes that mutated mitochondria with lower rates of respiration would suffer less ROS damage and thus escape autophagy recycling longer than more active mitochondria. As consequence, with passing rounds of mitogenesis in the course of normal chronological aging, the cell is enriched for "slow" mitochondria which cannot readily adjust their flux to meet ATP equivalent demand and eventually are incapable of meeting the pace of ATP equivalent consumption. This leads to the Catabolic Insufficiency Theory of Aging, proposed by Terman [198] in 2006. This idea has largely escaped attention.

Ferrer [199] reviews the evidence for general metabolic dysfunction which causes widespread oxidative damage requiring energy for repair and protein recycling and synthesis. Ferrer [199] goes on to point out that there is a shortage of ω-3 polyunsaturated fatty acids—critical fatty acid components of lipid rafts—which has knock-on effects on intra- and cell-cell communication as well as ER/Golgi and endosome trafficking resulting in the misprocessing of APP which proceeds to cause oxidative damage within the ECM. Proper ER/Golgi processing uses large amounts of ATP and NADPH. The fuel supply to neurons and astrocytes is outlined in Figure 2.4 along with the sources of ATP equivalents.

It has been discovered that fuel metabolism in the brain is disrupted with age [194]. Astrocytes feed the neurons lactate but with age the neurons are less able to utilize the lactate as the mitochondria malfunction. This malfunction was determined to be due to Complex IV diminishing relative to Complex II. The neurons, in turn, actively convert pyruvate into lactate due to a shift in expression from the lactate dehydrogenase A to B isoenzyme.

Phosphorylated AMPK was found in degenerating neurons prior to the development of tangles and plaques [86] adding weight to the argument that mitochondrial dysfunction and power supply could be the underlying mechanism of neurodegeneration of both neurons and glia. A similar energy deficit

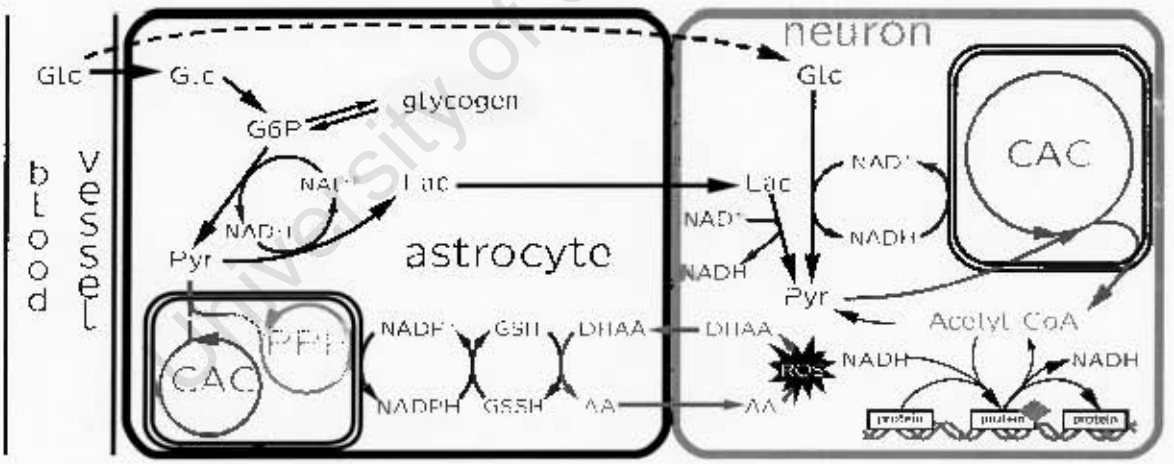

Figure 2.4: Cartoon of the astrocyte-neuron metabolic network whereby astrocytes support the metabolic needs of neurons. Astrocytes absorb glucose (Glc) from the blood which is converted to glucose-6-phosphate (G6P) which is either converted to glycogen or metabolized to pyruvate (Pyr). Some of the Pyr is used by the astrocyte for its metabolic needs and the rest is converted to lactate (Lac) which is exported to the neuron. In the astrocyte Pyr is used to drive the Citric Acid Cycle (CAC) and Pentose Phosphate Pathway (PPP) to generate NADPH which is used to synthesize GSH. The GSH is used to reduce dehydroascorbic acid (DHAA) to ascorbic acid (AA). The Lac taken up by the neuron is converted to Pyr and this Pyr is converted to acetyl-CoA in the mitochondria and converted to citrate. Citrate is exported from the mitochondria via the citrate shuttle to generate cytosolic acetyl-CoA which is used to acetylate proteins. Protein acetylation is used to monitor cellular power and resource supply. Information based in part from Allaman et al. [200].

is observed in aging skeletal muscle [193]. Both the ATP production capacity as well as expression of mitochondrial NADH dehydrogenase (part of Complex I) and $NADP^+$ isocitrate dehydrogenase 2 (a source of NADPH) decline with age. A decline in mitochondrial activity of complex I–IV has also been observed in middle age rats [201]. In the rats there was a decline in NAD^+ which is essential for the acceptance of electrons during glycolysis. Without NAD^+ glycolysis will slow down or stall, leading to glucose-6-phosphate accumulation which may cause the increase in GSK3β activity[9]. Low mitochondrial activity would upset the levels of acetyl-CoA which drives lysine acetylation (by lysine acetyltransferases). The role of lysine acetyltransferases in integrating transcriptional programing and fuel/resource abundance are reviewed by Patel et al. [202]. Sirtuins and histone deacetylases (HDACs) do the opposite, deacetylating lysine residues using NAD^+ as an electron carrier.

Catabolic insufficiency leads to a lower ratio of ATP to ADP, NAD^+ to NADH and higher levels of acetyl-CoA. Lower rates of ATP supply mean that protein processing (and other energy consumptive processes) are limited by an ever dwindling supply of ATP equivalents. This culminates in misfolded protein which can't afford to be repaired. Rising levels of acetyl-CoA and decreasing levels of NAD^+, due to a catabolic bottle neck in the slow mitochondria, impair the activities of NAD^+ dependent deacetylases (which would need to work against the cellular acetyl-CoA concentration). In this scenario cellular catastrophe is inevitable the moment mitochondrial energy efficiency first begins to wane. In addition to high acetyl-CoA and low NAD^+ and ATP, there would be lower levels of NADPH required for fatty acid synthesis [203] and GSH replenishment [92][10]. For the CNS, this also means that there would be a slower rate of vitamin C replenishment [205]. The rising levels of acetyl-CoA coupled with declining NAD^+ will set in motion the synthesis of lactate:

$$\text{pyruvate} + \text{NADH} + \text{H}^+ \longrightarrow \text{lactate} + \text{NAD}^+$$

The lactate serves as an electron sink, replenishing NAD^+, as well as clearing excess pyruvate. The cell could possibly persist in this state but it would be in no condition to cope with the vicissitudes of life.

David Fell reports that the actual enzymatic rates of enzymes within their metabolic pathways are 100 to 10 000 times lower than the maximal rate (V_{max}) [206]. As the flux approaches V_{max} the response coefficient, R, of the system tends to zero. Cells wherein slow mitochondria have multiplied are less able to respond to increased demand for ATP by the ER. This idea can be presented mathematically:

$$R_{ATP}^{ERpf} = C_{BiP}^{ERpf} \epsilon_{ATP}^{BiP}$$

The above expression (originally derived by Kacser & Burns [207] in the development of the mathematical framework for Metabolic Control Analysis)

[9] GSK3β's role in glycolysis is to activate glycogen synthase in the presence of excess glucose-6-phosphate.

[10] Fatty acid monodesaturation by NADPH is shown to be critical to longevity in *C. elegans* [204].

describes the response (R) of ER protein folding to ATP, where the ER protein folding ($ERpf$) is controlled (C, the control coefficient) by the enzymatic activity of BiP; and how this response is a product of the control exercised by BiP over the ER protein folding and the sensitivity (Elasticity, ϵ) of BiP to the ATP supply.

This foray into enzyme kinetcs and control analysis is to emphasize that the processes in the cell are connected in an complex network and that small changes in one pathway can have large effects on others. Central to the theory of Kascer and Burns is that no single enzyme controls flux through a pathway but instead control is shared among all members of the metabolic system, i.e *there is no rate limiting step* [208]. This applies to transcription factors and signaling cascades as well. As cells in the CNS are interconnected metabolically this means that neurodegenerative-aging cannot be understood by reducing the CNS to its components.

Catabolic insufficiency leading to chronic ER stress can explain both the manifestation of misfolded proteins and protein aggregates as observed in studies of neurodegeneration as well as many of the chronically activated signaling pathways, such as the AMPK cascade. If de Grey's Survival of the Slowest or Swerdlow's Mitochondrial Cascade hypothesis are correct (in only some of the cases of disease, and they are not mutually exclusive either) then it would mean that rather than free radicals being the cause it is the cell's excellent response to ROS damaged mitochondria which sets the stage for later catastrophe.

2.6 Conclusions

The chapter began by reviewing the aging-related pathologies of SPs and NFTs. Much was made of their mysterious etiology but potentially rendering the mystery of SPs and NFTs irrelevant is the growing doubt as to whether NFTs are in any way detrimental [172]. They are encountered in viable neurons with intact microtubule networks as well as persisting for decades in the cytoplasm without consequence. They are encountered in significant numbers in cognitively intact elderly people. Furthermore, tau hyperphosphorylation inhibits apoptosis by stabilizing β-catenin [118] which would be a neuroprotective role by NFTs. This stabilization is brought about by competitive inhibition of the β-catenin phosphorylation activity of GSK3β by tau. This anti-apoptotic effect of tau may be the emergency response of neurons which have lost contact with other neurons or laminin with the "hope" that contact can be reestablished and the neuron rescued. The question then is why aren't synaptic connections reestablished?

The idea of catabolic insufficiency leading to chronic ER stress and ensuing cellular degeneration is a simple idea which both links up many of the observations made in conjunction with Aβ and NFTs pathology as well as explains how protein aggregates can accumulate to pathological levels. Highlighting the importance of ER processing of protein, many RNA editing genes

have been found to be associated with extreme old age in humans and lifespan in *C. elegans* [209]. It is worth making mention of the ideas of Gavrilov & Gavrilova [210] who offer the Reliability Theory of Aging. This theory is based on the observation that organisms have an initial high load of damage which is compensated for by system component redundancy. As the redundancy is depleted (e.g. as the functional mitochondria are diluted by dysfunctional mitochondria) systems begin to malfunction until the organism dies. Their theory explains why mortality rates at advanced age are similar between populations even though the populations may exhibit vastly different average lifespans. AD and other dementias can be viewed as an expedited exhaustion of redundant capacity. Aging can be interpreted as the manifestation of the accumulated cellular insults and system malfunctions. Aging does not cause the insults, the insults cause the aging.

By limiting the insults or encouraging regeneration it may be possible to extend the healthspan and thus the median lifespan of humans. Whether or not the maximum lifespan can be affected is another matter which will be returned to in Chapter 7.

Together, the conspiracy of aging-related changes in cell function produce neurodegenerative-aging by the inability of the cell to keep pace with the energy demands for cellular maintenance. Once a critical number of neurons or glia have died or atrophied the system begins to malfunction and dementia, sensory or kinetic disorders manifest. In this scenario there is no need to invoke ever shortening telomeres[11] nor the Free Radical Theory of Harman [211] (which will be dealt with in Section 3.1 of the next chapter). All that is required is for one genetic error, be it slow mitochondria or defective γ-secretase, to be present for the entire system to collapse in later life. There may be a plethora of undetected genetic errors quietly conspiring to cause catastrophe later when the capacity of the cellular repair machinery is exceeded (as during disease) or the redundant units are exhausted (as during aging).

Nothobranchius offer several advantages for the study of neurodegenerative-aging. *Nothobranchius* possess only radial glia lining the brain surface and ventricles [212], by using wholemounts it is possible to study the neuron-glia interaction without introducing sectioning artifacts. A subpopulation of neurons exists in the stratum griseum superficiale of the optic tectum in close proximity to the radial glia. Using the antibodies listed in Table 1.1 it is possible to study SMI31 and GFAP accumulation, the distribution of L1 (via E587 antisera) as well as the abundance of TNR immunoreactive PNNs.

It is expected, using these antibodies, that SMI31 would be observed to accumulate in the OT neurons of normally aged fish and that resveratrol would counter this along with preserving neurons into advanced age. E587 immunoreactivity on neurons is also expected to decline with age and be protected by resveratrol-treatment based on the results of Valenzano et al. [5]. As FJB is now believed to indicate malfunctioning glia [25] and the FJB stained

[11] A problem postmitotic cells such as neurons wouldn't need to bother with in any case.

sections of *Nothobranchius* show considerable staining in the surface layer of the OT some level of radial glial degeneration is expected. This degeneration will most likely be concomitant with one or another form of protein misprocessing. Exercise has been shown to preserve (and restore) PNNs lost with age in rats [147], whether resveratrol will have the same effect is an open question. The data of Valenzano et al. [5] implies that the neural circuitry degenerates with age and is preserved by resveratrol. This indicates that the PNNs are also preserved. These questions will be answered in Chapters 5 and 6. The next chapter will serve to better equip the reader with what they can expect from polyphenols (such as resveratrol) regarding the retardation of neurodegenerative-aging.

Chapter 3

Mechanisms of polyphenol neuroprotection

> Is there a way to find the cure for this implanted in a pill?
> Well strip the bark right off a tree and just hand it this way.
> Don't even need a drink of water to make the headache go away.
>
> *Girl, you have no faith in medicine*, The White Stripes.

The question at hand is whether certain polyphenols have anti-aging properties, in particularly against neurodegenerative-aging; and if so, are certain polyphenols more beneficial than others and will ingesting more of these enable us to live healthier and longer lives? There are a multitude of reviews concerning the biological actions of polyphenols. In this review only those activities of polyphenols pertaining to neuroprotection or CNS metabolism will be addressed in any detail. Information from other fields will be drawn on to gain perspective of the effects that polyphenols have on cellular signaling. This review is not a search for a unifying hypothesis of the mechanism of polyphenol neuroprotection. The goal is not to review every bit of information but to present the information in such a way as to represent the multipotent properties of polyphenols which necessitate whole-animal experimentation. It is the assertion of the Author that polyphenol neuroprotection cannot be understood except by taking into account the many mechanisms by which they can synergistically affect physiological outcomes. More could be written but the information presented within the following pages is already more than adequate to present an integrated look at polyphenol action so far as neuroprotection is concerned.

A second goal in writing this chapter is to address the question of "what dose?" The fish experimented on by the Author were previously [5], and as part of this study, given 12 μg/fish/day. Large full grown *N furzeri* have a mass of ≈ 6 g at 12 weeks of age with smaller fish being ≈ 3 g. Adult *N. guentheri* are not much smaller. This equates to 4–8 mg/kg fish/day. How does this dose compare to that of other experiments and what can we expect from it?

The polyphenol rich diet of laboratory rodents together coupled with their low-risk environment has drawbacks for aging research. Barger et al. [213] report that resveratrol (at 4.9 mg/kg mouse/day) did not increase median lifespan in non-obese mice but did decrease the disease burden. This result fits neatly with Gavrilov's Reliability Theory of Aging [210] but also highlights why mice, kept in low-risk environments, are not advantageous in assessing the healthspan altering affects of polyphenols. The healthspan increasing effect of resveratrol was noticeable in high calorie fed obese mice (fed 22.4 mg/kg mouse/day) [214] because of the high extrinsic healthspan risk associated with this diet. Unless the animal model is exposed to healthspan risks which can deplete the redundant capacity of the animal no effect on median lifespan would be apparent. To this end insectivorous *Nothobranchius* are exposed both to low levels of dietary polyphenols and to extrinsic healthspan-risks in the aquarium water. *Nothobranchius* are superior model organisms to rodents in assessing the anti-aging properties of polyphenols.

As the molecular tools to study *Nothobranchius* physiology are poorly developed the only option is to employ antibody probes in search of aging-related and resveratrol-treatment dependent differences between experimental groups which can be inferred back to possible molecular mechanisms. There are several means by which polyphenols can exert a neuroprotective affect. These mechanisms proposed by other researchers will be briefly reviewed. Following the discussion of these the expectations of *Nothobranchius* low-dose resveratrol-treatment will be discussed and linked with the signs of neurodegeneration expected to be visible in *Nothobranchius* as discussed in the preceding chapter.

Several polyphenols will be discussed in this chapter. The structures of some of these neuroprotectively relevant polyphenols and structurally related compounds are presented in Figure 3.1. Also shown are two steroids, ursolic acid (a triterpenoid), and thioflavin-T which are reported to be neuroprotective. These are structurally similar compounds to polyphenols and will be discussed further on in this chapter. These compounds exert a neuroprotective affect despite not having a significant antioxidant potential. The chemical character of polyphenols empower them to act as antioxidants.

3.1 The Direct Antioxidant Hypothesis

The direct antioxidant hypothesis of polyphenol neuroprotection is born of the Free Radical Theory of aging which is reviewed by Beckman & Ames [215]. This theory holds that aging is a result of cumulative oxidative damage in the course of aerobic respiration and therefore antioxidants would prevent this damage and in so doing slow aging. Polyphenol compounds have direct antioxidant properties and they seem to retard aging or the onset of aging-related diseases. Therefore (according to proponents of the direct antioxidant hypothesis) polyphenols retard aging through their antioxidant properties. The Free Radical Theory of aging can no longer be regarded as a general model of aging

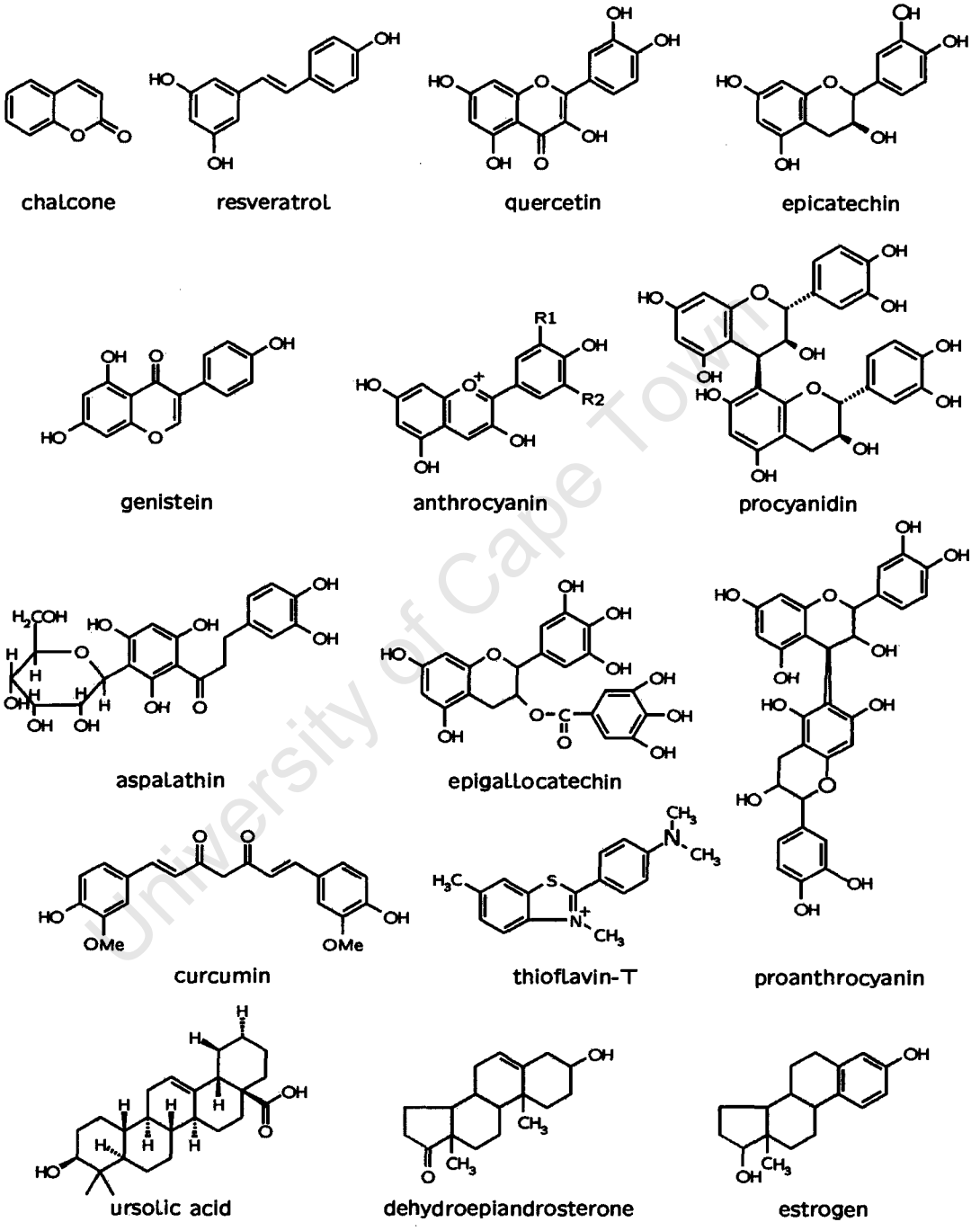

Figure 3.1: Structures of several biologically significant polyphenol compounds. Note the structural similarity to the structure of the steroids, triterpenoid and thioflavin-T.

on account of the naked mole rat, transgenic mice and *C. elegans* experiments.

The naked mole rat, *Heterocephalus glaber*, exhibits an exceptionally long life (more than 28 years) in respect to its diminutive size and also develops disproportionately high levels of oxidative damage to its proteins, DNA and lipids compared to other species of the same size and age [216]. It also has lower levels of antioxidant defense in the form of reduced GSH and redox status (as measured by the ratio of GSH to GSSG). In a mouse experiment where GPx4 (glutathione peroxidase 4, a phospholipid hydroperoxide glutathione peroxidase which is the key enzyme in the detoxification of lipid hydroperoxides) was knocked down the result was not early mortality but longer lifespan [151]. So far as rodents are concerned the Free Radical Theory of aging does not apply to them and probably not to *C. elegans* either. Experiments on *C. elegans* where superoxide dismutase (SOD) genes were systematically deleted the deletion of sod-2 resulted in an increase in oxidative damage to proteins *and* extended lifespan rather than shortening it [217]. The gene sod-2 codes for a SOD which localizes to the mitochondria so the mitochondrial Free Radical Theory of aging is also falsified as a general model of aging. Its deletion was compensated for by the upregulation of genes which increased mitochondrial efficiency and underpins the aging-related malfunction of cells and tissues (as discussed in the preceding chapter). Increased ROS does not result in a shorter lifespan as the Free Radical Theory predicts.

Further refutation of the antioxidant hypothesis of anti-aging comes from the experiments of Selman et al. [218] who report that life long vitamin C supplementation did not affect lifespan in mice but did decrease the expression of antioxidant protection genes. Mice might be poor subjects for such a study as they can synthesize vitamin C (unlike humans). Vitamin C supplementation, through negative feedback metabolic processes, could inhibit the synthesis of vitamin C synthesizing genes along with other antioxidant genes whose regulation is coded by the same response element. Human epidemiological data also yields no support for exogenous antioxidant supplementation having any effect on lifespan [219]. A recent placebo double-blind study has again presented evidence that long-term antioxidant supplementation has no effect on real or perceived health benefits [220]. This is to say that increasing the concentration of antioxidants beyond the minimum daily requirement does not affect healthspan nor, so far, lengthen lifespan as predicted from the Free Radical Theory of aging.

Experiments using the synthetic polyphenol, pterostilbene (40 mg/kg diet), produced plasma concentrations of 26 ng/mL ($\approx 0.095\ \mu$M) and a total of 1.3 ng in the rat hippocampus [221]. At these concentrations pterostilbene was able to *reverse* cognitive behavioral deficits in old rats. The improvement in working memory was correlated with the pterostilbene levels in the hippocampus. 150 μM quercetin was required to prevent oxidative stress in *C. elegans* [222]. It was estimated that 0.04 to 0.12 nmol quercetin was absorbed (after 20 hours incubation) per 1000 worms. *C. elegans* has an

adult volume of approximately 8.4×10^{-9} L [1], translating to 6.9–20.4 μM[2] tissue concentration. The adult rat hippocampus has a volume of approximately 50×10^{-6} L [224], implying a pterostilbene concentration of $\approx$0.14 μM, some 49 times less than for the worms incubated in quercetin. For comparison, the concentration of vitamin C in the human hippocampus ranges from 150 to 300 μg/g (wet weight) [225] which equates to between 1.2 and 2.4 μM which is at least five times less than for quercetin in *C. elegans* and nine times greater than for pterostilbene in the rat hippocampus. It is important to note that the rat brain is not limited in vitamin C. It is hard to accept that pterostilbene is acting as an antioxidant when surrounded by such an abundance of vitamin C.

In in vivo antioxidant assays by Rüweler et al. [226], luteolin and galangin almost completely quenched the oxidative activity of cumene hydroperoxide at 5–10 μM (Table 3.1) . In this assay, these two polyphenols were more potent than quercetin. While quercetin may have had an antioxidant activity at 150 μM in the *C. elegans* culture medium, it cannot be expected to have much of an antioxidant activity in situ at 6.9 μM when it lacks such potency, and where vitamin C is abundant.

It is important to reemphasize that pterostilbene *reversed* aging-related cognitive impairment in the rats [221]. Somehow the polyphenols were able to set the senescent cellular machinery in motion. Young rats can clear lipid peroxides from their membranes while old rats cannot [227]. The administration of rooibos tea[3] enabled aged rats to clear the lipid peroxide products from their membranes [156]. Inanami et al. [156] do not supply data concerning the rooibos dosage but a steeped aqueous extract has a polyphenol content of $\approx$ 2.6 mg/mL and rats ingest $\approx$ 11 mL/100 g rat per day [228] suggesting a polyphenol dose of $\approx$ 286 mg/kg rat/day. Lipid peroxides, unless immediately

[1] Calculated from [223].

[2] Assuming 70% wet weight being water.

[3] A beverage prepared by steeping the dried fermented twigs of the Rooibos (red bush), *Aspalathus linearis*, and which is rich in polyphenolics, particularly aspalathin.

Table 3.1: Table of intracellular potencies of polyphenol antioxidants. Values are IC_{50}s against 500 μM cumene hydroperoxide as measured using the C6 cell assay and a cell-free Trolox equivalent antioxidant capacity assay [226].

Polyphenol	IC_{50} for C6 cell assay (μM) blots	IC_{50} for cell-free assay (μM)
luteolin	1.0 ± 0.5	2.48 ± 0.23
ganlangin	2.1 ± 0.6	2.08 ± 0.11
kaempferol	8.0 ± 0.1	1.45 ± 0.08
quercetin	13.0 ± 1.2	4.84 ± 0.45
resveratrol	17.7 ± 6.8	2.88 ± 0.15
genistein	22.2 ± 6.8	2.96 ± 0.49
taxifolin	30.1 ± 8.2	3.09 ± 0.58

reduced, rapidly spread to adjacent lipids by acryl-radical cross-linking in a spontaneous and irreversible chain-reaction [229, 230]. The polyphenols of rooibos tea do not slow the process of lipid peroxide accumulation but *reverse* it.

The Author does not assert that ROS and the damage it causes are of no consequence in neurodegeneration, but instead that in the course of neurodegenerative-aging ROS is not the cause but a symptom of some other cellular dysfunction. The nature of that dysfunction is disputed. The Author believes it to be Catabolic Insufficiency (2.5, page 23) associated with mitochondrial inefficiency. Catabolic Insufficiency would result in ER stress and impair Golgi function which would prevent efficient recycling of cellular membranes and thus interfere with the maintenance of synaptic contacts.

The role of endogenous cellular and extracellular antioxidant measures are of critical importance in the nervous system. Lipofuscin accumulation alters the fluidity and permeability of the lipid membrane among many other potentially deleterious effects [23, 151]. This can affect the activity and cooperation of the cell surface receptor kinases and their detection of the ligands in the ECM [152]. As was discussed in Chapter 2, page 6, many of the CNS signaling complexes are imbedded in lipid rafts [48, 149, 157]. These rafts are enriched with polyunsaturated fatty acids which are especially sensitive to free radical attack and lipofuscin generation through acryl-radical cross-linking [231]. To protect against lipid peroxidation antioxidant enzymes are imbedded in the cell and organelle membranes. One such enzyme is GPx [232].

GPx enzymes use GSH to reduce oxidative damage on proteins and lipids [189], generating GSSH which is in turn reduced to GSH using NADPH [233]. It has been reported that GPx expression and activity declines with age in human endothelial progenitor cells [234], serving as a possible reason for the increase in lipofuscin levels with age. This may be interpreted as evidence for lipofuscin increase and GPx decrease being of importance in the aging process but as mentioned earlier there is at least one experiment suggesting that this is not the case. The GPx knock-down mice (retaining only 50% of GPx activity) lived longer than control mice and had a lower incidence of tumor lymphoma and glomerulonephritis but an increased susceptibility to oxidative stress-induced apoptosis [151]. Still, it was found that by supplying rats GSH monoester many of the membrane based aging-related enzyme deficits [81] were restored suggesting that the endogenous supply of GSH may be impaired in aging. But this is not the case with astrocytes which one study reports as showing no decline in GSH productivity [116].

In the nervous system the GABAergic neurons in the cortex seem especially prone to ROS damage following excitotoxic insult [137]. These GABAergic neurons of the hippocampus are ensheathed in PNNs. A decline in PPN ensheathed neurons have been observed in the motor cortex of the rat [147]. PNNs are made up of several proteins, many of which are glycosylated, such as CSPG [140]. CSPG affords these neurons protection from free radical damage and, as consequence, less prone to lipofuscin accumulation [135]. The

maintenance of the CSPG level is dependent on astrocyte activity [138] and an age-correlated atrophy of astocytes has been observed in AD model mice which is independent of SPs [110]. While astrocytes may retain their antioxidant capacity into old age there may be far fewer productive astrocytes later in life. This would also imply that there is a reduction in GSH supply necessary to maintain the ECM.

Without question the endogenous antioxidant defenses are critical to maintaining healthy cellular function into old age but it is unlikely that polyphenols are playing a direct role as antioxidants in vivo. There is evidence for polyphenols playing an indirect role as modulators of the endogenous antioxidant systems. For example: blueberry extracts administered before primary hippocampal neurons where exposed to Aβ caused an increase in ROS but reduced the toxic effects of the Aβ [235]. Further experimentation revealed that the blueberry extracts caused an increase in GSH levels in the cells via ERK and CREB signaling. This phenomenon of a mild stressor causing resistance to later stress is called hormesis and is the subject of the next section.

While the measurement of GSH levels is beyond the scope of this study it is expected that resveratrol would increase GSH supply. This could be achieved by either increasing GSH synthesis or preventing the age-associated atrophy of astrocytes. We know already from the research of Valenzano et al. [5] that lipofuscin levels are reduced in the livers of resveratrol-treated *N. furzeri* which indicates an improvement in GSH supply and membrane recycling relative to aged-match controls. As endogenous antioxidant supply is also vital to the maintenance of PNNs it is expected that resveratrol would also preserve these into old age. Both the question of resveratrol-treatment preserving astroglia and PNNs into old age will be answered in Chapter 6 using the GFAP and TNR antibodies.

3.2 Hormesis and energy metabolism

> "Hormesis refers to a process in which exposure to a low dose of a chemical agent or environmental factor that is damaging at higher doses induces a beneficial effect on the cell or organism."

The above quote from Mattson et al. [236] succinctly defines the concept of hormesis. It is an old idea popularized through homeopathy hocum. Hormesis is the simplest theory by which to explain the myriad of effects of polyphenols. The sections that follow should be interpreted in the light of this section. While polyphenols may be reported to work through native signaling cascades this effect is achieved by an exotic compound causing an unnatural activation of the signaling cascades. Given the rigorous regulation of these cascades this unnatural activation should be considered a source of cellular stress.

In the previous section it was reported that blueberry extracts induced ROS and this ROS caused a response which afforded protection against Aβ toxicity [235]. This response was effected via ERK and CREB which are down-

stream targets of PKA. Blueberry extracts have an anthrocyanin concentration of 877 mg/L (or ≈ 1.08 mM, average $M_r \approx 813$ g.mol^{-1} [4]) [237]. The cells used in the experiments by Brewer et al. [235] were given 125 μg/mL blueberry extract (or ≈153 μM). This can hardly be considered a *low* dose when genestein causes ROS damage at only 10 μM [226]. Still, the cells responded by becoming more stress resistant. Assuming pro-oxidant activity was restricted to the cell membrane a simple explanation can be hypothesized whereby JNK is activated by the small GTPase, Ral, in response to a drop in GSH concentration. This scheme is presented in Figure 3.2.

JNK activation coupled with deglutathionylation has been shown to result in the activation of SIRT1 (Silent Information Regulator 1) [238]. SIRT1 proceeds to deacetylate FoxO, p53 and nuclear factor κB (NF-κB) [239]. This deacetylation causes a shift from cell death to cell survival transcription modules which will be elaborated on in the next section. As part of the cell life transcription module is the expression of various antioxidant genes and Phase II enzymes such as protein chaperones. This response relies on the presence of a high NAD$^+$/NADH ratio and low levels of acetyl-CoA else SIRT would not have sufficient NAD$^+$ substrate while also having to contend with prod-

[4] Anthocyanins (which are a trimer of proanthrocyanin) polymerize and this is the monomer molecular mass, thus the stated molar concentration is most likely an over estimate of the actual concentration.

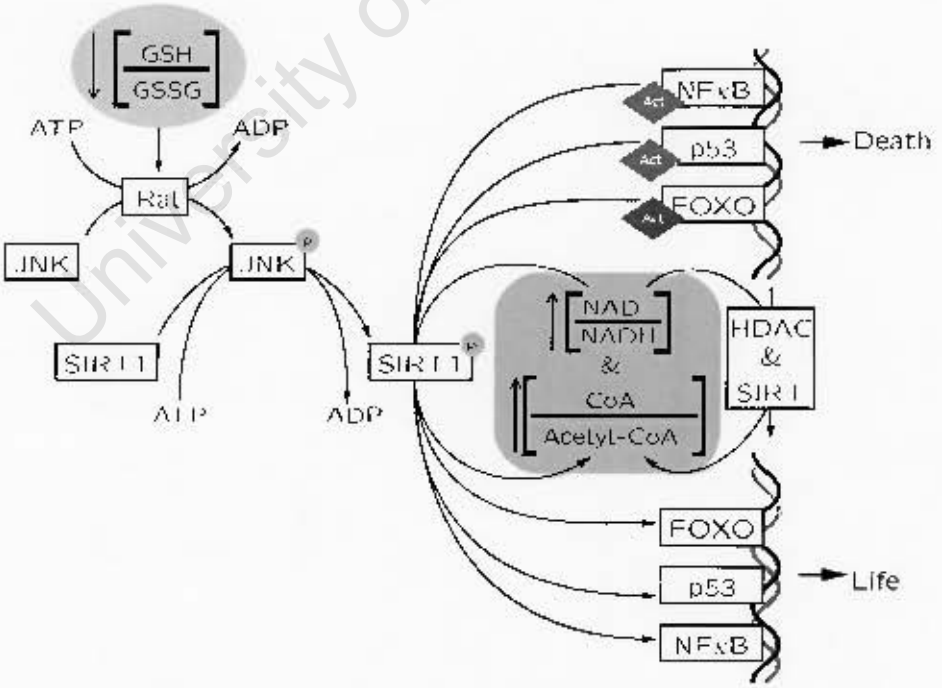

Figure 3.2: The choice between life and death as mediated by energy balance.

uct (acetyl-CoA) inhibition. This hypothesis relies on the cell being healthy to start with. Both middle age humans [193] and rats [201] show a decline in mitochondrial activity. In the rats, this decline was concomitant with a decline in the NAD^+/NADH ratio as well as sirtuin activity. There was also an increase in acetylated p53 indicating to the Author that unless there is sufficient mitochondrial fitness sirtuin cannot switch genomic expression programs from death to life.

There is evidence for sirtuin activation causing cell death in energetically compromised cells [240]. It can be expected that unsavable neurons would therefore be cleared from the brains of *Nothobranchius* on resveratrol-treatment (as resveratrol activates cell survival expression modules, and not because it necessarily activates sirtuins). Whether this neuron loss would be detectable among the neuroprotective effect of resveratrol is impossible to predict. Neuron numbers can be quantified using the SMI31 antibody. What effect resveratrol has on neuron survival will be revealed in Chapter 5.

Blueberry extracts (as well as spinach and strawberry extracts) can reverse age-related mental decline [237, 241] which suggests that a sirtuin based hypothesis (which simply protects cells against death) cannot fully explain the observations. Further complicating matters, while neuroprotection of adult rat hippocampal neurons relied on ERK activity [235], experiments employing mouse cerebral microglia and neuron cultures produced neuroprotection using blueberries by inhibiting ERK activity [242]. In the latter experiment, blueberry extract was effective at only 25 μg/mL ($\approx 30.6\ \mu$M) and the extract was added to the cell together with the Aβ, so at a lower concentration blueberry extract can prevent Aβ toxicity but through a different mechanism in a different cell type. This neuroprotective effect was only visible after 72 hours. At higher concentrations, significant neuroprotection was visible from 48 hours indicating a concentration dependent adaptive response was required in accordance with the Hormetic Theory of neuroprotection.

Son et al. [243] review the neurohormetic action of polyphenols. Their proposed mechanism is presented in Figure 3.3. A range of poylphenols have been observed to activate a variety of kinases, instigating the activation of a variety of expression modules. One such expression module is the antioxidant response element (ARE). The ARE is in part controlled by the activity of Nrf2. Nrf2 is kept inactive through covalent binding to Keap1 (via sulfide bridges). Sulforaphane, which is not a polyphenol, from broccoli has been shown to disrupt the sulfide bridges, allowing Nrf2 activity as well as inhibiting Nrf2's degradation. ARE expression results in the upregulation of antioxidant enzymes such as manganese superoxide dismutase (Mn-SOD), glutathione S-transferases, glutathione reductase, GPx, epoxide hydrolase, hemeoxygenase-1 (HO-1), catalase, NAD(P)H dehydrogenase quinone 1, UDP-glucuronosyltransferase (which is involved in the reprocessing of misfolded proteins) and various protein chaperones including Hsp70. Many of these have been shown to decline with age, be up-regulated in anti-aging therapies or otherwise been implicated in lifespan modulation.

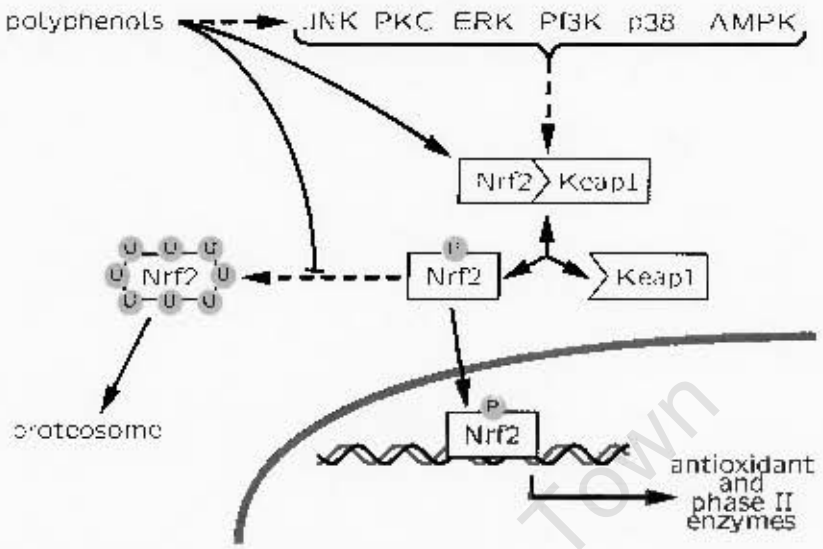

Figure 3.3: The nrf2 response to polyphenols is to initiate the transcription of antioxidant and phase II enzymes. Polyphenols can act via kinases or directly on the nrf2-keap1 complex or even on the degradation of nrf2. Schematic modified from [243]. The"U" stands for ubiquitin.

The hormetic activity of resveratrol is reviewed by Calabrese et al. [244]. Resveratrol was able to increase HO-1 expression in human aortic smooth muscle cells at only 0.1 μM. At 1.1 μg/mL (≈ 5 μM) it was able to increase the expression of SOD and GPx. Resveratrol, quercetin and epigallocatechin gallate, at 0.1–1 μM concentrations, were shown to increase the expression of endothelial nitric oxide synthase (eNOS) and vascular endothelial growth factor (VEGF) (genes important for cardiovascular health) and decrease the expression of endothelin-1 in cultured vascular endothelial cells [245]. 2.4 μM[5] resveratrol was achieved in brain tissue and at this concentration the levels of Aβ was reduced and AMPK activation increased [246]. The mice were given 3.5 g resveratrol/kg food. A 100 mg/kg mouse/day dose of purple sweet potato color extract was able to ameliorate the cognitive deficits in aging mice [247]. At this concentration of purple sweet potato color extract there was a decrease in GFAP, inducible NOS, cyclooxygenase-2, malondialadehyde content and nuclear translocation of NF-κB while the activity of Cu/Zn-SOD and catalase was increased. After 24 hours of incubation in ≈ 2.5 μM red wine extract cultured astrocytes were able to resist ROS damage [248]. These are low doses, far below what would be needed to invoke the direct antioxidant hypothesis, and are able to produce measurable effects on health. The pterostilbene experiments of Joseph et al. [221] which yielded a significant improvement in cognition employed 160 mg pterostilbene/kg rat/day and reached a concen-

[5] 1.7 nmol/g wet weight was retrieved from mouse brain homogenates. Assuming 70% wet weight being water and an M_r of 228 g/mol, 2.4 μM is estimated.

tration of 0.14 μM in the hippocampus. In Krikorian et al. [237], humans of 76.2 years average age, were given $\approx$ 7 mL blueberry juice per kilogram per day. This equated to 11.27 mg polyphenolics[6] per kilogram per day. This low dose was sufficient to produce a significant improvement in cognition. In another study, adults with mild cognitive impairment (78.2 years age average) were given approximately 7.5 mL concord grape juice per kilogram per day which also improved memory [249]. It is hard to believe that this low dose would approach 0.14 μM let alone 2.4 μM resveratrol at a cellular level. More impressive still, 4.9 mg resveratrol/kg mouse retarded several aging parameters in mice suggesting that very little is required to elicit beneficial effects [250].

Other polyphenols have been observed to exert biologically meaningful effects at low concentrations. A protective response to curcumin was observed at only 1 μM based on increases in RANTES[7] expression [251]. The curcumin was added to the cells for only one hour and then fresh medium was added and the cells left to recover for a further 23 hours. 50 mg/mL green tea extract was administered orally for 6 months to senescence accelerated mice with an improvement in spatial learning and the upregulation of synaptic plasticity related proteins: brain derived neurotrophic factor (BDNF), post-synaptic density protein-95 and CAMKII [252]. The same green tea dose given to C57BL/6J mice corrected the aging-related decrease in SOD and GPx activities as well as reduced the levels of thiobarbiturix acid reactive substances [253]. The loss of post-synaptic-density-95 and N-methyl-d-aspartate-receptor-1 in the hippocampus was also reduced as well as the activity of NF-κB. Rats given 0.96 mg/mL total green tea phenolics for 19 months had a higher GSH:GSSG ratio as well as higher activity of other antioxidant enzymes [254]. The levels of activated CREB and BDNF and Bcl-2 expression was also increased with green tea administration but there was no change in NF-κB activity suggesting that NF-κB activation may play no role in the long-term anti-aging response to green tea. Rats given 0.25 mg/kg genistein had a lower mean arterial blood pressure, increased NO bioavailability and lower malondialdehyde levels [255].

Rats given 200 mg/L grape seed flavanols in their drinking water developed less lipofuscin than controls [256] while rats given port flavanols did not benefit from the polyphenol content suggesting that the quality of the polyphenols could be important. A 592.5 mg grape seed extract per gram feed experiment on AD model mice, possessing the APP(Swe)/PS1dE9 mutation, resulted in a reduction of Aβ deposition and inflammation [257]. A 0.7 mg/g feed dose of curcumin given to the same mouse strain also reduced inflammation and Aβ deposition, indicating that some polyphenols are more potent than others at inducing a protective response. A range of blueberry extract fractions, applied at 0.5 mg/mL phenolics elicited various protective effects depending on

[6] Blueberry juice contains 734 mg/L hydroxycinnamic acid ester and 877 mg/mL anthocyanins.

[7] RANTES, regulated on activation normal T expressed and secreted, a cytokine which is expressed in brain tissue and has a neuroprotective function.

the fraction [258]. None of the individual polyphenol fractions had the same efficacy as the whole extract though each displayed different potencies against dopamine, aβ_{42} and lipopolysaccharide cytotoxicity. Most fractions as well as the whole extract increased levels of MAPK, JNK, p38 and NF-κB activity. The different fractions had different effects on the ROS levels depending on the stressor but in general increased ROS.

The Author has already referred to the importance of energy balance and mention was made as to the importance of the cellular levels of NAD^+ and acetyl-CoA. These levels, as far as they effect sirtuin activity, may be irrelevant to the anti-aging effects of polyphenols. Barger et al. [213] report that the bioactive dose of 4.9 mg/kg body weight/day resveratrol had *no* effect on Sir2 activity. The role of sirtuin in FoxO signaling will be discussed in Section 3.3.1. At low cellular concentrations of resveratrol there is an increase in AMPK activity [246] which is discussed in in Section 3.3.2.

Reviews of the bioactivity of resveratrol and other polyphenols neglect to report that they are inhibitors of the F_1F_0-ATP synthase of various species [259–262]. The IC_{50} values of the various polyphenols are given in Table 3.2. It is interesting to note that the two most physiologically potent polyphenols, (-)-epigallocatechin gallate (EGCG) and resveratrol, rank near the top.

It has been shown, using crystallography, that resveratrol, piceatannol and quercetin are non-competitive inhibitors binding to a common site between the β_{TP} and γ subunits of the F_1F_0-ATPase/synthase [263]. This binding impairs the rotary action of the ATPase and inhibits both ATPase and ATP synthase activities. While the IC_{50} values far exceed the polyphenol concentrations achieved in tissues this does not imply that they do not have an inhibitory action on ATP production. Fell [206] reviews non-competitive inhibition and its effect on the flux through pathways. The inhibitor effect varies with the control of the target enzyme over the flux through the system. For enzymes with a high flux control coefficient the response to the inhibitor quickly tends to zero with increasing concentration but grows more acute with decreasing concentration. Low levels of inhibitor can cause relatively large changes in flux. For enzymes with a low flux control coefficient the affect of the inhibitor is less severe at all concentrations but by no means negligible.

In brain and kidney tissue ATP synthase has a high flux control coefficient (0.26 and 0.27 respectively) over oxidative phosphorylation [264]. Complex I and pyruvate carrier have coefficients of 0.25 and 0.26 respectively in the brain. These three enzymes comprise 77% of the control over the production of ATP in the brain. Polyphenols can attain 0.1–1 μM in the bloodstream [265]. Based on the data of Zheng & Ramirez [259] this could imply a 0.26–2.6% decrease in the flux through oxidative phosphorylation. Theaflavins (from black tea) have been reported to inhibit both ATP synthesis and Complex I in vitro [266]. It was able to do this without increasing superoxide production. The IC_{50} values against ATP synthase by the theaflavins ranged between 10–60 μM for membrane bound enzyme and 0.7–4 μM for unbound enzyme. IC_{50} values against Complex I ranged from 7–45 μM. As both Complex I and ATP synthase both

Table 3.2: IC_{50} values of various polyphenols for the inhibition of F_0F_1 ATP synthase. Values taken from [259]. The concentrations for tannic acid (1701.2 g/mol), theaflavin (554 g/mol) and grape seed proanthrocyanidins (575 g/mol) were calculated using their respective average molecular masses and the mg/mL concentrations provided: 5, 20 and 30 respectively. Given the large size and complex structure of tannic acid, which would hinder its bioavailability, its low IC_{50} is probably an artifact of the assay.

Polyphenol	concentration (μM)
tannic acid	2.9
piceatannol	8
(-)-epigallocatechin gallate	17
resveratrol	19
theaflavins	36.1
curcumin	40
(-)-epicatechin gallate	45
quercetin	50
grape seed proanthocyanidin extract	52.1
genistein	55
kaempferol	55
morin	60
biochanin	65
apigenin	105
A Daidzein	127

have high control coefficients polyphenols could, at physiological concentrations, have a physiologically significant affect on oxidative phosphorylation.

Whether this inhibitory affect would cause the level of AMP to rise and activate AMPK is an open question. AMPK activation would lead not only to the execution of the ARE expression module but also the mitogenesis modules [267, 268]. This would correct any energy deficits as well as increase the concentration and supply of ATP equivalents (enabling the cell to better respond to its maintenance needs). In addition, more NAD^+ would be available, allowing for faster clearance of acetyl-CoA; improved fatty-acid synthesis and more mitochondrial endogenous antioxidants as well as GSH to counter ROS damage to the mitochondria. Ultimately, the consequences of the malfunctioning mitochondria of Short et al. [193] and de Grey [197] would be mitigated. The role of mitogensis and cellular stress in respect to aging and hormesis are reviewed by Calabrese et al. [268] who put particular focus on neurodegenerative disorders and neuroprotection showing that the inability to cope with cellular stress results in protein misfolding and proteotoxic stress, and hormetic treat-

ments ameliorate this proteotoxic stress through expression of what the authors call vitagenes (antioxidant and Phase II enzymes) and mitogensis. Short term blueberry enriched diet (20 mg blueberry extract/g feed/day) reverses object recognition memory loss in aging rats [269] implying a short stress can instigate a reparative response. It could also reverse aging-related Aβ deposition.

As the polyphenols can also inhibit the ATPase activity this could disrupt protein processing triggering the unfolded protein response. This would make more BiP and other chaperones available to ensure proper protein processing and recycling. This hypothesis has not yet been explored.

Polyphenols can interact with proteins in other ways. A range of polyphenols were tested by Riviére et al. [270] against Aβ aggregation. The results are shown in Table 3.3. The most effective polyphenols were stilbene dimers followed by resveratrol. The IC_{50} of resveratrol was 2.5× higher than the tissue concentration achieved by Vingtdeux et al. [246]. Resveratrol has been shown to selectively remodel soluble Aβ oliogmers, fibrillar intermediates and amyloid fibrils but not effect the autopoesis of non-toxic oligomers [271].

Resveratrol was found to block the lateral growth of the oligomer β-sheets [271]. With age there was a predilection for the aggregation of proteins in *C. elegans* which formed β-sheets [97]. It is possible that resveratrol could, in part, slow aging by hindering the aggregation of β-sheet proteins. Thioflavin-T, a small molecule (see Figure 3.1, page 31) which selectively binds to proteins which form β-sheets, was able to extend the lifespan of *C. elegans*. Thioflavin-T extended lifespan by 60% at 50 μM whereas 100 μM curcumin achieved 45% lifespan extension and there was no additive effect observed in combining the two compounds. The action of thioflavin-T relied on heat shock factor 1 and SKN-1, the *C. elegans* Nrf2 ortholog. *C. elegans* Hsp70 mRNA was up-

Table 3.3: The ability of polyphenols to disrupt Aβ aggregations is given in the table below as percentage inhibition and as IC_{50} values (where available). Only the most effective polyphenols are listed as well as two polyphenols mentioned previously in the text which were effective at retarding age-related cognitive decline. Data from [270]

Polyphenol	% Inhibition	IC_{50} (μM)
ϵ-viniferin glucoside	93 ± 3	0.2 ± 0.3
scirpusin A	80 ± 9	0.7 ± 0.3
resveratrol	63 ± 6	6 ± 2
piceid	62 ± 6	6 ± 2
ginsenoside A	46 ± 7	10 ± 2
curcumin	45 ± 9	10 ± 2
pterostilbene	35 ± 7	—
piceatannol	25 ± 9	—

regulated along with several other genes.

β-sheets are common structures in the cell [203]. Molecules that disrupt the stability of β-sheets could cause extensive cellular stress, prompting the expression of the unfolded protein response and Nrf-2/ARE modules to restore cellular homeodynamics. Indeed, several polyphenols (chlorogenic, ferulic, and gallic acids, quercetin, rutin, and isoquercetin) have been shown to bind to a range of proteins under physiological ionic conditions: human serum albumin, bovine serum albumin, soy glycinin, and lysozyme [272]. These polyphenols showed greater affinity to α-helices than β-sheets. As polyphenols are predominantly hydrophobic they are most likely to concentrate in membranes where proteins which are α-helix rich interact to maintain cellular homeodynamics (explaining why higher polyphenol concentrations are needed to achieve ATP synthase inhibition when the enzyme is membrane bound instead of in solution).

The physiological concentrations achieved by several polyphenols, most notably resveratrol, can both disrupt protein folding as well as ATP synthesis. One of the more biologically active polyphenols, genistein, could also cause ROS stress. This is accomplished at concentrations low enough to be considered hormetic. There is great interest in discovering the signaling mechanisms whereby this hormetic response is generated. This is with the hope that more potent stimulants can be designed to address specific ailments. There are four problems with this. Firstly, altering protein homeodynamics is far from a specific means to address a problem and secondly, as there does not appear to be any additive effect by administered polyphenols, a side salad rich in quercetin or ECGC rich cup of green tea might supply all the effective polyphenols one needs. Thirdly, the effectiveness of polyphenols may lie in their multipotent ability to disturb several cellular processes at once rather than a specific process, explaining why polyphenol-engineering attempts have largely failed to result in increased lifespan [273]. Lastly, as pointed out by Calabrese et al. [244] many polyphenols are toxic at higher concentrations though they may be beneficial at lower doses. A more potent hormetic could be toxic at much lower concentrations and circumvent the goal of producing a more effective hormetic. This toxic effect is manifest in the papers of Baur et al. [214] and Valenzano et al. [5] where resveratrol-treated groups exhibited a higher mortality rate in early phases of the experiment when compared to age-matched controls. This effect was absent at the lower dose used by Pearson et al. [250].

3.3 Polyphenols and cellular signaling

Polyphenols have been reported to affect several signaling pathways. The most notable is the PI3K/Akt/FoxO pathway but they also effect the activity of JNK, p53, AMPK and mTOR signaling. The subject of polyphenol signaling will be discussed with the purpose of pointing out that none of the individual pathways fully explain the effect polyphenols have on physiology, but that each pathway plays an important role in polyphenol-affected physiology. A serious

study of polyphenol lifespan extension cannot be conducted by only examining one pathway in a petri dish or focusing on one pathway in the animal. The organism must be studied as a whole.

3.3.1 PI3K, Akt, FoxO and sirtuins

The PI3K/Akt/GSK3β signaling cascade is linked to the development of taupathies and Aβ associated neurodegeneration [53, 73]. This same cascade is linked with longevity signaling to the FoxO transcription factors [114], Figure 3.4. This family of transcription factors play roles in development, cell cycle check points, stress response and regulates apoptosis.

Upon expression, FoxO transcription factors move into the nucleus where they remain unless phosphorylated by Akt where upon they are exported from the nucleus into the cytosol [274]. The transcriptionally active acetylated FoxO4a (the functional equivalent of the DAF-16 transcription factor of *C. elegans*) transcribes genes concerned with cell cycle arrest and apoptosis. FoxO4a also suppresses PP2A and PP2B activity as well as allows the transcription of insulin- and insulin-like receptor genes ensuring a negative feedback loop to keep FoxO activity under control [275]. The activation of FoxO transcription factors by resveratrol resensitizes PI3K-Akt [275] (resetting energy-state sensing) signaling among many other functions. Some of these other functions are up-regulating the expression of several cellular antioxidant enzymes (catalase and MnSOD) [276] and the unfolded protein response [277] which includes the upregulation of Hsp70 [276]. The activation of sirtuins (Figure 3.2), supposedly by resveratrol [106], results in the activation of the cell-survival properties of the mammalian FoxO3a (and *C. elegans* ortholog DAF-16) transcription factor [114, 278]. Resveratrol-treatment did restore PKC activity, a negative

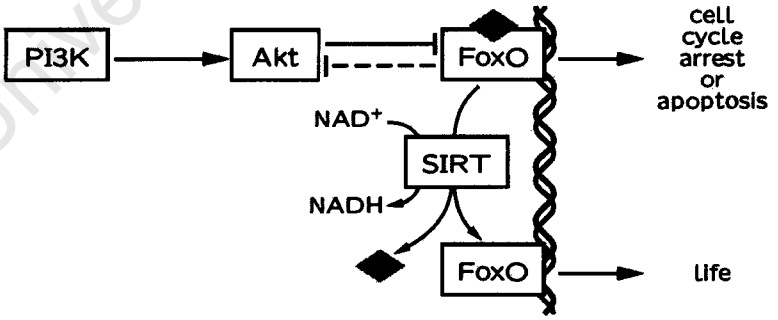

Figure 3.4: The PI3K/Akt/FoxO cascade and life and death decisions. Activated Akt phosphorylates FoxO causing it to dissociate from DNA and be exported from the nucleus. Deacetylation by sirtuin causes it to switch from expressing cell cycle check-point proteins and apoptosis sensitizing factors to the expression of cell survival modules such as the antioxidant response element and Phase II enzymes. Unphosphorylated FoxO transcribes both inhibitors of PP2B (which dephosphorylates Akt) as well as insulin and insulin-like receptors which enable PI3K activation.

regulator of GSK3β, which is dependent on chaperones to orchestrate its activity [1]. The resensitization of the PI3K/Akt pathway may also be instrumental in suppressing aberrant GSK3β activity.

Kaeberlein et al. [279] did not find any evidence of resveratrol activation of Sir2 in three strains of yeast nor any modulation of their lifespan by resveratrol. In vitro assays did demonstrate a substrate-specific activation of sirtuins (Sir2 and SIRT1) by resveratrol but only against the synthetic Fluor de Lys peptide. It was shown that SIRT1 does not normally have a high binding affinity to the Fluor de Lys peptide, but resveratrol improved this binding 8-fold [280]. The call by Kaeberlein et al. [279] to reexamine the putative sirtuin mechanism of longevity has been all but ignored. Instead, this mechanism still enjoys large support [281]. The observation that Sirt1 inhibitors are also neuroprotective have further complicated the issue inspiring Tang [239] to hypothesize that resveratrol may be neuroprotective because it is not a direct activator of Sirt1. Experimental results were recently published indicating that prior evidence that sirtuin over-expression increased lifespan was an artifact caused by not out-breeding the genetically modified experimental animals [282]. In outbred strains of *C. elegans* and *Drosophila* sirtuin over-expression had no effect on lifespan. Tang [239] believes that the AMPK pathway is the means by which resveratrol executes its protective effects. AMPK will be discussed in Section 3.3.2.

The effects of several polyphenols have been reported to be mediated via the PI3K/Akt pathway. Quercetin's lifespan extending effects were shown to be dependent on age-1/daf-2 (the homologs of PI3K and insulin-like growth factor receptor) signaling [283] and that there was a three fold increase in FoxO nuclear localization [222]. Curcumin mediated neuroprotection involved the activation of PI3K and MAPK signaling networks [251]. Whether or not curcumin activated Akt was not reported in that study. EGCG caused the upregulation of several FoxO regulated genes [284] but again no mention was made of Akt activity.

Interestingly, to increase longevity in *C. elegans* DAF-16 activity is only needed in the neuronal cell lineage [32]. Furthermore, lifespan extension via dietary restriction was reliant on a small group of neurons, the amphid neurons, which express insulin/insulin-like growth factor like ligands [285]. This offers the promise that long healthy life can be attained simply by preserving CNS function. This topic will be continued in Section 3.3.2 on AMPK.

Where does this leave the PI3K/Akt/FoxO pathway and sirtuins? Experiments in several model organisms reveal that the proper function of this pathway is vital to long and healthy life. Direct interaction was discovered between SIRT1 and the gene locus encoding presenilin 1 [286]. The increase in presenilin expression by SIRT1 activation resulted in an increase in glycosylated APPα and a decrease in APP fragments. In addition, there was a preservation of neuronal stem cell proliferative capacity in the mouse hippocampus. But when Balducci et al. [171] inhibited γ-secretase there was a reduction in intraneuronal APP/Aβ levels and tau hyperphosphorylation which indicates

that the upregulation of presinilin via increased SIRT1 activity may not be as meaningful as it first appears. Barger et al. [213] report that resveratrol had no effect on the PI3K/Akt/FoxO pathway but the age-related decline in glucose uptake was prevented in their mice. Bastianetto et al. [77] conducted a comprehensive review and report that resveratrol has no effect on the Akt and MAPK pathways. What does this mean? Experiments where SIRT or FoxO signaling has been disrupted only prove one thing: that the removal of SIRT or FoxO has detrimental consequences. Pietsch et al. [283], from their quercetin work, conclude that PI3K/Akt/FoxO signaling was coincidental to lifespan extension and not causal. The attenuation of lifespan and CNS healthspan is dependent on the concerted actions of several pathways working in symphony. As was claimed by Kascer and Burns back in 1979: control is shared among all members of the system [208]. The PI3K/Akt/FoxO pathway and sirtuins have an important share in this control but not a critical one.

3.3.2 Stress signaling

Both JNK and NF-κB are Redox sensitive. Via Redox sensing they are able to regulate cell survival programs. The activity of both are affected by polyphenols and the outcomes are generally beneficial. This section will briefly review the role of JNK and NF-κB in polyphenol protection in relation to the signaling pathways discussed previously and how they relate to AMPK signaling.

The p50 subunit of NF-κB is glutathionylated and the oxidation of the GSH group leads to the inhibition of NF-κB DNA binding [287] as does deacetylation by sirtuin [288]. The significance of this is debatable. NF-κB has a Jekyll and Hyde role in cell physiology. While its activity is associated with inflammation and cell survival functions there is evidence for its malfunction in the immune system being a protagonist in aging-related diseases [105, 289]. Supporting the idea of NF-κB driven inflam-aging, the suppression of NF-κB by resveratrol, curcumin and catechins result in neuroprotection in vitro and in disease model animals [290].

Resveratrol, quercetin [291] and curcumin [292] are known to inhibit the inflammatory response or reduce the cellular activity of NF-κB [293–296]. In the case of microglia NF-κB suppression seems key to neuroprotection [288]. NF-κB levels were reduced in a model of D-galactose induced brain injury when the aged mice were given purple sweet potato color polyphenols [247]. Likewise, NF-κB activity was reduced in another neuroprotective chronic green tea study on CF8BL/6J mice [253]. Conversely, in experiments testing the long term effect of green tea on age-dependent decline in hippocampal signaling there was no difference in NF-κB activation between treated and age matched controls [254]. The lack of NF-κB activity could be the result of the polyphenols preventing the neuronal insult which would ordinarily cause an inflammatory response. This would however also be evidence for NF-κB being inconsequential to neuroprotection. NF-κB plays an important role in the survival response of cells and it may need to be activated by polyphenols

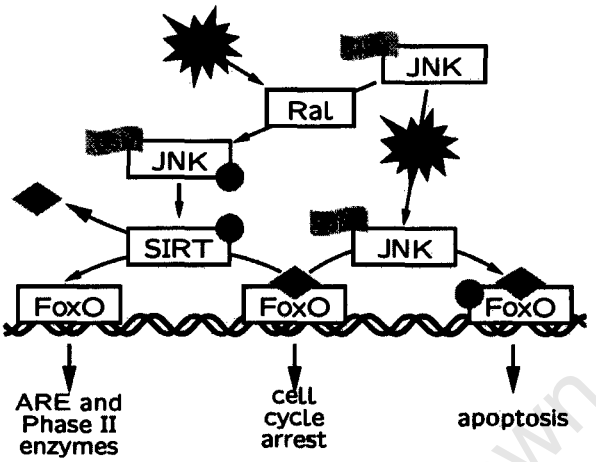

Figure 3.5: The JNK/SIRT/FoxO cascade and Redox switching between life and death. JNK can be activated by ROS in two ways: through the ROS activation of the Ral GTPase or by oxidation of GSH on glutathionylated JNK. Ral phosphorylated JNK activates sirtuins which switch FoxO from cell cycle arrest to cellular repair. Sustained activation of JNK by GSH oxidation causes JNK to phosphorylate FoxO activating apoptosis programs.

in certain cell types within the Hormetic Theory [236].

NF-κB does not function independently. Instead it is entangled in a complicated signaling network involving the PI3K/Akt/FoxO pathway as well as the JNK network and proinflammatory pathways [106]. It is impossible to experimentally determine the affect of NF-κB in polyphenol neuroprotection unless these complimentary pathways are simultaneously assessed.

The combination of FoxO3a and AP-1 activation by JNK puts into operation cell death programs that the additional deacetylation of FoxO3a by sirtuins can turn into cell survival responses [114, 297]. JNK plays a role in this switch from death to life, as illustrated in Figure 3.5. This switching is reviewed by Lam et al. [114]. In brief, JNK can be activated by the small GTPase, Ral. Ral phosphorylates JNK which in turn phosphorylates FoxO4a and SIRT1 (which then deacetylates FoxO3a) switching it from cell cycle arrest/death expression modules to cell survival and repair expression modules [238]. The target of JNK, c-Jun, is acetylated at its C-terminus and its deacetylation enables cell death transcription programs [298]. The acetylation of c-Jun is a response mediated by p300, an acetyltransferase under the control of ERK [299]. If the cell is stressed and energy supplies are low then c-Jun deacetylation may not occur on account of a build-up of NADH and acetyl-CoA (which would simultaneously drive acetylation). JNK is also glutathionylated and the oxidation of GSH results in sustained activity of JNK which then mediates the expression of apoptotic expression modules [300].

Ral is activated by a decline in the ratio of GSH to GSSG [238]. If, under stressful conditions, the dominant role of NF-κB is cell survival and that of

JNK is cell death in response to stress, then under conditions of excess ROS the oxidation of the GSH groups of JNK and NF-κB deactivates the cell survival expression modules controlled by NF-κB while activating the cell death expression modules of JNK. This is a simple means by which the cell can differentiate between mild damage (which can be repaired) and severe irrecoverable damage (where apoptosis would be preferential).

What roles do polyphenols have in JNK signaling? While resveratrol has not been shown to alter Ras-MAPK signaling, it does result in the down-regulation of the small guanine nucleotide exchange factor, Ras-GFR1 which is AP-1 inducible [301] suggesting that resveratrol promotes the survival/repair programs by suppressing AP-1. Recalling that FoxO3a activity can resensitize Akt, Akt can suppress JNK activation through its activation of IκB kinase [106] which would also activate NF-κB. In this model, transient activation of JNK leads to FoxO4a activation which in turn deactivates JNK (should the GSH group be in the reduced form). Further more, several polyphenols, including resveratrol, curcumin and catechins, are known to elevate the levels of GSH [189] and so ensure that JNK is not switched into sustained activation mode.

Genistein (from legumes) has been observed to have a pro-oxidant effect at low concentrations [226]. This pro-oxidant effect started at the concentration of only 2 μM. This effect may be severe enough to lead to a drop in GSH levels and activate the Ral/JNK/SIRT/FoxO3a pathways. Inhibition of ATP synthase [259] or disruption of β-sheet protein folding [270, 271] by resveratrol and other polyphenols could lead to cellular stress culminating in lowered GSH levels as well as the activation of AMPK [239]. Genistein has neuroprotective properties and will be discussed further on.

AMPK is the medium whereby whole body energy status is transmitted from the hormonal messengers to the requisite signaling networks to set in motion the correct transcription modules [302]. In most tissues it is activated by leptin and adiponectin (among other compounds). Both leptin and adiponectin are produced by adipocytes in response to low glucose levels. They activate AMPK which facilitates the merger of GLUT4 transporter-filled endosomes with the cell membrane. AMPK is negatively regulated by tumor necrosis factor-α and insulin. Leptin inhibits AMPK activation in the brain where adiponectin and ghrelin activate it. AMPK activation inhibits fatty acid synthesis and promotes β-oxidation. It also facilitates the transcription of the ARE, Phase II enzymes and mitogensis [239]. This response is evolutionary conserved from *C. elegans* to humans [93].

AMPK is also activated in response to increasing concentrations of AMP, Figure 3.6 [93, 239, 302]. Its activation by AMP allows more glucose to enter the cell as well as promote β-oxidation to correct the ATP deficit. AMPK also promotes gluconeogenesis, suppressing GSK3β activity. Insulin secretion in response to high blood glucose would deactivate AMPK via PI3K/Akt signaling and promote fatty acid synthesis, completing the negative feed back loop. AMPK negatively regulates the mTOR signaling cascade [267]. The mTOR signaling cascade regulates macro-autophagy and is activated in response to

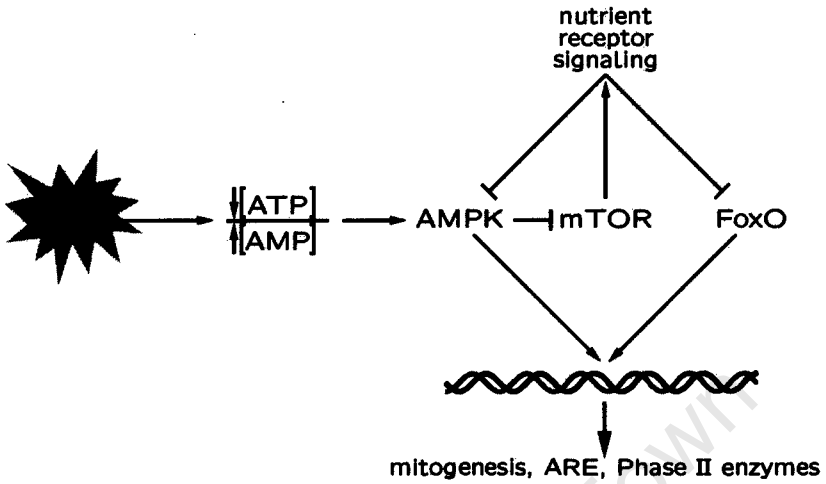

Figure 3.6: AMPK facilitation of lifespan extension through the depletion of ATP levels, brought on by cellular stress or nutrient deprivation. Activated AMPK inhibits mTOR which would ordinarily activate Akt to deactivate FoxO. The lack of nutrients and presence of leptin lead to FoxO activation through Akt inhibition. AMPK activation leads to the expression of mitogenic, ARE and phase II enzyme modules to extend lifespan.

nutrient supply levels (particularly essential amino acids such as methionine) [303]. While adequate nutrient levels are maintained mTOR is active and suppresses autophagy. mTOR signaling activates Akt and Akt activates mTOR to enforce cell growth during periods of adequate nutrient supply.

The mTOR pathway is emerging as the central pathway pertaining to life- and healthspan [94] and successfully explains the observations previously attributed to the inadequate Free Radical Theory of Aging. Inhibition of mTOR has resulted in lifespan extension of several species from *C. elegans* to mice [304]. Inhibition results in increased macro-autophagy and nutrient recycling. As mTOR inhibition and AMPK activation suppress protein synthesis, stimulate mitogensis and autophagy, activation of AMPK would address chronic ER stress and the resulting misfolding of proteins which culminate in APP misprocessing and neurodegeneration.

It is worth recalling from Chapter 2 that an impairment of autophagy results in an increase of PS-1 expression and γ-secretase activity [117]. Resveratrol, at 12.5 μM and above, has been found to suppress autophagy via S6K (the target of mTOR) [305]. This is contrary to what is expected of the polyphenol but this resveratrol dose is several times greater than what is shown to be beneficial in vitro. Using a much lower dose of 0.1–1 μM (i.e. physiological concentrations) resveratrol was shown to be cardioprotective by means of autophagy [306]. At 5 μM resveratrol was toxic to endothelial progenitor cells as well as several other healthy cell types while lower doses were protective [244]. At physiological concentrations resveratrol is able to activate AMPK and sup-

press S6K and mTOR activity to stimulate macro-autophagy and mitogenesis in accordance with the Theory of Hormesis.

Leptin has been shown to regulate tau phosphporylation and suppress Aβ production [307]. Several polyphenols have been observed to increase AMPK activity, these are EGCG, ginsenoside, resveratrol and quercetin [267]. Resveratrol has been shown to stimulate AMPK activity and impede Aβ formation at the low cellular concentration of 1.7 nmol/g wet weight brain material [246]. As discussed in Section 3.2 (page 35), green tea at similarly low concentrations was also able to invoke neuroprotective effects. EGCG has been reported to facilitate glucose uptake via an AMPK dependent mechanism. While leptin stimulates AMPK activity in most tissues, in the hypothalamus leptin suppresses AMPK activity in the periventricular and arcuate nuclei [302]. This causes appetite suppression, explaining the appetite suppressive properties of green tea. Dietary restriction was mediated via the nutrient sensing amphid nuclei in the *C. elegans* brain [285] and white adipose tissue lipolysis is under direct control by the sympathetic nervous system [308]. It is to tempting not to speculate that there may be a link between whole-body nutrient sensing and lifespan in vertebrates as there is in *C. elegans*. Quercetin has been demonstrated to reduce the expression of corticotropin-releasing factor and plasma levels of adrenocorticotropic hormone in Wistar rats administered 10 mg quercetin per kilogram [309]. Under fasting conditions this would inhibit cortisol production and glucogon cannot exert a gluconeogenic effect without cortisol [310]. Glucogon and cortisol also increase protein catabolism, which increases plasma levels of amino acids and free fatty acids. Together they act to counter a nutrient and fuel shortage which would suppress AMPK activation and mTOR inhibition (completing a feedback loop). Polyphenols can create physiological conditions which favour AMPK activation and mTOR inhibition. A refreshing cup of quercetin rich black tea between meals may be all that is needed to cause enough physiological stress to trigger a hormetic response via AMPK. There are several studies, reviewed by Ramassamy [293] and Mukhtar & Ahmad [294], linking black tea with increased lifespan and reduced probability of dementia.

AMPK has been observed to be dysregulated in AD where it phosphorylates tau, causing tangles [86]. AMPK is activated in pretangle neurons suggesting that there is a chronic energy deficiency leading up to tangle formation. This fits well with the Catabolic Insufficiency Theory of Terman [198]. This also suggests that polyphenol action via AMPK must be evoked before chronic energy insufficiency and metabolic collapse set in. This may not be strictly true in the case of neurodegenerative-aging where massive neuron loss is absent. That many polyphenols have been observed to reverse cognitive impairments in the aged suggests that the neuroprotective effects of polyphenols cannot be mediated through AMPK and mTOR alone.

The kinase p38 MAPK has important roles in cell survival [311]. Its role in polyphenol neuroprotection is still ambiguous. It has been explored with respect to cardiovascular protection but with conflicting results [244]: some

studies find an affect while others do not. An astrocyte study found that polyphenols increased p38 activity but this was in cells in culture and at a 100 μM resveratrol concentration [312] which is toxic to many cell types [244]. At 100 μM quercetin was shown not to alter p38 activity but this was in experiments designed to cause cell death [313]. A decline in p38 underlies immunosenescence in *C. elegans* [314] and increased lifespan is correlated with improved immunocompetence [315]. As polyphenols exert many beneficial effects, particularly in lifespan experiments, it would be expected to see an age-associated aberration in p38 activity which is restored by polyphenol-treatment.

3.3.3 Phytoestrogen potential

Several years ago phytoestrogens (such as genistein) and estrogen mimics were a popular research paradigm. There was great scientific interest and public alarm about chemicals in foods, plastics and drinking water which could have an estrogen-like effect on our biology, causing everything from the alleged sudden upsurge in male infertility to breast cancer. Surprisingly, few have taken the time to point out that the chemical structure of many polyphenols (and thioflavin-T) share a resemblance with that of the two steroids implicated in the aging process: estrogen and DHEA (Figure 3.1, page 31).

The decline in DHEA with age has been made into *the* explanation for aging, which one set of authors term "DHEA deficiency syndrome" [316]. The decline in DHEA levels has been implicated in a plethora of age-related diseases. Most notably, the decline in DHEA and its sulfate, DHEAS, are linked to aging-related and disease-related immune system malfunction [317]. DHEA is also linked to several neurological illnesses for which supplementation has proven a reliable treatment [318]. Likewise, the decline in estrogen levels in post menopausal women has been reported as the primary risk factor for dementia in women [319] and estrogen treatment has been beneficial in decreasing this risk [320]. Could polyphenols be acting as DHEA or estrogen substitutes? To properly explore this question we must remember that DHEA can be converted to estrogen in a three step processes catalyzed by 3β-hydroxysteroid dehydrogenase/isomerase, 17 ketosteroid reductase and P450 aromatase. All three enzymes are expressed in the CNS [321–323], chiefly the glia. DHEA may never reach neurons but its metabolites, particularly estrogen, may [324].

There is evidence that resveratrol can act as a mixed agonist/antagonist of the estrogen receptors α and β [325, 326] as well as bind to the androgen receptor [327], as can EGCG with a IC_{50} of 0.4 μM [328]. Resveratrol inhibited estrogen receptor activity at only 0.1 mM [329], well within the range of the biological concentration reported by Vingtdeux et al. [86]. Resveratrol induced stress resistance and MnSOD upregulation via estrogen receptor-β activation [330]. Blocking estrogen receptor-β activation prevented this effect while blocking estrogen receptor-α activation had no effect. Also, via the estrogen receptor, resveratrol administration to rats (30 mg/kg) caused a decrease in p38 MAPK

activity and an increase in HO-1 expression levels, protecting the rats against the effects of intestinal injury after trauma-hemorrhage [331]. Both MnSOD and HO-1 upregulation are a response common to most polyphenols. Estrogen has also been shown to induce the expression of HSPs in brain arteries, glia and neurons the same way as polyphenols do [332].

It is thus unsurprising that specific binding sites have been observed for both resveratrol and EGCG (as well as other polyphenols) in both the skin and the brain [333, 334]. Resveratrol displayed a K_i of 102 nM and EGCG a K_i of 25–45 nM. EGCG has been observed to up-regulate ADAM 10 via ERα [335]. This EGCG upregulation of ADAM 10 promoted non-amyloidogenic processing of APP. Genistein prevented Aβ induced inflammation in cultured astrocytes [336]. Estrogen had the same effect and both caused an increase in peroxisome proliferator activated receptor-γ expression [336]. The anti-inflammatory effect of estrogen in glial cells is mediated by RACK1 [337], the same PKC scaffolding protein involved in DHEA decline related memory loss [75] and is necessary for the neuroprotective effect of resveratrol [338] and EGCG [339]. Quercetin has also been reported to exert effects via estrogen receptor-α [340].

Han et al. [333] found that the resveratrol binding sites were widespread in the rat brain and enriched in the choriod plexus and subfornical organ. The choroid plexus, as well as being enriched for resveratrol binding sites, is also enriched for leptin receptors [341] (see section 3.3.2, page 46). Plasticity in the arcuate nucleus is determined by neurosteroid neuro-glial interaction [342]. This neuro-glia plasticity is dependent on polysialic acid rich NCAM expression which dietary restriction preserves into old age [166]. Han et al. [333] also point out that the choroid plexus secretes transthyretin[8] which is believed to play a neuroprotective role [343]. Watanabe et al. [344] has shown that *Gingko biloba* extracts were neuroprotective and up-regulated transthyretin mRNA. Estrogen has been shown to be neuroprotective and to exert this neuroprotection via glia [345, 346], such as the ependyma which line the choroid plexus. Several other studies implicate glia in playing a role in polyphenol-induced neuroprotection [248, 251, 347–350] and dietary restriction [166].

DHEA, its biological functions and its binding partners are reviewed by Webb et al. [351]. As well as binding to estrogen receptors (activating them), it also leads to the activation of peroxisome proliferator activated receptor-α, though apparently not by direct binding. Webb et al. [351] report that there are dedicated DHEA receptors in the brain, heart and other tissues; and that DHEA, at concentrations ranging from 0.010–10 μM, activated these membrane receptors and triggered kinase signaling cascades. Whether polyphenols can bind to these DHEA receptors and activate them remains to be determined. What is interesting is that DHEA is implicated in many aging-related diseases. DHEA and polyphenols both partake in a myriad of signaling cascades.

Another class of compounds, triterpenoids (Figure 3.1, page 31), are also

[8] Transthyretin binds and ferries thyroxin through the CNS and thus also plays a role in CNS nutrient sensing.

worth considering in this review. The physiological effects of the triterpenoids oleanolic and ursolic acid are reviewed by [352]. These compounds can be extracted from the waxy cuticle of fruits of the genus *Vaccinium* (e.g. blueberries) [353] and grapes [354]. Ursolic acid has been shown to protect neurons against excitotoxicity via the NMDA receptor [355]. The same has been reported of curcumin [356], EGCG [357] and resveratrol [358]. These compounds have been shown to exert the same effect on cancer growth and vascular function (the subject of the next Section) as polyphenols.

The multipotency of neuroactive steroids and polyphenols with regards to cellular signaling and physiological outcomes, together with the conserved structure, suggest that polyphenols could exert many of their effects by directly modulating steroid associated signaling cascades. As regards estrogen signaling, they can modulate estrogen signaling at concentrations well within the physiological concentrations achieved by polyphenols.

Studying the effects of resveratrol and other polyphenols on signaling cascades in *Nothobranchius* would be difficult. While identifying antibodies to active/inactive forms of the various kinases and transcription factors may be possible this would be a time consuming and expensive research direction and falls outside the scope of this study. Nevertheless, the body of research already suggests that their should be an upregulation in certain proteins such as protein chaperones (Hsp70) and proteins associated with synaptic plasticity (such as L1 which can be detected by the E587 antibody). If enough well characterized proteins can be identified it may be possible to nominate specific signaling cascades for further investigation. An important consideration to keep in mind is that the polyphenols may exert different affects not only in different cell types but cells of the same type in different locations may respond differently. Merely dissecting out a brain and extracting the proteins to develop on Western Blots may not be sufficient to detect the small changes in activity which may occur; and small changes in activity can have large effects [206]. The use of microarrays could also be useful but one cannot simply equate a change in expression with a change in protein concentration nor infer a change in the flux through a particular pathway.

The current data does suggest that glia would be affected by polyphenol-treatment. This should be apparent both by means of microscopy (assessing glial numbers and morphology) and by measuring the levels of GFAP and its isoforms [26].

3.4 Vascular health and neurogensis

The content of this section goes beyond the scope of the present study and is presented in brief because no review of the mechanisms of polyphenol neuroprotection would be complete without it.

Resveratrol and quercetin have been shown to cause changes in gene expression in vascular endothelial cells at concentrations as low as 0.1 μM [245]

which correlates well with resveratrol concentrations achieved in the rat brain [246] and is orders of magnitude below that achieved in human circulation [359]. Berry polyphenols have also been reported to reach plasma concentrations well above 0.1 μM [360]. The effects of polyphenols on vascular function and how these relate to vascular diseases (such as stroke and dementia) are reviewed by Ghosh & Scheepens [361] and West [362].

EGCG fed to aged guinea pigs at 30 mg/kg food/day for 28 days caused an improvement in vascular tone and sensitivity in addition to a decrease in erythrocyte malondialdehyde content and aggregation together with an improvement in erythrocyte deformability and viscosity [363]. This resulted in better oxygen supply and exchange rates. 15 days of high-polyphenol content dark chocolate (which is rich in chalcones and catechins) caused a reduction in blood pressure in glucose-intolerant hypertensive patients (as well as improved insulin sensitivity) [364]. Cranberry juice administered to patients with coronary artery disease resulted in a decrease in arterial stiffness [365]. Blueberries were also shown to improve vascular sensitivity [366] and tone [269] in both physiologically normal Sprague-Dawley and spontaneously hypertensive rats [367]. In other experiments on spontaneously hypertensive rats resveratrol prevented endothelial NOS uncoupling and the development of hypertension [89]. This uncoupling of NOS was attributed to S6K hyperactivity in endothelial cells and resveratrol or rapamycin treatment inhibited this hyperactivity [88]. Genistein improved NO bioavailability in aged Wistar rats [255] suggesting NO availability as one means by which polyphenols improve vascular function. This hypothesis is reviewed by Schewe et al. [368]. EGCG was shown to act through AMPK to inhibit the mTOR/S6K pathway [94, 267, 369].

Grape wine procyanidins have been linked to vascular health [370] and have been experimentally shown to improve the endothelium-dependent dilation of rat cerebral arterioles [371]. Other research shows that grape polyphenols do not affect vascular function in healthy men [372] implying that polyphenols do not disturb healthy physiological function. 45 mg/kg mouse/day resveratrol was able to regulate pathological angiogensis in mice and this was independent of sirtuin activity [373]. While blueberry supplementation did not affect vascularization of rat neural transplants it did improve graft growth and the efficiency of the blood-brain barrier [374] suggesting that there is more to the effects of polyphenols on the vasculature than improving vascular tone.

Ghosh & Scheepens [361] discusses the link between proper vascular function and stem cell maintenance. Resveratrol has been reported to reduce endothelial progenitor cell senescence [375] and rats fed resveratrol showed increased neurogensis [286]. Compound P7C3 has been shown to be proneurogenic as well as neuroprotective [376]. Interestingly, it also has a polyphenol-like structure and was active at very low concentrations. No data is available pertaining to how it affects the vascular system.

Whether polyphenols are having a direct effect on quiescent stem cells is yet to be proven. To achieve an over all pro-proliferative effect in culture 10

to 25 μM resveratrol was necessary [375]. Stem cells are sensitive to oxygen supply and nutrient availability and their neurological niches are tightly associated with blood supply [377]. Regular exercise improves CNS blood flow and oxygen supply and has also been shown to increase neurogenesis [378]. Furthermore, alleles positively associated with cardiovascular health are more frequent in long-lived human populations [379, 380] suggesting that maintaining vascular health may be all that is needed to ensure health into old age. Polyphenols have been demonstrated to improve vascular function. This provides a simple mechanism whereby they can benefit multiple systems at low doses and increase healthspan.

3.5 Conclusions

The Direct Antioxidant Hypothesis of polyphenol action, while not impossible under certain circumstances, fails to explain the multipotent effects of polyphenols. Furthermore, given the simplicity of the phytoestrogen activity and its affect on the vascular system at physiological polyphenol doses the Direct Antioxidant Hypothesis is also unnecessary. The bioactive and structural similarities between polyphenols and steroids is something which cannot be ignored. Polyphenols certainly exert effects via estrogen-mimic activities. The concept of polyphenols acting as hormetics which prime the organism's stress responses is a viable general explanation of the diverse actions of polyphenols.

As mentioned in the above section exercise (which is also a hormetic intervention) protects the cardiovascular system as well as being neuroprotective and neurogenerative. There is evidence for polyphenols not only remediating vascular problems associated with disease and old age, but that they act via signaling pathways implicated in lifespan regulation as were discussed in Section 3.3. Evidence for polyphenols binding to specific sites of receptors as well as interrupting β-sheets has also been discussed suggesting that polyphenols could trigger stress reactions by upsetting signaling cascades or by initiating them. Returning to hormesis, the inhibition of ATP synthase could be the trigger needed to activate AMPK whose activity is linked to the beneficial outcomes of polyphenol-treatment. Certainly the inhibition of ATPases would cause chaos in the cell.

As the same polyphenol can have multiple effects there cannot be one mechanism of polyphenol neuroprotection. As natural products, such a blueberries, contain multiple polyphenols there can be many different polyphenols affecting multiple pathways which can work synergistically. Many of the pathways converge onto common end effectors with common outcomes. While many individual polyphenols may have overlapping effects there is evidence that different polyphenol mixes can have different effects [258] which together can effect a common beneficial outcome. Joseph et al. [258] suggest that the naturally derived mix of polyphenols are more effective than the individual components.

This multiplicity of outcomes and possible mechanisms complicate re-

search. In simplifying the system to a single polyphenol acting on a single cell type or even single protein it is inevitable that incorrect or misleading conclusions will be drawn. While high doses are needed to elicit beneficial effects in culture much smaller doses are needed to elicit beneficial effects in situ (such as on the vascular system) which can have beneficial knock-on effects which are missed in reductionist experimental methods. What is more, reductionist methodologies neglect that these polyphenols are extensively metabolized in situ and mostly absorbed as conjugates [359]. As such, the beneficial effects can be missed in experiments using the basic compound when the beneficial effects are caused by or enhanced by the conjugates. There is evidence that glucoside and other conjugated stilbenes are more effective than the unconjugated analogues [221].

Only whole-animal experiments with an animal exposed to healthspan-risk and low levels of polyphenols in its normal diet, combined with a broad analysis of the whole organism, can accurately determine the efficacy of any single polyphenol. While such a methodology may preclude ultimate explanation of polyphenol action it would at least present an accurate reflection of the potency of the polyphenol or polyphenol mixture which reductionist methods cannot deliver.

The current research into polyphenol neuroprotection allows for the generation of several hypotheses which can be assayed using the antibodies introduced in Chapter 1. These have been mentioned in the course of this chapter. These hypotheses are that resveratrol would preserve healthy neurons into old age while eliminating degenerate neurons. This can be assayed using the SMI31 antibody. Resveratrol should cause the retention of proteins associated with cognitive function into old age. One such protein is L1 which can be monitored using the E587 antiserum. The literature also suggests that glial function should be maintained into old age. Using the anti-TNR and GFAP antibodies it is possible to quantify the numbers of astroglia and PNNs and their morphology. Assuming that gliosis is indeed detrimental then it would be expected for resveratrol-treatment to prevent gliosis. It is also expected that there should be a preservation of protein processing and homeodynamics. This can be assayed using GFAP antibodies as by Sloane et al. [101] and Korolainen et al. [381].

Chapter 4

Antibody markers for studying neurodegeneration in the *Nothobranchius* central nervous system

> And I heard, as it were the noise of thunder,
> one of the four beasts saying, Come and see.
> And I saw,
> And behold...
>
> *The man comes around*, Johnny Cash

This chapter was published in the Journal of Cytology & Histology, 2:1000120, 2011, reference [382]. The abstract of the article is not included here.

4.1 Introduction

Fish of the genus *Nothobranchius*, Peters, 1844 have a naturally short lifespan in which they develop several neurological biomarkers of aging [3]. Due to its short average lifespan of eight weeks (compared to three to five years for other vertebrate models) *Nothobranchius furzeri* is an excellent model organism for aging research. The aging of *N. furzeri* Jubb, 1971 progressed with an accumulation of lipofuscin and senescence associated β-galactosidase expression [3, 10] as well as a decline in operant learning and muscle strength which were correlated with neurodegeneration [5, 6, 10]. These age-related phenomena were retarded by resveratrol-treatment [5]. Further research of the neuroprotective effect of resveratrol and degeneration of the *Nothobranchius* CNS are

hampered by the lack of cell-type specific antibodies and other cellular markers of degenerative processes. Such markers are also needed to render results obtained in *Nothobranchius* comparable to other organisms for the elucidation of general mechanisms of aging and neuroprotection.

For our study frozen sections of *N. guentheri* were prepared on which to test the antibodies and lectin. We focused our research on the visual system as this is well characterized in fish and was the focus of Valenzano et al. [5]. We assembled a toolbox of markers to study the aging of the *Nothobranchius* CNS by testing CNS markers of development, regeneration and degeneration which have been used on other species. Of ten antibodies tested, the five mentioned below displayed useful reactivity in *N. guentheri*.

The SMI31 antibody recognizes phosphorylated neurofilament protein in neurons, axons, dendrites and neurofibrillary tangles (NFTs) in sections in a diverse array of species. Its accumulation in degenerate neurons is well documented [66, 67]. Glial fibrillary acid protein (GFAP), expressed by astroglia, is upregulated following CNS injury and in the process of neurodegeneration [119]. This pathological upregulation is typical of several model organisms making the availability of a GFAP antibody important to *Nothobranchius* aging research.

L1 is a glycoprotein neural recognition molecule of the CAM-immunoglobin superfamily related to NCAM [158] which has evolved from a family of evolutionary well conserved proteins [383]. It is expressed by astrocytes, oligodendrocytes and growing axons in zebrafish, and is involved in development, regeneration, plasticity and maintaining synaptic contact[123, 158, 163, 383]. It has also been implicated in neurodegeneration through the work of Strekova et al. [47].

Tenascin-R (TNR) is a matrix glycoprotein expressed by oligodendrocytes and is implicated in CNS regeneration and axonal path-finding [123, 384]. It has been reported to act as a barrier to microglial migration in tissue culture experiments [385] and plays what is thought to be a neuroprotective role. However, no such microglial repulsion effect was observed in the lizard species *Gallotia galloti* [384]. TNR is associated with lipid rafts where they form a scaffold for signaling proteins such as integrins [148]. Disruption of integrin signaling is linked with impaired neurogenesis [112, 386] and inhibition of apoptosis of degenerate neurons [118]. TNR appears to be linked to many facets of CNS development, maintenance and degeneration (as well as regeneration) but is largely unexplored in these regards.

Microglia are involved in CNS inflammation, after insult, and in the course of neurodegeneration [105, 119, 291]. Kim et al. [27] demonstrated an increase in microglial proliferation in mice in the course of normal aging and after CNS insult, as well as a relative decrease in aging associated proliferation with calorie restriction, using BS-I Isolectin B4 (also called GS-I isolectin B4). The role of microglia in degeneration is still disputed and it would be useful to know if and how resveratrol and other anti-aging interventions affect them during the course of aging. There is evidence that resveratrol exerts a neuroprotective

role in vitro by inhibiting neuroinflammation [291, 387]. The availability of a *Nothobranchius* microglial marker would enable us to test this hypothesis in situ using *Nothobranchius*.

Immunohistochemistry studies on sections show that these cellular probes reliably label specific cell types in the *Nothobranchius* CNS. This was supported by Western Blots which yielded similar banding patterns to other species using the aforementioned antibodies. These results enable research at the cellular level into neurodegeneration and resveratrol induced neuroprotection in *Nothobranchius*.

4.2 Methods and materials

4.2.1 Captive maintenance of *N. guentheri*

N. guentheri were obtained from Mr. O. Schmidt of Bishops Court, Cape Town, South Africa and maintained as per *N. furzeri* [388]. Fish were fed twice per day for six days and fasted one day per week. A 50% water change was performed weekly. Water for the water changes was prepared before the time using 15 g iodated coarse salt, 2 g $MgSO_4$, and 2 g $KHCO_3$ per 20 L and then filtered over limestone to compensate for the soft municipal tap water and its unstable pH. Fish were maintained in accordance with ethical standards of animal care.

4.2.2 Buffers

All dry chemicals, unless otherwise noted, were obtained from Merck.

The protein extraction buffer (pH 7.2) was composed of 0.1 M TRIS, 1% Nonidet P-40 substitute (Sigma, 74385), 0.01% SDS, 1 µg/mL Aprotinin (Roche, 10236624001) and 0.1 µM PMSF (Sigma P7626) (from a 0.1 M stock prepared in isopropanol). The buffer was chilled to 4 °C before use.

Phosphate buffed saline (PBS) solution consisted of 140 mM $NaC\ell$, 2.7 mM $KC\ell$, 8.8 mM Na_2HPO_4 and 1.47 mM KH_2PO_4 (pH 7.4). For Western Blots 500 µL of Tween (Sigma P1379) was added per L to produce the PBS-T. A TRIS buffered saline buffer (TBS) was employed for microglial staining with isolectin: 50 mM TRIS, 150 mM $NaC\ell$, 20 mM $MgC\ell$ and 10 mM $CaC\ell_2$ (pH 7.4). Blocking solution consisted of 1% BSA (Roche, 735078) in PBS or TBS. A 5% milk solution in PBS was used as blocking solution for Western Blots.

SDS-PAGE gels were prepared as per Current Protocols [389].

Tank buffer for SDS-PAGE was made up of 3 g TRIS together with 14.4 g glycine and 10 mL 10% SDS to 1 L with mQH_2O. Transfer buffer was composed of 44 mM TRIS, 182 mM glycine and 200 mL methanol diluted to 1 L with mQH_2O. 5× loading dye was prepared from 4 mL 10% SDS mixed together with 2 mL 100% glycerol, 1 mL β-mercaptoethanol, 2.5 mL 0.5 M TRIS (pH 6.8) and 0.003 g bromophenol blue and made up to 10 mL with mQH_2O.

Anti-fade mowiol mounting medium was prepared by adding 2.4 g mowiol (Farbwerker Hoescht, Frankfurt Germany) to 6 mL glycerol, left to stir until completely dissolved whereafter 6 mL mQH_2O was added. To this, 12 mL 0.2 M TRIS (pH 8.5) was added. The solution was incubated for 1 hour at 50 °C and then centrifuged at 12 000 ×g for five minutes. The supernatant was collected and stored at -20 °C. For use, an aliquot was thawed to room temperature and a spatula tip of n-propyl gallate (Sigma, P3130) was added, the aliquot vigorously shaken, left to stand overnight at 4 °C and then centrifuged at 12 000 ×g for five minutes. The anti-fade mowiol was stored at 4 °C.

4.2.3 Dissection and preparation of tissue samples

Fish were sacrificed and the tissue dissected in cold PBS as discussed in [5]. The lenses were removed following which the cranial bones were pried apart and the brain (with eyes attached) placed into 4 °C PBS and then into tissue freezing medium (Jung, 020108926) and left to stand on ice for 30 minutes to dehydrate the brain prior to freezing at -80 °C.

For protein extraction, the eyes were severed from the optic nerve and the spinal cord severed from the brain below the cranial nerves and then placed into an eppendorf test tube containing 200 μL protein extraction buffer. The tissue was homogenized and then centrifuged and the debris discarded. Protein samples were aliquoted and stored at -80 °C.

4.2.4 Histochemical staining

For wax mounting and sectioning whole fish were fixed in Bouin's Solution [390] and sectioned at 5 μm. Sections were stained with Kluver & Barrera Luxol Fast Blue/Cresyl Violet. All techniques, fixatives and stains prepared as in Bancroft & Gamble [391].

4.2.5 Immunohistochemistry of brain sections

Frozen brains with attached eyes were sectioned at 20 μm (for confocal analysis) at -20 °C in a cryostat and sections[1] fixed to APTES coated slides.

Sections were permeabilized in -20 °C methanol for 10 minutes and then given three washes in PBS. Sections where then incubated for one hour in blocking solution and then overnight at 4 °C in blocking solution with primary antibodies[2]. Antibody dilutions are summarized in Table 4.1. After incubation with primaries, the sections were washed three times in PBS and then incubated for 90 minutes at room temperature in the dark with anti-rabbit

[1] Transverse sections were cut through the ON and OT. Due to difficulty in orientating the small brain in tissue freezing medium and it shifting during freezing this ideal tissue orientation was rarely obtained.

[2] As negative controls sections were incubated with primary excluding secondary and without primary but including secondary. No-unspecific binding was observed with respect to the secondaries (data not shown). Preabsorption of the primary with the antigen was not feasible on account of budgetary constrains.

Alexa 488 (Molecular Probes, Invitrogen) and anti-mouse Cy3 (Jackson Immuno Research) (each diluted 1:1500). After secondary incubation, sections were washed in PBS and then mounted in anti-fade mowiol.

For biotinylated lectin staining, endogenous biotin was blocked for one hour at room temperature with DAKO Vector-Stain kit avidin-DH (Vectastain, PIC6100) added to TBS with 1% BSA according to the manufacturers specifications whereafter the slides were rinsed in TBS and incubated in 0.1 mg/mL biotin (Sigma, B4501) for 15 minutes and then washed in TBS. After washing, the BS-I isolectin B4 (Sigma, L3140) was incubated overnight on the sections at 1:60 dilution of 1 mg/mL isolectin solution into a TBS blocking solution of 0.1 mg/mL biotin and 1% BSA. After incubation, the sections were washed and incubated under streptavidin-Alexa 488 (Sigma) diluted 1:500 in TBS blocking solution for 90 minutes; and then washed and incubated under 0.5 μg/mL DAPI for 10 minutes before being washed and mounted in anti-fade mowiol.

4.2.6 SDS-PAGE and western blotting

Protein determinations of homogenates were done using the Pierce BCA protein assay (Pierce, 23225). Samples were read at 695 nm on a Kayto RT-2100C microplate reader.

Protein samples were incubated at 95°C in loading dye for two minutes. Samples which were to be incubated with E587, anti-TNR were incubated at 95 °C in a loading dye without β-mercaptoethanol. For the E587, TNR and

Table 4.1: Antibodies used in this study along with dilutions and reactivity results. Antibodies which were not reactive on IHC sections were not tested against Western Blots.

Antibody	Immunohistochemistry		Western Blots	
	dilution	reactivity	dilution	reactivity
E578 anti-L1[†]	1 : 2000	yes	1 : 2000	yes
GA-5 mab antiGFAP (Sigma G6171)	1 : 2000	yes	1 : 2000	yes
rabbit anti-bovine GFAP (DAKO Z0334)	1 : 2000	yes	1 : 2000	yes
SMI31(Covance SMI-310R)	1 : 400	yes	1 : 1000	yes
mab anti-rat TNR[‡]	1 : 400	yes	1 : 400	yes
rabbit anti-mouse S100 (Sigma S2644)	1 : 1000	inconsistent	1 : 1000	no
anti-Integrin β1 (Sigma SAB4501582)	1 : 200	no	N/A	N/A
rat anti-mouse MBP[§]	1 : 20	no	N/A	N/A
anti-zebrafish TAG[¶]	1 : 200	no	N/A	N/A
anti-mouse β-tubulin (Covance PRB-435P)	1 : 1000	no	N/A	N/A

[†] Gift from C. Stuermer, Konstanz Germany.
[‡] Gift from P. Persheva, Bonn Germany.
[§] Gift from C. Linington, Munich Germany.
[¶] Product from Lang et al. [123].

SMI31 blots, 20 μg protein was loaded onto a 7.5% SDS-PAGE gel (acrylamide, Sigma, A3574). For the GFAP blots, 5 μg protein was loaded onto 12% SDS-PAGE gels. pQGold IV protein marker (pQLab, 27-2116) was used. Electrophoresed protein was transferred to Amersham Hybond-ECL (General Electric) paper using transfer buffer at 100 V for one hour.

The blot was blocked for one hour in 5% commercial milk powder in PBS-T buffer whereafter the primary antibody was added together with 5% milk in PBS-T and incubated overnight at 4°C. Antibody dilutions are summarized in Table 4.1. The blot was washed four times in PBS-T and then the secondary antibodies were added: goat anti-rabbit-HRP (Biorad, 170-6515) and goat anti-mouse-HRP (Biorad, 170-6516) at 1:1500 dilution for 60 minutes. For autoradiograph visualization the blot was washed four times in PBS-T and then SuperSignal West Pico Chemiluminescent reagent (Pierce, 34080) was applied. Alternatively the blots were developed using a metal intensified DAB protocol based on Adams [392].

Sizes were calculated using a linear regression of a graph of molecular mass (kDa) vs the log of the migration distance (in millimeters) through the gel. The largest marker band was 170 kDa and the smallest 5 kDa.

4.2.7 Microscopy

Images were obtained using a Zeiss Confocal microscope (Jena, Germany). Images are representative of several specimens and were edited for publication using Adobe Photoshop CS2 v9.0.2.

4.3 Results and discussion

4.3.1 Results of SMI31 and anti-GFAP labeling

Figure 4.1 shows a luxul fast blue/cresyl violet stain of an 5 μm optic tectum (OT) section of *N. guentheri* and serves as reference for the below text[3].

It is expected that the SMI31 and rabbit anti-GFAP antibodies would label nerve fibers and astroglial-like structures (radial glia in particular as is typical for fish) respectively.

Figure 4.2 shows a section through the optic nerve (ON). The nerve is filled with SMI31 immunoreactive nerve fibers as well as large anti-GFAP immunoreactive glial processes. Signals do not colocalize. Figure 4.3A–G show a strong anti-GFAP immunoreactive layer corresponding with the stratum zonale (SZ, see Figure 4.1 in reference to OT layers) which is lined with radial glial cell bodies. This layer stretches into the stratum opticum (SO). There is also strong anti-GFAP reactivity in the stratum griseum periventriculare (SGPV) as would be expected for radial glia. The SMI31 signal is seen in five discrete zones: S1 the stratum griseum superficiale (SGS) and SO; S2 the

[3]The nomenclature for the layers is obtained from [393].

upper stratum griseum intermediale (uSGI); S3 the stratum griseum intermediale (SGI); S4 the stratum album intermediale (SAI); and S5 the SGPV which are composed mostly of axon fibers and dendritic projections as shown for goldfish [394]. SMI31 and anti-GFAP signal colocalize in cage-like structures in the SGS which are enlarged in Figures 4.3D–G. SMI31 signal was observed in both one week old fry (data not shown) and aged fish. In *Nothobranchius* species the epitope targeted by SMI31 may be present on neurofilament regardless of age and degenerative state as has been demonstrated by Lee et al. [395] in rats.

The SMI31 Western Blot(Figure 4.4) showed bands in the rat lane of approximately 226 and 155 kDa which corresponds with the predicted masses of the phosphorylated heavy and medium isoforms [66, 396]. This antibody produces a single band of ≈120 kDa in the zebrafish lane. Two bands are visible in the *N. guentheri* lane. These are approximately 114 and 134 kDa. With extended development a third band of ≈123 kDa became visible, which ultimately developed into a smear from 114 to 134 kDa. This multiple banding is typical of phosphorylated neurofilaments [67]. The size of the *N. guentheri* SMI31 immunoreactive bands and those of the mammalian medium chains, which range from 110 to 145 kDa, are coincidental. The lamprey neurofilament proteins range from 180 kDa to 50 kDa, with one neurofilament being 132 kDa [397]. The SMI31 antibody merely recognizes the same evolutionary conserved tyrosine-phosphorylation motif common to phosphorylated neurofilaments [398]. No smaller SMI31 reactive bands were observed.

The rabbit anti-cow GFAP antibody reacted with the homogenates to reveal several bands in each lane (rGFAP, Figure 4.4). Two bands were detected in the rat lane, the major band being ≈52 kDa, the other close to 70 kDa, possibly corresponding with neurofilament L which polyclonal GFAP antibodies are known to cross-react with [399]. A 50 kDa band is detected in the zebrafish lane with additional larger bands. Five bands are visible in the *N. guentheri* lane: the major band is ≈55 kDa (and appears to be a smear of two very similar sized bands), the two smaller bands are 45 and 51 kDa. One of the larger bands is ≈61 kDa and the other ≈69 kDa.

The polyclonal GFAP antibody used by the authors, Z0334 from DAKO, was used by Korolainen et al. [381] against aged and demented brain samples and also yielded a multiple banding pattern with a major band at 50 kDa and several smaller bands down to 35 kDa. The bands were confirmed to be GFAP and its post translational products by means of HPLC-ESI-MS/MS. This multiple banding pattern was observed for rainbow trout brain homogenates where a polyclonal anti-goldfish GFAP antibody was used [400]. However, trout astroglia grown in culture only produced a prominent band at 51 kDa suggesting that in fish, as in mammals, there is significant post-translational modification (as well as oxidation and degradation) of GFAP in the intact CNS in addition to multiple isoforms being expressed. It is known that the GFAPϵ isoform is post-translationally modified by presenilin proteins [169]. The multiple banding pattern observed on the blots shown in Figure 4.4 is the expected

outcome of using GFAP antibodies against brain homogenates. To obtain a solitary ≈50 kDa band would be extraordinary against a brain homogenate.

The neurofilament tyrosine-phosphorylation motif is common to GFAP and nuclear lamin [398] but SMI31 does not cross-react with other proteins on the blots. However, the polyclonal anti-GFAP does cross-react with proteins of approximately 61, 69 and 114 kDa as predicted from [398, 401]. Middledorp et al. [399] observed GFAP expression in degenerating neurons in culture using the Z0334 polyclonal GFAP antibody. This antibody was reacting against neurofilament L, a ≈68 kDa protein in humans. They hypothesize that the inclusion of neurofilament L into NFTs renders it susceptible to recognition by GFAP antibodies. On Western Blots using the GA-5 and Z0334 antibodies bands of 61 and 69 kDa are detected and the neurofilament L gene which has been cloned from the lamprey [397] is shown to share 44% amino acid sequence homology with the human neurofilament L and have an apparent molecular mass of 64 kDa. Nuclear lamins are ≈ 70 kDa but as the structures in Figure 4.3F occur outside of the nucleus it is unlikely to be cross reactivity with lamins but with the neurofilament L. An alternative explanation is that of ghost tangles. These are extracellular NFTs which are insoluble debris from degenerate neurons and have also been observed to be GFAP positive remains of astrocytic processes into the NFTs [120]. These ghost tangles do take on a cage-like appearance in sections.

As the SMI31 antibody did not cross react with neurofilament L on the blot the structures where SMI31 and polyclonal GFAP colocalize must also include the 114–132 kDa neurofilament proteins. Whether the GFAP signal in Figure 4.3F is the product of Z0334 reactivity against neurofilament L in NFTs or GFAP in ghost tangles remains to be determined. Research is underway to determine if the frequency of these cage-like structures can be correlated with age and the incidence and location of tangles and plaques in the OT of *N. guentheri*[4].

4.3.2 Results of GA-5 anti-GFAP and E587 labeling

We expect the E587 antiserum to colabel astroglia in the ON and OT as well as to label neurons and nerve fibers independently of the GA-5 monoclonal anti-GFAP antibody.

Figure 4.5 shows strong colocalization between E587 and GA-5 antibodies and the structures are consistent with those of astrocytic projections through the ON. In Figure 4.6 there is colocalization between E587 and GA-5 antibodies, both in the SZ and in radial glial-like structures which span the OT. The E587 signal is distributed through six distinct layers (Figure 4.6D): the SZ, SO, uSGI, SGI, SAI and SGPV. These results are consistent with the expected pattern of L1 distribution through the OT. Some large E587 cell bodies are visible in the OT (arrow head, Figure 4.6F).

[4]After publication of this article the quantification of the cage-like structures was suspended in favor of the work presented in the following chapters

The anti-human GFAP antibody, clone GA-5, reveals one band at ≈52 kDa for the rat brain homogenate (Figure 4.4). Zebrafish brain homogenate reacts with GA-5 to reveal two major proteins of approximately 43 kDa and 50 kDa in size. For *N. guentheri* there are five bands: a major band at 55 kDa paired with a smaller one of about 51 kDa; and another major band at ≈43 kDa together with two less prominent larger bands of approximately 45 and 48 kDa. The GA-5 clone is known to give the observed banding pattern, as can be seen for the Santa Cruz GA-5 antibody (sc-58766) [402], but still reliably labels astroglia only [398, 403]. Similarly, the J1-31 clone also gives a multiple banding pattern against whole brain homogenates but also reliably labels only astrocytes [401]. García et al. [401] attribute this multiple banding pattern to phosphorylation and degradation of GFAP. With longer exposure other bands manifested in all lanes when using both the rabbit anti-GFAP and GA-5 antibodies (data not shown). For all species, using the GFAP antibodies, bands appear between the 100 and 130 kDa. These could be the product of cross-reactivity between GFAP antibodies and neurofilaments.

The human L1 is 220 kDa and is cleaved at multiple sites by several different enzymes [47, 404]. The 220 kDa protein is cleaved into a membrane bound C-terminal fragment of 80 kDa and a soluble 140 (by plasmin) or 180 kDa fragment (by neuropsin). Cleavage by ADAM10 and 17 as well as γ-secretase results in a 28–32 kDa membrane bound fragment and a ≈200 kDa soluble fragment [159]. The concentration of the large soluble fragments in patients with dementia have been observed to increase compared to age-matched controls [47]. This array of post-translational modifications could generate an eight band pattern on a blot using a polyclonal serum. The multiple banding patterns shown in Figure 4.4 is expected for a protein which undergoes such extensive post-translational modification in addition to glycosylation.

The E587 antiserum detected bands of approximately 269, 238, 157, 125 and 85 kDa in the rat lane (bands R1–R5). Based on the human pattern a ≈30 kDa was expected but could not be resolved on the 7.5% gel. The band sizes which do arise are within the expected range for mammalian L1 [47, 159, 404] based on the errors associated with bands larger than 170 kDa. Bands of 190, 120 and 70 kDa are expected for E578 against zebrafish [164]. The authors, using a metal intensified DAB developed blot, demonstrate bands of 199, 125 and 97 kDa (Z1, 2 & 4 respectively, Figure 4.4) in addition to several other bands. The observed differences to Weiland et al. [164] could be due to differences in the origin of our zebrafish (an outbred aquarium strain) or the limits of the chemiluminescent method employed by Weiland et al. [164] which is prone to over-develop some bands at the expense of other bands. Z4, 5 & 6, of molecular masses 97, 52 and 42 kDa sum to 199 kDa which is the same size obtained for Z1. Similarly the three smallest visible bands in the *N. guentheri* lane, N4, 5 & 6 (68, 60 & 48 kDa), sum to 176 kDa which is the same size as N1. The E587 antibody is producing a similar banding pattern against the rat, zebrafish and *N. guentheri* brain samples. The observed differences between the banding patterns among the fish may represent differences

in post-translational modification of the full length protein as well a differences in total length. E587 is probably reacting against a structurally similar protein in each sample[5].

4.3.3 Results of SMI31 and E587 labeling

SMI31 and E587 signal is expected to colocalize in dendrites and in some axons fibers. E587 is also expected to label neurons. Figure 4.7 shows SMI31 signal in axon fibers in the ON as per Figure 4.2. Fibers are predominantly SMI31 positive but there is also strong E587 signal in some axons. E587 signal is also present in the astroglial projections in the ON as seen in Figure 4.5. The colocalization between SMI31 and E587 immunoreactivity in Figure 4.7 could be due to upregulation during axon extension and then down-regulation once the connection with the target neuron is established in accordance with its role in axon guidance [123, 405, 406].

Figure 4.8 shows five SMI31 positive layers in the OT as well as five of the six E587 layers seen in Figure 4.6. Layers L2–L6 and S1–S5 overlap (Figure 4.8d) and correspond with the SGS/SO, uSGI, SGI, SAI and SGPV. A complex of SMI31 and E587 positive fibers in the SGS/SO where fibers from the ON are expected to synapse with neurons in the SGS are visible in Figure 4.8E. The neurons of the SGS synapse with neurons in the uSGI and SGI. These fibers are strongly positive for both SMI31 and E587. These neurons synapse with neurons in the uSGI and SGI. These fibers are strongly positive for both SMI31 and E587 and are most likely dendrites expressing L1 in regard to L1's role in plasticity. In addition, the E587 antiserum also labels large cell bodies in the OT.

4.3.4 Results of anti-TNR and E587 labeling

Figure 4.9A–C shows anti-TNR signal restricted to the myelin layers of the ON, with no colocalization with the E587 signal which labels astroglia and nerve fibers. Figure 4.9D–F show the anti-TNR signal ordered over four layers corresponding with the SO (T1); uSGI (T2); SGI (T3); and SAI (T4) into the SGPV. These layers appear broader than the corresponding E587 layers and each layer fades in the direction of inner layers of the OT. Figure 4.9G–I shows that anti-TNR signal is localized to small cellular bodies. This punctate pattern of anti-TNR staining is unlike that of astroglial, neuronal or axonal labeling by the other antibodies. As expected, the anti-TNR antibody labels the myelinated nerve fiber tracts in the OT.

E587 labelled oligodendrocytes in the goldfish [406] though it did not colocalize with TNR in *N. guentheri*. It may be that *N. guentheri* oligodendrocytes

[5]See Appendix A.2.3.1 for further discussion with additional antibodies which were obtained after publication in an effort to resolve this question. The E587 antiserum is almost certainly reacting against the *Nothobranchius* L1 protein but there is probably also cross-reactivity with NCAM.

either do not express L1 at all or do not express an L1 recognizable by E587. It has been reported that glia and neurons express different forms of L1 [407].

The anti-TNR antibody produced three bands for the rat but only one for *N. guentheri* and zebrafish (Figure 4.4). These proteins are glycosylated in situ and as such the determinations of molecular masses by Western Blotare unreliable. Also, all prominent bands (except one of the rat bands) fall outside of the marker band range. Mammalian TNR has a molecular size of 160–180 kDa and can form dimers and trimers [408, 409]. Only the ≈165 kDa band falls within the marker range of the Western Blotand is of the expected size. The TNR antibody does not cross react with smaller proteins on the blot indicating high specificity. The fish anti-TNR reactive proteins did not migrate into the resolving gel and appears to be of similar size to the band at the top of the rat lane. No cross-reactivity with other proteins was observed in the *Nothobranchius* lane. The Western Blotdata together with the IHC data provides no evidence to suppose that the TNR antibody is not labeling TNR in *N. guentheri* tissues.

4.3.5 Results of labeling with BS-I Isolectin B4

Figure 4.10A–C is of the ON containing microglia labelled with isolectin and DAPI. Figure 4.10D–F are enlargements of the microglia indicated in A–C. These show the typical microglial form. Unexpectedly, the same sections used to observe microglia in the ON showed no microglia in the OT (data not shown). Within the OT the BS-I isolectin did bind to the cell walls of blood vessels confirming that the lectin was present over that part of the tissue section during the incubation step. The absence of BS-I isolectin positive microglia in the OT was unexpected. However, the possibility exists that there are microglia present in the OT but that they are not labelled by BS-I isolectin.

There is no evidence thus far that TNR is repulsive of *Nothobranchius* microglia.

4.3.6 Other antibodies tested

Five other antibodies were tested on *N. guentheri* sections but found to be inactive or inconsistent (results not shown). These are summarized in Table 4.1. The inactivity of the MBP antibody was surprising as it has been effective against goldfish, *Xenopus*, *Gallotia galloti* and rodents in our laboratory. The β-tubulin antibody has also been ineffective against zebrafish. The ineffectiveness of the TAG and integrin antibodies suggest that these proteins may be too evolutionary diverse in nature to be generally useful. Strong s100B staining was obtained in one cohort of aged *N. guentheri* but was totally absent in other aged cohorts. The s100B antibody did not react against protein on Western Blots.

4.4 Conclusions

The *Nothobranchius* research community now has available to it antibodies against nerve fibers (SMI31), astroglia[6] (anti-GFAP) and oligodendrocytes (anti-TNR)[7] in addition to the E587 antiserum which labels young axons and radial glial fibers, and the BS-I Isolectin which labels ON and retinal microglia.

SMI31 was consistent with expectations of neurofilament distribution in neuronal tissues. Together with the data from the Western Blots we find no evidence to believe that the SMI31 is not targeting neurofilament protein in *N. guentheri* and is a reliable label of axons and dendrites.

Some uncertainty exists as to the fidelity of E587 and GFAP antibodies. The combination of IHC and Western Blotdata indicate that the E587 antiserum is labeling an L1-like protein or proteins in *N. guentheri*. We cannot exclude that the E587 antiserum is not detecting other NCAMs in addition to L1 (such as CHL1, a 185 kDa protein in mammals), but if it is unreliable for detecting L1 in rat and *N. guentheri* brain homogenates then our blots reveal that it is equally unreliable for zebrafish as several additional bands developed on our blot compared to that published by Weiland et al. [164]. If the structures in Figure 4.3F prove to be neurodegenerative features then the reactivity of the polyclonal GFAP would be consistent with expectations based on the literature. Both GFAP antibodies reliability labelled astrocytes and did not label non-astrocytic structures.

Regardless of the uncertainties, all of the antibodies have been shown to reliably label expected cell types and structures in the *Nothobranchius* nervous system which makes it possible to detect aging-related changes at the cellular level in the *Nothobranchius* CNS. This research highlights the need to clone and express the respective proteins believed to be labelled by these antibodies and generate more specific antibodies against these proteins.

Experiments are underway to study neurodegeneration in *N. guentheri* using these antibodies as cellular markers as well as test them against other *Nothobranchius* species.

4.5 Acknowledgements

The authors wish to thank Mr. Otto Schmidt for supplying the fish. Also, Mrs T. Wiggins, S. Cooper, M. Petersen and Ms B. Kleemann for technical assistance. Funding was supplied by the author (TG), Mr Raymond Ackerman, Jean Huber (www.killi-data.org), the University of Cape Town and the South

[6] A later publication using the astoglial marker s100B showed that *Nothobanchius* have only radial glia lining the brain surfaces [410].

[7] A hypothesis not considered at the time was that the anti-TNR was labelling the nodes of Ranvier. There is evidence of oligodendrocytes forming periaxonal nets around the voltage-gated sodium channels [411]. These structures are composed of brevican [411] as well as versican and TNR [412]. Both versican and TNR are expressed only by oligodendrocytes [140] so this then unconsidered hypothesis does not affect the claim that TNR is a reliable marker of oligodendrocytes.

African National Research Foundation. We also wish to thank Mr. D.A. Wilcox for proof reading the manuscript and making valuable suggestions.

4.6 Figures

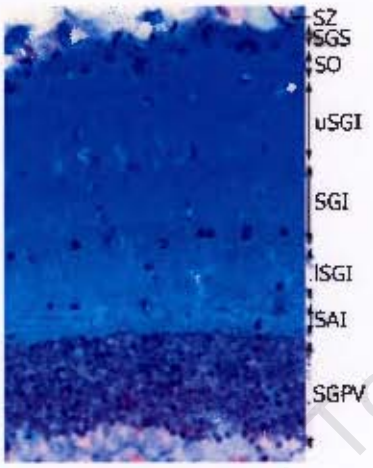

Figure 4.1: 5 μm fixed section of optic tectum of *Nothobranchius guentheri* stained with Luxol Fast Blue and Cresyl Violet. Optic tectum layers are labelled on the Figure: SZ, stratum zonale; SGS, stratum griseum superficiale; SO, stratum opticum; uSGI, upper stratum griseum intermediale; SGI, stratum griseum intermediale; lSGI, lower stratum griseum intermediale; SAI, stratum album intermediale; and SGPV, stratum griseum periventriculare. Neuronal cell bodies appear purple and myelin light blue. 400× magnification.

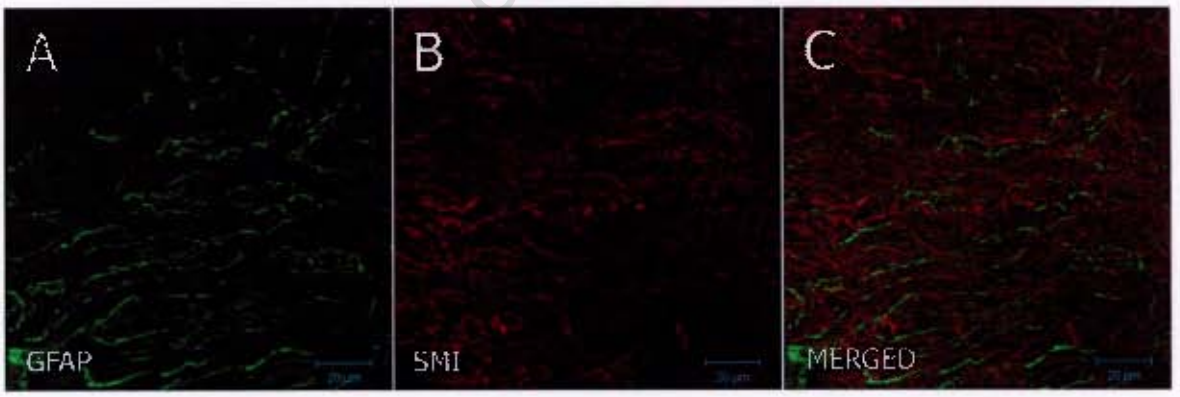

Figure 4.2: 20 μm frozen section of optic nerve of *Nothobranchius guentheri* probed with rabbit anti-cow GFAP and with SMI31 antibodies. The nerve is filled with axon fibers as well as large glial processes. Signals do not colocalize. Scale bar = 20 μm.

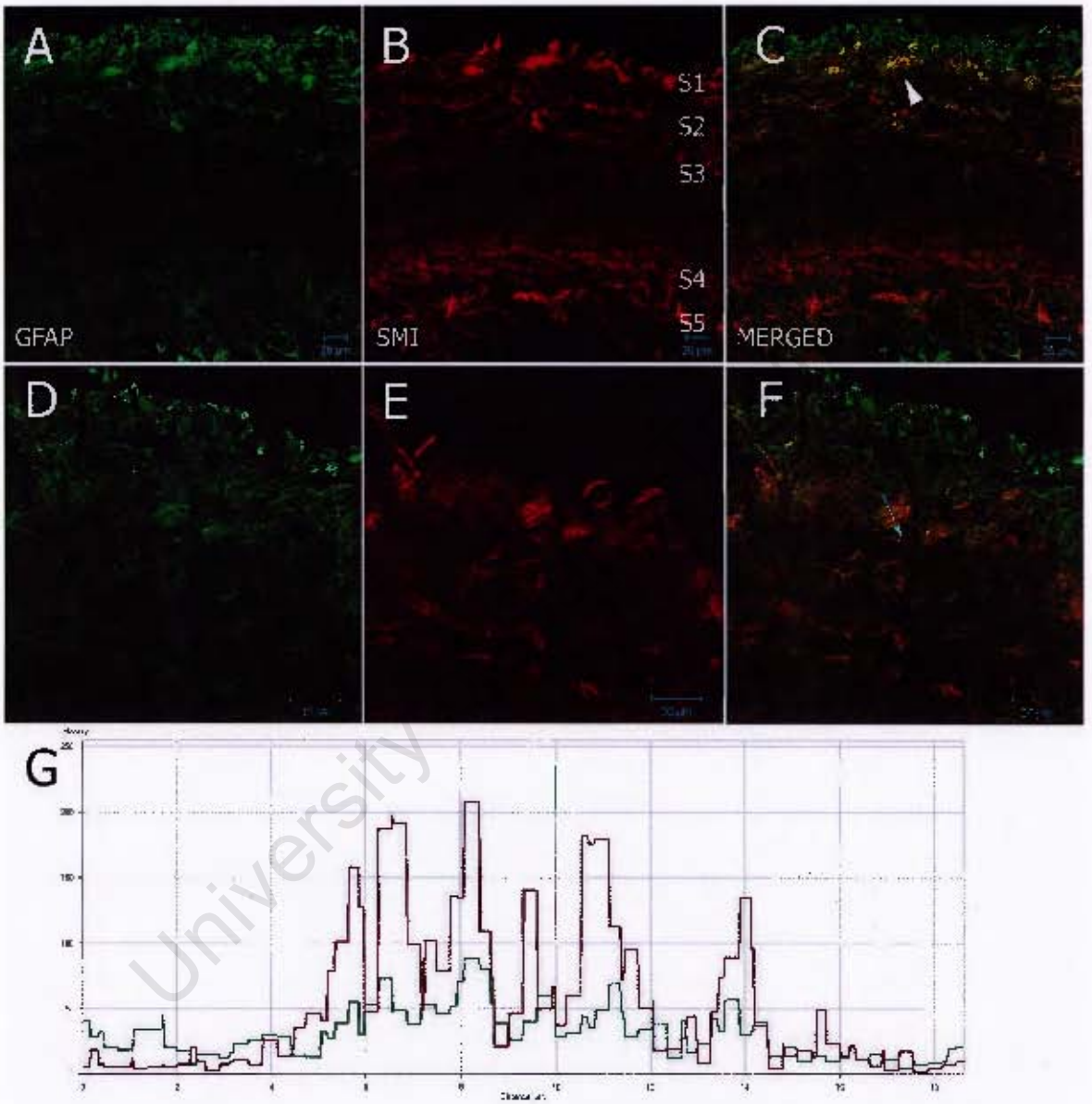

Figure 4.3: 20 μm frozen section of optic tectum of *Nothobranchius guentheri* probed with rabbit anti-cow GFAP and with SMI31 antibodies. There is a strong GFAP positive layer corresponding with the SZ into the SO (Figure 4.1) which is indicative of radial glia. The SMI31 signal is seen in five discrete zones: S1 the SGS & SO; S2 the uSGI; S3 the SGI; S4 the SAI; and S5 the SGPV. SMI31 and anti-GFAP signal are seen to overlap in cage-like structures in the SGS (arrow head in C) which are enlarged in Figures D–F. There is some co-localization of SMI31 and anti-GFAP signal (Figures F & G) in these structures. The arrow in F is the path along which the image was analyzed for colocalization shown in G. Scale bar = 20μm.

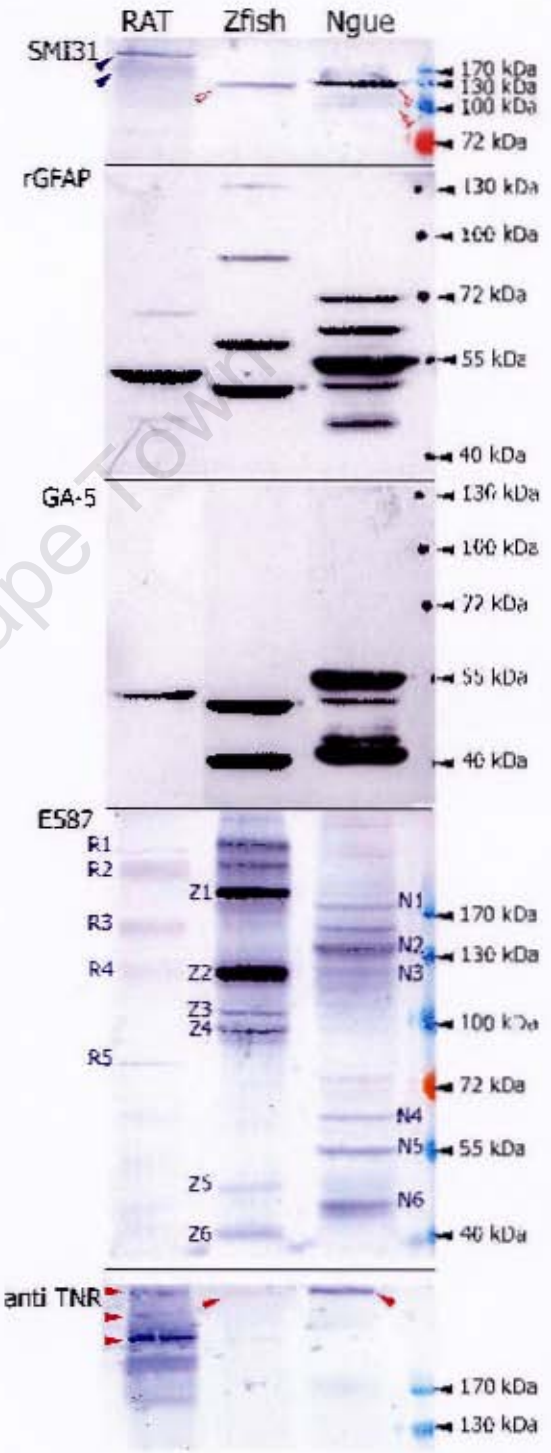

Figure 4.4: Western Blots against brain homogenates of rat, zebrafish (Zfish) and *N. guentheri* (Ngue). The antibodies used are SMI31 which should label neurofilament protein of approximately 110 to 230 kDa for the rat. Rat bands are indicated by blue arrowheads and fish in red. Two GFAP antibodies were used, the rabbit polyclonal anti-cow GFAP (rGFAP) and the mouse monoclonal anti-human GFAP (GA-5) which should label proteins of approximately 50 kDa. The E587 antiserum is generated against goldfish L1 and should label proteins of 190, 120 and 70 kDa. Rat bands are labels R1–5, zebrafish Z1–6 and *N. guentheri* N1–6. The monoclonal anti-TNR antibody labels three bands in the rat lane (blue arrowheads) and one band each in the fish lanes (red arrowheads). Marker band sizes are indicated to the right of the blots.

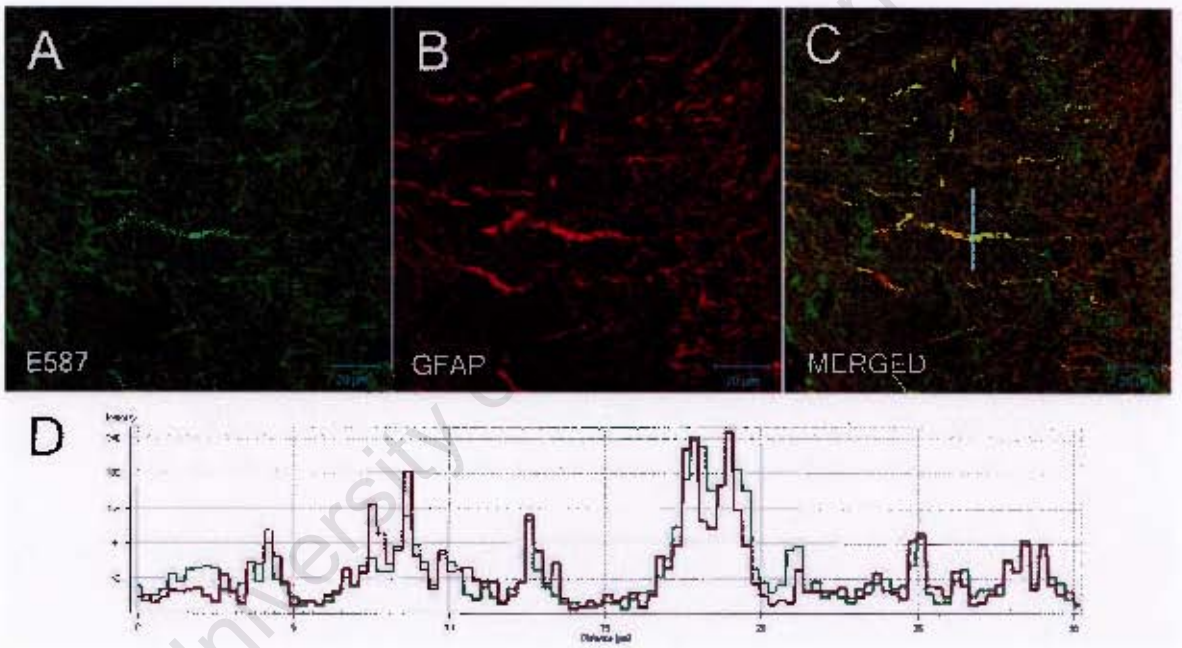

Figure 4.5: 20 μm frozen section of optic nerve of *Nothobranchius guentheri* probed with rabbit E587 antiserum and mouse anti-human GFAP. (C) shows a merged image of the red and green channels. The blue line indicates the optical section used to generate the profile in (D) which shows co-localization of red and green signal in the glial processes. Scale bar = 20 μm.

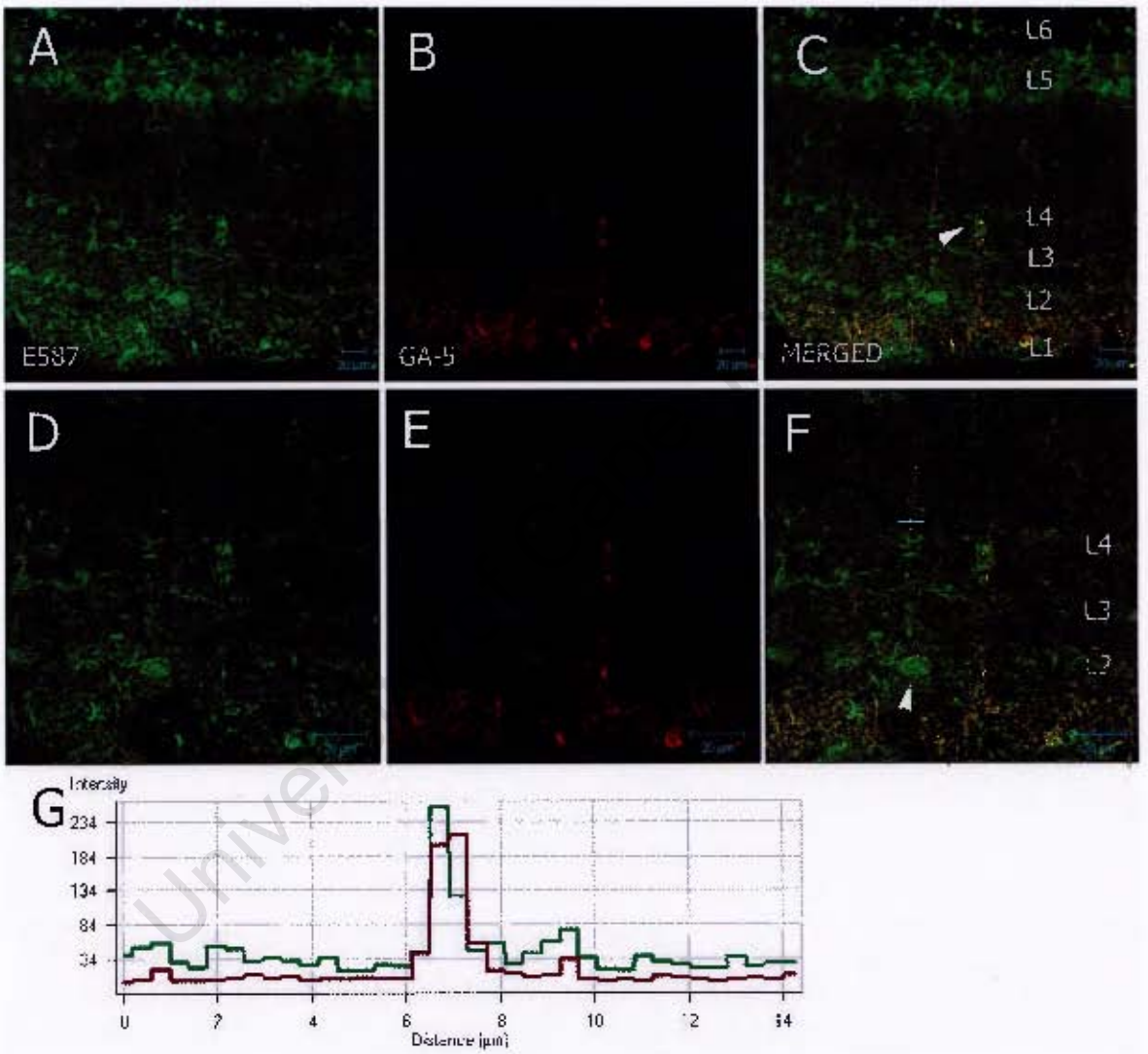

Figure 4.6: 20 μm frozen section of optic tectum of *Nothobranchius guentheri* probed with E587 antiserum and mouse anti-human GFAP. Arrow in (C) indicates a radial glial fiber which is the focus of Figures (D–F). Six anti-L1 layers can be discerned. Arrow in (F) indicates a large E587 cell body, most likely a neuron. L1 corresponds with the SZ; L2 with the SGS/SO; L3 and L4 with the fiber tracts in the uSGI and SGI; L5 with the fiber layer of the SAI; and L6 with the SGPV. (G) Radial fiber in (F) bisected showing that green and red signal colocalize in the radial glial fiber spanning the OT. Scale bar represents 20 μm.

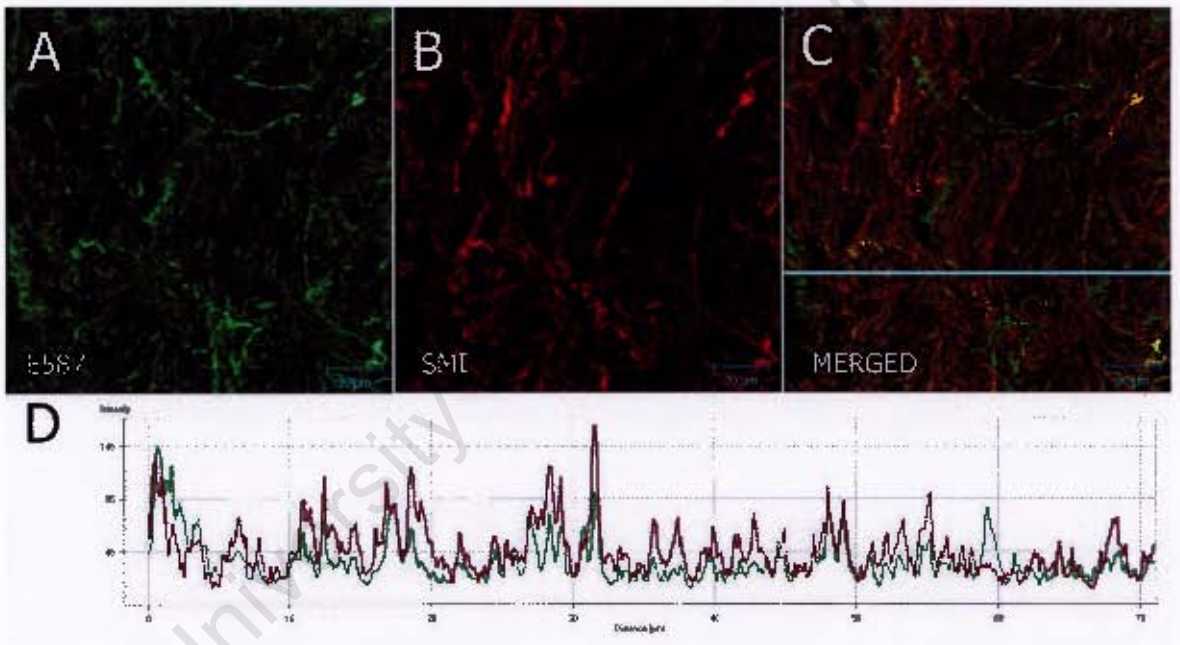

Figure 4.7: 20 μm frozen section of optic nerve of *Nothobranchius guentheri* probed with rabbit E587 antiserum and SMI31. (C) shows a merged image showing co-localization (D) of red and green signal in some of the nerve fibers. Some fibers show no red signal and are probably astrocytic processes. Scale bar = 20 μm.

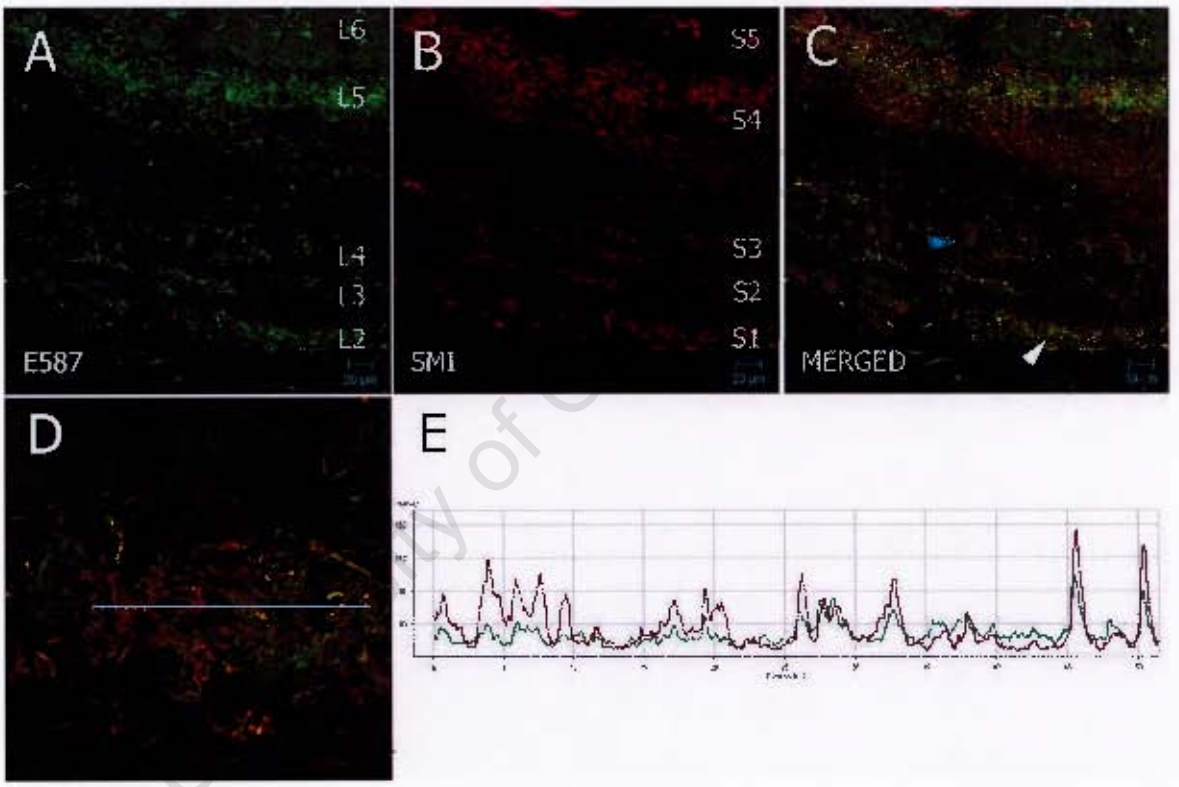

Figure 4.8: 20 µm frozen section of optic tectum of *Nothobranchius guentheri* probed with rabbit E587 antiserum and mouse SMI31. Several discrete SMI31 and E587 layers are evident in (A) and (B) which partially overlap in the merged image (C). Blue arrow in (C) indicates a large E587 cell body, possibly a neuron. White arrow in (C) serves as the center of focus for (D). Red and green signal in (D) colocalize (frame E) and show a complex of SMI31 and E587 positive fibers in the SGS/SO layer.

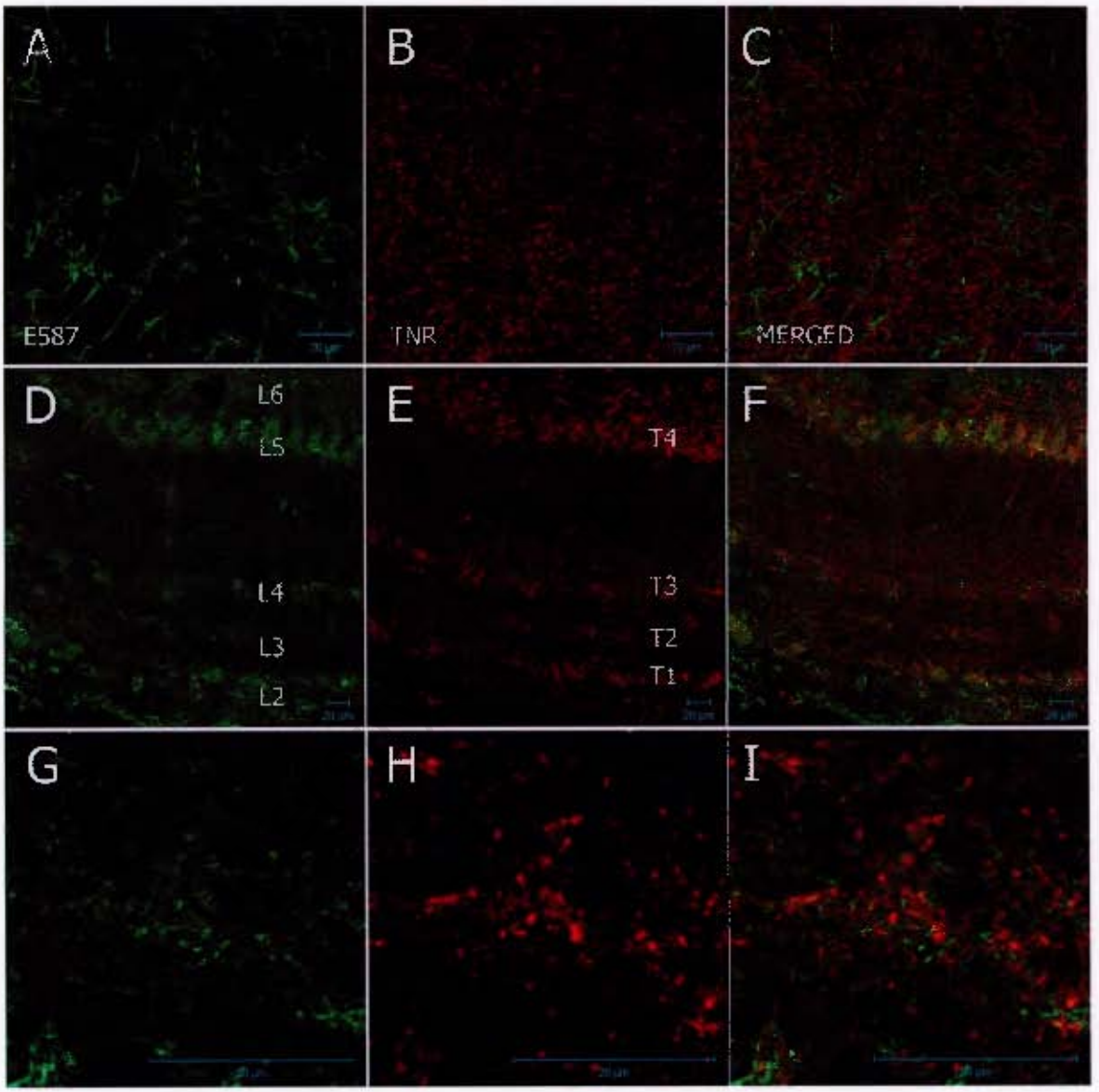

Figure 4.9: 20 μm frozen section of optic nerve and optic tectum of *Nothobranchius guentheri* probed with rabbit E587 antibody mouse anti-TNR. (A–C) shows images of the ON. E587 positive astrocytic processes are visible along with anti-TNR signal which appears restricted to specific cell bodies. There is no evidence for colocalization as in Figures 4.5 and 4.7. (D–F) shows images of the OT. The anti-TNR signal (E) is ordered in four layers corresponding with the SO (T1); uSGI (T2); SGI (T3); and SAI (T4) into the SGPV. These layers appear broader than the corresponding E587 layers and each layer fades in the direction of the inner layers of the tectum. (G–I) show magnified images of the OT which clearly show that E587 and anti-TNR signal do not colocalize. The anti-TNR signal is restricted to small cell bodies in the tissue. Scale bar = 20 μm.

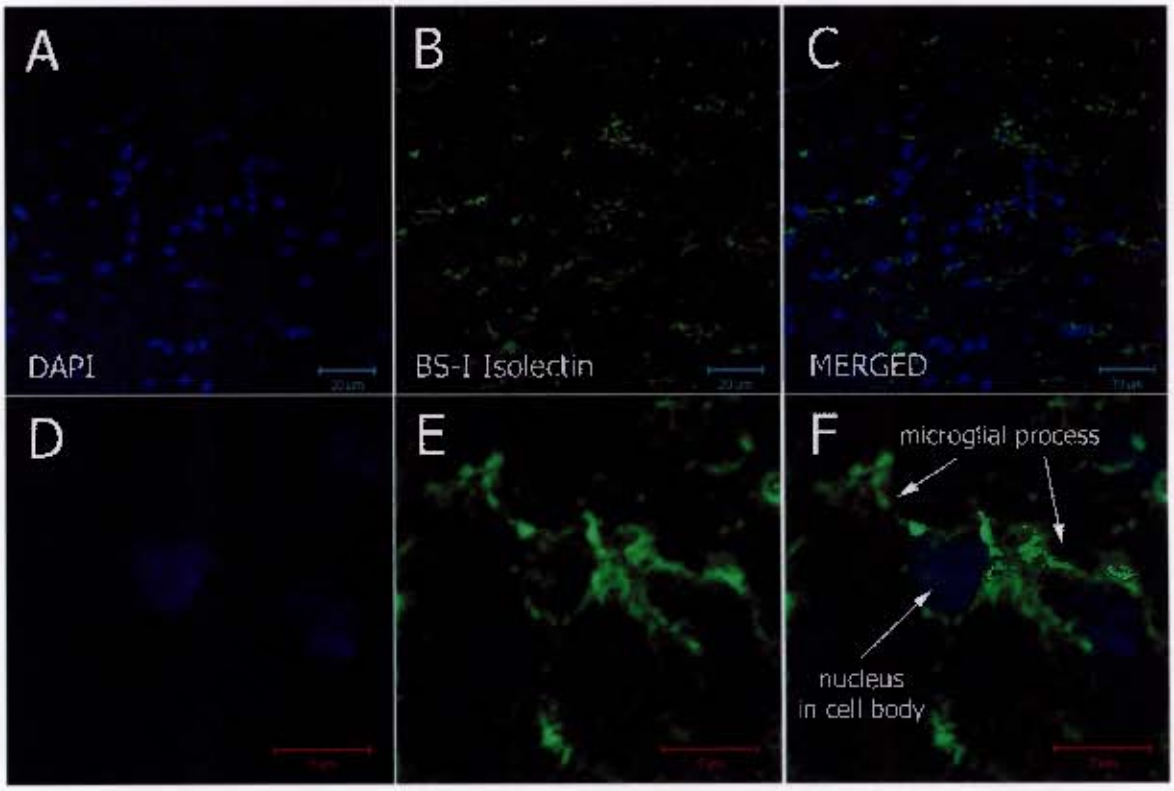

Figure 4.10: 20 μm frozen section of optic nerve of *Nothobranchius guentheri* probed with DAPI and biotinylated BS-I Isolectin B4. (A–C) shows images of the ON containing microglia labelled with BS-isolectin. Typical microglial morphology can be observed in the enlarged frames (D–F). Scale bars = 20 μm for (A–C) and 5 μm for (D–F).

Chapter 5

The effect of aging and resveratrol-treatment on neuron density in the optic tectum

I don't remember, it doens't ring a bell,
And when you call me everything is swell,
I tend to forget about the times we had,
Now it doesn't matter 'cause I feel so sad,
I've been disconnected.

Disconnected, Goo Goo Dolls.

5.1 Introduction

Polyphenols are reported to have a neuroprotective effect. Specifically, they are expected to prevent neuronal cell death caused by neurodegenerative processes or prevent these processes entirely [413]. As they inhibit neurodegenerative-aging they are expected to modulate lifespan by increasing healthspan. This increase in healthspan is expected to increase median lifespan as well as maximum lifespan.

Valenzano et al. [5] showed that *Nothobranchius furzeri* (of the extremely short lived Gonerezhou population) exhibited reduced operant conditioning and increased FJB signal in the OT as they grew older. This we[1] interpreted as a consequence neurodegeneration, in particular the accumulation of NFTs. These fish, fed a diet supplemented with resveratrol [5], lived longer than aged-matched controls as well as exhibited lower levels of FJB signal and improved operant conditioning. As neurodegeneration results in neuronal death

[1] The Author was a coauthor of the paper by Valenzano et al. [5].

we reasoned that the neuroprotective action of resveratrol was due to the preservation of neurons into old age. No cell-type specific probes were available to test this hypothesis. The Author recently published an antibody toolbox by which to investigate neurodegeneration in *Nothobranchius* [382] (Chapter 4) and set out to test whether resveratrol did preserve neurons into old age using the SMI31 antibody and E587 antiserum.

The SMI31 antibody was demonstrated to react against *Nothobranchius* neurons and axons. The SMI31 antibody recognizes abnormally phosphorylated neurofilament protein of the heavy and medium chain forms [66]. Abnormally phosphorylated neurofilaments have been found within NFTs [69, 70]. SMI31 has been used to label degenerating neurons wherein its epitope accumulates. This has been observed in culture and Alzheimer's Disease (AD) brain tissues [66] and using an AD model mouse [67]. This antibody has also been shown to label healthy neurons in rats [395].

The E587 antiserum has been used to label L1 in other fish species [123, 163, 164]. L1 is a member of the NCAM family and its role in neurodegeneration was reviewed in Chapter 2.4. It is expressed by a subset of neurons [414] where it plays a role in synaptogensis [415]. It occurs both on the neuronal and axonal surface [414] and within the synaptic cleft [162]. The L1 protein itself has been reported to be neuroprotective [416] while its signaling cascades have been implicated in neuroprotective responses [165]. The expression of L1 and other NCAM is down-regulated in aging [166]. This down-regulation is reversed by dietry restriction. The E587 antiserum was therefore used as a marker of neuron vitality and synaptic integration.

In this study the Author grew *N. guentheri* to old age, both with and without resveratrol-treatment. Resveratrol-treatment began at 12 weeks of age when the fish were sexually mature. Brains were sampled at two time points: 12 and 34 weeks of age. Whole brains were fixed and stained with SMI31 and E587 antibodies and the SGS examined. The FJB signal was most intense along the upper surface of the OT in *N. furzeri*. Because of this wholemounts were a convienient means to study the tissue without introducing sectioning artifacts or otherwise damaging the tissue through fixation, dehydration, freezing or wax imbedding. Differences were observed between the young and old fish and a detailed study of the SGS and glia limitants was performed and the neurons counted and analyzed.

Using immunostained wholemounts the Author presents evidence that SMI31 immunoreactivity accumulates in a particular subset of neurons with age along with a decrease in neuron density. In resveratrol-treated fish this subset of neurons is less abundant. We also present evidence that *N. guentheri* resveratrol-treated fish have a lower SGS neuron density per mm^2 compared to young and age-matched controls; but that the proportion of $E587^+$ neurons is similar to that of 12 weeks old fish.

5.2 Methods and materials

5.2.1 Animal care and experimentation

Fish were cared for as in Genade & Lang [382]. Fish were raised in our laboratory as described in Genade [388]. Experimental fish were given resveratrol (Sigma R5010) as described in Valenzano et al. [5]. The dose was ≈12 μg resveratrol/ fish/day. The fish were fed twice per day with a resveratrol-supplemented cube of *Chironomus* larvae set in 5% gelatine. The quantity of resveratrol was adjusted to the number of fish to which the cube of food was fed [388]. For *N. guentheri*, resveratrol-treatment began at 12 weeks of age after the fish had reached sexual maturity. Resveratrol stocks (1.2 mg/mL) were prepared in 96% ethanol to ensure chemical stability.

5.2.2 Dissection and immunohistochemistry

Wholemounts were chosen in preference over sections for several reasons. (1) The difficulty in positioning the brains for frozen sectioning which would have made obtaining reproducible date difficult (possibly culminating in wasting the fish). (2) Several artifacts were noticed in the sectioned tissue (such as the GFAP/SMI31 colocalization in Section 4.3.1 which were not noticed in the testing of the wholemount method. (3) In addition, during the freezing and sectioning process there was noticeable distortion of the tissue which made reaching anatomical conclusions difficult.

Fish were euthanized as described in Valenzano et al. [5] the whole brain carefully dissected out and the eyes severed. The brains were fixed for 10 minutes in 4% PFA and then post-fixed in -20°C methanol for another 10 minutes. This method was chosen over intracardially perfused due to the small size of the fish and that the current method of post-fixation was already standard practice for working with these fish.

Fixed brains were washed in 4°C PBS three times for 15 minutes and then incubated in PBS blocking solution of 1% bovine serum albumin and 1% DMSO. Whole brains were blocked for 24 hours at 4°C and then incubated with primary antibodies for 48 hours at 4°C. The following primary antibodies were used at 1:400 dilution in blocking solution: SMI31 (Covance SMI-31R) and counterstained with E578 anti-L1 antiserum (a gift from C. Stuermer, Konstanz Germany) or rabbit anti-bovine GFAP (DAKO Z0334). After primary antibody incubation the brains were washed three times in PBS and then incubated for 48 hours with the secondary antibodies diluted 1 in 500 blocking solution: anti-rabbit Alexa 488 (Molecular Probes, Invitrogen) and anti-mouse Cy3 (Jackson Immuno Research). After secondary staining the brains were washed three times in PBS and soaked in mowiol (with anti-fading agent n-propylgallate) overnight at 4°C. After the mowiol soak the brains were placed on coverslips in a drop of mowiol and gently pressed flat between two coverslips.

5.2.3 Microscopy and image analysis

Wholemount images were obtained using a Zeiss LSM S10 Meta NLO Confocal microscope (Jena, Germany). Images are representative of several specimens and were edited for publication using Adobe Photoshop CS2 v9.0.2.

Three $110.5 \times 110.5\,\mu m^2$ optical frames were recorded for each of the anterior, mid and posterior OT (henceforth referred to as aOT, mOT and pOT) as indicated in Figure 5.2, page 95. These areas were selected as examples of mature (aOT) and developing OT (pOT) with an intermediate area for a temporal analysis for any differences between the aOT and pOT. Each frame was 2.0 μm thick and spanned the SZ (containing the radial glia) and SGS. Due to inconsistency of the antibody penetration (which was often complete in young fish but only 10–15 μm in aged fish, data not shown) it was decided to only examine the upper layers (SZ–upper uSGI) for neurons. Within the 2 μm imaging depth all neurons of the SGS were included (see Figure 4.1) and in sharp focus (negating the need for the time consuming generation of a z-stack).

Within each of the large frames a smaller optical delimiter of $100 \times 100\,\mu m^2$ was used to count cells (Figure 5.3A, page 96). Images were obtained in the Cy3 channel with the maximum signal intensity threshholded to the most intensely SMI31 labelled cellular body. The image was manipulated in PhotoShop to intensify under-exposed cells. Cells which were clearly visible before PhotoShop enhancement were defined as $SMI31^{+++}$, i.e. neurons which have accumulated SMI31 epitope. Cells touching the bottom and left boundary of the delimiter were not counted. Some optic tecta were damaged during the dissection and could not be analyzed. The number of fish (N) and images analysied (n) are reported along with the corresponding data sets in the results section.

Neurons were categorized based on the pixel diameter of the PhotoShop Brush tool needed to completely obscure the neuron. Using the 50 μm scale bar as a size reference the pixel diameter was used to estimate the diameter of the neuron in μm. The numbers of neurons of a particular size were tallied and used to generate Figure 5.3E to determine the size categories. Neurons were categorized as small, large, giant, long or amorphous as described in Section 5.3.2 and Figure 5.3B & C.

5.2.4 Statistics

Survival analysis was carried out using the Log-rank test available online at http://in-silico.net/statistics/survivor developed by SA Joosse.

One-way Kruskal-Wallis Ranked ANOVA analysis were performed using SigmaPlot 11 (Systat Software, Inc., San Jose, CA USA) followed by Tukey, Dunn's or Holm-Sidak tests for statistical differences between the groups. Statistical differences between data sets are reported simply as being $p < 0.05$.

Statistical differences are indicated on the graphs by means of an asterisk for differences between the 12 weeks old and other groups; and an exclamation mark between the resveratrol-treatment and 34 weeks old groups. Error bars represent confidence intervals for $p = 0.05$ [417]. Where $0.05 > p < 0.10$ the

more stringent, but less powerful Mann-Whitney Rank Sum Test, was used to guard against false negatives.

5.3 Results and discussion

5.3.1 Resveratrol extends *N. guentheri* lifespan

Figure 5.1 shows the survival curves for the control and resveratrol-treated fish. Median survival for the resveratrol-treated *N. guentheri* was 50 weeks compared to 35 weeks for the non-treated control fish (a 42.9% increase in survival, $p < 0.0001$). Maximum (10%) survival was 62 weeks for the resveratrol-treated fish and 53 weeks for the controls (a 17.0% increase in survival). The oldest control fish died at 63 weeks of age and the oldest resveratrol-treated fish died at 66 weeks of age (a 4.8% difference).

Resveratrol-treatment had little effect on total lifespan but had a large effect on median lifespan which is associated with healthspan. These results mirror current experiments underway in Jena, Germany, by Prof. Cellerino (pers. comm.) using *N. furzeri*. The same *N. furzeri* strain which lived 8–9 weeks on average in Pisa, Italy is now living 12 weeks on average in Jena. The maximum lifespan has also increased suggesting that the resveratrol experiments carried out in Pisa [5] increased the healthspan of the fish under conditions of high extrinsic lifespan risk. Once the fish were removed from these risks their lifespan increased with total lifespan tending to the intrinsic maximum lifespan of the organism. Similarly, resveratrol-treated *N. guentheri* display a large sensitivity to increased extrinsic lifespan risk which is remedied by resveratrol-treatment. This could be on account of inbreeding in aquariums for several generations as is hypothesized for *N. furzeri* Gonarezhou [12]. The same phenomenon is observed when resveratrol was given to high-calorie fed mice and control mice [214, 250]. In accordance with Gavrilov's Reliability Theory of Aging: maximum lifespan is less affected by extrinsic lifespan risk and thus less susceptible to intervention strategies [210].

5.3.2 Neurons of various sizes occur in the SGS

228 neurons were measured to make an estimate of their size and the data graphed (Figure 5.3E, page 96). The graph revealed at least three size groups. The first group of small neurons was $4.7 \pm 0.6\,\mu$m SD. The cut-off point between small and large was designated as $5.9\,\mu$m based on the difference in the abundancies of the $5.4\,\mu$m and $6.1\,\mu$m neurons and large size interval between them of two small neuron standard deviations. Neurons from $5.9\,\mu$m diamter onwards had a more oval form. The large group was not as numerous in number nor as uniform in size as the small subset and no criteria by which to differentiate a medium subset could be found. The upper size limit of the large subset was designated as $11.7\,\mu$m. The large subset was $8.2 \pm 1.6\mu$m. The giant subset was $15.7 \pm 2.70\mu$m (Figure 5.3C) with one neuron being $22.8\,\mu$m.

Figure 5.3B is a representative image of the OT showing neurons of various sizes. Small neurons were often encountered as quartets of three small and one larger neuron (Figure 5.3D). Large neurons were often encountered in pairs. Members of these pairs were in close enough proximity to obscure one another. Using the E587 antiserum the borders of these neurons could be better discerned. Neurons classified as long were no wider than the diameter of a small neuron but at least three times longer than they were wide. Neurons were classified as amorphous if they had an irregular shape, the normal shapes being round, long or oval. Whether these neuron types represent genuine neuron subtypes or a progression from healthy to degenerate neurons will be discussed below.

5.3.3 Neuron density declines with age

To determine whether the total number of neurons in the SGS were declining with age all neurons in the SGS were counted. This data is presented in Figures 5.4 and 5.5 as well as Table 5.1. There is a decline in SMI31 immunoreactive neurons with the age of the fish (regardless of resveratrol supplementation) as well as an increase in neuronal density with the youth of the OT area. A subset of $SMI31^+$ neurons were immunoreactive with the E587 antiserum (Figure 5.4).

Using the sizing criteria established in Section 5.3.2 the neurons were counted in each OT area. This data is presented in Figure 5.5, page 98. On average, there is a statistical decline in neuron density with age between 12 and 34 weeks old fish. Relative to both the 12 and 34 weeks old fish, resveratrol-treated fish had a lower neuronal density. This difference was present between the 12 and 34 weeks old groups in the pOT. In the mOT both the 34 weeks old and resveratrol-treated fish neuron density was significantly less compared to the 12 weeks old fish. Resveratrol has a larger effect on the younger area of the OT than on the older areas.

When assessing the density of small neurons the resveratrol-treated group had significantly more neurons in the mOT compared to the 34 weeks old fish but not the 12 weeks old fish. Resveratrol-treated fish had on average more small neurons than the 12 and 34 weeks old groups. There were no significant differences between the resveratrol and control groups with respect to the large neurons. Resveratrol-treated fish had on average statistically fewer giant neurons compared to the 12 and 34 weeks old fish. There was no statistical difference in the number of giant neurons between the 12 and 34 weeks old fish. The 34 weeks old fish have consistently fewer giant neurons. A larger sample size may reveal a statistical difference. No significant difference was found in the pOT between any of the groups. In both the anterior and mOT resveratrol-treated fish had significantly fewer giant neurons compared to the 12 weeks old fish. When comparing the average values the resveratrol-treated fish had significantly fewer amorphous neurons compared to the 12 and 34 weeks old fish. This significant difference between the resveratrol and 34 weeks old controls was present in the posterior and anterior OT but not the mOT. Compared

Table 5.1: Table of statistical differences of SMI31$^+$ counts per mm^2 between the three OT areas within each experimental group: 12, 34 weeks old and resveratrol-treated (RT). Samples sizes were $N = 6$ & $n = 32$ for the 12 weeks old group; $N = 9$ & $n = 39$ for the 34 weeks old group; and $N = 5$ & $n = 27$ for the resveratrol-treatment group. Statistically significant results are underlined.

Total SMI31$^+$ per mm^2					
12 weeks old		**34 weeks old**		**RT**	
pOT > aOT	$\underline{p < 0.05}$	pOT > aOT	$\underline{p < 0.05}$	pOT > aOT	$\underline{p < 0.05}$
pOT > mOT	$\underline{p < 0.05}$	pOT > mOT	$\underline{p < 0.05}$	pOT > mOT	$\underline{p < 0.05}$
aOT vs mOT	$p > 0.05$	aOT vs mOT	$p > 0.05$	aOT vs mOT	$p > 0.05$
Proportion small SMI31$^+$ per total SMI31$^+$ per mm^2					
pOT vs aOT	$p = 0.653$	pOT vs aOT	$p = 0.967$	pOT vs aOT	$p = 0.123$
pOT vs mOT	$p = 0.653$	pOT vs mOT	$p = 0.967$	pOT vs mOT	$p = 0.123$
aOT vs mOT	$p = 0.653$	aOT vs mOT	$p = 0.967$	aOT vs mOT	$p = 0.123$
Proportion large SMI31$^+$ per total SMI31$^+$ per mm^2					
pOT vs aOT	$p = 0.259$[♣]	pOT vs aOT	$p = 0.442$	pOT vs aOT	$p = 0.217$[♣]
pOT vs mOT	$p = 0.259$[♣]	pOT vs mOT	$p = 0.442$	pOT vs mOT	$p = 0.217$[♣]
aOT vs mOT	$p = 0.259$[♣]	aOT vs mOT	$p = 0.442$	aOT vs mOT	$p = 0.217$[♣]
Proportion giant SMI31$^+$ per total SMI31$^+$ per mm^2					
pOT vs aOT	$p = 0.232$	pOT > aOT	$\underline{p < 0.05}$	pOT vs aOT	$p = 0.214$
pOT vs mOT	$p = 0.232$	pOT > mOT	$\underline{p < 0.05}$	pOT vs mOT	$p = 0.214$
aOT vs mOT	$p = 0.232$	aOT vs mOT	$p = 0.943$	aOT vs mOT	$p = 0.214$
Proportion amorphous SMI31$^+$ per total SMI31$^+$ per mm^2					
pOT vs aOT	$p > 0.05$	pOT vs aOT	$p = 0.882$	pOT vs aOT	$p = 0.663$
pOT > mOT	$\underline{p < 0.05}$	pOT vs mOT	$p = 0.882$	pOT vs mOT	$p = 0.663$
aOT > mOT	$\underline{p < 0.05}$	aOT vs mOT	$p = 0.8825$	aOT vs mOT	$p = 0.663$
Proportion long SMI31$^+$ per total SMI31$^+$ per mm^2					
pOT > aOT	$\underline{p < 0.05}$	pOT > aOT	$\underline{p < 0.05}$	pOT > aOT	$\underline{p < 0.05}$
pOT > mOT	$\underline{p < 0.05}$	pOT vs mOT	$p > 0.05$	pOT vs mOT	$p > 0.05$
aOT vs mOT	$p > 0.05$	aOT < mOT	$\underline{p < 0.05}$	aOT vs mOT	$p > 0.05$

[♣] A One-Way Analysis of Variance returned a p-value greater than 0.05 but the statistical power of the test (0.104) was below needed to be sure of the result (0.800). A more powerful analysis or more data may prove the difference to be significant.

to 12 weeks old fish the 34 weeks old fish had significantly fewer amorphous neurons in the pOT. This data could indicate that over time neurons are pruned from the neural network and that resveratrol-treatment encourages this pruning.

34 weeks old and resveratrol-treated fish had significantly more long neurons in both the mOT and on average compared to the 12 weeks old fish. Long neurons were often encountered lying adjacent to E587 immunoreactive blood vessels on the OT (Figure 5.4I).

That more small neurons exist on average in resveratrol-treated fish compared to controls suggests that newborn neurons are surviving in the established OT of resveratrol-treated fish. The alternative argument that the small neurons in resveratrol-treated fish are surviving better than in the young and old controls is not supported by this data. As much as one half of the total neurons are lost from the aOT with age but the small neurons increase by as much as 40% without upsetting the similarity in the proportion of large neurons between the groups. On the contrary, 34 weeks old fish also lose a significant proportion of their neurons from the aOT but exhibit no change in the proportion of small neurons in this area. In addition, while there are significant differences in neuronal density in the pOT with age and resveratrol-treatment, no difference is found in the proportion of small neurons in the pOT. Newborn (BrdU+) neurons have been observed in the aged OT of 34 weeks old and resveratrol-treated *N. guentheri* but were not quantified (Figure A.8, Appendix A.3). These neurons were observed along the dorsal edge of the OT, adjacent to the valvula cerebelli. Adult neurogenesis has been confirmed in *N. furzeri* and these newborn neuron do integrate [418]. These neurons arise in the torus longitudinalis adjacent to the valvula cerebelli and OT, and then migrate into the OT. Furthermore, resveratrol-treatment only began at 12 weeks so one can only expect the density of neurons in the anterior OT to decrease between the groups. They cannot increase unless new neurons were added to this area throughout the life of the fish. The long neurons could be new born neurons migrating into the OT. If so, then the 34 weeks old fish launch as great a regenerative effort as the resveratrol-treated fish. Why doesn't this regeneration succeed in 34 weeks old fish? Is it because the giant and amorphous neurons remain synaptically active and get in the way of the integration of newborn neurons? It has been reported that the rate of neuronal apoptosis mirrors the rate of neurogenesis and neuron integration in the hippocampus [122]. Degenerate neurons which fail to undergo apoptosis and make way for newborn neurons could upset this balance between neural pruning/neurogenesis and integration.

Whether the size groups (small, larger, giant and long) reflect specific cell types or a gradual increase in cell size with age is an open question requiring further investigation. Aging-related changes in neuron size have been reported for humans [38]. No differences were found in the average density of the large and long neurons suggesting that these could be specific neuronal types.

Table 5.2: Table of statistical differences of SMI31^{+++} counts per mm^2 between the three OT areas within each experimental group: 12, 34 weeks old and resveratrol-treated (RT). Samples sizes were $N = 6$ & $n = 32$ for the 12 weeks old group; $N = 9$ & $n = 39$ for the 34 weeks old group; and $N = 5$ & $n = 27$ for the resveratrol-treatment group. Statistically significant results are underlined.

Total SMI31^{+++} per mm^2					
12 weeks old		**34 weeks old**		**RT**	
pOT > aOT	$\underline{p < 0.05}$	pOT vs aOT	$p = 0.199$	pOT vs aOT	$p = 0.058^{\clubsuit}$
pOT > mOT	$\underline{p < 0.05}$	pOT vs mOT	$p = 0.199$	pOT vs mOT	$p = 0.058^{\clubsuit}$
aOT vs mOT	$p > 0.05$	aOT vs mOT	$p = 0.199$	aOT vs mOT	$p = 0.058^{\clubsuit}$
Proportion SMI31^{+++} of total neurons per mm^2					
pOT vs aOT	$p > 0.05$	pOT vs aOT	$p = 0.157$	pOT vs aOT	$p = 0.140$
pOT > mOT	$\underline{p < 0.05}$	pOT vs mOT	$p = 0.157$	pOT vs mOT	$p = 0.140$
aOT vs mOT	$p > 0.05$	aOT vs mOT	$p = 0.157$	aOT vs mOT	$p = 0.140$

$^{\clubsuit}$ The Mann-Whitney Rank Sum Test gives p-values of 0.124, 0.067 and 0.064 supporting the conclusion that these results are insignificant and not the result of low sampling size.

5.3.4 Changes in SMI31 immunoreactivity with age and resveratrol-treatment

SMI31 labels phosphorylated neurofilament proteins. These phosphorylated neurofilaments have been shown to be included in NFTs [68]. In this study neurons could be categorized based on whether they exhibit excessive SMI31 immunoreactivity, SMI31^{+++}, or those exhibiting a lower level of SMI31 immunoreactivity as described in Section 5.2.3. SMI31^{+++} neurons were counted and compared between the age groups and OT areas (Figure 5.6A, page 99). SMI31^{+++} neurons decreased with the age of the OT and the fish. Statistical difference between the OT areas within the groups are given in Table 5.2. The pOT of 12 weeks old fish had more SMI31^{+++} neurons than the aOT and mOT. There was no statistical difference in SMI31^{+++} neuron numbers between the OT areas of the 34 weeks old and resveratrol-treated fish.

Resveratrol-treated 34 weeks old fish had significantly less SMI31^{+++} neurons in the posterior and anterior OT compared to the 12 weeks old fish. Only the aOT was statistically different between the 34 weeks old and resveratrol-treated fish. There was no statistical difference between the 34 weeks old and resveratrol-treated fish in the mOT and pOT. On average, the number of SMI31^{+++} neurons was the same in 12 and 34 weeks old fish and significantly less in resveratrol-treated fish ($p < 0.05$). As with the case of the total neurons, there was a trend for the chronologically younger OT areas to possess more SMI31^{+++} neurons.

As neuronal density declines with age and resveratrol-treatment the question was posed as to whether there is a disproportionate increase in SMI31^{+++}

neurons? The density of SMI31^{+++} neurons were therefore expressed as a proportion of the total neurons in each OT area as well as on average. These results are shown in Figure 5.6B and Table 5.2. This analysis showed that on average the SMI31^{+++} neurons did accumulate disproportionally in 34 weeks old fish and that resveratrol-treated fish had significantly less. No difference in SMI31^{+++} abundance was observed between the different areas in 34 weeks old fish while the pOT of 12 weeks old fish had more SMI31^{+++} than the mOT. No difference was found between the resveratrol-treatment group OT areas.

Rather than be associated with age of the tissue, SMI31^{+++} neurons are associated with the youth of the tissue. It seems more reasonable, in the case of *N. guentheri*, to conclude that SMI31^{+++} neurons are unintegrated neurons. NFTs have been shown to inhibit apoptosis by disrupting β-catenin signaling [118]. This signaling pathway is involved in neurogensis [112], neural migration [419] and the integration of newborn neurons into the neural network [420]. When the neuron fails to establish synaptic contacts they could use NFTs to disrupt β-catenin signaling to stave off apoptosis while synaptic connections can be forged. In the pOT there are many more SMI31^{+++} neurons because many more neurons are produced than can be successfully integrated. As such, the mice of Yang et al. [67], could have accumulated a larger density of unintegrated neurons as Aβ disrupted the synaptic connections.

With the age of the fish there is an average increase in the proportion of SMI31^{+++} neurons as predicted from the work of Yang et al. [67] and Wang et al. [66] who report that the accumulation SMI31 immunoreactivity is a sign of neurodegeneration. It is reasonable to assume that these are NFT laden neurons undergoing either degeneration or a failure to integrate. Whether resveratrol is preventing neurodegeneration, aiding in neuron integration or stimulating degenerate neurons to undergo apoptosis instead of linger in the tissue is unknown. The data indicates that with age the proportion of unintegrated neurons increases. SMI31^{+++} neurons could serve as a marker of neuronal circuit malfunction. As there is no difference in the proportion of SMI31^{+++} neurons between the OT areas of 34 weeks old fish, SMI31^{+++} accumulation (as a proportion of total neurons) is a reliable indicator of CNS aging and dysfunction.

Resveratrol could be potentiating malfunctioning neurons to apoptosis or autophagy by restoring β-catenin signaling. There is some support for this hypothesis. Wu et al. [421] have reported that resveratrol induced autophagy in a cellular model of Parkinson's Disease. Furthermore, Liu et al. [240] speculate that resveratrol could cause neuronal death under excitotoxic stress, particularly of cells which are energetically compromised (as discussed in Chapter 2, Section 2.5 on page 20). Alternatively, resveratrol-treatment could be improving synaptogensis and aid the integration of neurons.

5.3.5 Changes in E587$^+$ neuron abundance with age and resveratrol-treatment

Using the sizing criteria established in Section 5.3.2 the number of E587 immunoreactive (E587$^+$) neurons were counted in each OT area. This data is presented in Figure 5.7 (page 100) and Table 5.3.

On average, resveratrol-treated fish had significantly more E587$^+$ neurons than the 34 weeks old control fish. There was no significant difference between the resveratrol-treatment and 12 weeks old fish. Both had significantly more E587$^+$ neurons than the 34 weeks old fish. These differences between the 12 weeks and resveratrol-treatment groups versus the 34 weeks old fish were also present in the pOT. Resveratrol-treated fish had more E587$^+$ neurons in the mOT, but not the aOT which had established before resveratrol-treatment began. 34 weeks old fish had fewer E587$^+$ neurons in the aOT than the 12 weeks old fish but there was no difference between the 12 weeks and resveratrol-treated fish. While resveratrol had not rescued E587 immunoreactivity to 12 weeks old levels in the aOT it had slowed E587$^+$ loss from this area.

With age there was a significant decline in the proportion of small E587$^+$ neurons both in the pOT and on average. Resveratrol-treated fish had a significantly higher proportion of E587$^+$ small neurons in the aOT, perhaps implying that resveratrol had preserved the functional capacity of this OT area. With the decrease in chronological age of the OT there was a decrease in the proportion of small E587$^+$ neurons in the resveratrol group whereas there was an increase in the 34 weeks old fish implying that resveratrol-treatment preserved the functional integrity of older OT areas. Increases in the 12 weeks old fish is concomitant with growth.

Referring to the proportion of large E587$^+$ neurons there was only a significant difference between the 12 and 34 weeks old fish in the aOT. The resveratrol-treated fish also had a lower proportion of large E587$^+$ neurons in the aOT. There was no difference between the 34 weeks old and resveratrol-treated groups in the aOT. On average, the resveratrol group had more E587$^+$ large neurons than the 34 weeks old fish but no difference to the 12 weeks old fish. Based on the successful lifespan extension by resveratrol in this species, as regards the SGS of the OT, it is most likely the small and large neurons which are functionally significant.

Resveratrol-treated fish had on average significantly fewer E587$^+$ giant and amorphous neurons compared to the 12 weeks old fish. Also, resveratrol-treated fish had significantly fewer amorphous but not giant E587$^+$ neurons compared to 34 weeks old fish. The proportion of E587$^+$ amorphous neurons is almost double that of E587$^+$ giant neurons. Comparing Figure 5.5E with its counterpart, Figure 5.7E, it is apparent that almost half of the amorphous neurons in the 34 weeks old OT are E587$^+$. 12 weeks old and Resveratrol-treated fish had fewer E587$^+$ neurons than the 34 weeks old fish suggesting that these neurons are the dysfunctional neuron subtype. Resveratrol-treatment selectively reduces the quantity of amorphous and SMI31^{+++} neurons compared to

Table 5.3: Table of statistical differences of the proportion E587$^+$ neurons of the total SMI31$^+$ neurons per mm^2 between the three OT areas within each experimental group: 12, 34 weeks old and resveratrol-treated (RT). Samples sizes were $N = 3$ & $n = 15$ for the 12 weeks old group; $N = 4$ & $n = 21$ for the 34 weeks old group; and $N = 5$ & $n = 27$ for the resveratrol-treatment group. Statistically significant results are underlined.

Proportion E587$^+$ of total SMI31$^+$ per mm^2					
12 weeks old		**34 weeks old**		**RT**	
pOT vs aOT	$p = 0.219$	pOT vs aOT	$p = 0.541$	pOT > aOT	$\underline{p < 0.05}$
pOT vs mOT	$p = 0.219$	pOT vs mOT	$p = 0.541$	pOT vs mOT	$p > 0.05$
aOT vs mOT	$p = 0.219$	aOT vs mOT	$p = 0.541$	aOT vs mOT	$p > 0.05$
Proportion small E587$^+$ per total SMI31$^+$ per mm^2					
pOT vs aOT	$p = 0.240$	pOT vs aOT	$p = 0.238$	pOT vs aOT	$p = 0.182$
pOT vs mOT	$p = 0.240$	pOT vs mOT	$p = 0.238$	pOT vs mOT	$p = 0.182$
aOT vs mOT	$p = 0.240$	aOT vs mOT	$p = 0.238$	aOT vs mOT	$p = 0.182$
Proportion large E587$^+$ per total SMI31$^+$ per mm^2					
pOT vs aOT	$p = 0.461$	pOT vs aOT	$p = 0.478$	pOT > aOT	$\underline{p < 0.05}$
pOT vs mOT	$p = 0.461$	pOT vs mOT	$p = 0.478$	pOT > mOT	$\underline{p < 0.05}$
aOT vs mOT	$p = 0.461$	aOT vs mOT	$p = 0.478$	aOT vs mOT	$p > 0.05$
Proportion giant E587$^+$ per total SMI31$^+$ per mm^2					
pOT vs aOT	$p = 0.246$	pOT vs aOT	$p = 0.306$	pOT vs aOT	$p = 0.155$
pOT vs mOT	$p = 0.246$	pOT vs mOT	$p = 0.306$	pOT vs mOT	$p = 0.155$
aOT vs mOT	$p = 0.246$	aOT vs mOT	$p = 0.306$	aOT vs mOT	$p = 0.155$
Proportion amorphous E587$^+$ per total SMI31$^+$ per mm^2					
pOT vs aOT	$p = 0.199$	pOT vs aOT	$p = 0.867$	pOT vs aOT	$p = 0.930$
pOT vs mOT	$p = 0.199$	pOT vs mOT	$p = 0.867$	pOT vs mOT	$p = 0.930$
aOT vs mOT	$p = 0.199$	aOT vs mOT	$p = 0.867$	aOT vs mOT	$p = 0.930$
Proportion long E587$^+$ per total SMI31$^+$ per mm^2					
pOT > aOT	$\underline{p < 0.05}$	pOT vs aOT	$p = 0.318$	pOT > aOT	$p = 0.067^{\clubsuit}$
pOT vs mOT	$p > 0.05$	pOT vs mOT	$p = 0.318$	pOT vs mOT	$p = 0.067$
aOT vs mOT	$p > 0.05$	aOT vs mOT	$p = 0.318$	aOT vs mOT	$p = 0.067$

$^{\clubsuit}$ The Mann-Whitney Rank Sum Test gives $p = 0.020$ for the difference between the pOT and aOT. The differences for pOT vs mOT and aOT vs mOT is still insignificant using this test ($p = 0.491$ and $p = 0.122$ respectively).

other neuron types in the SGS.

There were no differences between the groups as regards the proportion E587$^+$ long neurons but there is a consistent trend for resveratrol-treated fish to have more than the control groups. A larger sample size may prove this trend to be significant.

The average proportion of E587$^+$ neurons was significantly reduced in 34 weeks old fish compared to 12 weeks old fish; but the proportion of E587$^+$ neurons was preserved to the level of 12 weeks old fish in the resveratrol-treated fish (Figure 5.7A). Most of the E587$^+$ neurons were either small or large neurons (Figure 5.7B&C). 34 weeks old fish had reduced small, large and giant E587$^+$ neuron proportions but no change in the proportion of amorphous neurons. While 12 weeks old fish had signicantly more amorphous SMI31$^+$ neurons than 34 weeks old fish, 34 weeks old fish had the same amount of amorphous E587$^+$ neurons. In effect, aging increased the relative density of the amorphous neurons to the other neuron types. Resveratrol-treatment reduced the number of these amorphous neurons. It seems likely that it is the inability to remove malfunctioning neurons which could be driving *Nothobranchius* neurodegeneration, not the loss of neurons per se.

This restoration of E587 immunoreactivity in resveratrol-treated fish provides a beginning for a molecular explanation for the improved operant learning observed in *N. furzeri* given resveratrol [5] as well as in other species [221, 246].

5.4 General discussion and conclusions

Resveratrol neuroprotection is believed to be due to resveratrol activating cell survival programs, be this through the activation of AMP-kinase [246] or the inhibition of microglial activation [291]. Various mechanisms were reviewed in Chapter 3. Resveratrol is predicted to preserve neurons into old age but here the opposite is shown: that resveratrol-treated fish have fewer neurons than 12 and 34 weeks old fish (Figure 5.5)—and there is no question that resveratrol did extend *N. guentheri* lifespan. Articles pertaining to resveratrol's neuroprotective role are studies of CNS injury or disease and not normal aging, for example see references: Wang et al. [358], Lee et al. [422] and Liu et al. [423]. These studies of pathological aging could be presenting a false impression of the mechanism of resveratrol neuroprotection. Widespread neuron loss is not a feature of normal aging [28, 29] so the preservation of neurons into old age is not needed as it would be in pathological aging such as AD and PD.

The neurobiologist, Steven Rose, contends that during development the brain produces many more neurons than it needs and that as these extra neurons are pruned they are replaced with glia and synapses [424]. This enhances connectivity and improves brain function. The improvement in connectivity is, according to Rose, associated with the maturing of the brain while in later senescence the synapses atrophy, causing a decline in connectivity and brain function. There is also evidence for the atrophy of glia with age [26] so the de-

cline in neurons may, in itself, not be a sign of neurodegeneration in *N. guentheri*. In the rat there is significant neuron pruning in the superior colliculus after birth which does not affect the number of optic connections [425]. In the goldfish the synaptic terminals have been observed to shift with age as the fish grows [124]. As the zebrafish grows as much as 95% of the neurons in the OT are new cells which have integrated into the existing OT or have been added on to expand the organ. The fish is dependent on constant plasticity in the OT as well as persistent route markers, much like the mammalian basal ganglia and limbic system which must retain plasticity while still anchoring long-term memories. The increased immunoreactivity to the plasticity marker E587 antiserum, against goldfish L1 [123, 163, 164], in resveratrol-treated fish (Figure 5.7) is more meaningful than the loss of neurons.

The inability with age to clear the amorphous E587$^+$ neurons (which may have been unintegrated or disconnected degenerate neurons) could be what prevents or upsets the maturing of the OT. The inability to mature the OT could be what leads to the short-circuiting of the neural circuitry which manifests as cognitive deficits.

This study focused on the SGS of the OT. Antibody penetration was $\approx 10\ \mu m$ in old fish. The effect of aging and resveratrol on neuron density in the deeper layers is still unknown with respect to the antibodies used in this study. One criticism which could be voiced is that in flattening the wholemounts between the coverslips the surface area was deformed. Volume increases exponentially relative to surface area. In flattening out the wholemounts of the larger, older fish the surface area would be spread out more. This is a valid concern which must be kept in mind when interpreting these results. This could hide an accumulation of neurons with age or create a false impression of neuron loss. For this reason the E587 immunoreactive results are most valuable.

Whether or not dilution occurred with the flattening of the OT, the density of E587 immunoreactive neurons increased in the resveratrol-treated fish relative to the 34 weeks old fish and the proportion of giant and amorphous neurons was reduced. Also, there was no change in the proportion of SMI31$^+$ large neurons and an increase in the number of SMI31$^+$ small neurons indicating that dilution of the neuronal density was meager. Another possibility which was not explored is that the resveratrol brains may have been larger in volume than the 34 weeks old control fish but this option would still need to contend with the similarity of the average density of large neurons and the increase in the small neurons.

Another methodological issue is that of using the correct stereological tools [426]. The method applied to determine neuron size subsets is not an accurate way to determine neuron diameter. When consistently applied it is an accurate means to determine neuron subtypes by their relative size. Accurate neuron sizes need to be determined using the Nucleator tool.

These results inspire several interesting questions, the most important of which is whether the E587 immunoreactivty correlates with behavioral outcomes. Whether the different neuron size groups constitute a gradual increase

in neuron size from small to giant as the neurons become dysfunctional, or different types of neurons (fulfilling different functions) is another question which needs to be addressed. In OT sections this variety of neurons is missed and thus ignored by the literature. The long neurons are closely associated with blood vessels running over the OT. Are these newborn neurons migrating from the proliferative zone adjacent to the valvula cerebelli? Both the 34 weeks old and resveratrol-treated fish have a higher density of long neurons but only the resveratrol-treated fish have more E587$^+$ small and large neurons. Whether the E587 immunoreactivity correlates with increased synaptogenesis in the OT is another question which needs to be explored. Rose postulates that the dying neurons are replaced by glia and synapses. Does the density of synaptic contacts change with aging in *Nothobranchius* as in other animals [427]; and does resveratrol correct for any decline which may occur? Changes in glial density have been measured and will be the focus of Chapter 6.

With reference to Rose's postulate, we hypothesize that resveratrol-treatment allows *N. guentheri* to more thoroughly clear dysfunctional neurons and, by so doing, enhance synaptic connectivity. In accordance with this hypothesis the number of E587$^+$ neurons should correlate with behavioral outcomes and the level of spine density and other markers of synaptic activity.

5.5 Figures

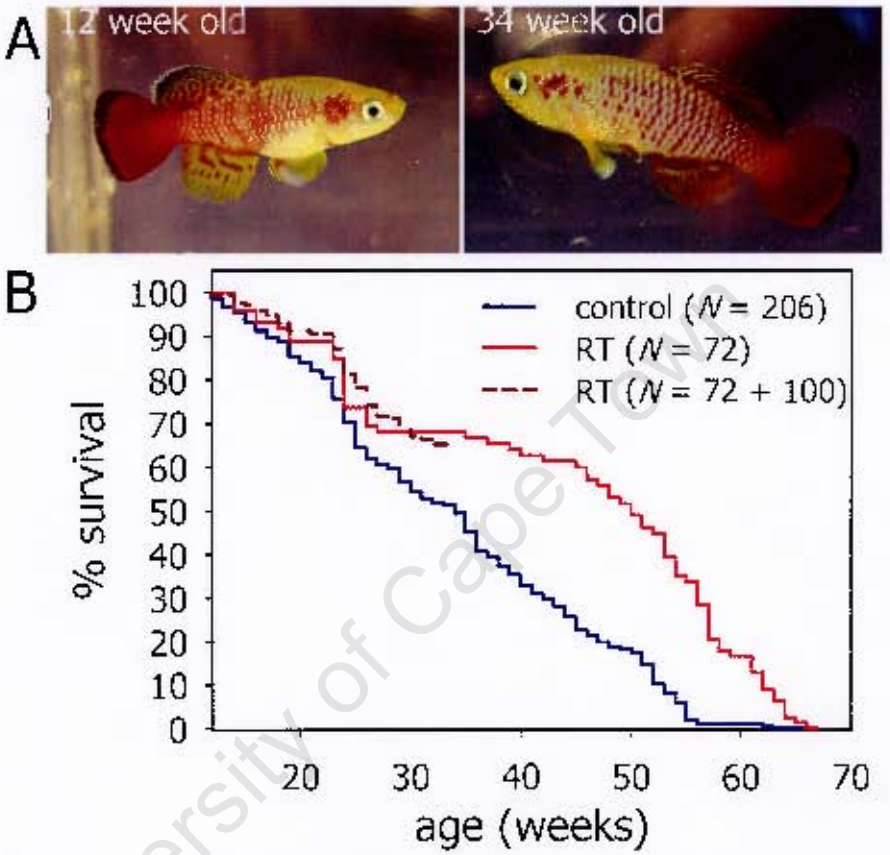

Figure 5.1: Survival curves for the *N. guentheri* control and resveratrol-treated groups. (A) Photos of a representative males of 12 weeks and 34 weeks of age. (B) 72 resveratrol-treated fish were left to live out their lives ($p < 0.0001$). A further 94 fish were raised to 34 weeks and sacrificed ($n = 100 + 72$, $p = 0.0127$). Median survival for the control group is 35 weeks and 50 weeks for the resveratrol-treated group. Maximum (10%) survival was 53 weeks for the control and 62 for the resveratrol-treated fish. The oldest control fish died at 63 weeks of age; and the oldest resveratrol-treated fish was 66 weeks of age.

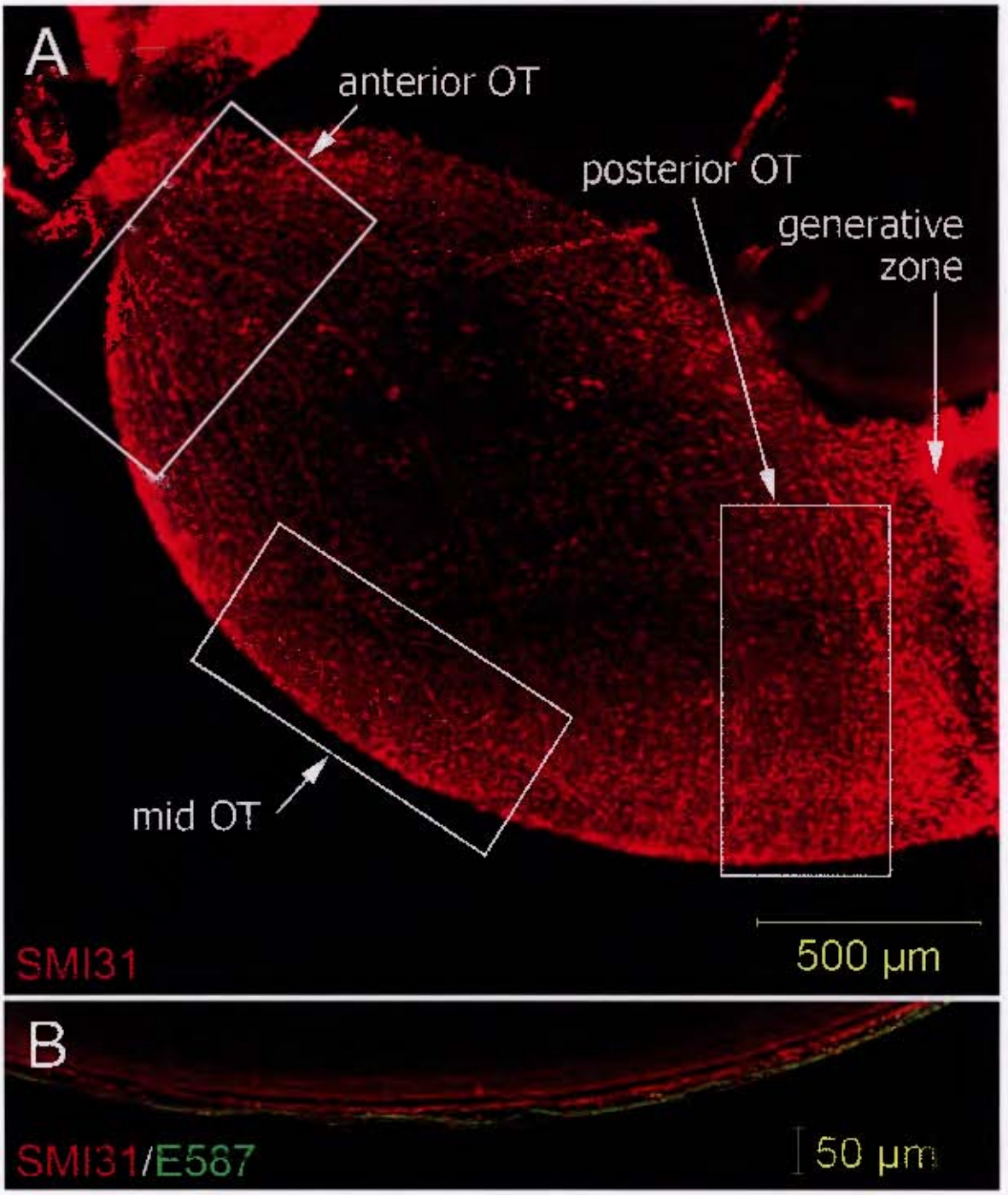

Figure 5.2: (A) Image of wholemount OT stained with SMI31 antibody. White boxes indicate areas examined for neuron counting. Note the position of the generative zone. (B) Tilescan along the edge of the OT along a deeper focal plane. Antibody penetration of 12 weeks old fish was complete in some specimens. Antibody penetration was ≈ 10 µm in aged fish.

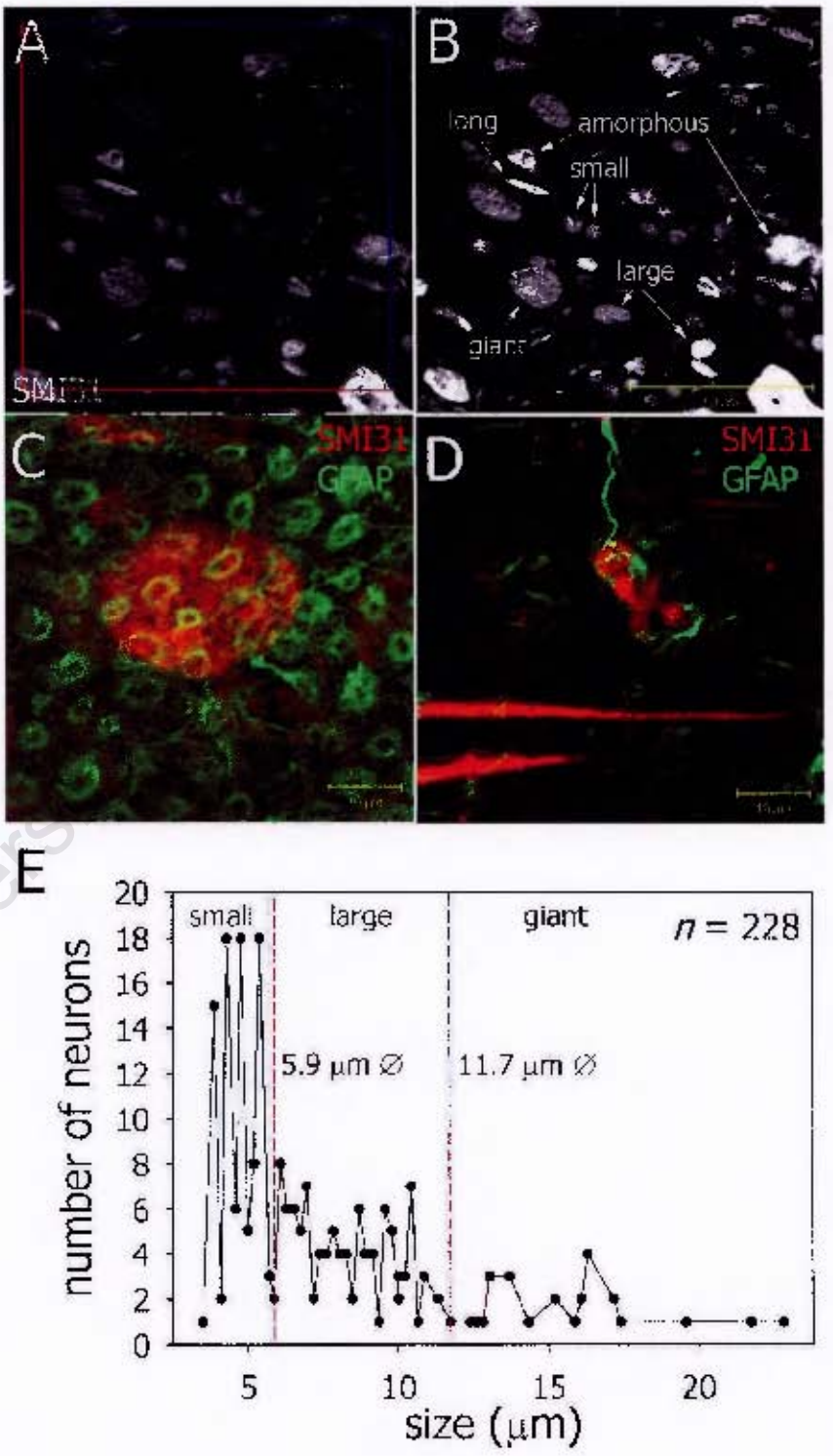

Figure 5.3: (A) Unenhanced grayscale image of neurons with SMI31 immunoreactivity. The red/blue-lined box indicate the limits for counting (neurons falling on the blue line were counted). (B) PhotoShop enhanced image of neurons with SMI31 immunoreactivity. The neuron sizes and/or types are visible. (C) Image of a giant neuron in the SGS. (D) A group of four small neurons serviced by an astrocytic process. (E) Graph of the number of neurons per size group with the demarcations between small, large and giant neurons indicated by a dashed line.

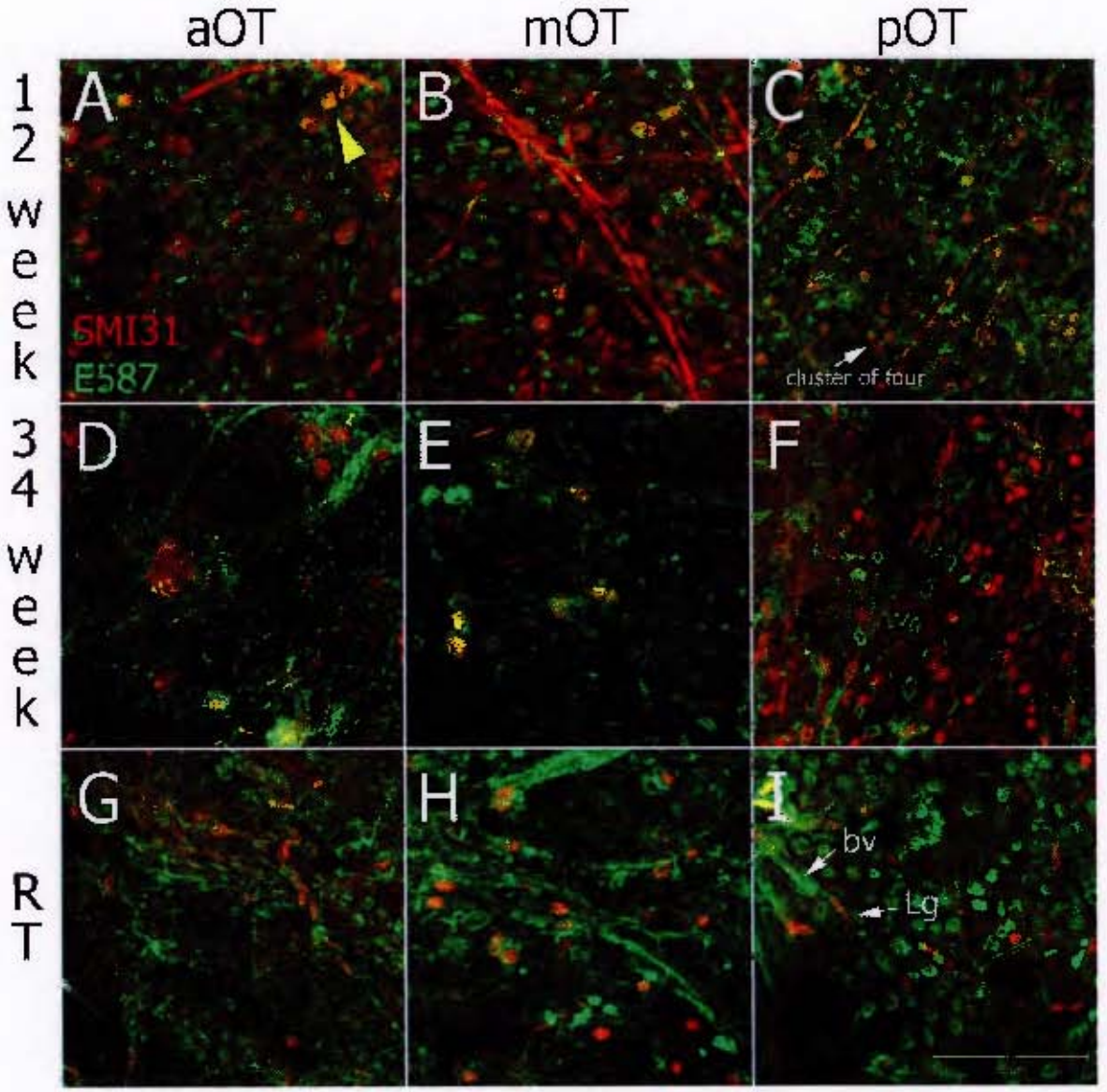

Figure 5.4: Panel of SMI31 immunoreactive neurons in the stratum griseum superficale lying among the E587 immunoreactive radial glia. An example of an E587^{+} neuron is indicated by the yellow arrow in (A). A group of four small neurons are indicated in image (C). Image (I) shows a long (Lg) neuron laying adjacent to an E587 immunoreactive blood vessel (bv). RT indicates the 34 weeks old resveratrol-treated group.

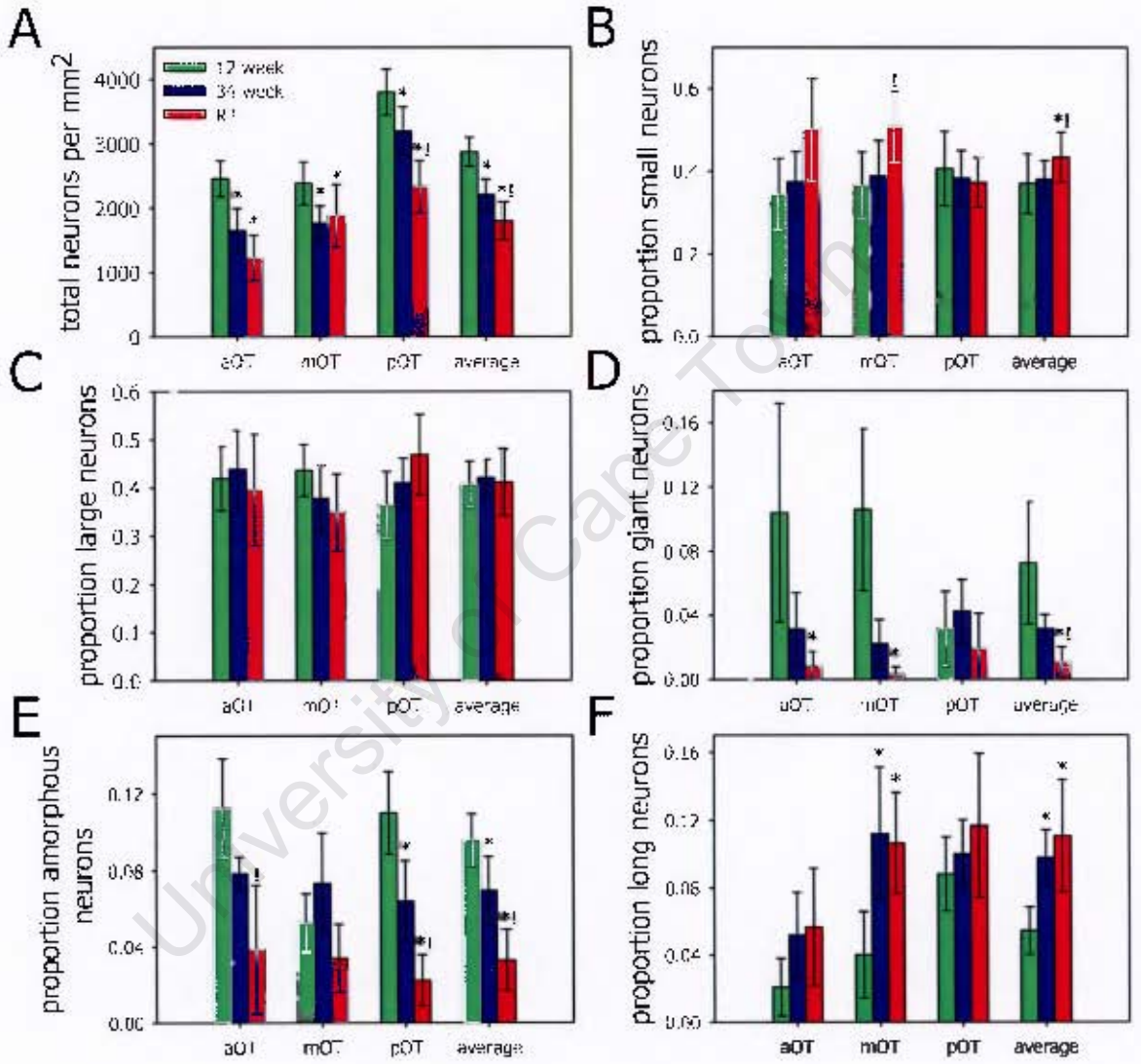

Figure 5.5: Graphs demonstrating the changes in neuronal density per OT area and average as measured by SMI31 immunoreactivity. (A) Age and resveratrol-treatment related changes in the total neurons of the SGS. Changes in the different types of neuron identified in Figure 5.3C are also shown expressed as the proportion total neurons (B–F). Asterisks indicate statistical significance between the 12 weeks group and the group under the asterisk. Exclamation marks indicate significance between the 34 weeks old and the resveratrol group. Error bars represent confidence intervals for $p = 0.05$. Samples sizes were $N = 6$ & $n = 32$ for the 12 weeks old group; $N = 9$ & $n = 39$ for the 34 weeks old group; and $N = 5$ & $n = 27$ for the resveratrol-treatment group.

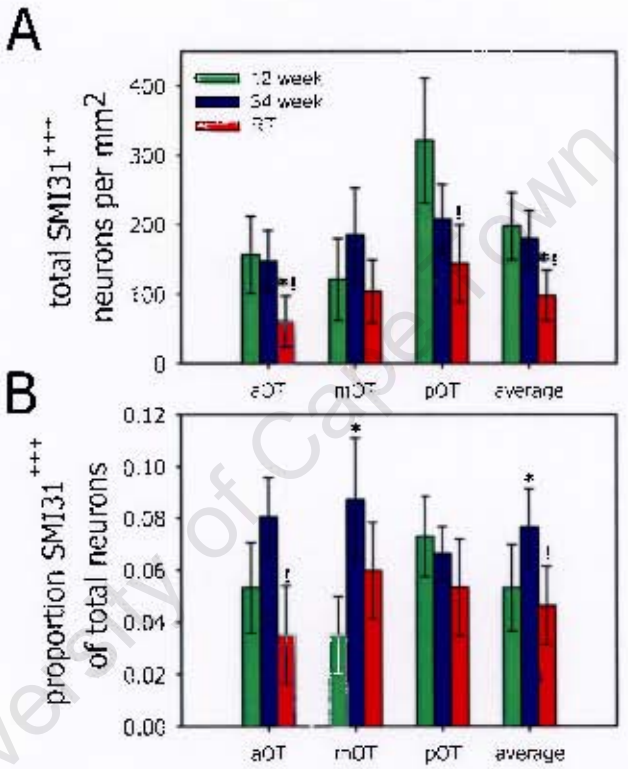

Figure 5.6: Graph of the number of neurons which have an accumulation of SMI31 immunoreactivity ($SMI31^{+++}$). (A) A graph of the number of $SMI31^{+++}$ neurons per mm^2 for each OT area as well as the average. There is no difference between the 12 and 34 weeks old fish average values but resveratrol-treated fish have less. (B) A graph of the proportion $SMI31^{+++}$ neurons of the total neurons per OT area. 34 weeks old fish have on average significantly more $SMI31^{+++}$ neurons than 12 weeks and resveratrol-treated fish. RT respresents the resveratrol-treated group. The asterisks indicate statistical significance between the 12 weeks group and the group under the asterisk. Exclamation marks indicate significance between the 34 weeks old and the resveratrol group. Error bars are confidence intervals for $p = 0.05$. Sample sizes are the same as for Figure 5.5.

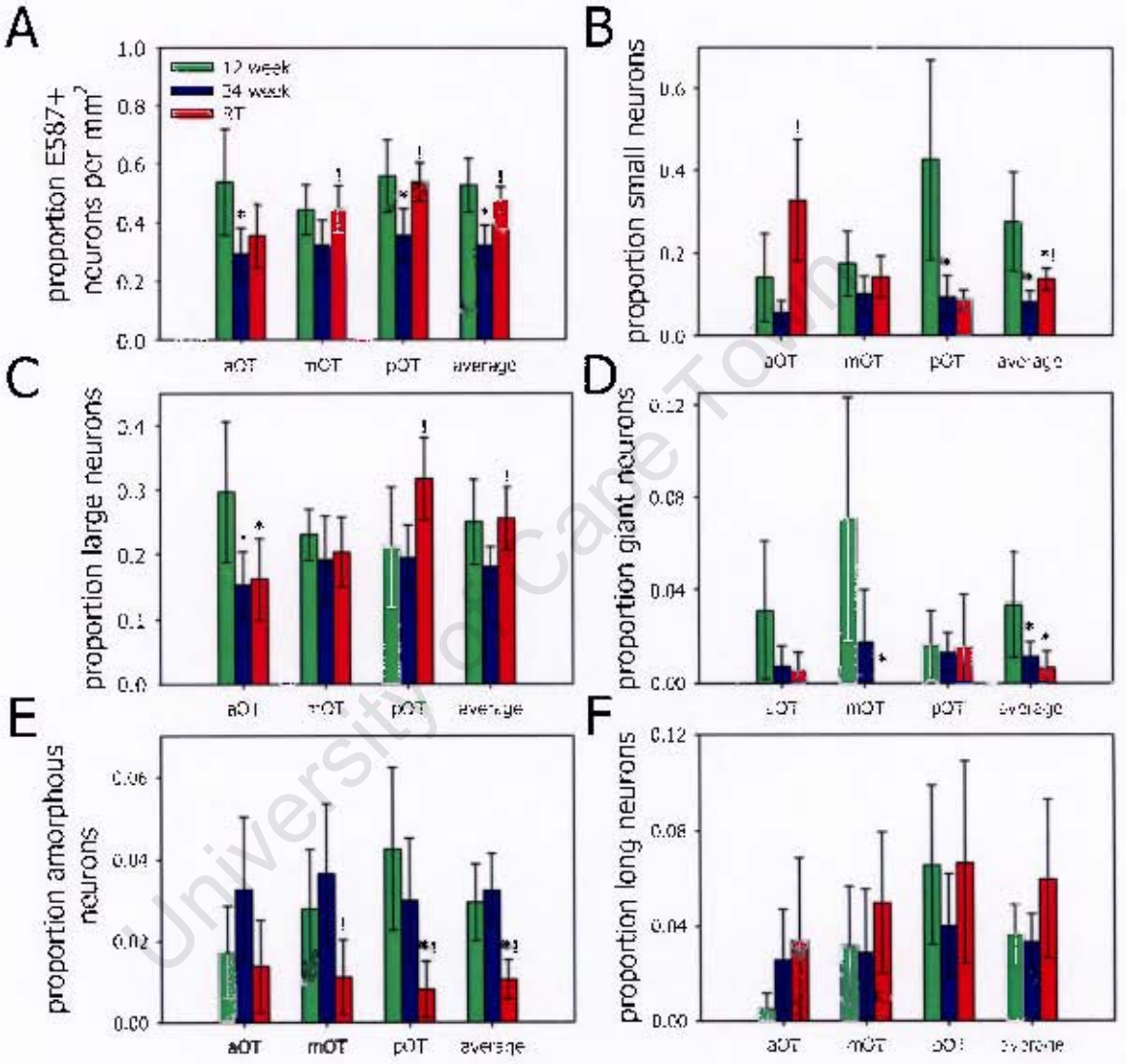

Figure 5.7: Graphs of the proportion of E587 immunoreactive neurons among the SM131 immunoreactive neurons. (A) Total E587$^+$ neurons in the SGS expressed as a proportion relative to the total number of neurons in Figure 5.5A. The proportion of each E587$^+$ neuron type is expressed as a proportion of the total number of neurons in panels B–F. RT is the resveratrol-treated group. Asterisks indicate statistical significance between the 12 weeks group and the group under the asterisk. Exclamation marks indicate significance between the 34 weeks old and the resveratrol group. Error bars represent confidence intervals for $p = 0.05$. Samples sizes were $N = 3$ & $n = 15$ for the 12 weeks old group; $N = 4$ & $n = 21$ for the 34 weeks old group; and $N = 5$ & $n = 27$ for the resveratrol-treatment group.

Chapter 6

The effect of age and resveratrol on *Nothobranchius* glia

You lacerate me with all of these memories,
And now I wear these scars out on my sleeve.

Chasing shadows at midnight, Pillar.

6.1 Introduction

In the previous chapter an age-related decline in OT neuron density was reported. This decline in neuron density was not remedied by resveratrol-treatment. Resveratrol-treatment did reduce the relative density of SMI31^{+++} neurons which can be interpreted as a decline in NFT bearing neurons. This was the interpretation of the resveratrol-treatment related decline in FJB signal reported by Valenzano et al. [5]. Damjanac et al. [25] reported that FJB labelled gliotic astrocytes and microglia. The FJB stain did stain the glia limitants of *N. furzeri* [10]. In the course of experiments to identify antibodies which could be used to label neurons and glia in the *Nothobranchius* CNS [382] differences were observed in the quality of the glia limitants between 12 and 34 weeks old *N. guentheri*. In this chapter the results of investigations of the *N. guentheri* glia limitans in the course of normal aging and resveratrol-treatment will be reported.

Wholemounts of 12 and 34 weeks old fish and resveratrol-treated 34 weeks old fish were prepared and incubated with antibodies against TNR, L1 and GFAP. These antibodies labelled defined CNS structures and cell types and are also implicated in synaptic plasticity.

TNR has a role in axon guidance [123] as well as the formation of PNNs which are involved in synaptic plasticity [137, 139]. Astrocytes are likewise in-

volved in plasticity: they are very active in laying down a suitable ECM which facilitates synapse formation. This is reviewed by Faissner et al. [138]. While PNNs are typically associated with oligodendrocytes the production of many PNN protein constituents are expressed by astrocytes and neurons [140]. TNR has been observed to associate with brevican (from astroglia) in PNNs [428]. While the E587 antiserum (against goldfish L1) labelled many structures and two cell types (neurons and astrocytes) in the *N. guentheri* CNS. It was used as an astrocyte marker.

PNN density has been observed to decline in specific brain regions in a functional and age-related manner in rats [147]. The knock out of cartilage link protein in mice resulted in persistent juvenile levels of ocular dominance plasticity as well as visual acuity sensitivity to visual deprivation [429] indicating that PNNs anchor neural circuits. PNNs have been demonstrated to play a role in establishing long-term memory [430]. They have also been shown to surround GABAergic neurons in the brain, the loss of which results in a loss of functional synaptic plasticity [137] implying that PNN surrounded neurons partake in top-down modulation of neural circuits. The operant learning assay employed by Valenzano et al [5, 6] was a visual task. It is reasonable that resveratrol may have exerted its operant learning preserving effect in *N. furzeri* by preserving the PNNs of the OT (and other brain regions). Such PNNs have previously been reported for gymnotiform fish [431] as well as goldfish [432]. TNR is reported to be expressed on the surface of oligodendrocytes in the CNS of mammals [140].

There is very little research on the effect of long term resveratrol supplementation on astrocytes and other glia. Most research has focused on astrocyte cultures or tissue slices. These results are reviewed by Quincozes-Santos & Gottfried [349]. Astrocytes are known to atrophy with age while a subset of astrocytes become gliotic and contribute to pathology [41, 110]. D'Angelo et al. [212] has demonstrated that *Nothobranchius* do not have astrocytes in the OT per se, but instead have radial glia lining the OT surface and ventricular zones. The Author thus set about comparing the state of the radial glia of young and old fish as well as fish administered resveratrol during the course of aging. As the OT was the object of focus in Valenzano et al. [5, 6] the Author continued to concentrate on this brain region.

Changes in radial glial density and morphology that were related to both aging and resveratrol-treatment were observed. Also observed were changes in the GFAP expression profile and the density of PNNs. In general, resveratrol had a positive effect on radial glial morphology, density per mm^2 and the number of large glial processes.

6.2 Methods and materials

6.2.1 Animal care and experimentation

Fish were cared for and killed as described in Chapter 5. All immunohistochemical experimental procedures are as described in Chapter 5. Differences from Chapter 5 are mentioned below.

6.2.2 Immunohistochemistry

The following primary antibodies were used at 1:400 dilution in blocking solution: E578 anti-L1 (gift from C. Stuermer, Konstanz Germany), GA-5 mab anti-GFAP (Sigma G6171), rabbit anti-bovine GFAP (DAKO Z0334) and mab anti-rat TNR (gift from P. Persheva, Bonn Germany).

6.2.3 PTAH staining for gliotic astrocytes

Fish were killed, the belly slit open, and fixed in Bouin's Solution for 24 hours. Fixed tissue was dehydrated in sequential 24 hour washes in 70% ethanol before being processed for paraffin impregnation. Fixed fish were imbedded in wax and sectioned at 5 μm and then fixed to APTES coated slides. Sections were taken to water and developed by the modified phosphotungstic acid hematoxylin (PTAH) method of Manlow & Munoz [433] after a 10 minute wash in 70% ethanol with a few drops of saturated lithium carbonate added (to extract the picric acid from the tissue).

6.2.4 Microscopy

Whole mount images were obtained using a Zeiss LSM S10 Meta NLO Confocal microscope (Jena, Germany). Images are representative of several specimens and were edited for publication using Adobe Photoshop CS2 v9.0.2.

For the counting of PNNs and large radial glial processes $221 \times 221\,\mu m^2$ optical frames were used. These frames were projections generated from a z-stack of $\approx 10\mu$m thick. For the counting of radial glia $110.5 \times 110.5\,\mu m^2$ optical frames were used. These frames were of a single 1.6 μm optical slice: PNNs and radial glia are present in the same plane. Only in-focus radial glia with a well defined shape were counted. Within the $110.5 \times 110.5\,\mu m^2$ frame a second $50 \times 50\,\mu m^2$ optical delimiter was applied for counting. Samples were taken as shown in Figure 6.1 and counts were made in triplicate for each area using $110.5 \times 110.5\,\mu m^2$ frames.

All PTAH positive cells in the entire stratum griseum periventriculare (SGPV) of the OT were counted. Only OT sections which passed though the valvula cerebelli (as in Woodhead & Pond [390]) were counted. Using a 40× lens the PTAH positive cells were counted by eye.

6.2.5 Western blotting

Western Blots were performed as in Genade & Lang [382] except that two extraction buffers were used: the NP-40 based buffer and a RIPA buffer. Composition of the RIPA buffer is as follows: 150 mM NaCℓ, 20 mM TRIS, 1% Triton X-100 (BDH, 30632) and deoxycholate (Sigma, D6750) and 0.1% SDS (Sigma, L4390). To complete the extraction buffer 20 μL 25x CPIC (Roche, 11697498001), 2.5 μL PMSF (Sigma P7626), 0.5 μL Aprotinin (Roche, 10236624001) and pepstatin A (Roche, 11359053001) was added to make up 500 μL buffer. The NP-40 buffer was composed as described in Chapter 4.2.2. The RIPA, on account of deoxycholate and SDS, is a strong disruptor of protein-protein interactions [434] whereas the NP-40 buffer is not. Extraction buffers were chilled to 4°C before use.

GA-5 was used for western blotting. The blots were developed using chloronaphthol as follows: after secondary antibody incubation the blots were washed in pH 7.4 50 mM TBS where after the developing medium was added. The developing medium consisted of 0.03% chloronaphthol in TBS. The mixture was filtered and H_2O_2 was added to a final concentration of 0.03% and then added to the blot. The blot was left to develop until the bands were resolved and the reaction stopped by rinsing in PBS. Blots were immediately dried and scanned. Blots which were to be compared were developed simultaneously in identical buffers and reagent solutions.

Scanned blots were analyzed using ImageJ [435]. Densitometric measures were standardized against the Ponceau S staining of the appropriate lane [436]. To determine relative changes in expression 12 weeks old and resveratrol-treated samples were measured and expressed as a fraction of the GFAP expression of the 34 weeks old control fish. To determine whether there was a change in the proportion of each GA-5 immunoreactive band between the age and treatment groups each band was measured relative to the total GA-5 immunoreactivity per lane.

6.2.6 Statistics

All statistical analyzes were performed as described in Chapter 5, page 82.

6.3 Results and discussion

6.3.1 Radial glial density declines with age and is partly reversed by resveratrol

Representative images of the OT of 12, 34 weeks old and resveratrol-treated 34 weeks old *N. guentheri* are shown in Figure 6.2 (page 115). Statistical differences between the OT areas pertaining to Figure 6.3 are given in Table 6.1.

With age the density of the radial glia declines (Figure 6.3A, page 116). Significant differences were recorded between 12 and 34 weeks old *N. guentheri* for all OT areas. Between 34 weeks old and resveratrol-treated *N. guentheri*

Table 6.1: Table of statistical differences of radial glia counts per mm^2 between the three OT areas within each experimental group: 12, 34 weeks old and resveratrol-treated (RT).

Radial glia per mm^2					
12 weeks old ($N = 10$ & $n = 38$)		**34 weeks old** ($N = 8$ & $n = 34$)		**RT** ($N = 4$ & $n = 24$)	
pOT > aOT	$p < 0.05$	pOT vs aOT	$p = 0.807$	pOT > aOT	$p < 0.001$
pOT > mOT	$p < 0.05$	pOT vs mOT	$p = 0.807$	pOT > mOT	$p < 0.001$
aOT vs mOT	$p > 0.05$	aOT vs mOT	$p = 0.807$	aOT < mOT	$p < 0.001$
Large radial glial processes per mm^2					
12 weeks old ($N = 7$)		**34 weeks old** ($N = 5$)		**RT** ($N = 4$)	
pOT < aOT	$p < 0.05$	pOT vs aOT	$p = 0.125$	pOT vs aOT	$p = 0.376^{\clubsuit}$
pOT vs mOT	$p > 0.05$	pOT vs mOT	$p = 0.125$	pOT vs mOT	$p = 0.376^{\clubsuit}$
aOT < mOT	$p < 0.05$	aOT vs mOT	$p = 0.125$	aOT vs mOT	$p = 0.376^{\clubsuit}$

$^{\clubsuit}$ A One-Way Analysis of Variance returned a p-value greater than 0.05 but the statistical power of the test (0.063) was below needed to be sure of the result (0.800). A more powerful analysis or more data may prove the differences to be significant.

significant differences were recorded between the mid, posterior and average radial glial counts. There was no statistical difference between the 12 weeks old and resveratrol-treated fish. Within the 12 weeks old group the glia become more diffuse with age and GFAP immunoreactivity becomes less. Comparing the 12 and 34 weeks old groups the glia have also become dysmorphic: they have lost their neat donut shape.

As well as there being a significant difference in radial glial density there was a visible change in radial glial morphology. There is a deterioration in the quality of the glia limitans with age both within the same age group moving from the anterior to posterior area as well as between age groups. As GFAP does not penetrate the fine processes [109] it was impossible to determine if these radial glia had differences in their domain size. It was impossible to control against different radial glial subtypes which would have confounded attempts to quantify the visible change in size. For these reasons no attempt was made to quantify this visible change in glial morphology. L1 is a surface protein in neurons and if so for glia as well then the colocalization of the E587 and GA-5 in Figure 6.2 could be taken as evidence for the shrinking of the glia with age. The radial glial cell bodies of 12 weeks old fish were well defined and rounded in shape compared to those of 34 weeks old fish (Figure 6.2). This rounder shape was retained by resveratrol-treated fish but the resveratrol-treated fish had larger radial glia as would be expected of gliotic glia. E587 labeling also revealed a more disorganized appearance (Figure 6.2), with the

E587 signal obscuring the radial glia.

Using E587 radial glia could be counted in young but not in aged fish. The E587 labelled wholemounts show that the glia are less well defined and obscured by some form of proteinaceous E587 serum immunoreactive matter. The brains of patients who had suffered from dementia have been reported to have more of the cleaved form of L1 (measured from the cerebrospinal fluid) compared to age-matched controls (with and without other neurodegenerative diseases) [47]. It is tempting to speculate that this E587 immunoreactive substance is cleaved L1 but until proteomic analysis of the E587 immunoreactive bands in Chapter 4 are completed this can only be an interesting, but undemonstrated, possibility. The glia limitans of resveratrol-treated fish had an appearance more like that of 12 weeks old fish: the glia were better defined (but still diffuse in the mid and anterior areas) but were also larger and showed stronger GFAP immunoreactivity.

A change was observed in the number of large glial processes (Figure 6.2, page 115 and Table 6.1) . These (including their branches) were counted by eye and the counts shown in Figure 6.3B, page 116. On average, 12 weeks old fish had more processes than 34 weeks old fish . As the OT ages (from posterior to anterior) the number of large processes increases significantly in 12 weeks old fish. In 34 weeks old fish there is no change in the number of large processes between the aOT and mOT while there were no large processes in the pOT. Resveratrol-treated fish exhibited large processes in all areas with the posterior areas having significantly more. The average across all areas was significantly different between the resveratrol-treated fish and 34 weeks old groups. There was no difference on average between the resveratrol and 12 weeks old fish.

The increase in the number of processes in 12 weeks old fish indicates that this is a sign of healthy aging and maybe functional maturity. In the rat, a decrease in astrocyte [437] and tanycyte [438] processes has been observed with age. This decline in processes was paralleled with an increase in GFAP in the rats. GFAP is one of several intermediate filament proteins in astrocytes which are involved in several physiological functions of astrocytes, not least of which is stabilizing the astrocytic processes [439].

Both the increase in large processes and hypertrophic form of the resveratrol-treated group glia are indicative of reactive gliosis [41]. In experiments using 3xTg-AD transgenic mice such hypertrophic astrocytes with large processes were observed associated with plaques [110]. Atrophic astrocytes were also observed and these correlated with the chronological age of the mice. It is now believed that reactive gliosis is an initially beneficial process (reviewed by Middeldorp & Hol [26]). The increase in processes may be an adaptive response to the aging/maturing tissue, perhaps making up for glia which have atrophied or the increase in synaptic maintenance. As can be seen from the data, this adaptive response is absent in aged fish.

As the glia in the aged brains carry a higher metabolic burden (they are more sparsely distributed over the same area) they may have greater metabolic

demands placed on them and hence become hypertrophic. As the fish grows over time the burden becomes greater but where normally aged glia are overcome the glia of the resveratrol-treated fish continue to react to the needs of the neurons. This would explain the observation that GFAP levels appeared to increase in dietary restricted *N. furzeri* [9]. The *N. furzeri* in the dietary restriction experiments also had improved operant learning indicating that their brains were healthier than age-matched controls.

6.3.2 PTAH staining shows an age-related increase in gliotic glia

The modified PTAH stain was used to assess the number of gliotic glia in each experimental group. Figure 6.4 (page 117) shows gliotic glia in the SGPV of 12 weeks, 34 weeks and resveratrol-treated 34 weeks old *N. guentheri*. There is a significant difference between 12 week and 34 weeks old fish but no statistical difference between 34 week and resveratrol-treated fish.

The PTAH stains confirm that in the SGPV of the OT there are gliotic radial glia in both the 34 week control and resveratrol-treated fish in the SGPV and that there is no meaningful difference between the counts. This stain could not be used to assay the number of gliotic glia in the glia limitans as the stain also binds to blood cells. The microtome-nicked blood cells were difficult to distinguish from nicked gliotic glia. It was impossible to estimate the number of processes in this area. That there are hypertophic/gliotic radial glia in both the SGPV and glia limitans but a significant lack of processes in the glia limitans of 34 weeks old control fish indicates to the Author that while the control group glia may stain PTAH positive, implying gliosis, these gliotic glia are no longer "reactive" to the extent that they do not participate in the compensation function of reactive glia in aging. Another method is required to distinguish between healthy and pathologically reactive glia.

6.3.3 Changes in GFAP Western Blotprofile with age

To confirm that GFAP levels were elevated in the resveratrol-treated fish Western Blots were developed using brain homogenates of the 12, 34 weeks old and resveratrol-treated fish. Proteomic analysis of GFAP from the brains of Alzheimer's Disease victims revealed that with age there is an increased misprocessing and concomitant aggregation of GFAP [381]. Protein was thus extracted using two different extraction buffers, the mild NP-40 based buffer and the harsher RIPA buffer. A formic acid extraction could not be performed at the time and there were only enough resveratrol-treated fish for the RIPA extraction. A large volume of protein was used in optimizing chemiluminescent detection. It was not possible to achieve adequate exposure of the faint bands without overexposure of the more prominent bands, rendering them unquantifiable. It was decided to revert to the chloronapthanol method which, being a simple cholormetric method, avoids the problem of overexposure of prominent bands.

Results pertaining to GA-5 anti-GFAP blotting are shown in Figure 6.5, page 118. The inset in Figure 6.5 is representative of anti-GFAP blots and shows four prominent GFAP bands from RIPA extracted 12, 34 weeks old and resveratrol-treated protein homogenates (each $N = 3$, $n = 6$) and NP-40 homogenates from 12 and 34 weeks old fish. The bands are 55, 51, 45 and 43 kDa. The 55–45 kDa bands are only clearly visible in aged and resveratrol-treated fish. 12 and 34 weeks old protein homogenates extracted using the NP-40 buffer were fainter. For the 12 weeks old fish only the 43 kDa band was clearly visible while larger bands are visible in the aged fish. Graph A of Figure 6.5 shows the relative change of each band compared to the protein levels of 34 weeks old fish while Graph B shows the proportion of each band compared to the total GFAP calculated from the sum of the bands for each fish.

For each band in Graph A there is an age-related increase. The GFAP levels of resveratrol-treated fish were less than for the 34 weeks old controls except for the 43 kDa band. 34 weeks old fish had twice as much GFAP as 12 weeks old fish. Resveratrol-treated fish had significantly less GFAP than 34 weeks old fish. 34 weeks old fish had significantly more of the 55 kDa band. Resveratrol-treatment restored the quantity of the 55 and 45 kDa bands to 12 weeks old levels.

Resveratrol-treated fish had a GFAP isoform proportion similar to that of 12 weeks old fish. There was no statistical difference between the 12 weeks old and resveratrol-treated proportions of the 55 and 43 kDa bands. This was even though there had been a relative increase in the quantity of the protein represented by the 43 kDa band with resveratrol-treatment.

Even though only three individuals of each age group were used for each of the RIPA and NP-40 extractions a clear difference was obtained between the three groups, with resveratrol preserving a level of GFAP expression closer to that of 12 weeks old fish. Also, there was less variation between the groups when comparing the ratios of the GFAP immunoreactive bands to the total immunoreactivity of the bands indicating that while the total quantities of GFAP

varies between individuals there is little inter-individual variation in the proportions of the isoforms. The relative proportions of the GFAP isoforms matters.

To make sense of the data in Figure 6.5 and understand how it can explain the observations of increased GFAP immunofluorescence in the whole-mounts we need recall that GFAP forms part of the cytoskeleton of glia and is involved in protein-protein interactions. The 55 kDa protein could be considered the full length protein and the others the degradation products [381]. Alternatively, the bands can be interpreted as different GFAP isoforms [26]. The isoforms vary in size, for example the human isoforms are GFAPα (49.9 kDa), GFAPδ/ϵ (49.5 kDA), GFAP-135, (44.5 kDa), GFAP-164 (42.1 kDa) and GFAP-exon6 (39.8 kDa) (E.M. Hol, pers comm, Netherlands Institute of Neuroscience). Fish do not have a full length exon 7a and thus do not make a GFAPδ of equal length as humans [440]. The GFAPδ isoform is associated with the human glia limitans and is indicative of cells with high cytoskeletal content. The ratio of the different isoforms to each other has been observed to affect the functionality of the cytoskeleton [441, 442]. A disproportionate increase in some isoforms causes a collapse of the cytoskeleton, generating protein aggregates [169, 441, 442].

The 55 kDa bands are not visible when the protein is extracted using the NP-40 buffer without deoxycholate. This indicates that the 55 kDa band is involved in strong protein-protein interactions and aggregated in the buffer, precipitating out of solution. 34 weeks old fish have significantly more of this isoform. As the disproportional expression of isoforms causes the collapse of the cytoskeleton this could explain the smaller size of the 34 weeks old radial glia (Figure 6.2). This could also explain the observed increase in GFAP immunoreactivity (as judged by IHC) of dietary restricted *N. furzeri* compared to age-matched controls [9] as well as the Author's observation of increased immunoreactivity in resveratrol-treated *N. guentheri*.

If the cytoskeleton collapses due to GFAP aggregation the GFAP epitopes would be unavailable for immunoreaction with antibodies. The increased immunoreactivity observed by the Author, as well as that observed by Terzibasi et al. [9], could be the result of the increased availability of the immunoreactive epitopes. The higher proportion of GFAP in the dietary restricted fish is a product of the low reactivity of the aggregated GFAP of old fish. The observed hypertrophy in Figure 6.2 is a consequence of increased metabolic demand on the surviving glia as well as the immuno-availability of the reactive epitope. Resveratrol-treated fish do have less GFAP than the age-matched controls. Repeating the dietary restriction experiments on *N. furzeri* along with proteiomic analysis could possibly confirm that those fish also have less GFAP and with age the GFAP is misprocessed.

Table 6.2: Table of statistical differences PNN counts per mm^2 between the three OT areas within each experimental group: 12, 34 weeks old and resveratrol-treated (RT). Samples sizes were $N = 4$ & $n = 11$ for the 12 weeks old group; $N = 4$ & $n = 7$ for the 34 weeks old group; and $N = 2$ & $n = 7$ for the resveratrol-treatment group.

PNN per mm^2					
12 weeks old		**34 weeks old**		**RT**	
pOT vs aOT	$p = 0.315$	pOT > aOT	$p = 0.073^{\blacklozenge}$	pOT vs aOT	$p = 0.127^{\blacklozenge}$
pOT vs mOT	$p = 0.315$	pOT vs mOT	$p = 0.073$	pOT vs mOT	$p = 0.127^{\blacklozenge}$
aOT vs mOT	$p = 0.315$	aOT vs mOT	$p = 0.073$	aOT vs mOT	$p = 0.127^{\blacklozenge}$

$^{\blacklozenge}$The Mann-Whitney Rank Sum Test gives $p = 0.017$ for this comparison. For the other sets $p = 0.376$ and 0.318 respectively. A larger dataset could provide statistically significant results.

$^{\blacklozenge}$The statistical power for this test was 0.239 which is below the desired power of 0.800. A more powerful test or additional data could determine a statistical difference.

6.3.4 Resveratrol preserves PNNs into old age

PNN are observed among the radial glia of the glia limitans of the OT (Figure 6.6, page 119). Antibodies penetrated approximately 10 μm deep in 34 weeks old fish and almost all the way through 12 weeks old fish. The Author cannot exclude the presence of PNNs in the deeper tissue of the tectum but has observed them around the nerves exiting/entering the spinal cord of wholemounted embryos which were ready to hatch (Figure A.10, page 148) indicating that they are widespread in the CNS of *Nothobranchius*.

With age there is a decline in PNN density between the 12 and 34 weeks old groups (Figures 6.6). Statistical difference between the OT areas is given in Table 6.2. PNNs are almost totally absent in the aOT in 34 weeks old fish. In both the mid and posterior section of the OT there is a statistically significant decrease in PNN density. There are almost three times as many PNNs in 12 weeks old fish compared to 34 weeks old fish. Resveratrol-treatment preserved PNNs with age in the mid and posterior areas of the OT. When averaging the total number of PNNs between old and resveratrol-treated fish a significant difference was recorded. There was also a significant difference between 12 and 34 weeks old fish. There was large variation between fish and even between OT hemispheres. There was no statistical difference between the OT areas within each age group indicating that the changes in PNN density are the consequence of intrinsic aging of the fish and does not have anything to do with the maturation of the OT.

Resveratrol-treatment partially preserved the density of PNNs in the anterior area of old fish while totally preserving PNNs in the mid and posterior areas. This indicates that not only did resveratrol preserve existing PNNs into old age but also preserved the functional capacity of the fish CNS. This is also seen in the $E587^{+}$ dataset were resveratrol-treatment increased the proportion of small neurons. Unless the neurons in the PNNs are integrated into neural

circuits, and these circuits are used, they would be lost [147]. The rescue of the PNNs in the mid and posterior areas could indicate that the brain retains aspects of plasticity which are lost in 34 weeks old controls. Regrettably, behavioral studies with the *N. guentheri* were not performed.

The decline in PNNs parallels the decline in radial glial density. The counter stain for the PNN counts was the rabbit anti-GFAP antibody or E587 antiserum and these stains were used to derive the radial glial counts and in so doing effectively linking the two datasets. While the PNN data set is small it is supported by the larger radial glial dataset. There is evidence for astrocytes regulating the expression of TNR [443]. In the enlarged images (Figure 6.6D, H & L) glial processes can be seen to penetrate the PNNs. Astrocytes (and oligodendrocytes) lay down the ECM which forms the PNNs so the preservation of active astrocytes may be all that is needed to preserve the PNNs [138]. Astrocyte transplants have restored visual system plasticity [134]. The inability of aged radial glia to support the PNNs could be a reason for their decline. The preservation of PNNs with the preservation of the radial glia is to be expected.

6.4 General discussion and conclusions

Fish grow throughout their lives. In the case of the OT, growth is from the anterior to the posterior, with new cells added at the posterior edge. Thus the anterior area of the OT is chronologically older than the posterior area. This provides the opportunity to assess the effect of aging not only on existing tissues but also on newly formed tissues. Data was presented which shows that the quality and quantity of the radial glia and PNNs change in the course of aging and resveratrol-treatment.

Radial glia and astrocytes play an important role in plasticity and synaptogenesis along with their role as metabolic support cells [444]. Terzibasi et al. [9] has demonstrated an increase in GFAP in dietary restricted *N. furzeri* which was concomitant with improved operant learning. Resveratrol is regarded as a dietary restriction mimic [278] so the lack of any increase in GFAP in resveratrol-treated fish is unexpected given the results in *N. furzeri*. This discrepancy can be explained away by Terzibasi et al. [9] not performing Western Blots to confirm the GFAP levels of the fish. GFAP has been reported to be misprocessed with age in humans [381], monkeys [101] and now *N. guentheri*. This misprocessing has been demonstrated to cause cytoskeletal collapse which would hide GFAP-antibody epitopes creating a false impression of reduced GFAP in age-matched controls. This discontinuity between the results of IHC (Figure 6.2) and Western Blots (Figure 6.5) highlight the need for reliable controls when comparing anti-aging interventions to age-matched controls. As discussed in Chapter 2.5, protein aggregation anomalies are common in aging. FJB could be staining dysfunctional glia in *Nothobranchius* along with degenerate neurons. The interpretation of results from *N. furzeri* where the FJB stain was used should be treated with caution.

Resveratrol has been reported to decrease gliotransmitter levels and p38

MAPK activation in cultured astrocytes [312] indicating that it does affect glia beneficially. It is possible that the increased activity of the glia in the dietary restricted and resveratrol-treated *Nothobranchius* is what ensures successful neurological aging in these species and the preservation of the PNNs which are required for cognitive retention [430], plasticity [139] and motor acuity [147]. It is also possible that resveratrol is directly disrupting protein aggregation [270] which would ordinarily cripple a cell (see Chapter 3.2, page 42).

The retention of the PNNs and active astrocytes into old age is one hypothetical means whereby operant learning is retained into old age in *Nothobranchius*. Karetko-Sysa et al. [445] showed that following discrete cortical injury, the PNNs adjacent to the injury were lost but there was little loss of neurons. They suggest that the loss of PNNs may be to release the brakes on synaptic plasticity [139] so that the brain may functionally regenerate, however, in old *N. guentheri* they do not regenerate. Neurons in the SGS are lost with advancing age (Chapter 5) and in particular E587$^+$ neurons. With the decline in E587$^+$ neurons, indicating a decline in synaptogenesis, the neurons in the PNNs may be unable to reintegrate into the neural circuitry (and thus never reform the PNN). PNNs not only put the brakes on synaptic plasticity but also serve as anchors for the neural circuits. The loss of the PNNs would prevent surviving neurons from functionally integrating into the OT as well as hinder attempts at regeneration.

Sample sizes for the determination of radial glial density, PTAH positive gliotic astroctyes and the number of processes were sufficient for statistical analysis. The Western Blotdata correlates with the statistically meaningful results and the PNN counts are linked to the statistically relevant glial density data as a counter stain. The Western Blotdata becomes more meaningful in conjunction with the larger data sets, both explaining and reaffirming the conclusions drawn from the larger datasets. It is the opinion of the Author, based on the coherency of the data, that with age there was a dysregulation of the GFAP isoforms represented by the four bands (whether these are protein degradation products or genuine isoforms the Author cannot conclude at this time); and that resveratrol-treatment returned the banding profile to that of 12 weeks old fish. With regard to PNNs, there is an age associated loss of PNNs. Resveratrol-treatment preserved the PNNs implying that resveratrol improved OT health and function.

To aid further research the cloning and characterization of the *Nothobranchius* GFAP gene and its processing, together with proteomic analysis of identified bands are needed. Antibodies specific to each band are essential to allow for cytological studies, not only to observe where the various isoforms localize to but how they interact with the cytoskeleton. More interesting, is determining whether there are radial glia subtypes [26, 399] in *Nothobranchius* which may play different physiological roles. In light of the glial simplicity and accessibility of this model organism it could be exceedingly useful in learning the roles of the various glial subtypes (should they exist in the fish as in mammals). This is all the more pressing in light of the stronger correlation between

glial atrophy and human age (and senile dementia) than with pathological neuron loss (which drives Alzheimer's Disease research) [41].

6.5 Figures

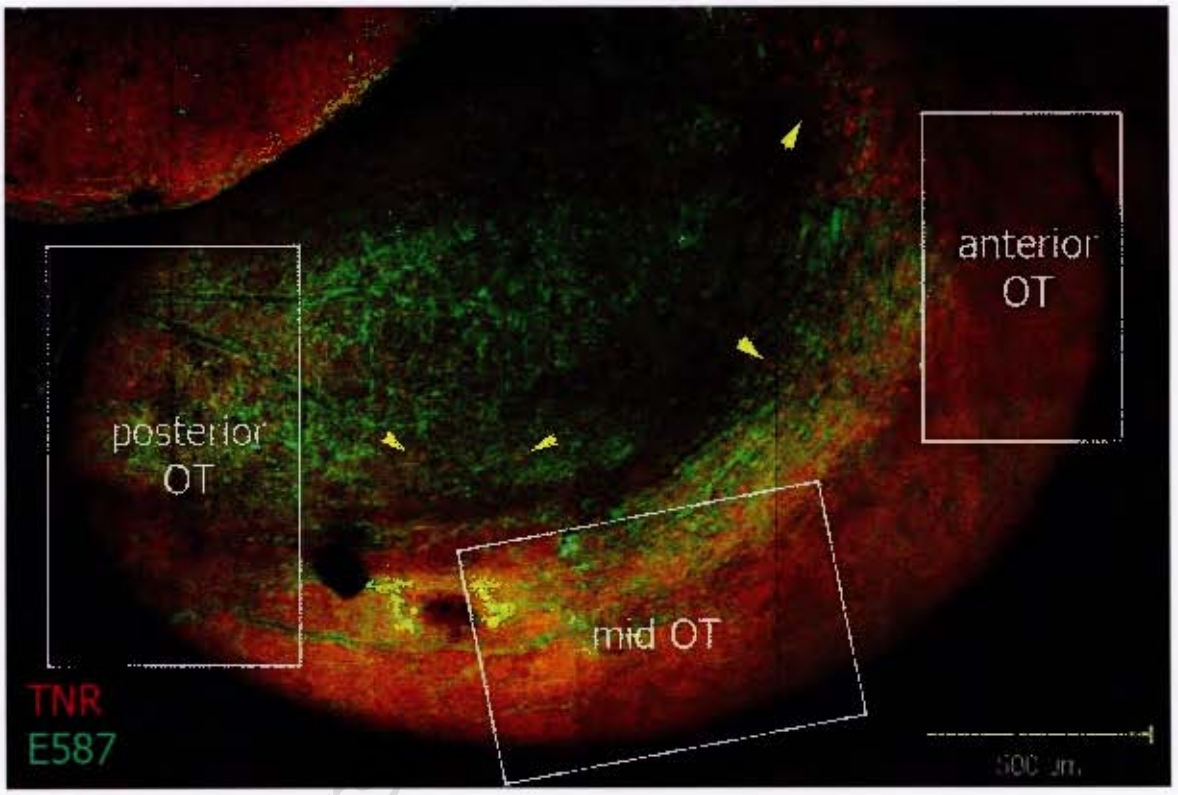

Figure 6.1: Tilescan of wholemounted *N. guentheri* optic tectum stained with anti-TNR and E587 antiserum. The areas of interest are indicated on the figure. PNNs (examples indicated by yellow arrowheads) are visible lying on the OT surface in the glia limitans.

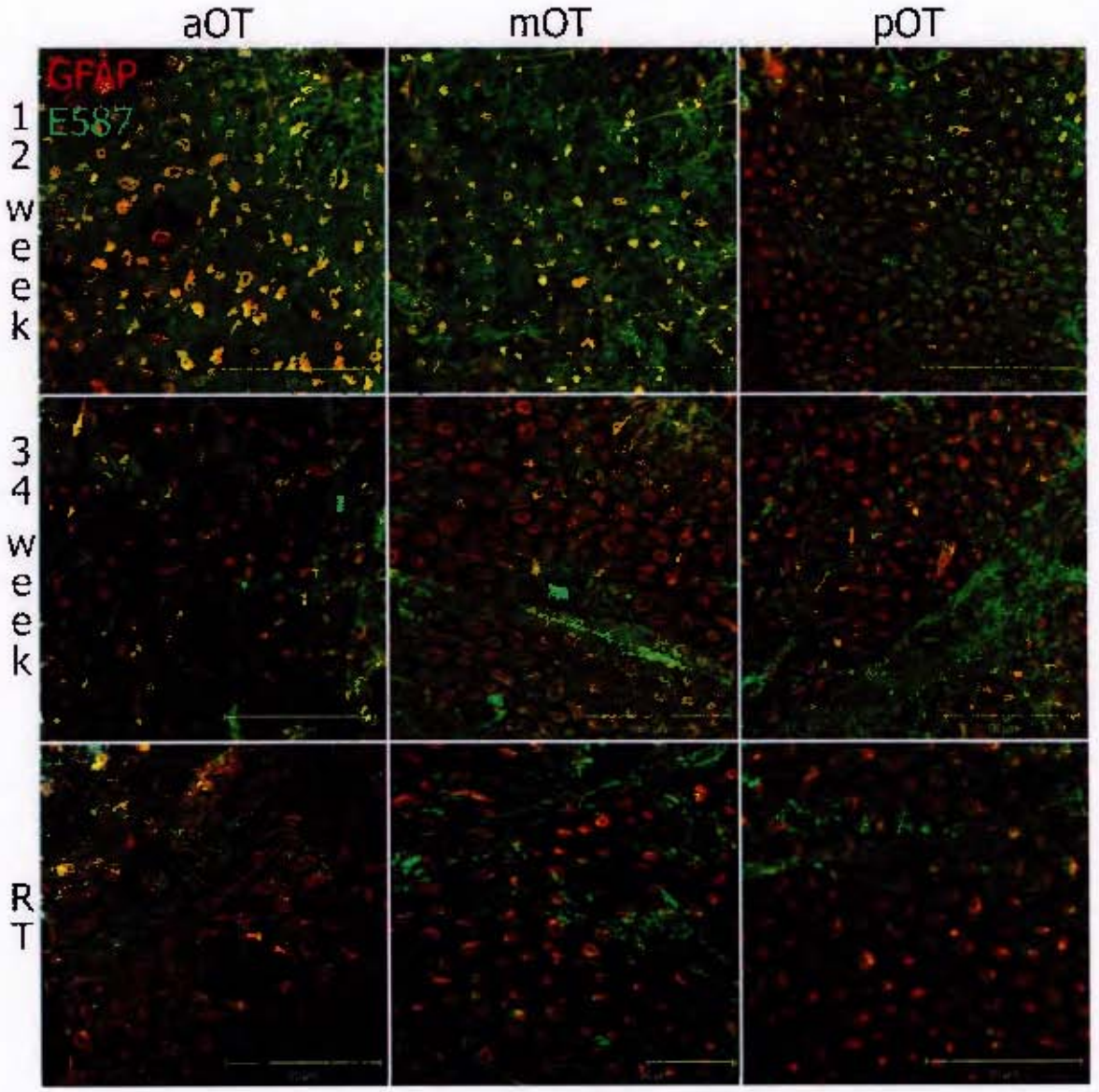

Figure 6.2: GA-5 anti-GFAP and E587 antiserum labelled OT of 12 week, 34 week and 34 week resveratrol-treated (RT) *N. guentheri*. Representative images are shown for the anterior, mid and posterior areas of the OT. GA-5 anti-GFAP and E587 antiserum colocalize on radial glia in the glia limitans. Note the larger radial glia in older fish as well as the older areas of the OT in 12 weeks old fish. 12 weeks old fish have more E587 immunoreactive background in the tissue compared to older fish.

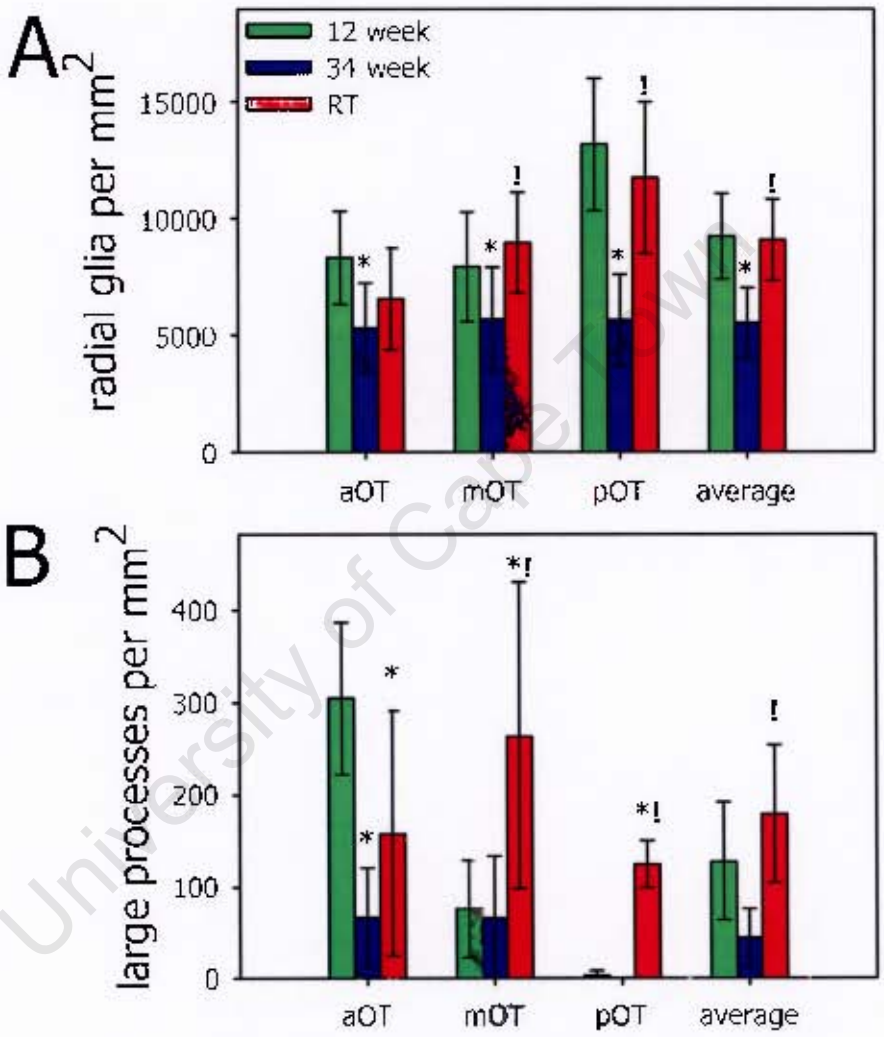

Figure 6.3: Graphs comparing (A) radial glial density per mm^2 and (B) large processes between 12, 34 and resveratrol-treated 34 weeks old *N. guentheri*. Asterisks denote significant differences between 12 and 34 weeks old groups; and exclamation marks denote significant differences between 34 weeks old and resveratrol-treated fish. Error bars represent 95% confidence intervals. For (A), 12 weeks old group is $N = 10$, $n = 38$; 34 weeks old group is $N = 8$, $n = 55$; and resveratrol group $N = 4$, $n = 24$. For (B) $N = 7$, 5 and 4 respectively.

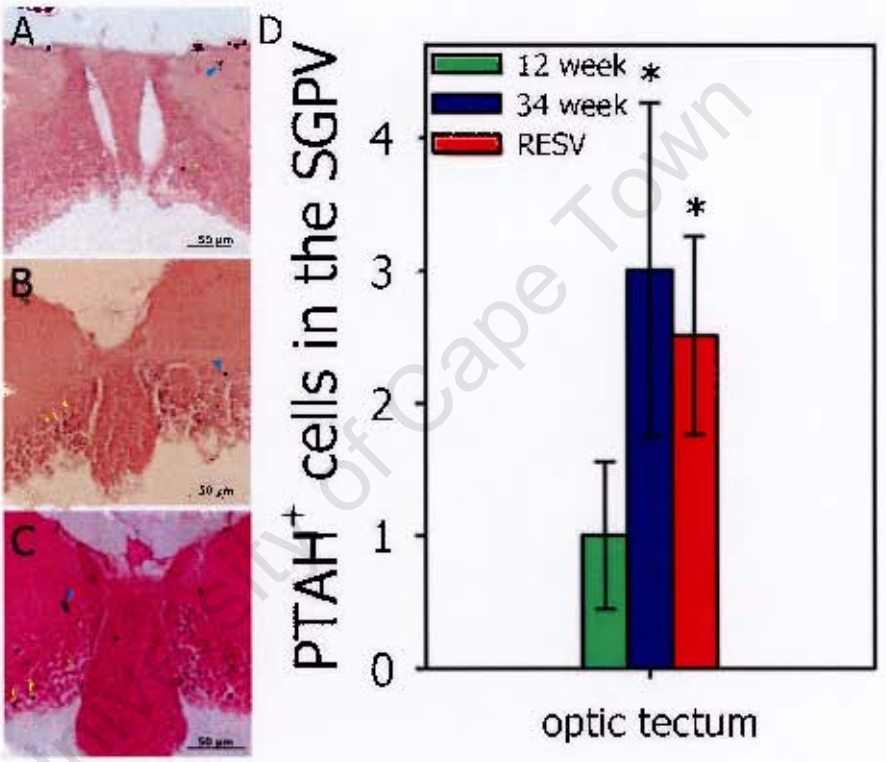

Figure 6.4: Modified PTAH stained gliotic glia in the SGPV of the OT lying adjacent to the valvula cerebelli. A) 12 weeks old fish, B) 34 weeks old fish and C) resveratrol-treated fish. Graph D shows an increase of PTAH positive cells in 34 weeks ($N = 6$, $n = 17$) and resveratrol-treated fish ($N = 5$, $n = 17$) relative to 12 weeks old fish ($N = 6$, $n = 11$). Yellow arrow heads indicate PTAH positive cells; blue arrows indicate possible nicked blood cells. Asterisks indicate statistical differences comparing 12 weeks old fish to each of the other groups ($p \ll 0.05$). Error bars represent 95% confidence intervals.

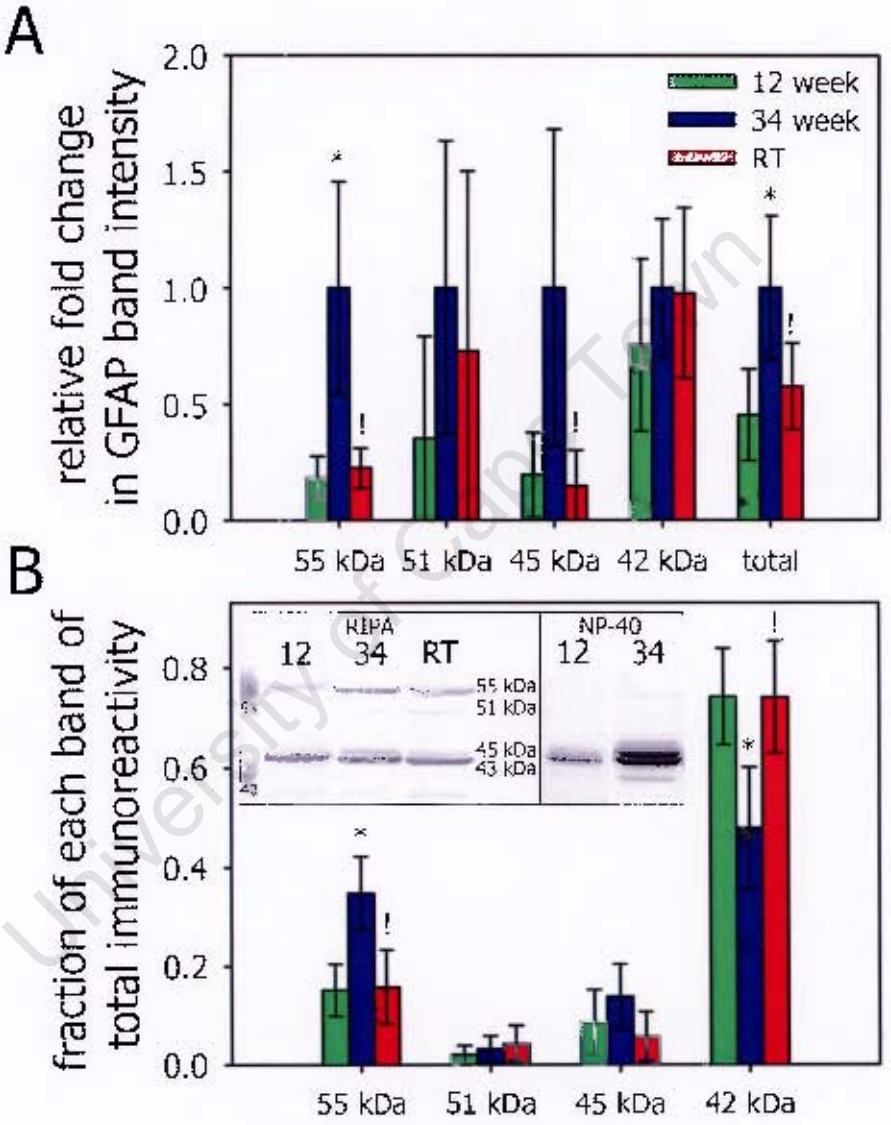

Figure 6.5: Comparison of GFAP expression between 12, 34 and resveratrol-treated 34 weeks old *N. guentheri*. Inset: representative blot denoting analyzed anti-GFAP reactive bands. (A) Differences in GFAP bands relative to 34 weeks old fish. (B) Differences in each GFAP band relative to total GFAP of each fish. Error bars represent 95% confidence intervals. $N = 3$ and $n = 6$ for each group.

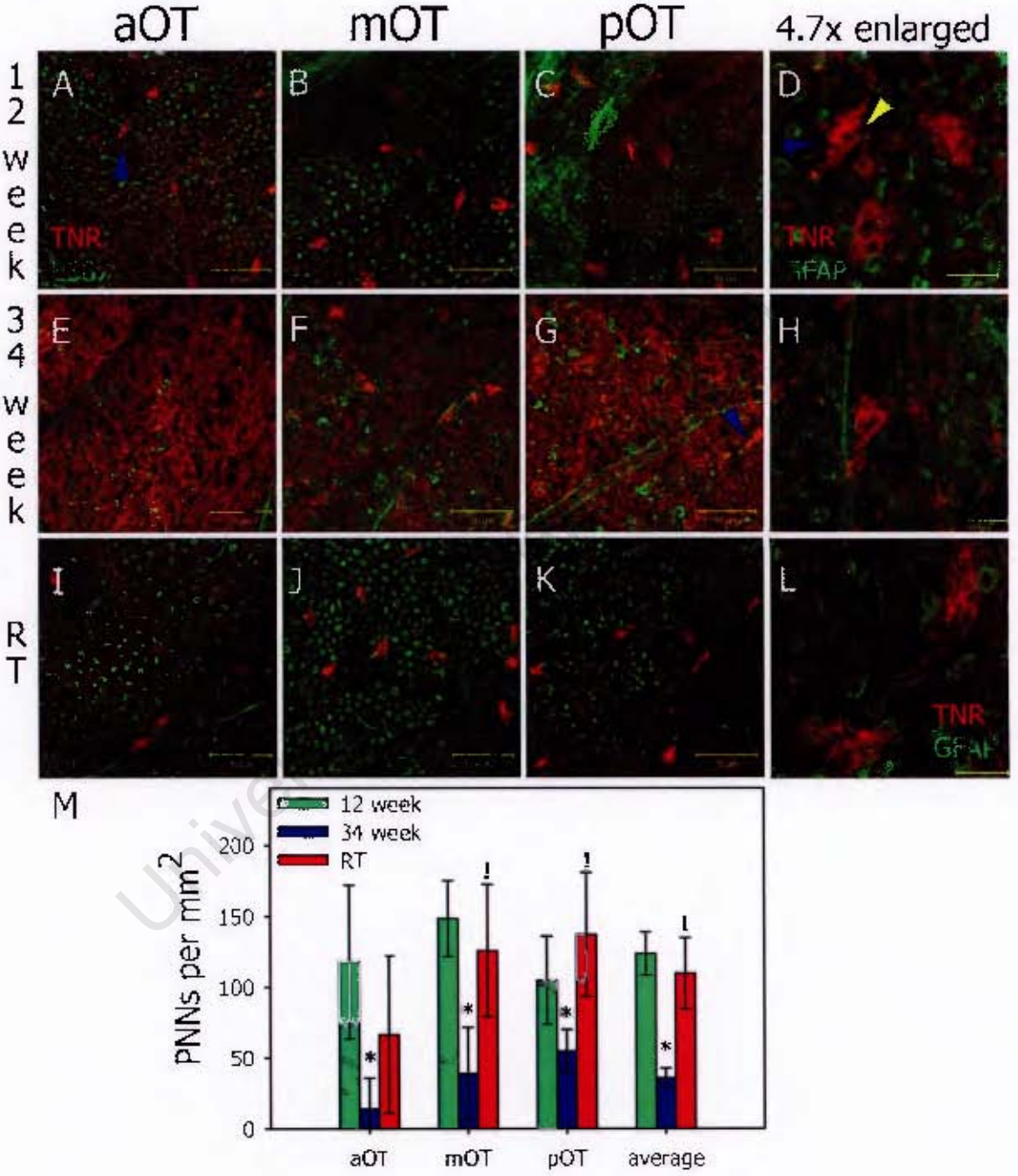

Figure 6.6: Comparison of PNN density between 12 weeks (N = 4, n = 11), 34 weeks old (N = 4, n = 7) and resveratrol-treated(N = 2, n = 7) *N. guentheri*. A–D of 12 weeks old fish PNNs (examples indicated by blue arrows) and images E–H of 34 weeks old fish PNNs; staining with anti-TNR and E587 antiserum. I–L, images of resveratrol-treated fish PNNs; staining with anti-TNR and anti-GFAP. Images D, H and L are enlargements of PNNs. Note glial interactions with the PNN (yellow arrow image D). Graph M compares PNN density as PNNs per mm^2. Asterisks indicate significance between 12 and 34 weeks old fish. Exclamation marks indicate significance between 34 week control and resveratrol-treated fish. Error bars are confidence intervals for p = 0.05.

Chapter 7

General Discussion and Conclusions

Who is this man?
Caesar, he is but a soothsayer,
he is old and his brain is addled,
pay him no mind!

Caeser, Iggy Pop.

The purpose of this study was to identify cytological probes by which to study neurodegeneration in *Nothobranchius*. To accomplish this purpose *N. guentheri* was selected as our experimental subject on account of its ease of culture and longer lifespan. The longer lifespan allowed for better temporal resolution between youth and old age which could allow for easier identification of aging-dependent cellular and anatomical changes. Three experiments were performed. In the first experiment: fish were raised to sexual maturity and allowed to age normally with the intention of analyzing 12 and 34 weeks old brains in search of aging-dependent changes. In the second experiment: fish were raised to sexual maturity and treated with resveratrol through the course of their natural lives with the intent of identifying resveratrol-treatment dependent differences between resveratrol-treated and 34 weeks old control fish. Thirdly, while the fish aged a variety of antibodies were tested for immunoreactivity against *N. guentheri* tissue and protein extracts. The results of these experiments are discussed in this chapter with references to the expected outcomes raised in the review chapters and within the framework of aging research. Also included in this chapter (because it would have necessitated a large digression from the focus of Chapter 5) are the results and discussion of the hazard functions pertaining to resveratrol-mediated lifespan extension of *N. guentheri*. In the last section future research directions will be discussed.

7.1 Review of the antibody toolkit

The results of antibody testing are reported in Chapter 4. The E587 antiserum and SMI31, GA-5 anti-GFAP and Z0334 anti-GFAP and anti-TNR proved useful but unanswered questions persist. The nature of the multiple GFAP immunoreactive bands needs to be resolved, particularly with respect to Chapter 6. Likewise, just what E587 is reacting against needs to be determined. It is almost certainly reacting against *Nothobranchius* L1-NCAM but may in addition be reacting against other NCAMs. These antibodies were effective for the purpose they were used for: labeling particular cellular structures and cell types as well as determining age-related changes.

While the fish neurofilament proteins are of various sizes [397] they are used much the same across the evolutionary lineages [396]. The SMI31 antibody labels a specific evolutionary conserved phosphorylated neurofilament epitope [398]. These phosphorylation sites are important for the dynamic regulation of the neurofilaments [396]. The dynamics of *Nothobranchius* neurofilaments are probably not very much different to that of mammals. Similarly, the evolutionary conserved L1 [383, 446] seems to be at work in *Nothobranchius* as in other species: playing a role in neuron preservation [165, 416] and possibly synaptogenesis [415]. As in rodents L1 appears here to also be expressed by only a subset of neurons [414].

The GFAP banding is remarkable. While most demonstration blots (by antibody manufacturers) only show a single band of the typical size the reality is that GFAP antibodies label several bands over a defined size range [381]. The human GFAP exists as several isoforms ranging in size from 49.9 to 38.9 kDa. A similar variety of GFAP bands were observed against the *Nothobranchius* brain homogenates implying that *Nothobranchius* GFAP may be processed much the same as in mammals.

Further research is required to confirm the identities of the antigens labelled by the antibodies as well as confirm the function of these proteins in *Nothobranchius*. In so doing the changes observed at the cellular level can be related to molecular physiology of these proteins.

7.2 Does *N. guentheri* age like other species?

For *Nothobranchius* to be useful models of aging they must manifest signs of aging common to other species and in particular they should show signs of aging in common with mammals. Several signs of neurodegenerative-aging were discussed and from them predictions were made of what would be discovered using the antibodies introduced in Chapter 1.

These predictions are as follows:

- *Nothobranchius* would accumulate SMI31 epitope in a subset of their neurons as in other species undergoing neurodegeneration.
- That L1 and other NCAM positive neurons would decrease with aging.

- GFAP expression would increase in the course of aging as...
- ...glia are observed to malfunction.
- *Nothobranchius* would show a decrease in PNNs with age.
- That neurodegenerative-aging would involve one or several protein aggregates or misprocessed proteins.

The neurodegeneration literature predicts massive neuronal loss but this is based on pathological aging, not normal aging. Normal aging correlates more with a general atrophy of the white matter, not that of the gray matter. Whether *Nothobranchius* neurodegeneration would show pathological aging (with massive neuron loss) or normal aging, characterized by glial atrophy, was a question the Author wished to answer.

7.2.1 SMI31 epitope accumulates with age

In Chapter 5 evidence was presented supporting the use of the SMI31 antibody to label degenerating neurons. With age SMI31 immunoreactivity did accumulate in a subset of neurons in *Nothobranchius* even though it also labelled healthy neurons as has been previously reported and discussed in Section 5.1 (Figure 5.6). Using the SMI31 antibody several possible neuron subtypes could be discerned in the OT of *Nothobranchius*. Of interest were the small and large neurons which appear to be the normal, functional neurons. This was hypothesized based on changes in the expression of E587 antigen on the neurons (discussed in Section 5.4).

The accumulation of SMI31, which is linked with the accumulation of NFTs in neurons, supports our initial interpretation of FJB accumulation in *N. furzeri* being due to an increase in NFTs [5]. However, as there is also evidence of glial malfunction, the increase in FJB signal could be the consequence of glial malfunction as well as NFT accumulation. In the light of Damjanac et al. [25] it is better to consider FJB a general marker of neurodegeneration than a specific indicator of NFTs or glial malfunction.

7.2.2 Neuronal expression of E587 antigen declines with age

The use of the E587 antiserum, raised against goldfish L1, revealed that there is a $E587^+$ population of neurons in the *Nothobranchius* OT (Figure 5.7). The $E587^+$ subpopulation of neurons declines with age as predicted from research performed on mammals [47, 166] where the loss of NCAM was concomitant with the decline in cognition of mammalian model organisms. *Nothobranchius* have been demonstrated to exhibit such a decline in cognition with age. This is useful information for the formulation of hypotheses to tie functional outcomes with molecular events.

7.2.3 GFAP expression and misprocessing increased with age

With age GFAP accumulated in the radial glia of *N. guentheri* (Chapter 6, Figure 6.5). Analysis of Western Blots indicates that with age there is a significant increase in one of the GFAP immunoreactive protein bands and that the proportion of the GFAP isoforms was disturbed. Western Blots of protein homogenates extracted using different buffers indicate that the disproportionate increase in the 55 kDa GFAP isoform caused the GFAP filaments to aggregate and precipitate out of solution. This discovery explained why, even though the 34 weeks old fish had more GFAP than the 12 weeks old fish, the wholemounts of 12 weeks old fish appeared to express more GFAP. A similar misprocessing of human GFAP is reported by Korolainen et al. [381].

7.2.4 Radial glia atrophy with age

There was a significant decline in the abundance of radial glia as the fish aged (Chapter 6, Figure 6.3). This is congruent with research on mammals where similar glial atrophy has been observed [110] even while there was an age (or disease) related increase in GFAP expression [447] in the same organism. The aged glia of *N. guentheri* were not only fewer in number but also less responsive as judged by the number of large processes emanating from them.

7.2.5 PNN abundance declines with age

With age the number of PNNs declined (Figure 6.6). The loss of PNNs with age in mammals has been associated with a decline in CNS cognitive and motor function [147]. Further more, this loss in PNNs was brain-region specific. The loss of the PNNs of the OT can be regarded as evidence of an age-related loss in OT use and/or functionality. As PNNs are the concerted product of the astroglia, neurons and oligodendrocytes their decline is evidence of a possible general dysfunction of the CNS at the cellular level.

With age the ECM of *N. guentheri* was observed to change but this change could not be quantified (Section 6.3.1). As discussed in Chapter 2 the ECM is both the foundation on which the cells of the CNS organize themselves as well as the conduit by which the cells communicate with each other. Changes in the expression of the ECM proteins, TNR and NCAMs (such as L1), would disrupt the CNS milieu and perhaps facilitate (if not exacerbate) the loss of the PNNs, neurons and glia with age as these changes hinder regeneration in the course of injury and disease [448].

7.2.6 Protein aggregation in the *Nothobranchius* CNS

Two types of protein aggregation have already been mentioned in this chapter. These were misprocessed GFAP and NFTs. Whether there are other forms of protein aggregation is not known at this time. Further research will, in all probability, confirm the existence of other forms of protein aggregation. This

increase in protein aggregation will probably be correlated with the decline in mitochondrial efficiency in *Nothobranchius* [22].

7.2.7 Massive neuron loss is not a feature of *Nothobranchius* OT aging

The SGS of the *N. guentheri* OT did not show evidence of massive neuron loss (Figure 5.5). Neuron loss was moderate with aging. The loss of E587$^+$ neurons was greater than the general loss of neurons (39% vs 23%) and this difference was more meaningful as these are probably the functional neurons. 40% of the radial glia were lost with age which is far greater than that of the average neuron loss. These results mirror studies of mammalian aging which found that the loss of glia correlates better with age than the loss of neurons [28, 102, 110].

Analysis of other brain regions with respect to the decline in neuronal density and rescue of glial and PNN density needs to be performed. Whether neurodegenerative-aging is wholesale in the *Nothobranchius* brain or restricted to certain areas as in other species (such as humans which suffer degeneration selectively in the frontal and temporal lobes, hippocampus and substantia nigra) is an important question which needs to be answered. Bielschowski silver staining of Bouin's fixed sections (Figure 7.1) suggested that the midbrain could be subject to a greater level of degeneration relative to other brain regions but as Bouin's Solution interferes with silver staining[1] these results need confirmation. Davidson's fixative has been identified as an alternative to Bouin's Solution for fixing and softening the bony tissues for sectioning.

[1] Bouin's Solution was selected for its property of fixing and softening tissue without causing excessive soft tissue shrinking while preserving antibody epitopes. No silver staining had been planned at the outset of the project.

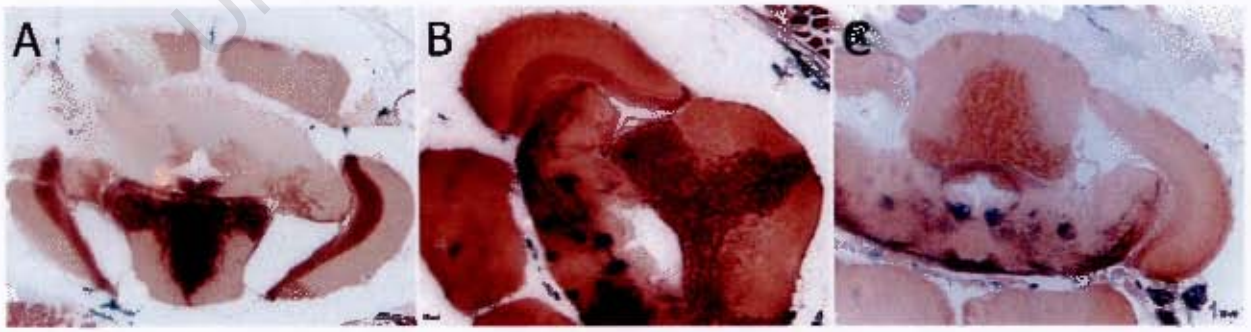

Figure 7.1: Photos of Bielschowski silver stained sections through the brain of *N. guentheri*. Sections (A, 12 weeks old; B, 34 weeks old; C, resveratrol-treated) were developed at the same time. Tissue was fixed in Bouin's Solution which is known to interfere with silver staining. Large difference in stain intensity are visible between the sections.

7.3 *N. guentheri* lived longer on resveratrol-treatment

Aging has been defined as the accumulation of biological changes that render organisms progressively more likely to die [30]. From this definition, and critical to a successful anti-aging experiment, is the demonstration of a significant decrease in the likelihood of death. Such evidence is presented in Figures 5.1 and 7.3 (to be discussed in the next section). If resveratrol had not extended lifespan then the observed cellular differences between the aged and resveratrol-treatment groups could not be described as evidence of resveratrol mediated anti-aging.

Resveratrol-treatment was expected to affect *Nothobranchius* aging in several ways. These were mentioned in Chapter 3 and are restated below:

- *Nothobranchius* would have fewer degenerate neurons than age-matched controls.
- Proteins associated with synaptic plasticity would be up-regulated.
- Glia would be positively affected.
- The problem of protein aggregates would be ameliorated.

7.3.1 Resveratrol-treated *Nothobranchius* have fewer degenerate neurons

Resveratrol-treatment increased the loss of neurons from the *N. guentheri* OT (Figure 5.5). There was a 38% loss of neurons in resveratrol-treated fish compared to the 23% loss with age. Whereas there was a 31% increase in the proportion of $SMI31^{+++}$ neurons with age there was an 8% decrease following resveratrol-treatment (compared to 12 weeks old fish) and a 33% decrease relative to the age-matched controls (Figure 5.6). Resveratrol-treatment did cause there to be fewer degenerate neuron in the OT of aged *N. guentheri* OT but there were also less neurons in total.

This is a new finding in a neuroprotective paradigm which purports that resveratrol protects neurons against death [239]. That resveratrol caused a loss of neurons, and the large scale of this loss of neurons, is unexpected and difficult to explain. As discussed in Chapter 3.2 (page 35), the probability of noticing the removal of energetically compromised neurons by resveratrol was small in anticipation of the larger neuroprotective action of resveratrol. While the explanations given may be largely speculative they do at least provide hypotheses for testing.

Were it not for the increase in lifespan with resveratrol-treatment these results of exacerbated neuron loss would be cause for serious concern. Resveratrol-treatment could well extend human lifespan but the evidence presented here speaks against resveratrol as an elixir of youth. It could slow the

mortality rate in midlife but exacerbate the mortality rate at advanced age. This subject will be elaborated on in the next section.

7.3.2 Proteins associated with synaptic plasticity are up-regulated

Resveratrol-treatment resulted in a proportional increase in E587$^+$ neurons among aged fish (Chapter 5, Figure 5.7). The proportion of E587$^+$ neurons was retained to that of 12 weeks old fish. It also preserved PNNs into old age which imply a preservation of OT function (Chapter 6, Figure 6.6). These results are in accordance with experiments on *N. furzeri* where resveratrol improved cognitive and motor function into old age.

While resveratrol-treatment may have exacerbated the loss of neurons with age it selectively preserved E587$^+$ neurons suggesting that it is these neurons which are important for youthful OT function. While it cannot be determined whether the neurons in the PNNs were lost with age or the TNR PNN component was lost—the PNN can persist even though one or several of its components are absent [144]—it can be claimed that resveratrol-treatment preserved the PNNs and this simultaneously preserves the function of the neurons enclosed by the PNN.

These results again force us to reconsider our theories of neuroprotection. These theories aim for wholesale preservation of neurons. The experiments with *N. guentheri* imply that CNS function can be preserved even though neurons are lost and it is the preservation of synaptic plasticity which is crucial to lifespan extension.

7.3.3 Radial glia were preserved

Resveratrol-treatment preserved radial glia into old age as well as preserved their ability to react to their environment (Chapter 6, Figure 6.3). This is a novel finding.

Resveratrol research on glia has focused on cell culture experiments employing high concentrations of resveratrol. Here, with a low dose of resveratrol, the aging-related loss of glia was prevented. These glia remained reactive, that is to say they were able to react to their cellular environment rather than they were gliotic glia (which are considered to be pathological). The resveratrol-treated glia did appear to be larger than those of 12 weeks old fish and could have been hypertrophic and considered to be gliotic glia; but this would add weight to the emerging belief that gliotic glia are not themselves pathological [26]. The number of PTAH stained gliotic glia did not change between aged and resveratrol-treated fish supporting the idea that there may be a difference between pathological gliotic glia and non-pathological responsive glia.

7.3.4 GFAP Protein aggregation was ameliorated

34 weeks old control fish had an unbalanced proportion of the observed GFAP isoforms relative to 12 weeks old fish. Resveratrol-treatment restored the GFAP isoform proportions to that of 12 weeks old fish as well as reducing total GFAP (Figure 6.5). This restoration of the GFAP isoform proportions could have prevented intracellular aggregation of the GFAP which would have caused the collapse of the glial cytoskeleton.

While it cannot be claimed that resveratrol-treatment prevented NFT formation it did clear the NFTs by either preventing the NFT formation or causing the death of the NFT bearing neurons.

7.4 *Nothobranchius* neurodegenerative-aging and neuroprotection in context

Rose [424] put forward that as the brain matures, excess neurons are shed and replaced with synapses and glia. The data shows that with the chronological age of the OT there is a decline in neuron density in 12 weeks old fish (Figure 5.5) but, as predicted by Rose, there is no change in the level of $E587^+$ (synaptically active) neurons. We also see that with chronological age of the OT there is an increase in glial processes while the number of glia remain constant (Figure 6.3, page 116). Rose reports that as the animal ages synapses are lost. While synapses were not quantified the markers of synaptogenesis and plasticity ($E587^+$ and PNNs) did decline with age. This decline was concomitant with an increased loss of neurons. Resveratrol-treatment either restored the markers of synaptogenesis to 12 weeks old levels or increased them beyond those levels but had no positive effect on the total number of neurons.

These data indicate that neuronal plasticity is key to polyphenol neuroprotection, and not neuron survival alone. The rescue of E587 immunoreactivity together with glial and PNN density indicate that the functioning of the CNS is dependent on proper interaction between neurons and glia and further experimentation should take this into account. The small size of *Nothobranchius* and their short lifespan makes them accessible to more thorough examination. As argued by Genade et al. [3], *Nothobranchius* are excellent models of aging and readily accessible for experimentation and examination.

7.5 Aging, anti-aging and the benefits of using *Nothobranchius*

A selection of hypothetical survival curves, to aid in the discussion of anti-aging, are presented in Figure 7.2. The goal of many anti-aging researchers is an overall increase in lifespan (Curve B) but this comes with a set of problems. One serious problem, from a human perspective, is a longer working life to pay for a longer retirement. If, as in Curve B, there is a large tail to the right

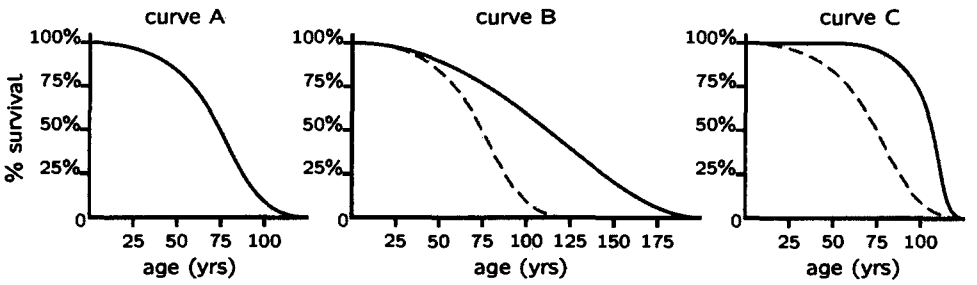

Figure 7.2: Survival curves and two hypothetical options to lifespan extension. Curve A is a hypothetical normal curve for human beings with median life expectancy of 75 years of age (included as a dashed line in B & C). Curve B is the hypothetical doubling of lifespan. Note the longer tail period of lower quality of life. Curve C represents an extension of median lifespan by increasing health span. Maximum lifespan is unaffected. Note the short tail to the right of low quality life.

into old age then this option would also be associated with a longer period of low quality life and debilitation. The cost on society with respect to financial resources and time for the care of the elderly will be tremendous [2]. Curve B is not the ideal. The ideal is to shorten the tail to the right as much as possible, that is to increase the *healthspan*. This is graphically presented by Curve C. In Curve C median lifespan is extended but maximum lifespan doesn't change. The tail to the right is compressed meaning that individuals are likely to live long healthy lives with a brief period of debilitation. Some would argue that the ideal is a curve with the shape of C but age range of B. This matter will be returned to below when Gavrilov's Reliability Theory of Aging is revisited.

Resveratrol-treatment of *N. guentheri* extended median lifespan by 42.9% without extending maximum lifespan by very much (4.8%). This is contrary to *N. furzeri* where median lifespan was increased 33% and maximum lifespan 27% [5]. The extremely short lifespan of the Gonarezhou *N. furzeri* is extraordinary and resveratrol lifespan extension may not be typical in this species[2] Resveratrol-treatment had no effect on the lifespan of standard-diet fed mice but it did improve health [250]. In those mouse experiments there was a small but statistically insignificant increase in median lifespan. This subject was discussed in Chapter 5.3.1, page 83.

Gavrilov's analysis of the lifespans of various human populations shows that the death rate at advanced age approaches the same rate for all populations regardless of the factors affecting their median lifespans [210]. This could imply that there is an intrinsic limit to lifespan beyond which lifespan cannot be extended. In this analysis Curve B is unlikely to become reality but Curve C becomes possible. It is precisely the approaching of Curve C which resveratrol hints at in the *N. guentheri* and mouse experiments.

[2]Dr. Alexander Dorn (pers comm.), who is conducting resveratrol experiments at the Leibniz Institute for Age Research, Fritz Lipmann Institute of Jena on *N. furzeri*, reports that the large increase in total lifespan has disappeared under the water conditions there. In addition, the median lifespan of controls has increased to 12 weeks suggesting environmental factors affect aging in that species.

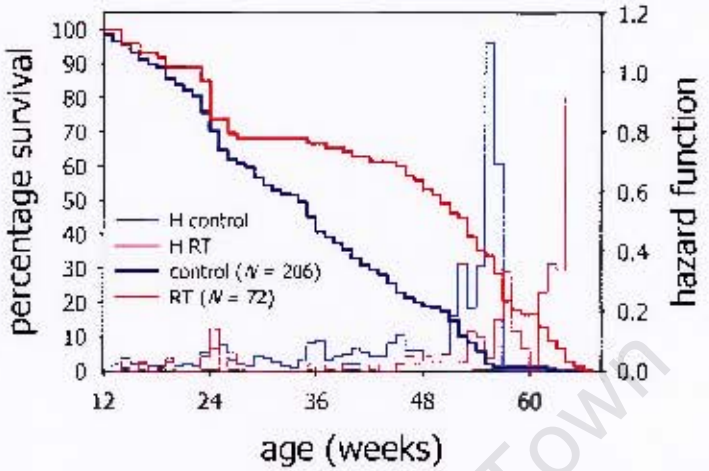

Figure 7.3: Comparison of survival and hazard plots shows that with age the Kaplan-Meier hazard function (probability of death) of each group increases. This increase occurs later in the resveratrol-treatment (RT) group than the control group. The statistical difference between the control and resveratrol-treatment hazard function plots is $p = 0.027$. For most the duration of the trial the hazard function of the control group is larger than the resveratrol-treatment group.

As the fish age their probability of death (hazard function) increases (Figure 7.3). Resveratrol-treatment succeeds in delaying not only the increase in the hazard function but for most the lifespan of the resveratrol-treated fish their hazard functions are lower than that of the control fish. Aging has effectively been staved off. But, when one examines the life trajectories and hazard functions at various ages a different set of conclusions can be drawn. Table 7.1 gives a selection of hazard function values at ages which correspond with the 75%, 50%, 25% and 10% survival marks of the groups. At 10%, exactly as predicted from Gavrilov's theories, the hazard functions are equivalent. Old resveratrol-treated fish are as likely to die as old control fish. At both the 25 and 50% survival marks the hazard functions of the resveratrol-treated fish is greater than that of the control fish; but at the control-group 50% survival mark the hazard of the resveratrol-treated fish is zero. At the 25% survival mark the resveratrol-treated fish had double the probability of death as the control group. What is more, at the control group 50% survival mark there has been a significant decline in neurons (i.e. redundant capacity) rather than preserving them, even though function was retained. Resveratrol-treatment delays aging (system failure) but accelerates the aging-related decline later in life—the exhaustion of redundant capacity makes the fish more likely to suffer a fatal insult. Resveratrol-treatment corresponds with Curve C and is *not* the elixir of youth.

Resveratrol anti-aging results are not as clear in mouse experiments [250]. The reason for the small difference between standard fed and resveratrol-

Table 7.1: Comparison of hazard functions between the control and resveratrol-treatment (RT) groups at specific ages. At the 10% survival point the hazard function (probability of death) is the same for both groups. At 25% survival the hazard function of the resveratrol-treatment group is 2.75× greater than the control.

age	Control Group		RT-group	
(weeks)	% survival	hazard function	% survival	hazard function
25	75%	0.073	75%	0.140
35	50%	0.038	68%	0.000
46	25%	0.120	60%	0.023
51	17%	0.054	50%	0.053
53	10%	0.357	49%	0.030
58	1%	0.000	25%	0.330
63	0%	N/A	10%	0.357

treated mice's median lifespan can be explained by the high living standards and low-risk lifestyles of the mice (that is, fed a high quality diet and kept in clean conditions where they are not exposed to pathogens). Similarly, as medical technology has advanced, so the median lifespan of humans has increased in low-risk human populations. Returning to Gavrilov's Reliability Theory of Aging, the low-risk environment means a slower exhaustion of the redundant capacity of our physiological systems. Given the high polyphenolic diet (salads, fruits, juices etc...) associated with low-risk populations (i.e. those who exercise what is currently considered a healthy lifestyle) resveratrol may have no measurable effect at all. Indeed, it may be only because of the carnivorous nature of *Nothobranchius* that resveratrol-treatment (in the absence of confounding polyphenols in the natural diet) can have such remarkable results. Recalling the results of high-calorie fed resveratrol supplemented mice, the resveratrol did eliminate the health risk associated with a high-calorie diet [214], so resveratrol can compensate for a high-risk lifestyle. The question is just what risks can it counter? As pessimistic as this analysis is, it is important to retain the glimmer of hope afforded by the research of Krikorian et al [237, 249] which indicates that berry phenolics can improve the mental function of aged humans.

Nothobranchius have several qualities which make them excellent models of aging. Their carnivorous diet which is naturally low in exogenous polyphenols makes them good models to test polyphenols for anti-aging properties. The nature of their environment and social structure exposes them to extrinsic lifespan risk which enables the experimenter to better detect effects on healthspan and median lifespan. It can be argued that the sterile low risk conditions which mice are maintained under are essential for elucidating the mechanisms of polyphenol action but such conditions are not the natural state of mice nor men; and how is it possible to elucidate the mechanisms of

polyphenol anti-aging if the anti-aging effect cannot be observed in the experimental system? In addition, as discussed in Chapter 3, deducing this mechanism of action may be impossible given the limits of our technology. *Nothobranchius* age like other organisms. Based on neuroprotection experiments performed on mammalian models predictions were made as to what the outcomes of *Nothobranchius* polyphenol anti-aging experiments would be and these predictions proved true. The causes of aging are evolutionary conserved and give rise to a process which is common among multicellular organisms. *Nothobranchius* represent an excellent compromise between a short lifespan, experimental accessibility and a common vertebrate biology. This is not to say that there is no room for mice, only that there is also room for *Nothobranchius*.

7.6 Looking forward

The results reported in this thesis inspire further inquiry. These research avenues have been discussed in Chapters 4 through 6 and will not be repeated here. In this section research options inspired from this chapter will be addressed.

The markers of synaptic plasticity indicate that the OT of resveratrol-treated fish is more synaptically active than age-matched controls. This data corresponds with various experiments (examples are indicated in Chapter 3) which indicate that resveratrol preserves CNS function into old age. Taken together with the results of Krikorian et al [237, 249] there is hope that resveratrol could be a useful supplement to improve cognition in the elderly. What needs to be determined is whether this improvement in cognitive function by late-in-life polyphenol supplementation will have the same effect on life- and healthspan as long term supplementation. There is a stark difference in the magnitude in operant outcomes comparing the resveratrol-treated *N. furzeri* [5] and the subjects of Krikorian et al.

In this Chapter there has been discussion of the problem of distinguishing glia which remain responsive and gliotic glia. HSP27 (also called HSP25 or HSPB1) antibodies could be used to distinguish between pathological and responsive glia [449]. HSP27 is expressed in response to cellular injury and may play a role in stabilizing the glial cystoskeleton. Glia which are still functioning normally (that is to say glia which are still responsive) would expresses more HSP27 than glia which are dysfunctioning. Initial data from Western Blots suggest that the relative proportions of the GFAP immunoreactive bands could serve as a marker of properly functioning glia. In aged fish there should be a reduction in the 43 kDa band and an elevation of the 55 kDa band. Antibodies specific to these bands could be used to detect dysfunctional glia in wholemounts and sections.

The SMI31 and E587 antibodies could not be used to identify distressed neurons or neurons which were neurodegenerative. If resveratrol functions by a purely hormetic mechanism, where it causes mild injury, then knowing which neurons are dying is important. Clarke et al. [450] propose a one-hit

model of neuron death which is a consequence of the random initiation of apoptosis due to cellular insult. If resveratrol is causing the death of degenerate neurons then this is a good outcome. If, instead, it is causing the death of neurons at random then this is a deleterious outcome which may increase median lifespan but, by exhausting the redundant capacity of the CNS, would reduce maximum lifespan. To this purpose the anti-phospho-c-Jun antibody, which has been used to label distressed neurons in the retinal ganglion cell layer, could be useful [451]. If there is a selective decrease in phospho-c-Jun following resveratrol-treatment then this would confirm that resveratrol is clearing degenerate neurons.

There is a need to identify more markers of neurodegeneration, regeneration and plasticity for *Nothobranchius* in order to properly take advantage of the rapid aging and anti-aging intervention experiments employing these fish. The nature of GFAP and E587 immunoreactivity needs to be clarified. The nature of the gliotic glia in *Nothobranchius* needs to be further investigated to address the question of whether there are different glial subtypes in the SGS of the OT, and whether the GFAP immunoreactive bands correspond with different subtypes. Behavioral experiments also need to be performed and the results correlated with the neuron, glial and PNN density to better elucidate which plays the larger role in resveratrol lifespan extension. While the modified PTAH stain of Manlow & Munoz [433] is a simple and easy way to assess the aging-related increase in gliosis it is not very useful in differentiating between normal aging and resveratrol retarded aging. Thicker fixed sections will need to be made of the brain and probed using the GFAP antibodies to determine if the PTAH positive cells in the SGPV represent pathological glia or not.

Resveratrol-treatment is expected to modulate the immune system. BS-isolectin has been established as a means to monitor microglia in the *Nothobranchius* retina and ON. This analysis needs to be completed. As the BS-isolectin did not label microglia in the brain there is a question of whether this is a limitation of the BS-isolectin stain or an indication that the *Nothobranchius* brain does not contain microglia. Additional microglia markers are needed to answer the question of whether the *Nothobranchius* brain does or does not contain microglia.

The antibodies mentioned in this thesis need to be tested against other *Nothobranchius* species to prove their effectiveness. Repeating the neuronal and glial experiments in *N. furzeri* (both long and short-lived strains) is an important next step to confirm whether these are evolutionary conserved processes of aging in *Nothobranchius*. Whether the plasticity related features of *N. furzeri* Gonarezhou decline faster than the long-lived strains is an important question which needs answering.

Appendix A

Miscellaneous data

Now, mama, don't you worry none,
From small things, mama, big things one day come.

From small things big things come, Bruce Springsteen.

A.1 Introduction

This appendix contains data of two sorts: results which were uninformative or of a poorly substantiated nature for inclusion in the main narrative but which could still prove to be useful; and data which supports the results reported in Chapter 5 and 6 but also had no real place in the main narrative. These results were gathered in the process of identifying targets for detailed research which would yield informative and interesting data for hypothesis generation. These results will be afforded neither narrative or detailed discussion in this chapter. They are presented here as a matter of record and for the benefit of those who would continue the *Nothobranchius* aging research.

A.2 Additional antibodies tested

A.2.1 Aim

Further antibodies were sought which could label CNS proteins and cells or which could be used as protein loading controls. These antibodies are listed in Table A.1 along with the protein they were generated against.

Commentary from reviewers of Genade & Lang [382] prompted the Author to conduct further tests to determine how reliable the E587 antisera was reacting against L1. Three other antibodies were available and Western Blots were prepared in the hope of definitively demonstrating that the E587 antiserum is reacting against L1 and not other NCAMs. These results are reported in Section A.2.3.1.

Table A.1: Additional antibodies used in this study along with dilutions and reactivity results.

Antibody	Cellular target	Western Blots		IHC	
		dilution	reactivity	dilution	reactivity
rabbit E987 antiserum†	goldfish L1 NCAM	1 : 500	yes	N/A	N/A
E587 mab♣	goldfish L1 NCAM	1 : 200	yes	N/A	N/A
rabbit anti-L1♣	rat L1 NCAM	1 : 500	yes	N/A	N/A
acetyl-tubulin (Sigma T7451)	tubulin in neurons	1 : 1000	yes	1 : 200	yes
rabbit anti-p38 (Sigma M0800)	p38, all cells	1 : 1000	yes	N/A	N/A
rabbit anti-BDNF (Sigma AV41970)	BDNF in neurons	1 : 200	yes	N/A	N/A
rabbit anti-tau♠	tau in neurons	1 : 200	yes	1:200	yes

† Gift from C. Stuermer, Konstanz Germany.
♣ Generated by Dirk. M. Lang in the lab of C. Stuermer, Konstanz Germany.
♠ 17025 antibody produced by Dr. Virginia Lee, Univ. Pennsylvania.

From Chapter 3.3.2 it was hypothesized that resveratrol would effect p38 expression and activity. Other researchers in the lab were employing p38 as a loading control on their blots. Western Blots were performed and probed using the Sigma polyclonal antibody. This antibody had been used to label p38 of the killifish, *Fundulus heteroclitus* [452]. The result of this experiment is reported in Section A.2.3.2.

The acetyl-tubulin antibody has been used to label the neurons and neuronal processes of zebrafish [453]. This antibody was tested in order to identify an antibody which could label all neurons in the *Nothobranchius* CNS and in so doing determine whether the SMI31 antibody was labeling all neurons in the OT or just a subset thereof.

Exercise has been shown to increase BDNF expression [378]. Green tea and *Gingko biloba* extracts [252, 454] as well as oral resveratrol-treatment [455] have also been reported to increase BDNF expression. Whether resveratrol-treatment of *Nothobranchius* also caused an increase in BDNF was an important question to answer and a BDNF antibody to answer this question was sought.

Hyperphosphorylated tau is the cause for the development of NFTs. There are six isoforms of tau in mammals and these are incorportated into NFTs at different proportions to one another [456]. Being able to observe tau by IHC and quantify its expression with age and anti-aging treatments is an important requirement to fully utilize *Nothobranchius*. A sample of the 17025 tau antibody was obtained and tested against *N. guentheri*.

A.2.2 Materials and Methods

All methods and materials, unless otherwise recorded here, were as per Chapters 4–6. Antibody dilutions are recorded in Table A.1 along with their efficacy. Proteins were extracted using either a NP-40 based buffer or a RIPA buffer. Unless otherwise stated, *Nothobranchius* protein samples are pooled samples of four 12 weeks old and four 34 weeks old fish.

For Western Blots using the Sigma M0800 p38 antibody the blot was blocked with 5% milk in PBS for one hour followed by primary incubation in PBS without milk.

Images of Western Blots have been manipulated in PhotoShop. Lanes of the same blot were spliced together for display purposes. Spliced blots will be indicated in the figure legends.

A.2.3 Results and discussion

A.2.3.1 E987 antiserum and E587 monoclonal and anti-L1 polyclonal antibody efficacy

Results of blotting using four different L1 antibodies are shown in Figure A.1, page 141. All antibodies detected a band of ≈220 kDa in each lane. In the anti-rat blot this band is clearly a doublet of approximately 220 and 200 kDa, the latter being the product of the first cleavage [159]. Both the E587 and anti-rat L1 blots show a band in the *Nothobranchius* lane of ≈50 kDa. The anti-rat L1 antibody gives a similar banding pattern as that shown for zebrafish on the E587 blot and *Nothobranchius* on the E943 blot. There is a band of ≈130 kDa. The enzymatic processing of L1 and the expected band sizes were discussed in Chapter 4.3.2, page 64. Both the 50 and 130 kDa bands, which are common among the blots, are expected from the sequential enzymatic cleavage of the full length protein.

The E587 and E943 antisera could be reacting against NCAM but the blots demonstrate that these antisera are definitely also binding L1. Proteomic analysis and protein sequencing are required to be absolutely sure of the identity of E587's protein target.

A.2.3.2 p38 MAPK antibody efficacy

The Sigma M0800 p38 antibody proved a reliable marker of *Nothobranchius* p38. This antibody labelled many bands on the blot (Figure A.2). The identity of these bands is unknown.

No significant difference in p38 expression was observed ($p = 0.412$) but the power of the test (One Way Anova) was below that needed (0.049 vs the required 0.80) to yield a reliable result. The observed elevation in p38 expression in *N. guentheri* could be real. A larger sample size is required to resolve the question of the significance of the increased p38 expression in resveratrol-treated fish.

The data indicates that p38 is possibly not a reliable loading control for protein blotting.

A.2.3.3 Acetyl-tubulin antibody efficacy

Western Blots (Figure A.3) and wholemounts (Figure A.4) were prepared using the acetyl-tubulin antibody.

Western Blots revealed a band of 60 kDa for all three species and in accordance with the expected band size. For all three species two smaller bands of 38 and 35 kDa were also detected. The *Nothobranchius* bands were not sharp and could indicate that there are multiple isoforms, each with a small difference in size. Alternatively these could be phosphorylated forms of the protein. When run on a non-denaturing gel two bands are visible of 52 and 50 kDa. This indicates that there could be protein-protein interactions which the β-mercaptoethanol disrupts. Densitometry of the blots run on the non-denaturing gel showed no aging-related difference. Densitometry of the bands on the denatured protein indicates that the abundance of the small isoforms changes with the age of the fish. This difference was not explored further but could be indicative of neurodegeneration or an artifact of sample preparation.

Staining of wholemounts with the acetyl-tubulin antibody was uninformative. No clear differences were apparent by eye and no in depth study of the wholemounts was undertaken (other research directions promised to be more informative). Whether the holes in acetyl-tublin immunoreactivity correlate with the density of PNNs is one interesting avenue of research. No cell bodies in the OT were apparent at low magnification using this antibody but such cell bodies were visible in other brain regions (data not shown). This could indicate that only certain neurons expressed acetyl-tubulin. Whether the acetyl-tubulin was expressed by the neurons enclosed in the PNN could not be tested as both the acetyl-tubulin and TNR antibodies were both mouse monoclonals.

Acetyl-tubulin expression is continuous in mature integrated neurons but fragmented in degenerating and apoptotic neurons [453]. It could serve as a useful marker by which to quantify the level of disconnectivity in degenerating brain tissue. Using an antibody against neurofilament-light as counter stain the expression of acetyl-tubulin along dendrites could be monitored. Synaptophysin could be another interesting counter-stain. The use of this antibody in Western Blotting as a marker of the total number of neurons between age-groups is not possible as it only gives an indication of the synaptically stable axons and neurites. In addition, as the fish grow with age and more neurons are added to the brain along with new synaptic connections any decrease in acetyl-tublin associated with aging or neurodegeneration could be masked. Without another protein which is known to be stably expressed through aging by which to compare acetyl-tubulin expression this antibody can tell the experimenter nothing about the state of the fish CNS.

A.2.3.4 Sigma AV41970 BDNF antibody efficacy

Results of western blotting are shown in Figure A.5. Protein extracted without deoxycholate (which disrupts protein-protein interactions) should yield bands of ≈29 kDa. Protein extractions with deoxycholate would yield bands of ≈15 kDa. The *N. guentheri* proteins were extracted using RIPA which has 1% deoxycholate and a band of ≈16 kDa was observed.

The densitometry of the blot shows that there was a change in BNDF expression with age. 34 weeks old fish had on average less BDNF than 12 weeks old fish. BDNF expression of resveratrol-treated fish could not be performed as the protein had been exhausted.

BDNF expression changes with age and resveratrol-treatment need to be examined more extensively in future.

A.2.3.5 17025 Tau antibody efficacy

Mammalian tau ranges from 55–65 kDa in size [457]. The multiple banding smear pattern in the rat lane shown in Figure A.6 is typical of a protein expressed as multiple isoforms which undergo phosphorylation. A similar banding pattern was obtained for the fish samples but of a slightly different size range. Most rat bands were between 64 and 39 kDa while for *N. guentheri* most bands were between 40 and 26 kDa. Zebrafish and goldfish tau ranges from 32–55 kDa [458]. *Nothobranchius* tau is probably processed differently to that of mammals and fish of the family Cyprinidae (such as gold- and zebrafish).

Wholemounts of 34 weeks old fish brains were incubated with anti-tau and SMI31 (Figure A.7). The tau antibody reacted against neuron cell bodies as well as fine processes between them. There was no colocalization between the tau antibody and SMI31. Some colocalization of SMI31 and tau was expected as hyperphosphorylated tau is found in NFTs along with abnormally phosphorylated neurofilament protein. This could be because the tau epitope was unavailable within the NFT. The tau antibody reacted against the periphery of the neurons and fine processes but did not react against the SMI31$^+$ axons. This is unexpected as tau plays a role in stabilizing neurofilaments and would be expected to colocalize with SMI31$^+$ axons. Counter staining using a neurofilament-L antibody which binds to dendrites would confirm whether the tau antibody is labeling dendrites.

The Western Blotand wholemount shows that the 17025 antibody is probably reacting against *Nothobranchius* tau. This could be a useful structural label in *Nothobranchius* aging research.

A.2.4 Conclusions

Preliminary testing of the antibodies discussed above indicate that they could be useful in *Nothobranchius* aging research. The acetyl-tubulin and BDNF antibodies are particularly promising as they show that there are aging-related

changes in expression and protein processing. Changes in tau expression with age could not be tested for on account of damage to the blot over the 12 weeks old lane. Future research conducted using these antibodies could yield valuable data regarding *Nothobranchius* aging and resveratrol-treatment.

A.3 BrdU positive cells occur in the epidermis and optic tectum of 34 weeks old fish

A.3.1 Aim

Resveratrol had been demonstrated to extend the mitotic lifespan of progenitor cells in culture [375] and is expected to preserve stem cell proliferative capacities in vivo [459]. The aim of this experiment was to determine whether aged fish have a lower rate of mitosis than young fish; and whether resveratrol-treated fish have a rate of mitosis similar to that of 12 week or 34 weeks old fish. Bromodioxyuridine (BrdU) was used to gauge the level of mitosis.

A.3.2 Materials and Methods

Only female fish were used and females have a more uniform growth than males (anecdotal observation). No growth curves were made to control for this.

BrdU was prepared as a 5 mg/mL solution in aquarium water. Female fish were incubated in the solution for four days with the solution replenished on the second day. On the fourth day, 96 hours after BrdU exposure was began, the fish were killed and fixed in Bouin's Solution as described in Section 6.2.3.

Sections were rehydrated and the Bouin's extracted in 70% ethanol with several drops of saturated lithium carbonate added (10 minute wash). There after the protocol of Tang et al. [460] was followed using the Becton-Dickinson antibody (#347580). Anti-mouse Cy3 (Jackson Immuno Research) was used as secondary. Fixation caused autofluoresence in the Alexa 488 channel. This autofluoresences was used as a convenient counter stain.

A.3.3 Results and discussion

A sample of results are shown in Figure A.8. There were many BrdU positive cells in the epidermis of the normal skin as well as the layer which covers the eye. BrdU positive cells were observed in the brain of all 34 weeks old fish examined. These cells were observed emerging from the torus longitudinalis adjacent to the valvula cerebelli. No such cells were observed in 12 weeks old fish. Five fish were examined of both age groups.

The observation of BrdU positive cells in aged brain but not young brain was unexpected. 12 weeks was the age where the fish sexed out and became reproductively active. It could be that at this age there is a momentary pause in growth as energy is devoted to reproduction. As no growth curves were made there was no means to prove that growth paused at this point in the lifecycle of the female fish. This line of inquiry was suspended in order to pursue more promising research options.

This line of inquiry should be returned to and the proper controls applied.

A.4 PTAH positive glia in the retina

A.4.1 Aim

The goal was to determine whether resveratrol-treatment decreased the incidence of gliotic glia in the *N. guentheri* CNS. The PTAH stain [433] was employed to answer this question. Half of the results are reported in Chapter 6.3.2.

A.4.2 Materials and Methods

All methods as in Chapter 6.

A.4.3 Results and discussion

No statistical difference was found between 34 weeks old and resveratrol-treated *N. guentheri* with regard to the number of gliotic glia in the OT. However, a significant difference was present in the retina between the 34 weeks old fish and resveratrol-treated fish (Figure A.9, $p < 0.001$). This difference in resveratrol-treatment response was unexpected and cannot be explained without fanciful speculation. It was thus excluded from discussion from the main body of the thesis. There were 4.7× as many PTAH positive cells in the 34 weeks old retina as compared to the OT ($p < 0.001$) indicating that the retina may be under more metabolic stress than the OT.

Referring back to Chapter 4, microglia have only thus far been observed in the retina and ON. This difference in microglial distribution could be the cause of the disparity between the OT and retinal gliotic glia. The aid of microglia in dealing with any neuron loss may reduce the stress on the glia. Microglia are yet to be investigated with respect to age and resveratrol-treatment.

Also, additional methods are needed to confirm the absence of microglia in the *Nothobranchius* brain.

A.5 Perineuronal nets along the spinal cord

A.5.1 Aim

Early on in the project an attempt was made to study normal neurological development using the antibodies mentioned in Table 1.1. To this end fully developed unhatched *N. guentheri* embryo wholemounts were prepared.

A.5.2 Materials and Methods

Wholemounts were prepared as in Chapter 5 and anti-TNR was used as in Chapter 6. Fully developed embryos (identifiable by a blue-gold iridescent ring around the developed eye) were dissected out of the egg, the yolk sack removed, and fixed in 10% PFA.

A.5.3 Results and discussion

On account of the dark pigmentation and advanced state of *Nothobranchius* fry development antibody signal could not be observed in the spinal cord and cranium of the fry. Nerves exiting the spinal cord were visible. Only the anti-TNR antibody experiment yielded useful data.

Figure A.10 is a projection of a z-stack of confocal images. TNR positive PNNs are visible along the spinal cord. Similar structures have been observed in rats [461] and zebrafish[462] providing some evidence for TNR being used for the same structural purpose in fish and rats.

Until an albino strain of *Nothobranchius* is obtained for experimentation this use of wholemount embryos will be of little use in studying the *Nothobranchius* CNS. Albino strains of *N. rachovii* and *rubripinnis* do exist.

A.6 Figures

Figure A.1: Comparative blots using four L1 antibodies: the E587 and E943 antisera, the E587 monoclonal and anti-rat L1 polyclonal antibody. Each lane contains brain homogenate extracted using NP-40 based extraction buffer of the species rat (R), goldfish, (G), zebrafish (Z) and *Nothobranchius guentheri* (N). Areas of the anti-rat L1 blot are digitally enhanced to reveal the faint bands. All antibodies detected a band of ≈220 kDa at the top of each lane. In the anti-rat blot this band is clearly a doublet. Both the E587 and anti-rat L1 blots show a band in the *Nothobranchius* lane of ≈50 kDa. The anti-rat L1 antibody gives a similar banding pattern as that shown for zebrafish on the E587 blot and *Nothobranchius* on the E943 blot. There is a prominent band of ≈130 kDa common to the fish E587, E943 and rat anti-rat L1 blots.

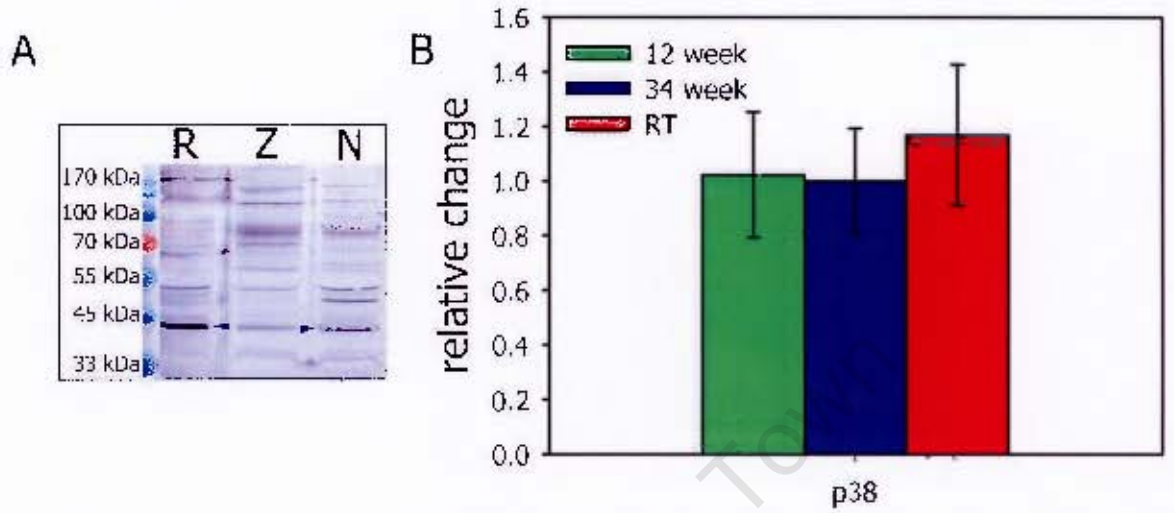

Figure A.2: The Sigma M0800 p38 antibody reliably labels p38. (A) The Western Blotof rat (R), zebrafish (Z) and *N. guentheri* (N) brain protein homogenates shows several bands with a particularly prominent band of ≈38 kDa common to all three lanes. (B) Densitometric analysis of the p38 band shows that expression of p38 is elevated in resveratrol-treated (RT) fish. This difference is not statistically significant. There is no change in expression with age. $N = 3$ and $n = 9$ for each age group. One Way Anova was used to test for statistical significance. Error bars are confidence intervals for $p = 0.05$. The blot was manipulated in PhotoShop to group the R, Z and N lanes together.

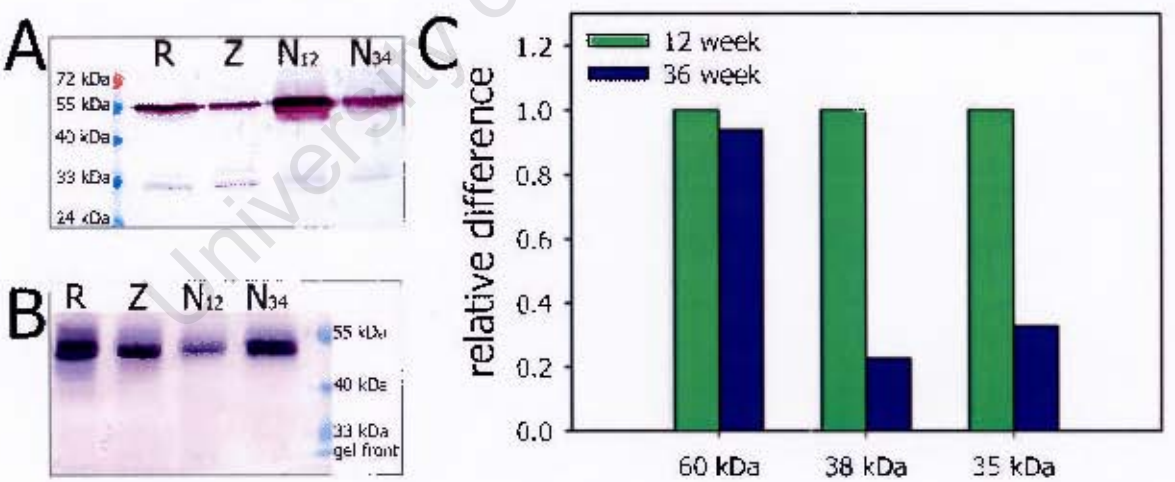

Figure A.3: The acetyl-tubulin (Sigma T7451) antibody was used against rat (R), zebrafish (Z) and *N. guentheri* (N) brain homogenates electrophoresed under denaturing conditions (A) and non-denaturing conditions (B). The *Nothobranchius* lane consists of pooled samples from four fish of the 12 (N12) and 34 weeks old (N34) age groups. Blot (A) shows three bands common to each species of 60, 38 and 35 kDa. *Nothobranchius* protein was extracted using RIPA extraction buffer with 1% deoxycholate which disrupts protein-protein interactions. Densitometry was performed on the denatured blot and the results shown in (C). (B) NP-40 extraction buffer without deoxycholate was used. The two smaller bands are absent from gels run under non-denaturing conditions. The difference in expression between the age groups could be significant and indicate differences in protein processing.

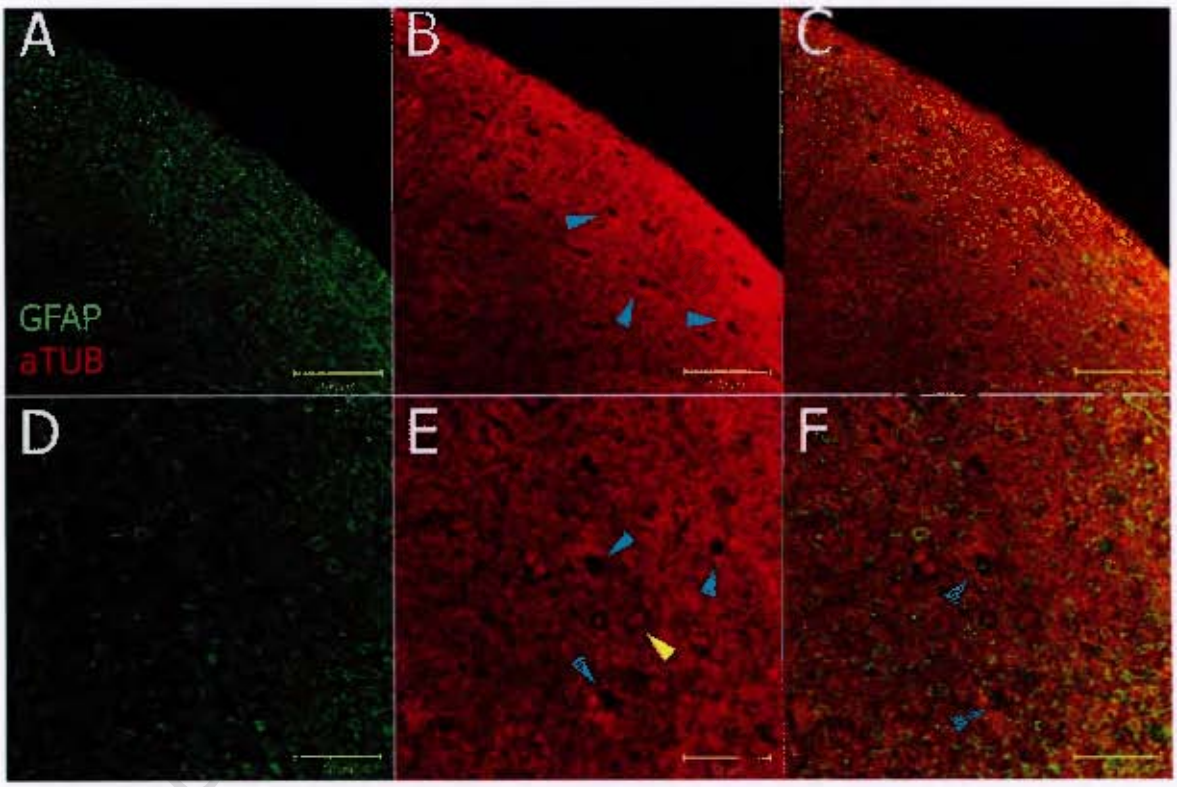

Figure A.4: Wholemounts of 34 weeks old fish were incubated with acetyl-tubulin and DAKO Z0334 (anti-GFAP) antibodies. At low magnification (B–C) holes (pale blue arrowheads) are visible on the surface of the OT stained with the acteyl-tubulin antibody. The DAKO Z0334 staining (A & C) show that this is not damage to the OT but that these are areas of non-acetyl-tubulin immunoreactivity. Higher magnification (D–E) reveal that in some of the holes there are acetyl-tubulin immunoreactive cell bodies (yellow arrowhead, E).

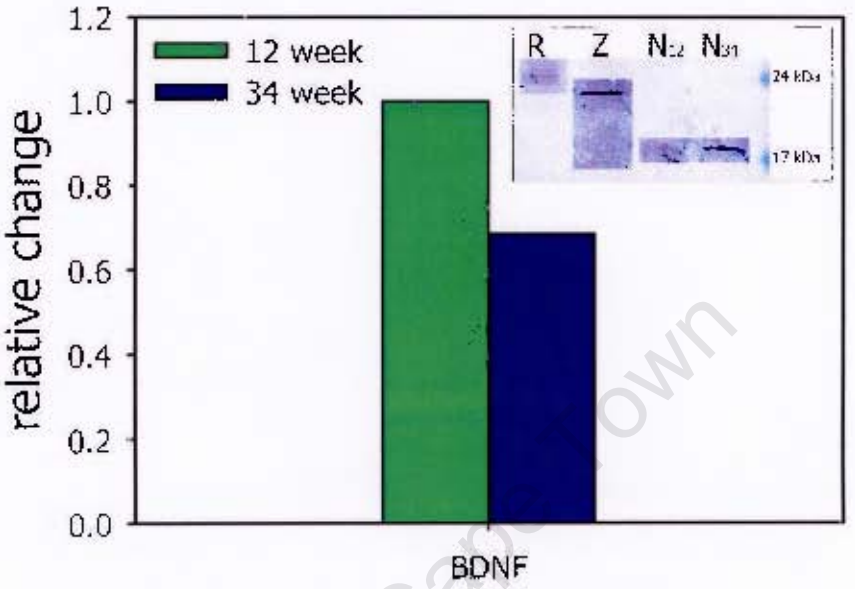

Figure A.5: The Sigma AV41970 BDNF antibody reacts against a single *N. guentheri* protein band. The Western Blotis included as an insert in the graph of the relative change in expression between 12 weeks (N12) and 34 weeks old (N34) old *N. guentheri* (each age group is a pooled sample of four fish). The rat homogenate (extracted with NP-40 based buffer) shows two bands of approximately 26 and 25 kDa. The zebrafish protein homogenate (also extracted using NP-40 based buffer) shows a single ≈23 kDa band. The *N. guentheri* (extracted using RIPA) lane shows a single ≈16 kDa band. Full length BDNF has an expected size of ≈ 29kDa but it is a dimer of two equally sized protein fragments which yield bands of ≈15 kDa [463]. BDNF bands were faint and are digitally enhanced on the blot.

Figure A.6: The 17025 tau antibody labelled several bands in each lane. In the rat lane (R) more than 6 bands were labelled by the antibody. Similarly, multiple bands were observed in the zebrafish (Z) and *N. guentheri* (N) lanes. An additional *N. guentheri* lane has been edited out of image on account of physical damage to the blot.

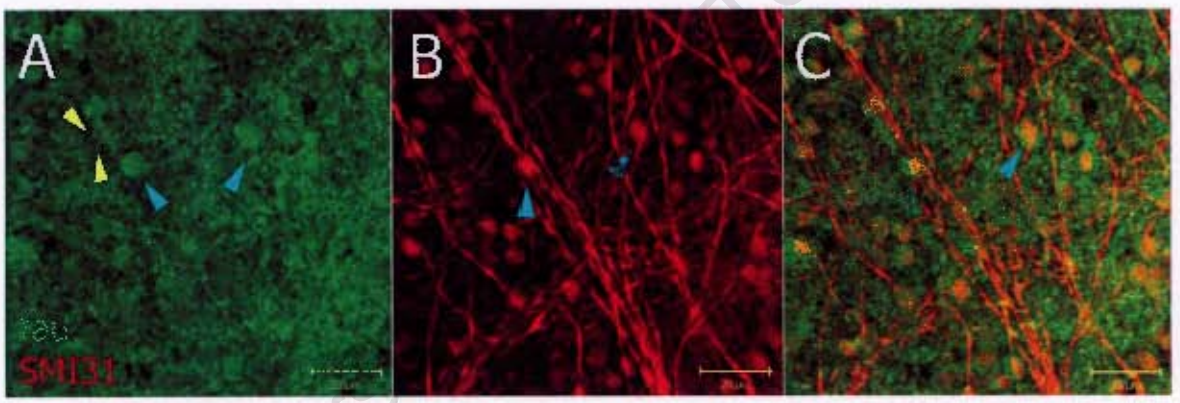

Figure A.7: 34 weeks old fish brains were incubated with 17025 tau antibody and SMI31. The tau antibody reacted against neurons and fibers. Thin fibers are visible and indicated by the yellow arrowheads in A. These thin fibers are not SMI31 immunoreactive. SMI31 immunoreactive fibers were not tau immunoreactive. The tau antibody also labels the periphery of neurons (pale blue arrowheads in A and C). Mammalian tau ranges in size from 55–65 kDa and zebra- and goldfish tau is 32–55 kDa.

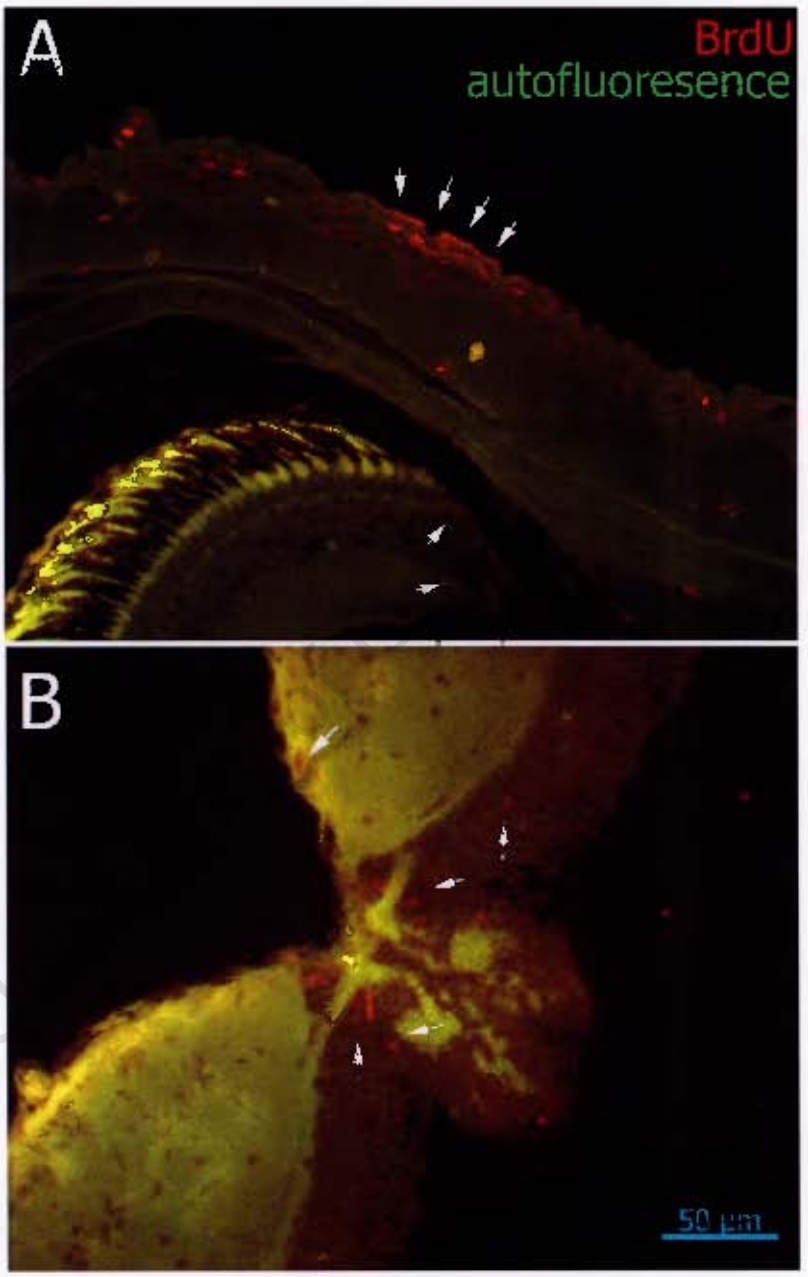

Figure A.8: BrdU positive cells in the aged tissues of *N. guentheri*. A) BrdU positive cells in the epidermis of the lens in 34 weeks old *N. guentheri*. BrdU positive cells are also visible in the retina. B) BrdU positive cells emerging from the torus longitudinalis adjacent to the valvula cerebelli. Possible BrdU positive cells having migrated into the OT are indicated by white arrow heads.

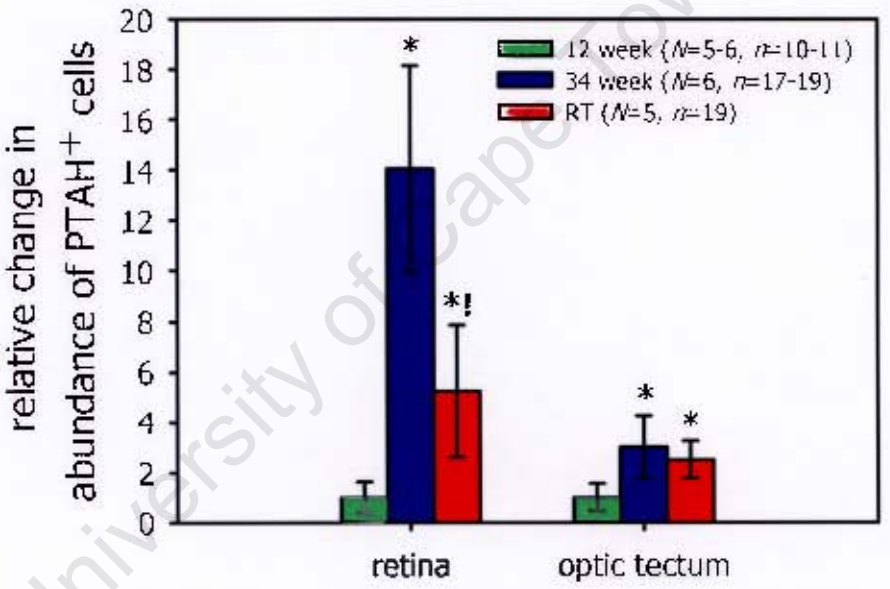

Figure A.9: Gliotic glia decline in the retina with resveratrol-treatment ($p < 0.001$) but not the OT. Error bars represent confidence intervals for $p = 0.05$.

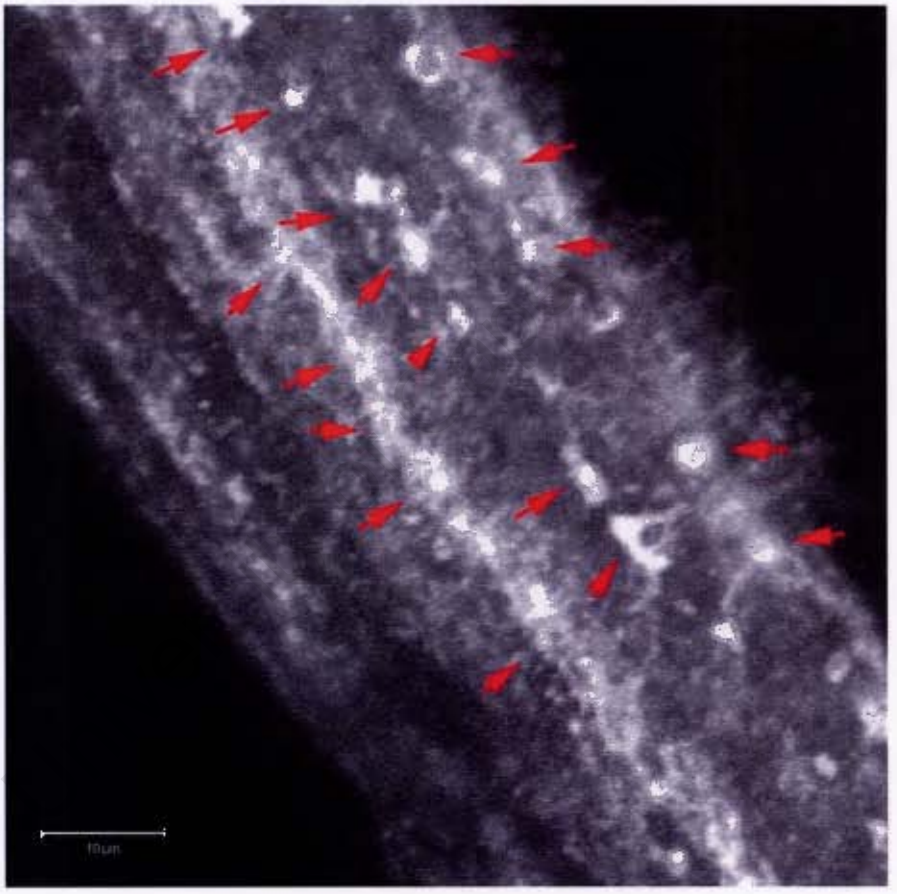

Figure A.10: PPNs along the spinal cord of a just born *N. guentheri* fry are indicated by the red arrow heads. PNNs are also visible along what could be interpreted as the sympathetic trunk of paravertabral ganglia.

References

[1] **Pascale A., Amadio M., Govoni S. & Battaini F.** (2007) The aging brain, a key target for the future: the protein kinase C involvement. *Pharmacol. Res.*, 55:560–569. URL http://www.ncbi.nlm.nih.gov/pubmed/17553691.

[2] **Chenais J.C.** (1990) Demographic transition patterns and their impact on the age structure. *Pop. & Dev. Rev.*, 16:327–336. URL http://www.jstor.org/pss/1971593.

[3] **Genade T., Benedetti M., Terzibasi E., Roncaglia P., Valenzano D.R., Cattaneo A. & Cellerino A.** (2005) Annual fishes of the genus *Nothobranchius* as a model system for aging research. *Aging Cell*, 4:223–233. URL http://www.ncbi.nlm.nih.gov/pubmed/16164422.

[4] **Valdesalici S. & Cellerino A.** (2003) Extremely short lifespan in the annual fish Nothobranchius furzeri. *Proc. Biol. Sci.*, 270 **Suppl** 2:S189–191. URL http://www.ncbi.nlm.nih.gov/pubmed/14667379.

[5] **Valenzano D.R., Terzibasi E., Genade T., Cattaneo A., Domenici L. & Cellerino A.** (2006) Resveratrol prolongs lifespan and retards the onset of age-related markers in a short-lived vertebrate. *Curr. Biol.*, 16:296–300. URL http://www.ncbi.nlm.nih.gov/pubmed/16461283.

[6] **Valenzano D.R., Terzibasi E., Cattaneo A., Domenici L. & Cellerino A.** (2006) Temperature affects longevity and age-related locomotor and cognitive decay in the short-lived fish *Nothobranchius furzeri*. *Aging Cell*, 5:275–278. URL http://www.ncbi.nlm.nih.gov/pubmed/16842500.

[7] **Podrabsky J.E. & Somero G.N.** (2004) Changes in gene expression associated with acclimation to constant temperatures and fluctuating daily temperatures in an annual killifish *Austrofundulus limnaeus*. *Exprimental Biology*, 207:2237–2254. URL http://www.ncbi.nlm.nih.gov/pubmed/15159429.

[8] **Liu R.K., Leung B.E. & Walford R.L.** (1975) Effect of temperature-transfer on growth of laboratory populations of a South American annual fish *Cynolebias bellottii*. *Growth*, 39:337–43. URL http://www.ncbi.nlm.nih.gov/pubmed/1183853.

[9] **Terzibasi E., Lefrancois C., Domenici P., Hartmann N., Graf M. & Cellerino A.** (2009) Effects of dietary restriction on mortality and age-related phenotypes in the short-lived fish *Nothobranchius furzeri*. *Aging Cell*, 8:88–99. URL http://www.ncbi.nlm.nih.gov/pubmed/19302373.

[10] **Terzibasi E., Valenzano D.R., Benedetti M., Roncaglia P., Cattaneo A., Domenici L. & Cellerino A.** (2008) Large differences in aging phenotype between strains of the short-lived annual fish *Nothobranchius furzeri*. *PLoS ONE*, 3:e3866. URL http://www.ncbi.nlm.nih.gov/pubmed/19052641.

[11] **Valenzano D.R., Kirschner J., Kamber R.A., Zhang E., Weber D., Cellerino A., Englert C., Platzer M., Reichwald K. & Brunet A.** (2009) Mapping loci associated with tail color and sex determination in the short-lived fish *Nothobranchius furzeri*. *Genetics*, 183:1385–1395. URL http://www.ncbi.nlm.nih.gov/pubmed/19786620.

[12] **Reichwald K., Lauber C., Nanda I., Kirschner J., Hartmann N., Schories S., Gausmann U., Taudien S., Schilhabel M.B., Szafranski K., Glockner G., Schmid M., Cellerino A., Schartl M., Englert C. & Platzer M.** (2009) High tandem repeat content in the genome of the short-lived annual fish *Nothobranchius furzeri*: a new vertebrate model for aging research. *Genome Biol.*, **10**:R16. URL http://www.ncbi.nlm.nih.gov/pubmed/19210790.

[13] **Hsu C.Y., Chiu Y.C., Hsu W.L. & Chan Y.P.** (2008) Age-related markers assayed at different developmental stages of the annual fish *Nothobranchius rachovii*. *J. Gerontol. A. Biol. Sci. Med. Sci.*, **63**:1267–1276. URL http://www.ncbi.nlm.nih.gov/pubmed/19126839.

[14] **Seluanov A., Hine C., Azpurua J., Feigenson M., Bozzella M., Mao Z., Catania K.C. & Gorbunova V.** (2009) Hypersensitivity to contact inhibition provides a clue to cancer resistance of naked mole-rat. *Proc. Natl. Acad. Sci. U. S. A.*, **106**:19352–19357. URL http://www.ncbi.nlm.nih.gov/pubmed/19858485.

[15] **Lucas A., Almaida-Pagan A., Mendiola P.F. & de Costa P.** (2009) Characterization of *Nothobranchius korthausae* as a model for studying aging physiology. *Acta Physiol.*, **195**:S667:P40. URL http://www.blackwellpublishing.com/aphmeeting/abstract.asp?MeetingID=754&id=73085.

[16] **Costa W.J.E.M.** (2009) Species delimitation among populations of the eastern Tanzanian seasonal killifish *Nothobranchius korthausae* (Cyprinodontiformes: Nothobranchiidae). *Ichthyol. Explor. Freshwaters*, **20**:111–126. URL http://www.pfeil-verlag.de/04biol/pdf/ief20_2_03.pdf.

[17] **Lucas A., Almaida-Pagan A., Mendiola P.F. & de Costa P.** (2009) Effect of photoperiod on incubation time, survival and growth of *Nothobranchius korthausae*. *Acta Physiol.*, **195**:S667:P41. URL http://www.blackwellpublishing.com/aphmeeting/abstract.asp?MeetingID=754&id=73086.

[18] **Lucas-Sanchez A., Almaida-Pagan P.F., Madrid J.A., de Costa J. & Mendiola P.** (2011) Age-related changes in fatty acid profile and locomotor activity rhythms in *Nothobranchius korthausae*. *Exp Gerontol*. URL http://www.ncbi.nlm.nih.gov/pubmed/21896325.

[19] **di Cicco E., Tozzini E.T., Rossi G. & Cellerino A.** (2010) The short-lived annual fish *Nothobranchius furzeri* shows a typical teleost aging process reinforced by high incidence of age-dependent neoplasias. *Mech. Ageing. Dev.*, **46**:249–256. URL http://www.ncbi.nlm.nih.gov/pubmed/21056099.

[20] **Markofsky J. & Milstoc M.** (1979) Histopathological observations of the kidney during aging of the male annual fish *Nothobranchius guentheri*. *Exp. Geront.*, **14**:149–155. URL http://www.ncbi.nlm.nih.gov/pubmed/456446.

[21] **Markofsky J. & Milstoc M.** (1979) Aging changes in the liver of the male annual cyprinodont fish, *Nothobranchius guentheri*. *Exp Gerontol.*, **14**:11–20. URL http://www.ncbi.nlm.nih.gov/pubmed/456435.

[22] **Hartmann N., Reichwald K., Wittig I., Drose S., Schmeisser S., Luck C., Hahn C., Graf M., Gausmann U., Terzibasi E., Cellerino A., Ristow M., Brandt U., Platzer M. & Englert C.** (2011) Mitochondrial DNA copy number and function decrease with age in the short-lived fish Nothobranchius furzeri. *Aging Cell*, **10**:824–831. URL http://www.ncbi.nlm.nih.gov/pubmed/21624037.

[23] **Brunk U.T. & Terman A.** (2002) Lipofuscin: mechanism of age-related accumulation and influence on cell function. *Free Radic. Biol. Med.*, **33**:611–619. URL http://www.ncbi.nlm.nih.gov/pubmed/12208347.

[24] **Schmued L.C. & Hopkins K.J.** (2000) Fluoro-Jade B: a high affinity fluorescent marker for the localization of neuronal degeneration. *Brain Res.*, **874**:123–130. URL http://www.ncbi.nlm.nih.gov/pubmed/10960596.

[25] **Damjanac M., Rioux B.A., Barrier L., Pontcharraud R., Anne C., Hugon J. & Page G.** (2007) Fluoro-Jade B staining as useful tool to identify activated microglia and astrocytes in a mouse transgenic model of Alzheimer's disease. *Brain. Res.*, **1128**:40–49. URL http://www.ncbi.nlm.nih.gov/pubmed/17125750.

[26] **Middeldorp J. & Hol E.M.** (2011) GFAP in health and disease. *Prog. Neurobiol.*, 93:421–443. URL http://www.ncbi.nlm.nih.gov/pubmed/21219963.

[27] **Kim K.Y., Ju W.K. & Neufeld A.H.** (2004) Neuronal susceptibility to damage: comparison of the retinas of young, old and old/caloric restricted rats before and after transient ischemia. *Neurobiol. Aging.*, 25:491–500. URL http://www.ncbi.nlm.nih.gov/pubmed/15013570.

[28] **Morrison J.H. & Hof P.R.** (1997) Life and death of neurons in the aging brain. *Science*, 278:412–419. URL http://www.ncbi.nlm.nih.gov/pubmed/9334292.

[29] **Anderton B.H.** (1997) Changes in the aging brain in health and disease. *Philos. Trans. R. Soc. Lond. (Biol.)*, 352:1781–1792. URL http://www.ncbi.nlm.nih.gov/pubmed/9460061.

[30] **Medawar P.B.** (1952) *An Unsolved Problem of Biology*. H. K. Lewis, London.

[31] **Lynch G., Rex C.S. & Gall C.M.** (2006) Synaptic plasticity in early aging. *Ageing Res. Rev.*, 5:255–280. URL http://www.ncbi.nlm.nih.gov/pubmed/16935034.

[32] **Wolkow C.A., Kimura K.D., Lee M.S. & Ruvkun G.** (2000) Regulation of *C. elegans* life-span by insulinlike signaling in the nervous system. *Science*, 290:147–150. URL http://www.sciencemag.org/content/290/5489/147.abstract.

[33] **Simonsen A., Cumming R.C., Brech A., Isakson P., Schubert D.R. & Finley K.D.** (2008) Promoting basal levels of autophagy in the nervous system enhances longevity and oxidant resistance in adult *Drosophila*. *Autophagy*, 4:176–184. URL http://www.ncbi.nlm.nih.gov/pubmed/18059160.

[34] **Dimakopoulos A.C.** (2005) Protein aggregation in Alzheimer's disease and other neuropathologcal disorders. *Curr. Alzheimer Res.*, 2:19–28. URL http://www.ncbi.nlm.nih.gov/pubmed/15977986.

[35] **Armstrong R.A.** (2006) Plaques and tangles and the pathogenesis of Alzheimer's disease. *Folia Neuropathol.*, 44:1–11. URL http://www.ncbi.nlm.nih.gov/pubmed/16565925.

[36] **Maldonado T.A., Jones R.E. & Norris D.O.** (2002) Timing of neurodegeneration and Beta-amyloid (Aβ) peptide deposition in the brain of aging Kokanee salmon. *Neurobiol.*, 53:21–35. URL http://www.ncbi.nlm.nih.gov/pubmed/12360580.

[37] **Delacourte A., David J.P., Sergeant N., Buée L., Wattez A., Vermersch P., Ghozali E., Fallet-Bianco C., Pasquier F., Lebert F., Petit H. & Di Menza C.** (1999) The biochemical pathway of neurofibrillary degeneration in aging and Alzheimer's disease. *Neurology*, 52:1158–1165. URL http://www.neurology.org/content/52/6/1158.

[38] **Dani S.U., Pittella J.E.H., Boehme A., Hori A. & Schneider B.** (1997) Progressive formation of neuritic plaques and neurofibrillary tangles is exponentially related to age and neuronal size. *Demt. Geriatr. Cogn. Disord.*, 8:217–227. URL http://www.ncbi.nlm.nih.gov/pubmed/9213066.

[39] **La Ferla F.M.** (2010) Pathways linking Aβ and tau pathologies. *Biochm. Soc. Trans.*, 38:993–995. URL http://www.ncbi.nlm.nih.gov/pubmed/20658991.

[40] **Haass C.** (2004) Take five–BACE and the γ-secretase quartet conduct Alzheimer's amyloid β-peptide generation. *EMBO J.*, 33:483–488. URL http://www.ncbi.nlm.nih.gov/pubmed/14749724.

[41] **Unger J.W.** (1998) Glial reaction in aging and Alzheimer's Disease. *Microsc. Res. Tech*, 43:24–28. URL http://www.ncbi.nlm.nih.gov/pubmed/9829455.

[42] **Puzzo D., Privitera L., Fa M., Staniszewski A., Hashimoto G., Aziz F., Sakurai M., Ribe E.M., Troy C.M., Mercken M., Jung S.S., Palmeri A. & Arancio O.** (2010) Endogenous amyloid-β is necessary for hippocampal synaptic plasticity and memory. *Ann. Neurol.*, 69:819–830. URL http://www.ncbi.nlm.nih.gov/pubmed/21472769.

[43] **Parihar M.S. & Brewer G.J.** (2010) Amyloid beta as a modulator of synaptic plasticity. *J. Alzheimers Dis.*, 22:741–763. URL http://www.ncbi.nlm.nih.gov/pubmed/20847424.

[44] **Zhang Y.W., Thompson R., Zhang H. & Xu H.** (2011) APP processing in Alzheimer's disease. *Mol. Brain.*, 4:3. URL http://www.ncbi.nlm.nih.gov/pubmed/21214928.

[45] **Wang J.Z., Grundke-Iqbal I. & Iqbal K.** (2007) Kinases and phosphatases and tau sites involved in Alzheimer neurofibrillary degeneration. *Eur. J. Neurosci.*, 25:59–68. URL http://www.ncbi.nlm.nih.gov/pubmed/17241267.

[46] **Wright J.W. & Harding J.W.** (2010) Contributions of matrix metalloproteinases to neural plasticity, habituation, associative learning and drug addiction. *Neural Plast.*, epub:579382. URL http://www.ncbi.nlm.nih.gov/pubmed/20169175.

[47] **Strekova H., Bihmann C., Kleene R., Eggers C., Saffell J., Hemperly J., Weiler C., Müller-Thomsen T. & Schachner M.** (2006) Elevated levels of neuronal recognition molecule L1 in the cerebrospinal fluid of patients with Alzheimer diseae and other dementia syndromes. *Neurobiol. Aging*, 27:1–9. URL http://www.ncbi.nlm.nih.gov/pubmed/16298234.

[48] **Urano Y., Hayashi I., Isoo N., Ried P.C., Shibasaki Y., Noguchi N., Tomita T., Iwatsubo T., Hamakubo T. & Kodama T.** (2005) Association of active γ-secretase complex with lipid rafts. *J. Lipid. Res.*, 46:904–912. URL http://www.ncbi.nlm.nih.gov/pubmed/15716592.

[49] **Fei M., Jianghua W., Rujuan M., Z. W. & Qian W.** (2011) The relationship of plasma aβ levels to dementia in aging individuals with mild cognitive impairment. *J. Neuro. Sci.*. URL http://www.ncbi.nlm.nih.gov/pubmed/21440911.

[50] **Sánchez L., Madurga S., Pukala T., Vilaseca M., López-Iglesias C., Robinson C.V., Giralt E. & Carulla N.** (2011) Aβ40 and aβ42 amyloid fibrils exhibit distinct molecular recycling properties. *J. Am. Chem. Soc.*, 133:6505–6508. URL http://www.ncbi.nlm.nih.gov/pubmed/21486030.

[51] **Sullivan C.P., Jay A., Stack E., Pakaluk M., Wadlinger E., Fine R.E., Wells J.M. & Morin P.J.** (2011) Retromer disruption promotes amyloidogenic APP processing. *Neurobiol. Dis.*, 43:338–345. URL http://www.ncbi.nlm.nih.gov/pubmed/21515373.

[52] **Iqbal K. & Grundke-Iqbal I.** (2007) Alzheimer neurofibrillay degeneration: significance, etiopathogenesis, therapeutics and prevention. *J. Cell Mol. Med.*, 12:38–55. URL http://www.ncbi.nlm.nih.gov/pubmed/18194444.

[53] **Ferrer I., Gomez-Isla T., Puig B., Freixes M., Ribé E., Dalfó E. & Avila J.** (2005) Current advances on different kinases involved in tau phosphorylation, and implications in Alzheimer's disease and taupathies. *Curr. Alzheimer Res.*, 2:3–18. URL http://www.ncbi.nlm.nih.gov/pubmed/15977985.

[54] **Liu F., Grundke-Iqbal I., Iqbal K. & Gong C.X.** (2005) Contributions of protein phosphatase PP1, PP2A, PP2B and PP5 to the regulation of tau phosphorylation. *Eur. J. Neurosci.*, 22:1942–1950. URL http://www.ncbi.nlm.nih.gov/pubmed/16262633.

[55] **Kins S., Kurosinki P., Nitsch R.M. & Götz J.** (2003) Activation of the ERK and JNK signaling pathways caused by neuron-specific inhibition of PP2A in transgenic mice. *Am. J. Pathol.*, 163:833–843. URL http://www.ncbi.nlm.nih.gov/pubmed/12937125.

[56] **Houslay M.D.** (2006) A RSK(y) relationship with promiscuous PKA. *Sci. STKE.*, 349:pe32. URL http://www.ncbi.nlm.nih.gov/pubmed/16926362.

[57] **Garelick M.G. & Kennedy B.K.** (2011) TOR on the brain. *Exp. Gerontol.*, 46:155–163. URL http://www.ncbi.nlm.nih.gov/pubmed/20849946.

[58] **Goldberg J.L.** (2003) How does an axon grow? *Genes Dev.*, 17:941–958. URL http://www.ncbi.nlm.nih.gov/pubmed/12704078.

[59] **Kandel E.R., Schwartz J.H. & Jessell T.M.** (2000) *Principles of Neural Science, 4th edition*. McGraw-Hill, USA, 4th edition.

[60] **Roberson E.D., English J.D., Adams J.P., Selcher J.C., Kondratick C. & Sweatt J.D.** (1999) The mitogen-activated protain kinase cascade couples PKA and PKC to cAMP response element binding protein phosphorylation in are CA1 of hippocampus. *J. Neurosci.*, 19:4337–4348. URL http://www.ncbi.nlm.nih.gov/pubmed/10341237.

[61] **Carlson M.E., Silva H.S. & Conboy I.M.** (2008) Aging of signal transduction pathways, and pathology. *Exp. Cell. Res.*, 314:1951–1961. URL http://www.ncbi.nlm.nih.gov/pubmed/18474281.

[62] **Goldberg Y.** (1999) Protein phosphatase 2A: who shall regulate the regulator? *Biochem. Pharmacol.*, 57:321–328. URL http://www.ncbi.nlm.nih.gov/pubmed/9933020.

[63] **Lopes J.P. & Agostinho P.** (2011) Cdk5: multitasking between physiological and pathological conditions. *Prog. Neurobiol.*, 94:49–63. URL http://www.ncbi.nlm.nih.gov/pubmed/21473899.

[64] **Obulesu M., Venu R. & Somashekhar R.** (2011) Tau mediated neurodegeneration: an insight into Alzheimer's Disease pathology. *Neurochem. Res.*, 36:1329–1335. URL http://www.ncbi.nlm.nih.gov/pubmed/21509508.

[65] **Li X., Kumar Y., Zempel H., Mandelkov E.M., Biernat J. & Mandelkow E.** (2011) Novel diffusion barrier for axonal retention of Tau in neurons and its failure in neurodegeneration. *EMBO J.*, 30:4825–4837. URL http://www.ncbi.nlm.nih.gov/pubmed/22009197.

[66] **Wang J., Tung Y.C., Wang Y., Li X.T., Iqbal K. & Grundke-Iqbal I.** (2001) Hyperphosphorylation and accumulation of neurofilament proteins in Alzheimer Disease brain and in okadaic acid-treated SY5Y cells. *FEBS Lett.*, 507:81–87. URL http://www.ncbi.nlm.nih.gov/pubmed/11682063.

[67] **Yang X., Yang Y., Luo Y., Li G. & Yang E.S.** (2009) Hyperphosphorylation and accumulation of neurofilament proteins in transgenic mice with Alzheimer presenilin 1 mutation. *Cell. Mol. Neurobiol.*, 29:497–501. URL http://www.ncbi.nlm.nih.gov/pubmed/19137424.

[68] **Rudrabhatla P., Jaffe H. & Pant H.C.** (2011) Direct evidence of phosphorylated neuronal intermediate filament proteins in neurofibrillary tangles (NFTs): phosphoproteomics of Alzheimer's NFTs. *FASEB J.*, 25:3896–3905. URL http://www.ncbi.nlm.nih.gov/pubmed/21828286.

[69] **Perry G., Rizzuto N., Autilio-Gambetti L. & Gambetti P.** (1985) Paired helical filaments from Alzheimer Disease patients contain cytoskeletal components. *Proc. Natl. Acad. Sci. USA*, 82:3916–3920. URL http://www.ncbi.nlm.nih.gov/pubmed/3889918.

[70] **Sternberger N.H., Sternberger L.A. & Ulrich J.** (1985) Aberrant neurofilament phosphorylation in Alzheimer Disease. *Proc. Natl. Acad. Sci. USA*, 82:4274–4276. URL http://www.ncbi.nlm.nih.gov/pubmed/3159022.

[71] **Giese K.P.** (2009) GSK-3: a key player in neurodegeneration and memory. *IUBMB Life*, 61:516–521. URL http://www.ncbi.nlm.nih.gov/pubmed/19391164.

[72] **Jackson G.R., Wiedau-Pazos M., Sang T.K., Wagle N., Brown C.A., Massachi S. & Geschwind D.H.** (2002) Human wild-type tau interacts with wingless pathway components and produces neurofibrillary pathology in *Drosophila*. *Neuron*, 34:509–519. URL http://www.ncbi.nlm.nih.gov/pubmed/12062036.

[73] **Jimenez S., Torres M., Vizuete M., Sanchez-Varo R., Sanchez-Mejias E., Trujillo-Estrada L., Carmona-Cuenca I., Caballero C., Ruano D., Gutierrez A. & Vitorica J.** (2011) Age-dependent accumulation of soluble Abeta oligomers reverses the neuroprotective effect of sAPPalpha by modulating Pi3K/Akt-GSK-3beta pathway in Alzheimer mice model. *J. Biol. Chem.*, 286:18141–18425. URL http://www.ncbi.nlm.nih.gov/pubmed/21460223.

[74] **Phukan S., Babu V.S., Kannoji A., Hariharan R. & Balaji V.N.** (2010) GSK3β: role in therapeutic landscape and development of modulators. *Br. J. Pharmacol.*, 160:1–19. URL http://www.ncbi.nlm.nih.gov/pubmed/20331603.

[75] **Racchi M., Govoni S., Solerte S.B., Galli C.L. & Corsini E.** (2001) Dehydroepiandrosterone and the relationship with aging and memory: a possible link with protein kinase C functional machinery. *Brain Res. Res. Rev.*, 37:287–293. URL http://www.ncbi.nlm.nih.gov/pubmed/11744093.

[76] **Lynch M.J., Baillie G.S. & Houslay M.D.** (2007) cAMP-specific phosphodiesterase-4D5 (PDE4D5) provides a paradigm for understanding the unique non-redundant roles that PDE4 isoforms play in shaping compartmentalized cAMP cell signalling. *Biochem. Soc. Trans.*, 35:938–941. URL http://www.ncbi.nlm.nih.gov/pubmed/17956250.

[77] **Bastianetto S., Brouillette J. & Quirion R.** (2007) Neuroprotective effects of natural products: interaction with intracellular kinases, amyloid peptides and a possible role for transthyretin. *Neurochem. Res.*, 32:1720–1725. URL http://www.ncbi.nlm.nih.gov/pubmed/17406978.

[78] **Ameyar M., Wisniewska M. & Weitzman J.B.** (2003) A role for AP-1 in apoptosis: the case for and against. *Biochimie*, 85:747–752. URL http://www.ncbi.nlm.nih.gov/pubmed/14585541.

[79] **Janssens V. & Goris J.** (2001) Protein phosphatase 2A: a highly regulated family of serine/threonine phosphatases implicated in cell growth and signalling. *Biochem. J.*, 353:417–439. URL http://www.ncbi.nlm.nih.gov/pmc/articles/PMC1221586.

[80] **Fioretti B., Castigli E., Micheli M.R., Bova R., Sciaccaluga M., Harper A., Franciolini F. & Catacuzzeno L.** (2006) Expression and modulation of the intermediate conductance Ca^{2+} activated K^+ channel in glioblastoma GL-15 cells. *Cell Physiol. Biochem.*, 18:47–56. URL http://www.ncbi.nlm.nih.gov/pubmed/16914889.

[81] **Murali G., Panneerselvam K.S. & Pannerselvam C.** (2008) Age-related alterations of lipofuscin, membrane-bound ATPases and intracellular calcium in cortex, striatum and hippocampus of rat brain: protective role of glutathione monoester. *Int. J. Dev. Neurosci.*, 26:211–215. URL http://www.ncbi.nlm.nih.gov/pubmed/18242929.

[82] **Brenman J.E. & Bredt D.S.** (1997) Synaptic signaling by nitric oxide. *Curr. Opin. Neurobiol.*, 7:374–378. URL http://www.ncbi.nlm.nih.gov/pubmed/9232800.

[83] **Nakamura T. & Lipton S.A.** (2011) Redox modulation by S-nitrosylation contributes to protein misfolding, mitochondrial dynamics, and neuronal synaptic damage in neurodegenerative diseases. *Cell Death Differ.*, 18:1478–1486. URL http://www.ncbi.nlm.nih.gov/pubmed/21597461.

[84] **Berndt C., Lillig C.H. & Holmgren A.** (2007) Thiol-based mechanisms of the thioredoxin and glutaredoxin systems: implications for diseases in the cardiovascular system. *Am. J. Physiol. Heart Circ. Physiol.*, 292:H1227–1236. URL http://www.ncbi.nlm.nih.gov/pubmed/17172268.

[85] **Bustamante J., Czerniczyniec A., Cymeryng C. & Lores-Arnaiz S.** (2008) Age related changes from youth to adulthood in rat brain cortex: nitric oxide synthase and mitochondrial respiratory function. *Neurochem. Res.*, 33:1216–1223. URL http://www.ncbi.nlm.nih.gov/pubmed/18259860.

[86] **Vingtdeux V., Davies P., Dickson D.W. & Marambaud P.** (2011) AMPK is abnormally activated in tangle- and pre-tangle-bearing neurons in Alzheimer's disease and other tauopathies. *Acta Neuropathol.*, 121:337–349. URL http://www.ncbi.nlm.nih.gov/pubmed/20957377.

[87] **Ceolotto G., Becilacqua M., Papparella I., Baritono E., Franco L., Corvaja C., Mazzoni M., Semplicini A. & Avogaro A.** (2004) Insulin generates free radicals by an NAD(P)H, phosphatidylinositol 3'-kinase-dependent mechanism in human skin fibroblasts ex vivo. *Diabetes*, 53:1344–1351. URL http://www.ncbi.nlm.nih.gov/pubmed/15111505.

[88] **Rajapakse A.G., Yepuri G., Carvas J.M., Stein S., Matter C.M., Scerri I., Ruffieux J., Montani J.P., Ming X.F. & Yang Z.** (2011) Hyperactive S6K1 mediates oxidative stress and endothelial dysfunction in aging: inhibition by resveratrol. *PloS One*, 6:e19237. URL http://www.ncbi.nlm.nih.gov/pubmed/21544240.

[89] **Bhatt S.R., Lokhandwala M.F. & Banday A.A.** (2011) Resveratrol prevents endothelial nitric oxide synthase uncoupling and attenuates development of hypertension in spontaneously hypertensive rats. *Eur. J. Pharmacol.*, 667:258–264. URL http://www.ncbi.nlm.nih.gov/pubmed/21640096.

[90] **Rous P.P. & Blenis J.** (2004) ERK and p38 MAPK-activated protein kinases: a family of protein kinases with diverse biological functions. *Microbiol. Mol. Biol. Rev.*, 68:320–344. URL http://www.ncbi.nlm.nih.gov/pubmed/15187187.

[91] **Meng T.C., Lou Y.W., Chen Y.Y., Hsu S.F. & Huang Y.F.** (2006) Cys-oxidation of protein tyrosine phosphatases: its role in regulation of signal transduction and its involvement in human cancers. *J. Canc. Mol.*, 2:9–16. URL http://www.mupnet.com/jocm%202(1)%209.htm.

[92] **Lillig C.H., Berndt C. & Holmgren A.** (2008) Glutaredoxin systems. *Biochim. Biophys. Acta.*, 1780:1304–1317. URL http://www.ncbi.nlm.nih.gov/pubmed/18621099.

[93] **Curtis R., O'Connor G. & DiStefano P.S.** (2006) Aging networks in *Caenorhabditis elegans*: AMP-activated protein kinase (aak-2) links multiple aging and metabolism pathways. *Aging Cell*, 5:119–126. URL http://www.ncbi.nlm.nih.gov/pubmed/16626391.

[94] **Blagosklonny M.V.** (2008) Aging: ROS or TOR. *Cell Cycle*, 7:3344–3354. URL http://www.ncbi.nlm.nih.gov/pubmed/18971624.

[95] **Johnston J.A., Ward C.L. & Kopito R.R.** (1998) Aggresomes: a cellular response to misfolded proteins. *J. Cell. Biol.*, 143:1883–1898. URL http://www.ncbi.nlm.nih.gov/pubmed/9864362.

[96] **Cash A.D., Aliev G., Siedlak S.L., Nunomura A., H. F., Zhu X., Ratina A.K., Vinters H.V., Tabaston M., Johnson A.B., Paula-Barbosa M., Avila J., Jones P.K., Castellani R.J., Smith M.A. & Perry G.** (2003) Microtubule reduction in Alzheimer's disease and aging is independent of tau filament formation. *Am. J. Pathol.*, 162:1623–1627. URL http://www.ncbi.nlm.nih.gov/pubmed/12707046.

[97] **David D.C., Ollikainen N., Trinidad J.C., Cary M.P., Burlingame A.L. & Kenyon C.** (2010) Widespread protein aggregation as an inherent part of aging in *C. elegans*. *Plos Biol.*, 8:e1000450. URL http://www.ncbi.nlm.nih.gov/pubmed/20711477.

[98] **Riederer B.M., Leuba G., Vernay A. & Riederer I.M.** (2011) The role of the ubiquitin proteasome system in Alzheimer's disease. *Exp. Biol. Med. (Maywood)*, 236:e268–276. URL http://www.ncbi.nlm.nih.gov/pubmed/21383047.

[99] **Li R., Johnson A.B., Salomons G., Goldman J.E., Naidu S., Quinlan R., Cree B., Ruyle S.Z., Banwell B., D'Hooghe M., Sibert J.R., Rolf C.M., Cox H., Reddy A., Gutiérrez-Solana L.G., Collins A., Weller R.O., Messing A., van der Knaap M.S. & Brenner M.** (2005) Glial fibrillary acidic protein mutations in infantile, juvenile, and adult forms of Alexander Disease. *Ann. Neurol.*, 57:310–326. URL http://www.ncbi.nlm.nih.gov/pubmed/15732097.

[100] **Chin S.S. & Goldman J.E.** (1996) Glial inclusions in CNS degenerative diseases. *J Neuropathol Exp Neurol*, 55:499–508. URL http://www.ncbi.nlm.nih.gov/pubmed/8627339.

[101] **Sloane J.A., Hollander W., Rosene D.L., Moss M.B., Kemper T. & Abraham C.R.** (2000) Astrocytic hypertrophy and altered GFAP degradation with age in subcortical white matter of the rhesus monkey. *Brain Res.*, 862:1–10. URL http://www.ncbi.nlm.nih.gov/pubmed/10799662.

[102] **Streit W.J., Braak H., Xue Q.S. & Bechmann I.** (2009) Dystrophic (senescent) rather than activated microglial cells are associated with tau pathology and likely precede neurodegeneration in Alzheimer's Disease. *Acta. Neuropathol.*, 118:475–485. URL http://www.ncbi.nlm.nih.gov/pubmed/19513731.

[103] **Sansoni P., Vescovini R., Fagnoni F., Biasini C., Zanni F., Zanlari L., Telera G. A. Lucchini, Passeri G., Monti D., Franceschi C. & Passeri M.** (2008) The immune system in extreme longevity. *Exp. Gerontol.*, 43:61–65. URL http://www.ncbi.nlm.nih.gov/pubmed/17870272.

[104] **von Bernhardi R., Tichauer J.E. & Eugenin J.** (2010) Aging-dependent changes of microglial cells and their relevance for neurodegenerative disorders. *J. Neurochem.*, 112:1099–1114. URL http://www.ncbi.nlm.nih.gov/pubmed/20002526.

[105] **Salminen A., Huuskonen J., Ojala J., Kauppinen A., Kaarniranta K. & Suuronen T.** (2008) Activation of innate immunity system during aging: NF-κB signaling is the molecular culprit of inflamm-aging. *Ageing Res. Rev.*, 7:83–105. URL http://www.ncbi.nlm.nih.gov/pubmed/17964225.

[106] **Salminen A., Ojala J., Huuskonen J., Kauppinen A., Suuronen T. & Kaarniranta K.** (2008) Interaction of aging-associated signaling cascades: Inhibition of NF-κB signaling by longevity factors FoxOs and SIRT1. *Cell. Mol. Life. Sci.*, 65:1049–1058. URL http://www.ncbi.nlm.nih.gov/pubmed/18193389.

[107] **Campuzano O., Castillo-Ruiz M.M., Acarin L., Castellano B. & Gonzalez B.** (2008) Distinct pattern of microglial response, cyclooxygenase-2, and inducible nitric oxide synthase expression in the aged rat brain after excitotoxic damage. *J. Neurosci. Res.*, 86:3170–3183. URL http://www.ncbi.nlm.nih.gov/pubmed/18543338.

[108] **Tabner B.J., Turnbull S., Fullwood N.J., German M. & Allsop D.** (2005) The production of hydrogen peroxide during early-stage protein aggregation: a common pathological mechanism in different neurodegenerative disease? *Biochem. Soc. Trans.*, 33:548–450. URL http://www.ncbi.nlm.nih.gov/pubmed/16042541.

[109] **Pekny M. & Nilsson M.** (2005) Astrocyte activation and reactive gliosis. *Glia*, 50:427–434. URL http://www.ncbi.nlm.nih.gov/pubmed/15846805.

[110] **Olabarria M., Noristani H.N., Verkhratsky A. & Rodrǵuez J.J.** (2010) Concomitant astroglial atrophy and astrogliosis in a tripple transgenic animal model of Alzheimer's Disease. *Glia*, 58:831–838. URL http://www.ncbi.nlm.nih.gov/pubmed/20140958.

[111] **Sen J. & Belli A.** (2007) S100B in neuropathologic stats: the CRP of the brain? *J. Neurosci. Res.*, 85:1373–1380. URL http://www.ncbi.nlm.nih.gov/pubmed/17348038.

[112] **Esposito G., Scuderi C., Lu J., Savani C., de Filippis D., Iuvone T., Steardo J. L, Sheen V. & Steardo L.** (2008) S100B induces tau protein hyperphosphorylation via Dickopff-1 upregulation and disrupts the Wnt pathway in human neuronal stem cells. *J. Cell. Mol. Med.*, 12:914–927. URL http://www.ncbi.nlm.nih.gov/pubmed/18494933.

[113] **Luo X., Puig O., Hyun J., Bohmann D. & Jasper H.** (2007) Foxo and Fos regulate the decision between cell death and survival in response to UV radiation. *EMBO J.*, 26:380–390. URL http://www.ncbi.nlm.nih.gov/pubmed/17183370.

[114] **Lam E.W., Francis R.E. & Petkovic M.** (2006) FOXO transcription factors: key regulators of cell fate. *Biochem. Soc. Trans.*, 34:722–726. URL http://www.ncbi.nlm.nih.gov/pubmed/17052182.

[115] **Salminen A., Ojala J., Kaarniranta K., Haapasalo A., Hiltunen M. & Soininen H.** (2011) Astrocytes in the aging brain express characteristics of senescence-associated secretory phenotype. *Eur. J. Neurosci.*, 34:3–11. URL http://www.ncbi.nlm.nih.gov/pubmed/21649759.

[116] **Liddell J.R., Robsinson S.R., Dringen R. & Bishop G.M.** (2010) Astrocytes retain their antioxidant capacity into advanced old age. *Glia*, 58:1500–1509. URL http://www.ncbi.nlm.nih.gov/pubmed/20648641.

[117] **Ohta K., Mizuno A., Ueda M., Li S., Suzuki Y., Hida Y., Hayakawa-Yano Y., Itoh M., Ohta E., Kobori M. & Nakagawa T.** (2010) Autophagy impairment stimulates PS1 expression and gamma-secretase activity. *Autophagy*, 6:345–352. URL http://www.ncbi.nlm.nih.gov/pubmed/20168091.

[118] **Li H.L., Wang H.H., Liu S.J., Deng Y.Q., Zhang Y.J., Tian Q., Wang X.C., Chen X.Q., Yang Y., Zhang J.Y., Wang Q., Xu H., Liao F.F. & Wang J.Z.** (2007) Phosphotylation of tau antagonizes apoptosis by stabilizing β-catenin, a mechanism involved in Alzheimer's neurodegeneration. *Proc. Nat. Acad. Sci. USA*, 104:3591–3596. URL http://www.ncbi.nlm.nih.gov/pubmed/17360687.

[119] **Nagele J. R. G. Wegiel, Venkataraman V., Imaki H., Wang K.C. & Wegiel J.** (2004) Contribution of glial cells to the development of amyloid plaques in Alzheimer's Disease. *Neurobiol. Aging*, 25:663–674. URL http://www.ncbi.nlm.nih.gov/pubmed/15172746.

[120] **Ikeda K., Haga C., Oyanagi S., Iritani S. & Kosaka K.** (1992) Ultrastuctural and immunohistochemical study of degenerate neurite-bearing ghost tangles. *J. Neurol.*, 239:191–194. URL http://www.ncbi.nlm.nih.gov/pubmed/1597685.

[121] **Allaman I., Gavillet M., Belanger M., Laroche T., Viertl D., Lashuel H.A. & Magistretti P.J.** (2010) Amyloid-beta aggregates cause alterations of astrocytic metabolic phenotype: impact on neuronal viability. *J. Neurosci.*, 30:3326–3338. URL http://www.ncbi.nlm.nih.gov/pubmed/20203192.

[122] **Sairanen M., Lucas G., Ernfors P., Castrén M. & Castrén E.** (2005) Brain-derived neurotrophic factor and antidepressant drugs have different but coordinated effects on neuronal turnover, proliferation, and survival in the adult dentate gyrus. *J. Neurosci.*, 25:1089–1094. URL http://www.ncbi.nlm.nih.gov/pubmed/15689544.

[123] **Lang D.M., Warren J.T., Klisa C. & Stuermer C.A.O.** (2001) Topographic restriction of TAG-1 expression in the developing retinotectal pathway and target dependent reexpression during axon regeneration. *Mol. Cell. Neurosci.*, 17:398–414. URL http://www.ncbi.nlm.nih.gov/pubmed/11178876.

[124] **Easter S.S. & Stuermer C.A.O.** (1984) An evaluation of the hypothesis of shifting terminals in goldfish optic tectum. *J. Neurosci.*, 4:1052–1063. URL http://www.ncbi.nlm.nih.gov/pubmed/6325603.

[125] **Adolf B., Chapouton P., Lam C.S., Topp S., Tannhäuser B., Strähle U., Götz M. & Bally-Cuif L.** (2006) Conserved and acquired features of adult neurogenesis in the zebrafish telencephalon. *Dev. Biol.*, 295:278–293. URL http://www.ncbi.nlm.nih.gov/pubmed/16828638.

[126] **Zupanc G.K., Hinsch K. & Gage F.H.** (2005) Proliferation, migration, neuronal differentiation, and long-term survival of new cells in the adult zebrafish brain. *J. Comp. Neurol.*, 488:290–319. URL http://www.ncbi.nlm.nih.gov/pubmed/15952170.

[127] **Zupanc G. & Horschke I.** (1995) Proliferation zones in the brain of adult gymnotiform fish: a quantitative mapping study. *J. Comp. Neurol.*, 353:213–233. URL http://www.ncbi.nlm.nih.gov/pubmed/7745132.

[128] **Dali M., Richter M., Godement P. & Pasquale E.B.** (2006) Eph receptors inactive R-Ras through different mechanisms to achieve cell repulsion. *J. Cell Sci.*, 119:1244–1254. URL http://www.ncbi.nlm.nih.gov/pubmed/16522685.

[129] **Jenkins G.** (2002) Molecular mechanisms of skin ageing. *Mech. Ageing. Dev.*, 123:801–810. URL http://www.ncbi.nlm.nih.gov/pubmed/11869737.

[130] **Romero J.R., Vasan R.S., Beiser A.S., Au R., Benjamin E., DeCarli C., Wolf P.A. & Seshadri S.** (2010) Association of matrix metalloproteinases with MRI indices of brain ischemia and aging. *Neurobiol. Aging.*, 31:2128–2135. URL http://www.ncbi.nlm.nih.gov/pubmed/19128858.

[131] **Jucker M. & Ingram D.K.** (1994) Age-related fibrillar material in mouse brain. assessing its potential as a biomarker of aging and as a model of human neurodegenerative disease. *Ann. N. Y. Acad. Sci.*, 719:238–247. URL http://www.ncbi.nlm.nih.gov/pubmed/8010596.

[132] **Syková E.** (2001) Glial diffusion barriers during aging and pathological states. *Prog. Brain Res.*, 132:339–363. URL http://www.ncbi.nlm.nih.gov/pubmed/11545002.

[133] **Ethell I. & Ethell D.W.** (2007) Matrix metalloproteinases in brain development and remodeling: synaptic functions and targets. *J. Neurosci. Res.*, 85:2813–2823. URL http://www.ncbi.nlm.nih.gov/pubmed/17387691.

[134] **Müller M. & Best J.** (1989) Ocular dominance plasticity in adult cat visual cortex after transplantation of cultured astrocytes. *Nature*, 342:427–430. URL http://www.ncbi.nlm.nih.gov/pubmed/2586611.

[135] **Morawski M., Brückner M.K., Riederer P., Brückner G. & Arendt T.** (2004) Perineuronal nets potentially protect against oxidative stress. *Exp. Neurol.*, 188:309–315. URL http://www.ncbi.nlm.nih.gov/pubmed/15246831.

[136] **Morawski M., Bruckner G., Jager C., Seeger G. & Arendt T.** (2010) Neurons associated with aggrecan-based perineuronal nets are protected against tau pathology in subcortical regions in Alzheimer's disease. *Neuroscience*, 169:1347–1363. URL http://www.ncbi.nlm.nih.gov/pubmed/20497908.

[137] **Brenneke R., Schachner M., Elger C.E. & Lie A.A.** (2004) Up-regulation of extracellular matrix glycoprotein tenascin-R during axonal reorganization and astrogliosis in the adult rat hippocampus. *Epilepsy Res.*, 58:133–143. URL http://www.ncbi.nlm.nih.gov/pubmed/15120744.

[138] **Faissner A., Pyka M., Geissler M., Sobik T., Frischknecht R., Gundelfinger E.D. & Seidenbercher C.** (2010) Contributions of astrocytes to synapse formation and maturation—potential functions of the perisynaptic extracellular matrix. *Brain Res. Rev.*, 63:26–38. URL http://www.ncbi.nlm.nih.gov/pubmed/20096729.

[139] **Baveliar D., Levi D.M., Li R.W., Dan Y. & Hensch T.K.** (2010) Removing brakes on adult brain plasticity: from molecular to behavioral interventions. *J. Neurosci.*, 30:14964–14971. URL http://www.ncbi.nlm.nih.gov/pubmed/21068299.

[140] **Carulli D., Rhodes K.E., Brown D.J., Bonnet T.P., Pollack S.J., Oliver K., Strata P. & Fawcett J.W.** (2006) Composition of perineuronal nets in the adult rat cerebellum and the cellular origin of the their components. *J. Comp. Neurol.*, 494:559–577. URL http://www.ncbi.nlm.nih.gov/pubmed/16374793.

[141] **John N., Krugel H., Frischknecht R., Smalla K.H., Schultz C., Kreutz M.R., Gundelfinger E.D. & Seidenbecher C.I.** (2006) Brevican-containing perineuronal nets of extracellular matrix in dissociated hippocampal primary cultures. *Mol. Cell. Neurosci.*, 31:774–784. URL http://www.ncbi.nlm.nih.gov/pubmed/16503162.

[142] **Milev P., Maurel P., Chiba A., Mevissen M., Popp S., Yamaguchi Y., Margolis R.K. & Margolis R.U.** (1998) Differential regulation of expression of hyaluronan-binding proteoglycans in developing brain: aggrecan, versican, neurocan, and brevican. *Biochem. Biophys. Res. Commun.*, 247:207–212. URL http://www.ncbi.nlm.nih.gov/pubmed/9642104.

[143] **Ajmo J.M., Bailey L.A., Howell M.D., Cortez L.K., Pennypacker K.R., Mehta H.N., Morgan D., Gordon M.N. & Gottschall P.E.** (2010) Abnormal post-translational and extracellular processing of brevican in plaque-bearing mice over-expressing APPsw. *J. Neurochem.*, 113:784–795. URL http://www.ncbi.nlm.nih.gov/pubmed/20180882.

[144] **Saitoh Y., Matsui E, Chiba Y., Kawamura N., Keino H., Satoh M., Kumagai N., Ishii S., Yoshikawa K., Shimada A., Maeda N., Oohira A. & Hosokawa M.** (2008) Reduced expression of MAb6B4 epitopes on chondroitin sulfate proteoglycan aggrecan in perineuronal nets from cerebral cortices of SAMP10 mice: a model for age-dependent neurodegeneration. *J. Neurosci. Res.*, 86:1316–1323. URL http://www.ncbi.nlm.nih.gov/pubmed/18044762.

[145] **Bukalo O., Schachner M. & Dityatev A.** (2001) Modificaton of extracellular matrix by enzymatic removal of chondroitin sulfate and by lack of tenascin-R differentially affects several forms of synaptic plasticity in the hippocampus. *Neurosci.*, 104:359–369. URL http://www.ncbi.nlm.nih.gov/pubmed/11377840.

[146] **Saghatelyan A.K., Gorissen S., Albert M., Hertlein B., Schackner M. & Dityatev A.** (2001) The extracellular matrix molecule tenascin-R and its HNK-1 carbohydrate modulate perisomatic inhibition and long-term potentiation in the CA1 region of the hippocampus. *Eur. J. NeuroSci.*, 12:3331–3342. URL http://www.ncbi.nlm.nih.gov/pubmed/10998116.

[147] **Hilbig H., Bidmon H.J., Steingrüber S., Reinke H. & Dinse H.R.** (2002) Enriched environmental conditions reverse age-dependent gliosis and losses of neurofilaments and extracellular matrix components but do not alter lipofuscin accumulation in the hindlimb area of the aging rat brain. *J. Chem. Neuroanat.*, 23:199–209. URL http://www.ncbi.nlm.nih.gov/pubmed/11861126.

[148] **Kappler J., Baader S.L., Franken S., Pesheva P., Schilling K., Rauch U. & Gieselmann V.** (2002) Tenascins are associated with lipid rafts isolated from mouse brain. *Biochem. Biophys, Res. Comm.*, 294:742–747. URL http://www.ncbi.nlm.nih.gov/pubmed/12056833.

[149] **Del Pozo M.A.** (2004) Integrin signaling and lipid rafts. *Cell Cycle*, 3:725–728. URL http://www.ncbi.nlm.nih.gov/pubmed/15197344.

[150] **Montine T.J., Neely M.D., Quinn J.F., Beal M.F., Markesbery W.R., Roberts L.J. & Morrow J.D.** (2002) Lipid peroxidation in aging brain and Alzheimer's Disease. *Free Rad. Biol. & Med.*, 33:620–626. URL http://www.ncbi.nlm.nih.gov/pubmed/12208348.

[151] **Ran Q., Liang H., Ikeno Y., Qi W., Prolla T.A., Roberts L.J., Wolf N., Van Remmen H. & Richardson A.** (2007) Reduction in glutathione peroxidase 4 increases life span through increased sensitivity to apoptosis. *J. Gerontol.*, 62:932–942. URL http://www.ncbi.nlm.nih.gov/pubmed/17895430.

[152] **Teng K.K. & Hempstead B.L.** (2004) Neurotrophins and their receptors: signaling trios in complex biological systems. *Cell Mol. Life Sci.*, 61:35–48. URL http://www.ncbi.nlm.nih.gov/pubmed/14704852.

[153] **Theodosis D.T., Poulain D.A. & Oliet S.H.** (2008) Activity-dependent structural and functional plasticity of astrocyte-neuron interactions. *Physiol. Rev.*, 88:983–1008. URL http://www.ncbi.nlm.nih.gov/pubmed/18626065.

[154] **Bernhardt R.R.** (1999) Cellular and molecular basis of axonal regeneration in the fish central nervous system. *Expr. Neurol.*, 157:223–240.

[155] **Chen H. & Firestein B.I.** (2007) RhoA regulates dendrite branching in hippocampal neurons by decreasing cypin protein levels. *J. Neurosci.*, 27:8378–8386. URL http://www.ncbi.nlm.nih.gov/pubmed/17670984.

[156] **Inanami O., Asanuma T., Inukai T. N. Jin & Shimokawa S.** (1995) The suppression of age-related accumulation of lipid peroxides in rat brain by administration of Rooibos tea (*Aspalathus lineatis*). *Neurosci Lett*, 196:85–88. URL http://www.ncbi.nlm.nih.gov/pubmed/7501264.

[157] **Decker L., Baron W. & French-Constant C.** (2004) Lipid rafts: microenvironments for integrin-growth factor interactions in neural development. *Biochem. Soc. Trans.*, 32:426–430. URL http://www.ncbi.nlm.nih.gov/pubmed/15157152.

[158] **Schmid R.S. & Maness P.F.** (2008) L1 and NCAM adhesion molecules as signaling coreceptors in neuronal migration and process outgrowth. *Curr. Opin. Neurobiol.*, 18:245–250. URL http://www.ncbi.nlm.nih.gov/pubmed/18760361.

[159] **Maretzky T., Schulte M., Ludwig A., Rose-John S., Blobel C., Hartmann D., Altevogt P., Saftig P. & Reiss K.** (2005) L1 is sequentially processed by two differently activated metalloproteases and presenilin/γ-secretase and regulates neural cell adhesion, cell migration, and neurite outgrowth. *Mol. Cell. Biol.*, 25:9040–9053. URL http://www.ncbi.nlm.nih.gov/pubmed/16199880.

[160] **Bartsch U., Kirchhoff F. & Schachner M.** (1989) Immunohistological localization of the adhesion molecules L1, NCAM, and MAG in the developing and adult optic nerve of mice. *J. Comp. Neurol.*, 284:451–462. URL http://www.ncbi.nlm.nih.gov/pubmed/2474006.

[161] **Lochter A. & Schachner M.** (1993) Tenascin and extracellular matrix glycoproteins: from promotion to polarization of neurite growth in vitro. *J. Neurosci.*, 13:3986–4000. URL http://www.ncbi.nlm.nih.gov/pubmed/7690068.

[162] **Schuster T., Krug M., Stalder M., Hackel N., Gerardy-Schahn R. & Schachner M.** (2001) Immunoelectron microscopic localization of the neural recognition molecules L1, NCAM, and its isoform NCAM180, the NCAM-associated polysialic acid, beta1 integrin and the extracellular matrix molecule tenascin-R in synapses of the adult rat hippocampus. *J. Neurobiol.*, 49:142–158. URL http://www.ncbi.nlm.nih.gov/pubmed/11598921.

[163] **Becker T. & Becker C.G.** (2001) Regenerating descending axons preferentially reroute to the gray matter in the presence of a general macrophage/microglial reaction to a spinal transection in adult zebrafish. *J. Comp. Neurol.*, 433:131–147. URL http://www.ncbi.nlm.nih.gov/pubmed/11283955.

[164] **Weiland U.M., Ott H., Bastmeyer M., Schaden H., Giordano S. & Stuermer C.A.** (1997) Expression of L1-related cell adhesion molecule on developing CNS fibre tracts in zebrafish and its functional contribution to axon fasciculation. *Mol. Cell. Neurosci.*, 9:77–89. URL http://www.ncbi.nlm.nih.gov/pubmed/9204481.

[165] **Li Y.L., Wu G.Z., Dawe G.S., Zeng L., Cui S.S., Loers G., Tilling T., Sun L., Schachner M. & Xiao Z.C.** (2008) Cell surface sialylation and fucosylation are regulated by L1 via phospholipase Cγ and cooperate to modulate neurite outgrowth, cell curvival and migration. *PloS One*, 3:e3841. URL http://www.ncbi.nlm.nih.gov/pubmed/19048108.

[166] **Kaur M., Sharma S. & Kaur G.** (2008) Age-related impairments in neuronal plasticity markers and astrocytic GFAP and their reversal by late-onset short term dietary restriction. *Biogerontology*, 9:441–454. URL http://www.ncbi.nlm.nih.gov/pubmed/18763049.

[167] **Jessberge S., Aigner S., Clemenson G.D., Toni N., Lie D.C., Karalay O., Overall R., Kempermann G. & Gage RH.** (2008) Cdk5 regulates accurate maturation of newborn granule cells in the adult hippocampus. *PloS. Bio.*, 6:e272. URL http://www.ncbi.nlm.nih.gov/pubmed/18998770.

[168] **Li B.S., Zhang L., Gu J., Amin N.D. & Pant H.C.** (2000) Integrin $\alpha 1,\beta 1$ mediated activation of cyclin-dependent kinase 5 activity is involved in neurite outgrowth and human neurofilament protein H Lys-Ser-Pro tail domain phosphorylation. *J. Neurosci.*, 20:6055–6062. URL http://www.ncbi.nlm.nih.gov/pubmed/10934255.

[169] **Nielsen A.L., Holm I.E., Johansen M., Boven B., Jørgensen P. & Jørgensen A.L.** (2002) A new splice variant of glial fibrillary acidic protein, GFAPϵ, interacts with the presenilin proteins. *J. Biol. Chem.*, 277:29983–29991. URL http://www.ncbi.nlm.nih.gov/pubmed/12058025.

[170] **Placania L., Zhu L. & Li Y.M.** (2009) Gender- and age-dependent γ-secretase activity in mouse brain and its implication in sporadic alzheimer disease. *PLoS One*, 4:e5088. URL http://www.ncbi.nlm.nih.gov/pubmed/19352431.

[171] **Balducci C., Mehdawy B., Mare L., Giuliani A., Lorenzini L., Sivilia S., Giardino L., Calzá L., Lanzillotta A., Sarnico I., Pizzi M., Usiello A., Viscomi A.R., Ottonello S., Villetti G., Imbimbo B.P., Nisticó G., Forloni G. & Nisticó R.** (2011) The γ-secretase modulator CHF5074 restores memory and hippocampal synaptic plasticity in plaque-free Tg2576 mice. *J. Alzheimers Dis.*, 24:799–816. URL http://www.ncbi.nlm.nih.gov/pubmed/21321397.

[172] **Castellani R.J., Nunomura A., Lee H.G., Perry G. & Smith M.A.** (2008) Phosphorylated tau: toxic, protective, or none of the above. *Alzheimers Dis.*, 14:377–383. URL http://www.ncbi.nlm.nih.gov/pubmed/18688087.

[173] **Ellgaard L. & Helenius A.** (2003) Quality control in the endoplasmic reticulum. *Nat. Rev. Mol. Cell. Biol.*, 4:181–191. URL http://www.ncbi.nlm.nih.gov/pubmed/12612637.

[174] **Naidoo N.** (2009) ER and aging—protein folding and the ER stress response. *Ageing Res. Rev.*, 8:150–159. URL http://www.ncbi.nlm.nih.gov/pubmed/19491040.

[175] **Naidoo N., Ferber M., Master M., Zhu Y. & Pack A.I.** (2008) Aging impairs the unfolded protein response to sleep deprivation leads to proapoptotic signaling. *J. Neurosci.*, 28:6539–6548. URL http://www.ncbi.nlm.nih.gov/pubmed/18579727.

[176] **Paz Gavilan M., Vela J., Castano A., Ramos J.C. B. del Rio, Vitorica J. & Ruano D.** (2006) Cellular environment facilitates protein accumulation in aged rat hippocampus. *Neurobiol. Aging*, 27:973–982. URL http://www.ncbi.nlm.nih.gov/pubmed/15964666.

[177] **Hussain S.G. & Ramaiah K.V.** (2007) Reduced eIF2alpha phosphorylation and increased proapoptotic proteins in aging. *Biochem. Biophys. Res. Commun.*, 355:365–370. URL http://www.ncbi.nlm.nih.gov/pubmed/17300747.

[178] **Nuss J.E., Choksi K.B., DeFord J.H. & Papconstantinou J.** (2008) Decreased enzyme activities of chaperons PDI and BiP in aged mouse livers. *Biochem. Biophys. Res. Commun.*, 365:355–361. URL http://www.ncbi.nlm.nih.gov/pubmed/17996725.

[179] **Rabek J.P., Boyston III W.H. & Papaconstantinou J.** (2003) Carbonylation of ER chaperone proteins in aged mouse liver. *Biochem. Biophys. Res. Commun.*, **305**:566–572. URL http://www.ncbi.nlm.nih.gov/pubmed/12763031.

[180] **Prostko C.R., Brostrom M.A. & Brostrom C.O.** (1993) Reversible phosphorylation of eukaryotic initiation factor 2 alpha in response to endoplasmic reticular signaling. *Mol. Cell. Biochem.*, **127–128**:255–265. URL http://www.ncbi.nlm.nih.gov/pubmed/7935356.

[181] **Calfon M., Zeng H., Urano F., Till J.H., Hubbard S.R., Harding H.P., Clark S.G. & Ron D.** (2002) IRE1 couples endoplasmic reticulum load to secretory capacity by processing XBP-1 mRNA. *Nature*, **415**:92–96. URL http://www.ncbi.nlm.nih.gov/pubmed/11780124.

[182] **Lee L. K. Neigeborn & Kaufman R.J.** (2003) The unfolded protein response is required for haploid tolernace in yeast. *J. Biol. Chem.*, **278**:11818–11827. URL http://www.ncbi.nlm.nih.gov/pubmed/12560331.

[183] **Lee K., Tirasophon W., Shen X., Michalak M., Prywes R., Okada T., Yoshida H., Mori K. & Kaufman R.J.** (2002) IRE1-mediated unconventional mRNA splicing and S2P-mediated ATF6 cleavage merge to regulate XBP1 insignaling the unfolded protein response. *Genes Develop.*, **16**:452–466. URL http://www.ncbi.nlm.nih.gov/pubmed/11850408.

[184] **Yoshida H., Matsui T., Hosokawa N., Kaufman R.J., Nagata K. & Mori K.** (2003) A time-dependent phase shift in the mamalian unfolded protein response. *Devel. Cell*, **4**:265–271. URL http://www.ncbi.nlm.nih.gov/pubmed/12586069.

[185] **Yoshida H., Matsui T., Yamamoto A., Okada T. & Mori K.** (2001) XBP1 mRNA is induced by ATF6 and spliced by IRE1 in response to ER stress to produce a highly active transcription factor. *Cell*, **107**:881–891. URL http://www.ncbi.nlm.nih.gov/pubmed/11779464.

[186] **Yoshida H., Haze K., Yanagi H., Yura T. & Mori K.** (1998) Identification of the cis-acting endoplasmic reticulum stress response element responsible for transcriptional induction of mammalian glucose-regulated proteins. involement of basic leucin zipper transcription factors. *J. Biol. Cell.*, **273**:33741–33749. URL http://www.ncbi.nlm.nih.gov/pubmed/9837962.

[187] **van der Vlies D., Pap E.H., Post J.A., Celis J.E. & Wirtz K.W.** (2002) Endoplasmic reticulum resident proteins of normal human dermal fibroblasts are the major targets for oxidative stress induced by hydrogen peroxide. *Biochem. J.*, **366**:825–830. URL http://www.ncbi.nlm.nih.gov/pubmed/12071860.

[188] **Hwang C., Sinskey A.J. & Lodish H.F.** (1992) Oxidized redox state of glutathione in the endoplasmic reticulum. *Science*, **257**:1496–1502. URL http://www.ncbi.nlm.nih.gov/pubmed/1523409.

[189] **Moskaug J., Clarlsen H., Myhrstad M.C.W. & Blomhoff R.** (2005) Polyphenols and glutathione synthesis regulation. *Am. J. Clin. Nutr.*, **81(suppl)**:277S–283S. URL http://www.ncbi.nlm.nih.gov/pubmed/15640491.

[190] **van der Vlies D., Woudenberg J. & Post J.A.** (2003) Protein oxidation in aging: endoplasmic reticulum as a target. *Amino Acids*, **25**:397–407. URL http://www.ncbi.nlm.nih.gov/pubmed/14661099.

[191] **Erickson R.R., Dunning L.M. & Holtzman J.L.** (2006) The effect of aging on the chaperone concentrations in the hepatic, endoplasmic reticulum of male rats: the possible role of protein misfolding due to the loss of chaperones in the decline in physiological function seen with age. *J. Gerontol. A Biol. Sci. Med. Sci.*, **61**:435–443. URL http://www.ncbi.nlm.nih.gov/pubmed/16720739.

[192] **Tomassini B., Malisan F., Franchi L., Nicolo C., Calvo G.B., Saito T. & Testi R.** (2004) Calnexin suppresses GD3 synthase-induced apoptosis. *FASEB J.*, **23**:1889–1899. URL http://www.ncbi.nlm.nih.gov/pubmed/15319364.

[193] **Short K.R., Bigelow M.L., Kahl J., Singh R., Coenen-Schimke J., Raghavakaimal S. & Nair K.S.** (2005) Decline in skeletal muscle mitochondrial function with aging in humans. *PNAS*, **102**:5618–5623. URL http://www.ncbi.nlm.nih.gov/pubmed/15800038.

[194] **Ross J.M., Öberg J., Brené G. Coppotelli, Terzioglu M., Pernold M.G., Sitnikov R., Kehr J., Trifunovic A., Larsson N.G., Hoffer B.J. & Olson L.** (2010) High brain lactate is a hallmark of aging and caused by a shift in the lactate dehydrogenase A/B ratio. *Proc. Natl. Acad. Sci. USA.*, **107**:20087–20092. URL http://www.ncbi.nlm.nih.gov/pubmed/21041631.

[195] **Swerdlow R.H., Burns J.M. & Khan S.M.** (2010) The Alzheimer's disease mitochondrial cascade hypothesis. *J. Alzheimers Dis.*, **20S2**:S265–279. URL http://www.ncbi.nlm.nih.gov/pubmed/20442494.

[196] **Morais V.A. & De Strooper B.** (2010) Mitochondria dysfunction and neurodegenerative disorders: cause or consequence. *J. Alzheimers Dis.*, **20S2**:S255–263. URL http://www.ncbi.nlm.nih.gov/pubmed/20463408.

[197] **de Grey A.D.** (2004) Mitochondrial mutations in mammalian aging: an over-hasty about turn? *Rejuvenation Res.*, **7**:171–174. URL http://www.ncbi.nlm.nih.gov/pubmed/15588517.

[198] **Terman A.** (2006) Catabolic insufficiency and aging. *Ann. N. Y. Acad. Sci.*, **1067**:27–36. URL http://www.ncbi.nlm.nih.gov/pubmed/16803967.

[199] **Ferrer I.** (2009) Altered mitochondria, energy metabolism, voltage-dependent anion channel, and lipid rafts converge to exhaust neurons in Alzheimer's disease. *J. Bioenerg. Biomembr.*, **41**:425–431. URL http://www.ncbi.nlm.nih.gov/pubmed/19798558.

[200] **Allaman I., Bélanger M. & Magistretti P.J.** (2011) Astrocyte-neuron metabolic relationships: for better and for worse. *Trends. Neurosci.*, **34**:76–87. URL http://www.ncbi.nlm.nih.gov/pubmed/21236501.

[201] **Braidy N., Guillemin G.J., Mansour H., Can-Ling T., Poljak A. & Grant R.** (2011) Age related changes in NAD+ metanolism oxidative stress and SIRT1 activity in Wistar rats. *PLoS One*, **6**:e19194. URL http://www.ncbi.nlm.nih.gov/pubmed/21541336.

[202] **Patel J., Pathak R.R. & Mujtaba S.** (2011) The biology of lysine acetylation integrates transcriptional programming and metabolism. *Nutr. Metab. (Lond)*, **8**:12. URL http://www.ncbi.nlm.nih.gov/pubmed/21371315.

[203] **Garret R.H. & Grisham C.M.** (1995) *Biochemistry*. Saunders College Publishing.

[204] **Groudeau J., Bellemin S., Toselli-Mollereau E., Shamalnasab M., Chen Y. & Aguilaniu H.** (2011) Fatty acid desaturation links germ cell loss to longevity through NHR-80/HNF4 in *C. elegans*. *PloS Biol.*, **9**:e1000599. URL http://www.ncbi.nlm.nih.gov/pubmed/21423649.

[205] **Wilson J.X.** (1997) Antioxidant defense of the brain: a role for astrocytes. *Can. J. Physiol. Pharmacol.*, **75**:1149–1163. URL http://www.ncbi.nlm.nih.gov/pubmed/9431439.

[206] **Fell D.** (1997) *Understanding the control of metabolism*. Portland Press, London.

[207] **Kacser H. & Burns J.A.** (1973) The control of flux. *Symp. Soc. Exp. Biol.*, **32**:65–104. URL http://www.ncbi.nlm.nih.gov/pubmed/4148886.

[208] **Kascer H. & Burns J.A.** (1979) Molecular democracy: who shares the controls? *Biochem. Soc. Trans.*, **7**:1149–1160. URL http://www.ncbi.nlm.nih.gov/pubmed/389705.

[209] **Sebastiani P., Montano M., Puca A., Solovieff N., Kojima T., Wang M.C., Melista E., Meltzer M., Fischer S.E., Andersen S., Hatley S.H., Sedgewick A., Arai Y., Bergman A., Barzilai N., Terry D.F., Riva A., Anselmi C.V., Malovini A., Kitamoto A., Sawabe M., Arai T., Gondo Y., Steinberg M.H., Hirose N., Atzmon G., Ruvkun G., Baldwin C.T. & Perls T.T.** (2009) RNA editing genes associated with extreme old age in humans and with lifespan in *C. elegans*. *PloS One*, **4**:e8210. URL http://www.ncbi.nlm.nih.gov/pubmed/20011587.

[210] **Gavrilov L.A. & Gavrilova N.S.** (2003) The quest for a general theory of aging and longevity. *SAGE KE*, **28**:1–10. URL http://www.ncbi.nlm.nih.gov/pubmed/12867663.

[211] **Harman D.** (1992) Free radical theory of aging. *Mutat. Res.*, 275:257–266. URL http://www.ncbi.nlm.nih.gov/pubmed/1383768.

[212] **D'Angelo L., de Girolamo P., Cellerino A., Tozzini E.T., Castaldo L. & Lucini C.** (2011) Neurotrophin Trk receptors in the brain of a teleost fish, *Nothobranchius furzeri*. *Microsc. Res. Tech.*. URL http://www.ncbi.nlm.nih.gov/pubmed/21678525.

[213] **Barger J.L., Kayo T., Vann J.M., Arias E.B., Wang J., Hacker T.A., Wang Y., Raederstorff D., Morrow J.D., Leeuwenburgh C., Allison D.B., Saupe K.W., Cartee G.D., Weindruch R. & Prolla T.A.** (2008) A low dose of dietry resveratrol partially mimics caloric restriction and retards aging parameters in mice. *Plos ONE*, 3:e2264. URL http://www.ncbi.nlm.nih.gov/pubmed/18523577.

[214] **Baur J.A., Pearson K.J., Price N.L., Jamieson H.A., Lerin C., Kalra A., Prabhu V.V., Allard J.S., Lopez-Lluch G., Lewis K., Pistell P.J., Poosala S., Becker K.G., Boss O., Gwinn D., Wang M., Ramaswamy S., Fishnein K.W., Spencer R.G., Lakatta E.G., Le Couteur D., Shaw R.J., Navas P., Puigserver P., Ingram D.K., de Cabo R. & Sinclair D.A.** (2006) Resveratrol improves health and survival of mice on a high-calorie diet. *Nature*, 444:337–342. URL http://www.ncbi.nlm.nih.gov/pubmed/17086191.

[215] **Beckman K.B. & Ames B.N.** (1998) The free radical theory of aging matures. *Physiol. Rev.*, 78:547–581. URL http://www.ncbi.nlm.nih.gov/pubmed/9562038.

[216] **Andziak B., O'Conner T.P., Qi W., DeWaal E.M., Pierce A., Chaudhuri A.R., Van Remmen H. & Buffenstein R.** (2006) High oxidative damage levels in the longest-living rodent, the naked mole-rat. *Aging Cell*, 5:463–471. URL http://www.ncbi.nlm.nih.gov/pubmed/17054663.

[217] **Van Raamsdonk J.M. & Hekimi S.** (2009) Deletion of the mitochondria superoxide dismutase sod-2 extends lifespan in *Caenorhabditis elegans*. *PloS Genet*, 5:e1000361. URL http://www.ncbi.nlm.nih.gov/pubmed/19197346.

[218] **Selman C., McLaren J.S., Meyer C., Duncan J.S., Redman P., Collins A.R., Duthie G.G. & Speakman J.R.** (2006) Life-long vitamin C supplementation in combination with cold exposure does not affect oxidative damage or lifespan in mice, but decreases expression of antioxidant protection genes. *Mech. Ageing Dev.*, 127:897–904. URL http://www.ncbi.nlm.nih.gov/pubmed/17092545.

[219] **Pham D.Q. & Plakogiannis R.** (2005) Vitamin E supplementation in cardiovascular disease and cancer prevention. *Ann. Pharmacother.*, 39:1870–1878. URL http://www.ncbi.nlm.nih.gov/pubmed/16189282.

[220] **Brian con S., Boini S., Bertrais S., Guillemin E, Galen P. & Hercberg S.** (2011) Long-term antioxidant supplementation has no effect on health-related quality of life: the randomized, double-blind, placebo-controlled, primary prevention SU.VI.MAX trial. *Int. J. Epidemiol.*, 40:1605–1616. URL http://www.ncbi.nlm.nih.gov/pubmed/22158670.

[221] **Joseph J.A., Fisher D.R., Cheng V., Rimando A.M. & Shukitt-Hale B.** (2008) Cellular and behavioral effects of stilbene resveratrol analogues: implications for reducing the deleterious effects of aging. *J. Agric. Food Chem.*, 56:10544–10551. URL http://www.ncbi.nlm.nih.gov/pubmed/18954071.

[222] **Kampkötter A., Timpel C., Zurawski R.F., Ruhl S., Chovolou Y., Proksch P. & Wätjen W.** (2008) Increase of stress resistance and lifespan of *Caenorhabditis elegans* by quercetin. *Comp. Biochem. Physiol. B. Biochem. Mol. Bio.*, 149:314–323. URL http://www.ncbi.nlm.nih.gov/pubmed/18024103.

[223] **Knight C.G., Patel M.N., Azevedo R.B. & Leroi A.M.** (2002) A novel mode of ecdysozoan growth in *Caenorhabditis elegans*. *Evol. Dev.*, 4:16–27. URL http://www.ncbi.nlm.nih.gov/pubmed/11871396.

[224] **Kalisch R., Schubert M., Jacob W., Kessler M.S., Hemauer R., Wigger A., Landgraf R. & Auer D.P.** (2006) Anxiety and hippocampus volume in the rat. *Neuropsychopharmacology*, 31:925–932. URL http://www.ncbi.nlm.nih.gov/pubmed/16192979.

[225] **Oke A.F., May L. & Adams R.N.** (1987) Ascorbic acid distribution patterns in human brain: a comparison with nonhuman mammalian species. *Ann. N. Y. Acad. Sci.*, 498:1–12. URL http://www.ncbi.nlm.nih.gov/pubmed/3304058.

[226] **Rüweler M., Anker A., Gülden M., Maser E. & Seibert H.** (2008) Inhibition of peroxide-induced radical generation by plant polyphenols in C6 astroglioma cells. *Toxicol. In. Vitro.*, 22:1377–1381. URL http://www.ncbi.nlm.nih.gov/pubmed/18406568.

[227] **Noda Y., McGeer P.I. & MacGeer E.G.** (1983) Lipid peroxides in brain during aging and the effects of hyperbaric oxygen. *J. Nuerochem.*, 40:1329–1332. URL http://www.sciencedirect.com/science/article/pii/0197458082900379.

[228] **Marnewick J.L., van der Westhuizen F.H., Joubert E., Swanevelder S., Swart P. & Gelderblom W.C.A.** (2009) Chemoprotective properties of rooibos (*Aspalathus linearis*), honeybush (*Cyclopia intermedia*) herbal and green and black (*Camellia sinensis*) teas against cancer promotion induced by fumonisin B1 in rat liver. *Food & Chem. Toxicol.*, 47:220–229. URL http://www.ncbi.nlm.nih.gov/pubmed/19041360.

[229] **Buettner G.R.** (1993) The pecking order of free radicals and antioxidants: lipid peroxidation, alpha-tocopherol, and ascorbate. *Arch. Biochem. Biophys.*, 300:535–543. URL http://www.ncbi.nlm.nih.gov/pubmed/8434935.

[230] **Mylonas C. & Kouretas D.** (1999) Lipid peroxidation and tissue damage. *In Vivo*, 13:295–309. URL http://www.ncbi.nlm.nih.gov/pubmed/10459507.

[231] **Crawford M.A., Bazinet R.P. & Sinclair A.J.** (2009) Fat intake and CNS functioning: ageing and disease. *Ann. Nutr. Metab.*, 55:202–228. URL http://www.ncbi.nlm.nih.gov/pubmed/19752543.

[232] **Limón-Pacheco J.H. & Gonsebatt M.E.** (2010) The glutathione system and its regulation by neurohormone melatonin in the central nervous system. *Cent. Nerv. Syst. Agents Med. Chem.*, 10:287–297. URL http://www.ncbi.nlm.nih.gov/pubmed/20868358.

[233] **Foyer C.H. & Noctor G.** (2011) Ascorbate and glutathione: the heart of the redox hub. *Plant. Physiol.*, 155:2–18. URL http://www.ncbi.nlm.nih.gov/pubmed/21205630.

[234] **He T., Joyner M.J. & Katusic Z.S.** (2009) Aging decreses expression and activity of glutathione peroxidase-1 in human endothelial progenitor cells. *Microvasc. Res.*, 78:447–452. URL http://www.ncbi.nlm.nih.gov/pubmed/19733578.

[235] **Brewer G.J., Torricelli J.R., Lindsey A.L., Kunz E.Z., Neuman A., Fisher D.R. & Joseph J.A.** (2010) Age-related toxicity of amyloid-β associated with increased pERK and pCREB in primary hippocampal neurons: reversal by blueberry extract. *J. Nutr. Biochem.*, 21:991–998. URL http://www.ncbi.nlm.nih.gov/pubmed/19954954.

[236] **Mattson M.P., Son T.G. & Camandola S.** (2007) Viewpoint: mechanims of action and therapeutic potential of neurohormetic phytochemicals. *Dose Response*, 5:174–186. URL http://www.ncbi.nlm.nih.gov/pubmed/18648607.

[237] **Krikorian R., Shidler M.D., Nash T.A., Kalt W., Vinqvist-Tymchuk M.R., Shukitt-Hale B. & Joseph J.A.** (2010) Blueberry supplementation improves memory in older adults. *J. Agric. Food Chem.*, 58:3996–4000. URL http://www.ncbi.nlm.nih.gov/pubmed/20047325.

[238] **Essers M.A., Weijzen S., Vries-Smits A.M., Saarloos I., de Ruiter N.D., Bos J.L. & Burgering B.M.** (2004) FOXO transcription factor activation by oxidative stress mediated by the small GTPase Ral and JNK. *EMBO J.*, 23:4802–4812. URL http://www.ncbi.nlm.nih.gov/pubmed/15538382.

[239] **Tang B.L.** (2010) Resveratrol is neuroprotective because it is not a direct activator of Sirt1–a hypothesis. *Brain Res. Bull.*, 81:359–361. URL http://www.ncbi.nlm.nih.gov/pubmed/20026255.

[240] **Liu D., Gharavi R., Pitta M., Gleichmann M. & Mattson M.P.** (2009) Nicotinamide prevents NAD^+ depletion and protects neurons against excitotoxicity and cerebral ischemia: NAD^+ consumption by SIRT1 may endanger energetically compromised neurons. *Neuromol. Med.*, 11:28–42. URL http://www.ncbi.nlm.nih.gov/pubmed/19288225.

[241] **Joseph J.A., Skukitt-Hale B., Denisova N.A., Bielinski D., MArtin A., McEwen J.J. & Bickford P.C.** (1999) Reversals of age-related decline in neuronal signal transduction, cognitive, and motor behavioral deficits with blueberry, spinach, or strawberry dietry supplementation. *J. Neurosci*, 19:8114–8121. URL http://www.ncbi.nlm.nih.gov/pubmed/10479711.

[242] **Zhu Y., Bickford P.C., Sanberg P., Giunta B. & J. T.** (2008) Blueberry opposes β-amyloid peptide induced microglial activation via inhibition of p44/42 mitogen-activation protein kinase. *Rejuvenation Res.*, 11:891–901. URL http://www.ncbi.nlm.nih.gov/pubmed/18789000.

[243] **Son T.G., Camandola S. & Mattson M.P.** (2008) Hormetic dietry phytochemicals. *Neuromolecular Med.*, 10:236–246. URL http://www.ncbi.nlm.nih.gov/pubmed/18543123.

[244] **Calabrese E.J., Mattson M.P. & Calabrese V.** (2010) Resveratrol commonly displays hormesis: occurence and biomedical significance. *Hum. Exp. Toxicol.*, 29:980–1015. URL http://www.ncbi.nlm.nih.gov/pubmed/21115559.

[245] **Nicholson S.K., Tucker G.A. & Brameld J.M.** (2009) Physiological concentrations of dietry polyphenols regulate vascular endothelial cell expression of genes important in cardivascular health. *Br. J. Nutr.*, 21:1–6. URL http://www.ncbi.nlm.nih.gov/pubmed/20021702.

[246] **Vingtdeux V., Giliberto L., Zhao H., Chandakkar P., Wu Q., Simon J.E., Janle E.M., Lobo J., Ferruzzi M.G., Davies P. & Marmbaud P.** (2010) AMP-activated proteins kinase signaling activation by resveratrol modulates amyloid-beta peptide metabolism. *J. Biol. Chem.*, 285:9100–9113. URL http://www.ncbi.nlm.nih.gov/pubmed/20080969.

[247] **Shan Q., Lu J., Zheng Y., Li J., Zhou Z., Hu B., Zhang Z., Fan S., Mao Z., Wang Y.J. & Ma D.** (2009) Purple sweet potato color ameliorates congnition deficits and attenuates oxidative damage and inflammation in aging mouse brain induced by d-galactose. *J. Biomed. Biotechnol.*, 2009:564737. URL http://www.ncbi.nlm.nih.gov/pubmed/19865488.

[248] **Gómez-Serranilos M.P., Martin S., Ortega T., Palomino O.M., Prodanov M., Vacas V., Hermández T., Estrella I. & Carretero M.E.** (2009) Study of red wine neuroprotection on astrocytes. *Plant Foods Hum. Nutr.*, 64:238–243. URL http://www.ncbi.nlm.nih.gov/pubmed/19821030.

[249] **Krikorian R., Nash T.A., Shidler M.D., Shukitt-Hale B. & Joseph J.A.** (2010) Concord grape juice supplementation improves memory function in older adults with mild cognitive impairment. *Br. J. Nutr.*, 103:730–734. URL http://www.ncbi.nlm.nih.gov/pubmed/20028599.

[250] **Pearson K.J., Baur J.A., Lewis K.N., Peshkin L., Price N.L., Labinskyy N., Swindell W.R., Kamara D., Minor R.K., Perez E., Jamieson H.A., Zhang Y., Dunn S.R., Sharma K., Pleshko N., Woolett L.A., Csiszar A., Ikeno Y., Le Couteur D., Elliott P.J., Becker K.G., Navas P., Ingram D.K., Wolf N.S., Ungvari Z., Sinclair D.A. & de Cabo R.** (2008) Resveratrol delays age-related deterioration and mimics transcriptional aspects of dietary restriction without extending lifespan. *Cell Metab.*, 8:157–168. URL http://www.ncbi.nlm.nih.gov/pubmed/18599363.

[251] **Lin M.S., Hung K.S., Chiu W.T., Sun Y.Y., Tsai S.H., Lin J.W. & Lee Y.H.** (2011) Curcumin enhances neuronal survival in N-methyl-d-aspartic acid toxicity by inducing RANTES expression in astrocytes via PI-3K and MAPK signaling pathways. *Prog. Neuropsychopharmacol. Biol. Psychiatry*, 35:931–938. URL http://www.ncbi.nlm.nih.gov/pubmed/21299667.

[252] **Li Q., Zhao H.F., Zhang Z.F., Liu Z.G., Pei X.R., Wang J.B. & Li Y.** (2009) Long-term green tea catechin administration prevents spatial learning and memory impairment in senescence-accelerated mouse prone-8 mice by decreasing aβ1-42 oligomers and upregulating synaptic plasticity-related proteins in the hippocampus. *Neurosci.*, 285:9100–9113. URL http://www.ncbi.nlm.nih.gov/pubmed/20080969.

[253] **Li Q., Zhao H., Zhang Z. & Li Y.** (2010) Chronic green tea catechins administration prevents oxidative stress-related brain aging in C57BL/6J mice. *Brain Res.*, 1353:28–35. URL http://www.ncbi.nlm.nih.gov/pubmed/20682303.

[254] **Assunção M., Santos-Margues M.J., Carvalho F. & Andrade J.P.** (2010) Green tea averts age-dependent decline of hippocampal signaling systems related to antioxidant defenses and survival. *Free Radic. Biol. Med.*, **48**:831–838. URL http://www.ncbi.nlm.nih.gov/pubmed/20064606.

[255] **Eksakulkla S., Suksom D., Siriviriyakul P. & Patumraj S.** (2009) Increased NO bioavailablity in aging male rats by genistein and exercise training: using 4, 5-diaminofluorescein diacetate. *Reprod. Biol. Endocrinol.*, **7**:93. URL http://www.ncbi.nlm.nih.gov/pubmed/19735570.

[256] **Assunção M., de Freitas V. & Paula-Barbosa M.** (2007) Grape seed flavanols, but not Port wine, prevent ethanol-induced neuronal lipofuscin formation. *Brain Res.*, **1129**:72–80. URL http://www.ncbi.nlm.nih.gov/pubmed/17156755.

[257] **Wang Y.J., Thomas P., Zhong J.H., Bi F.F., Kasaraju S., Pollard A., Fenech M. & Zhou X.F.** (2009) Consumption of grape seed extract prevents amyloid-β deposition and attenuates inflammation in brain of an Alzheimer's disease mouse. *Neurotox. Res.*, **15**:3–14. URL http://www.ncbi.nlm.nih.gov/pubmed/19384583.

[258] **Joseph J.A., Shukitt-Hale B., Brewer G.J., Weikel K.A., Kalt W. & Fisher D.R.** (2010) Differential protection among fractionated blueberry polyphenolic families against DA-, Abeta(42)- and LPS-induced decrements in Ca(2+) buffering in primary hippocampal cells. *J. Agric. Food Chem.*, **58**:8196–8204. URL http://www.ncbi.nlm.nih.gov/pubmed/20597478.

[259] **Zheng J. & Ramirez V.D.** (2000) Inhibition of mitochondrial proton F_0F_1-ATPase/ATP synthase by polyphenolic phytochemicals. *Br. J. Pharmacol.*, **130**:1115–1123. URL http://www.ncbi.nlm.nih.gov/pubmed/10882397.

[260] **Lang D.R. & Racker E.** (1974) Effects of quercetin and F_1 inhibitor on mitochondrial ATPase and energy-linked reactions in submitochondrial particles. *Biochim. Biophys. Acta.*, **333**:180–186. URL http://www.ncbi.nlm.nih.gov/pubmed/19400030.

[261] **Di Pietro A., Godinot C., Bouillant M.L. & Gautheron D.C.** (1975) Pig heart mitochondrial ATPase: properties of purified and membrane-bound enzyme: effects of flavonoids. *Biochimie.*, **57**:959–967. URL http://www.ncbi.nlm.nih.gov/pubmed/130941.

[262] **Zheng J. & Ramirez V.D.** (1999) Piceatannol, a stilbene phytochemical, inhibits mitochondrial F_0F_1-ATPase activity by targeting the F_1 complex. *Biochem. Biophys. Res. Commun.*, **261**:499–503. URL http://www.ncbi.nlm.nih.gov/pubmed/10425214.

[263] **Gledhill J.R., Montgomery M.G., Leslie A.G.W. & Walker J.E.** (2007) Mechanism of inhibition of bovine F_1-ATPase by resveratrol and related polyphenols. *Proc. Natl. Acad. Sci. USA*, **104**:13632–13637. URL http://www.ncbi.nlm.nih.gov/pubmed/17698806.

[264] **Rossingnol R., Letellier T., Malgat M., Rocher C. & Mazat J.P.** (2000) Tissue variation in the control of oxidative phosphorylation: implication for mitochondrial diseases. *Biochem. J.*, **347**:45–53. URL http://www.ncbi.nlm.nih.gov/pubmed/10727400.

[265] **Scalbert A. & Williamson G.** (2000) Dietary intake and bioavailability of polyphenols. *J. Nutr.*, **130**:2073S–2085S. URL http://www.ncbi.nlm.nih.gov/pubmed/10917926.

[266] **Li B., Vik S.B. & Tu Y.** (2011) Theaflavins inhibit the ATP synthase and the respiratory chain without increasing superoxide production. *J. Nutr. Biochem.*, **Epub**. URL http://www.ncbi.nlm.nih.gov/pubmed/21924889.

[267] **Hwang J.T., Kwon D.Y. & Yoon S.H.** (2009) AMP-activated protein kinase: a potential target for the disease prevention by natural occuring polyphenols. *N. Biotechnol.*, **26**:17–22. URL http://www.ncbi.nlm.nih.gov/pubmed/19818314.

[268] **Calabrese V., Cornelius C., Stella A.M. & Calabrese E.J.** (2010) Cellular stress responses, mitostress and carnitine insufficiencies as critical determinants in aging and neurodegeneration disorders: role of hormesis and vitagenes. *Neuochem. Res.*, **35**:1880–1915. URL http://www.ncbi.nlm.nih.gov/pubmed/21080068.

[269] **Del Bo' C., Kristo A.S., Kalea A.Z., Ciappellano S., Riso P., Porrini M. & Klimis-Zacas D.** (2010) The temporal effect of a wild blueberry (*Vaccinium angustifolium*)-enriched diet on vasomotor tone in the Sprague-Dawley rat. *Nutr Metab Cardiovasc Dis*. URL http://www.ncbi.nlm.nih.gov/pubmed/20709513.

[270] **Riviére C., Papastamoulis Y., Fortin P.Y., Delchier N., Andriamanarivo S., Waffo-Teguo P., Kapche G.D., Amira-Guebalia H., Delaunay J.C., Mérillon J.M., Richard T. & Monti J.P.** (2010) New stilbene dimers against amyloid fibril formation. *Bioorg. Med. Chem. Lett.*, 20:3441–3443. URL http://www.ncbi.nlm.nih.gov/pubmed/20452207.

[271] **Ladiwala A.R., Lin J.C., Bale S.S., Marcelino-Cruz A.M., Bhattacharya M., Dordick J.S. & Tessier P.M.** (2010) Resveratrol selectively remodels soluble oligomers and fibrils of amyloid Aβ into off-pathway conformers. *J. Biol. Chem.*, 285:24228–24237. URL http://www.ncbi.nlm.nih.gov/pubmed/20511235.

[272] **Rawel H.M., Meidtner K. & Kroll J.** (2005) Binding of selected phenolic compounds to proteins. *J. Agric. Food Chem.*, 53:4228–4235. URL http://www.ncbi.nlm.nih.gov/pubmed/15884865.

[273] **Zarse K., Schmeisser S., Birringer M., Falk E., Schmoll D. & Ristow M.** (2010) Differential effects of resveratrol and SRT1720 on lifespan of adult *Caenorhabditis elegans*. *Horm. Metab. Res.*, 42:837–839. URL http://www.ncbi.nlm.nih.gov/pubmed/20925017.

[274] **Cheng Z. & White M.F.** (2011) Targeting Forkhead box O1 from the concept to metabolic diseases: lessons from mouse models. *Antioxid. Redox. Signal.*, 14:649–661. URL http://www.ncbi.nlm.nih.gov/pubmed/20615072.

[275] **Ni Y.G., Wang N., Cao D.J., Sachan N., Morris D.J., Gerard R.D., Kuro-O M., Rothermel B.A. & Hill J.A.** (2007) FoxO transcription factors activate Akt and attenuate insulin signaling in heart by inhibiting protein phosphatases. *Proc. Natl. Acad. Sci. USA.*, 104:20517–20522. URL http://www.ncbi.nlm.nih.gov/pubmed/18077353.

[276] **Carter M.E. & Brunet A.** (2007) FoxO transcription factors. *Cur. Biol.*, 17:113–114. URL http://www.ncbi.nlm.nih.gov/pubmed/17307039.

[277] **Salminen A. & Kaamiranta K.** (2010) ER stress and hormetic regulation of the aging process. *Ageing Res. Rev.*, 9:211–217. URL http://www.ncbi.nlm.nih.gov/pubmed/20416402.

[278] **Wood J., Rogina B., Lavu S., Howitz K., Helfand S., Tatar M. & Sinclair D.A.** (2004) Sirtuin activators mimic caloric restriction and delay ageing in metazoans. *Nature*, 430:686–689. URL http://www.ncbi.nlm.nih.gov/pubmed/15254550.

[279] **Kaeberlein M., McDonagh T., Heltweg B., Hixon J., Westman E.A., Caldwell S.D., Napper A., Curtis R., Di Stefano P.S., Fields S., Bedalov A. & Kennedy B.K.** (2005) Substrate-specific activation of sirtuins by resveratrol. *J. Biol. Chem.*, 280:17038–17045. URL http://www.ncbi.nlm.nih.gov/pubmed/15684413.

[280] **Borra M.T., Smith B.C. & Denu J.M.** (2005) Mechanism of human SIRT1 activation by resveratrol. *J. Biol. Chem.*, 280:17187–17195. URL http://www.ncbi.nlm.nih.gov/pubmed/15749705.

[281] **Baur J.A., Chen D., Chini E.N., Chua K., Cohen H.Y., de Cabo R., Deng C., Dimmeler S., Gius D., Guarente L.P., Helfand S.L., Imai S., Itoh H., Kadowaki T., Koya D., Leeuwenburgh C., McBurney M., Nabeshima Y., Neri C., Oberdoerffer P., Pestell R.G., Rogina B., Sadoshima J., Sartorelli V., Serrano M., Sinclair D.A., Steegbom C., Tatar M., Tissenbaum H.A., Tong Q., Tsubota K., Vaquero A. & Verdin E.** (2010) Dietry restriction: standing up for sirtuins. *Science*, 329:5995. URL http://www.ncbi.nlm.nih.gov/pubmed/20798296.

[282] **Burnett C., Valentini S., Cabreiro F., Goss M., Somogyvári M., Piper M.D., Hoddinott M., Sutphin G.L., Leko V., McElwee J.J., Vazquez-Manrique R.P., Orfila A.M., Ackerman D., Au C., Vinti G., Riesen M., Howard K., Neri C., Bedalov A., Kaeberlein M., Söti C., Partridge L. & Gems D.** (2011) Absence of effects of Sir2 overexpression on lifespan in *C. elegans* and *Drosophila*. *Nature*, 477:482–485. URL http://www.ncbi.nlm.nih.gov/pubmed/21938067.

[283] **Pietsch K., Saul N., Menzel R., Stürzenbaum S.R. & Steinberg C.E.** (2009) Quercetin mediated lifespan extension in *Caenorhabditis elegans* is modulated by age-1, daf-2, sek-1 and unc-43. *Biogerontology*, **10**:565–578. URL http://www.ncbi.nlm.nih.gov/pubmed/19043800.

[284] **Srividhya R., Jyothilakshmi V., Arulmathi K., Senthilkumaran V. & Kalaiselvi P.** (2008) Attention of senescence-induced oxidative exacerbations in aged rat brain by (-)-epigallocatechin-3-gallate. *Int. J. Dev. Neurosci.*, **26**:217–223. URL http://www.ncbi.nlm.nih.gov/pubmed/18207349.

[285] **Collins J.J., Evason K., Pickett C.L., Schneider D.L. & Kornfeld K.** (2008) The anticonvulsant ethosuximide disrupts sensory function to extend *C. elegans* lifespan. *PLoS Genet.*, **4**:e1000230. URL http://www.ncbi.nlm.nih.gov/pubmed/18949032.

[286] **Torres G., Dileo J.N., Hallas B.H., Horowitz J.M. & Leheste J.R.** (2011) Silent information regulator 1 mediates hippocampal plasticity through presenilin1. *Neurosci.*, **179**:32–40. URL http://www.ncbi.nlm.nih.gov/pubmed/21277951.

[287] **Pineda-Molina E., Klatt P., Vázquez J., Marina A., Garcia de Lacoba M., Pérez-Sala D. & Lamas S.** (2001) Glutathionylation of the p50 subuit of NFκB: a mechanism for redox induced inhibition of DNA binding. *Biochemistry.*, **40**:14134–14142. URL http://www.ncbi.nlm.nih.gov/pubmed/11714266.

[288] **Chen J., Zhou Y., Mueller-Steiner S., Chen L.F., Kwon H., Yi S., Mucke L. & Gan L.** (2005) SIRT1 protects against microglia-dependent amyloid-β toxicity through inhibiting NF-κB signaling. *J. Biol. Chem.*, **280**:40364–40374. URL http://www.ncbi.nlm.nih.gov/pubmed/16183991.

[289] **Adler A.S., Sinha S., Kawahara L.A., Zhang J.Y., Segal E. & Chang H.Y.** (2007) Motif module map reveals enforcement of aging by continual NF-κB activity. *Genes & Develop.*, **21**:32443257. URL http://www.ncbi.nlm.nih.gov/pubmed/18055696.

[290] **Rahman I., Biswas S.K. & Kirkham P.A.** (2006) Regulation of inflammation and redox signaling by dietry polyphenols. *Biochem. Pharmacol.*, **72**:1439–1454. URL http://www.ncbi.nlm.nih.gov/pubmed/16920072.

[291] **Bureau G., Longpré F. & Martinoli M.G.** (2008) Resveratrol and quercetin, two natural polyphenols, reduce apoptotic neuronal cell death induced by neuroinflammation. *J. Neurosci. Res.*, **86**:403–410. URL http://www.ncbi.nlm.nih.gov/pubmed/17929310.

[292] **Sikora E., Scapagnini G. & Barbagallo M.** (2010) Curcumin, inflammation, ageing and age-related disease. *Immun. Ageing*, **7**:1. URL http://www.ncbi.nlm.nih.gov/pubmed/20205886.

[293] **Ramassamy C.** (2006) Emerging role of polyphenolic compounds in the treatment of neurodegenerative disease: a review of their intracellular targets. *Eur. J. Pharmacol*, **545**:51–64. URL http://www.ncbi.nlm.nih.gov/pubmed/16904103.

[294] **Mukhtar H. & Ahmad N.** (2000) Tea polyphenols: prevention of cancer and optimizing health. *Am. J. Clin. Nutr.*, **71(suppl)**:1698S–1702S. URL http://www.ncbi.nlm.nih.gov/pubmed/10837321.

[295] **Biesalski H.K.** (2007) Polyphenols and inflammation: basic interactions. *Curr. Opin. Clin. Nutr. Metab. Care*, **10**:724–728. URL http://www.ncbi.nlm.nih.gov/pubmed/18089954.

[296] **Kraft T.E., Parisotto D., Schempp C. & Efferth T.** (2009) Fighting cancer with red wine? Molecular mechanisms of resveratrol. *Crit. Rev. Food Sci. Nutr*, **49**:782–799. URL http://www.ncbi.nlm.nih.gov/pubmed/20443159.

[297] **Brunet A., Sweeney L.B., Sturgill J.F., Chua K.F., Greer P.L., Lin Y., Tran H., Ross S.E., Mostoslavsky R., Cohen H.Y., Hu L.S., Cheng H.L., Jedrychowski M.P., Gygi S.P., Sinclair D.A., Alt F.W. & Greenberg M.E.** (2004) Stress-dependent regulation of FOXO transcription factors by the SIRT1 deacetylase. *Science*, **303**:2011–2015. URL http://www.ncbi.nlm.nih.gov/pubmed/14976264.

[298] **Raivich G.** (2008) c-Jun expression, activation and function in neural cell death, inflammation and repair. *J. Neurochem.*, 107:898–906. URL http://www.ncbi.nlm.nih.gov/pubmed/18793328.

[299] **Vries R.G., Prudenziati M., Zwartjes C., Verlaan M., Kalkhoven E. & Zentema A.** (2001) A specific lysine in c-Jun is required for transcriptional repression by E1A and is acetylated by p300. *EMBO J.*, 20:6095–6103. URL http://www.ncbi.nlm.nih.gov/pubmed/11689449.

[300] **Lu G.D., Shen H.M., Chung M.C. & Ong C.N.** (2007) Critical role of oxidative stress and sustained JNK activation in aloe-emodin mediated apoptotic cell death in human hepatoma cells. *Carcinogenesis.*, 28:1937–1945. URL http://www.ncbi.nlm.nih.gov/pubmed/17698970.

[301] **Stefani M., Markus M.A., Lin R.C.Y., Pinese M., Dawes I.W. & Morris B.J.** (2007) The effect of resveratrol on a cell model of human aging. *Ann. N. Y. Acad. Sci.*, 1114:407–418. URL http://www.ncbi.nlm.nih.gov/pubmed/17804521.

[302] **Dzamko N.L. & Steinberg G.R.** (2009) AMPK-dependent hormonal regulation of whole-body energy metabolism. *Acta Physiol. (Oxf)*, 196:115–127. URL http://www.ncbi.nlm.nih.gov/pubmed/19245657.

[303] **Stephan J.S., Yeh Y.Y., Ramachandran V., Deminoff S.J. & Herman P.K.** (2009) The Tor and PKA signaling pathways independently target the Atg1/Atg13 protein kinase complex to control autophagy. *PNAS*, 106:17049–17054. URL http://www.ncbi.nlm.nih.gov/pubmed/19805182.

[304] **Sharp Z.D.** (2011) Aging and TOR: interwoven in the fabric of life. *Cell Mol. Life Sci.*, 68:587–597. URL http://www.ncbi.nlm.nih.gov/pubmed/20960025.

[305] **Armour S.M., Baur J.A., Hsieh S.N., Land-Bracha A., Thomas S.M. & Sinclair D.A.** (2009) Inhibition of mammalian S6 kinase by resveratrol suppresses autophagy. *Aging (Albany NY)*, 1:515–528. URL http://www.ncbi.nlm.nih.gov/pubmed/20157535.

[306] **Gurusamy N., Lekli I., Mukherjee S., Ray D., Ahsan M.K., Gherghiceanu M., Popescu L.M. & Das D.K.** (2010) Cardioprotection by resveratrol: a novel mechanism via autophagy involving the mTORC2 pathway. *Cardiovasc. Res.*, 85:103–112. URL http://www.ncbi.nlm.nih.gov/pubmed/19959541. Prof. Das has come under investigation for research fraud. Several papers have been retracted but not this one. Of the papers retracted Gurusamy was a lead author of several.

[307] **Greco S.J., Sarkar S., Johnston J.M. & Tezapsidis N.** (2009) Leptin regulates tau phosphorylation and amyloid through AMPK in neuronal cells. *Biochem. Biophys. Res. Commun.*, 380:98–104. URL http://www.ncbi.nlm.nih.gov/pubmed/19166821.

[308] **Bartness T.J., Shrestha Y.B., Vaughan C.H., Schwartz G.J. & Song C.K.** (2010) Sensory and sympathetic nervous system control of white adipose tissue lipolysis. *Mol. Cell. Endocrinol.*, 318:34–43. URL http://www.ncbi.nlm.nih.gov/pubmed/19747957.

[309] **Kawabata K., Kawai Y. & Terao J.** (2010) Suppressive effect of quercetin on acute stress-induced hypothalamic-pituitary-adrenal axis response in Wistar rats. *J. Nutr. Biochem.*, 21:374–380. URL http://www.ncbi.nlm.nih.gov/pubmed/19423323.

[310] **Ganong W.F.** (1997) *Review of Medical Physiology*. Appleton and Lange, Stamford, Connecticut, 18th edition.

[311] **Thorntoon T.M. & Rincon M.** (2009) Non-classical p38 map kinase functions: cell cycle checkpoints and survival. *Int. J. Biol. Sci.*, 5:44–52. URL http://www.ncbi.nlm.nih.gov/pubmed/19159010.

[312] **Zhou H., Chen Q., Kong D.L., Guo J., Wang Q. & Yu S.Y.** (2011) Effects of resveratrol on gliotransmitter levels and p38 activities in cultured astrocytes. *Neurochem. Res.*, 36:17–26. URL http://www.ncbi.nlm.nih.gov/pubmed/20842424.

[313] **Kim Y.H., Lee D.H., Jeong J.H., Guo Z.S. & Lee Y.J.** (2008) Quercetin augments TRAIL-induced apoptotic death: involvement of the ERK signal transduction pathway. *Biochem. Pharmacol.*, 75:1946–1958. URL http://www.ncbi.nlm.nih.gov/pubmed/18377872.

[314] **Youngman M.J., Rogers Z.N. & Kim D.H.** (2011) A decline in p38 MAPK signaling underlies immunosenescence in *Caenorhabditis elegans*. *PLoS Gen.*, 7:e1002082. URL http://www.ncbi.nlm.nih.gov/pubmed/21625567.

[315] **Garsin D.A., Villanueva J.M., Begun J., Kim C.D. D. H. andSifri, Calderwood S.B., Ruvkun G. & Ausubel F.M.** (2003) Long-lived *C. elegans daf*-2 mutants are resistant to bacterial pathogens. *Science*, 300:1921. URL http://www.ncbi.nlm.nih.gov/pubmed/12817143.

[316] **Hinson J.P. & Raven P.W.** (1999) DHEA deficiency syndrome: a new term for old age? *J. Endocrinology*, 163:1–5. URL http://www.ncbi.nlm.nih.gov/pubmed/10495400.

[317] **Chen C.C. & Parker C.R.** (2004) Adrenal androgens and the immune system. *Semin. Reprod. Med.*, 22:369–377. URL http://www.ncbi.nlm.nih.gov/pubmed/15635504.

[318] **Gassoir M., Carter R.B. & Witkin J.M.** (1999) Neuroactive steroids: potential therapeutic use in neurological and psychiatric disorders. *TiPS*, 20:107–112. URL http://www.ncbi.nlm.nih.gov/pubmed/10203866.

[319] **Henderon V.W. & Brinton R.D.** (2010) Menopause and mitochondria: windows into estrogen effects on Alzheimer's disease risk and therapy. *Prog. Brain Res.*, 182:77–96. URL http://www.ncbi.nlm.nih.gov/pubmed/20541661.

[320] **Craig M.C. & Murphy D.G.** (2010) Estrogen therapy and Alzheimer's dementia. *Ann. N. Y. Acad. Sci.*, 1205:245–253. URL http://www.ncbi.nlm.nih.gov/pubmed/20840280.

[321] **Mukai H., Tsurugizawa T., Ogiue-Ikeda M., Murakami G., Hojo Y., Ishii H., Kimoto T. & Kawato S.** (2006) Local neurosteroid production in the hippocampus: influence on synaptic plasticity of memory. *Neuroendorcrinology*, 84:255–263. URL http://www.ncbi.nlm.nih.gov/pubmed/17142999.

[322] **Tsuruo Y.** (2005) Topography and function of androgen-metabolizing enzymes in the central nervous system. *Anat. Sci. Int.*, 80:1–11. URL http://www.ncbi.nlm.nih.gov/pubmed/15794125.

[323] **Bruzzone R., O Rego J.L., Luu-The V., Pelletier G., Vallarino M. & Vaudry H.** (2010) Immunohistochemical localization and biological activity of 3β-hydroxysteroid dehydrogenase and 5α-reductase in the brain of the frog, *Rana esculenta*, during development. *J. Chem. Neuroanat.*, 39:35–50. URL http://www.ncbi.nlm.nih.gov/pubmed/19665548.

[324] **Azcoitia I., Yague J.G. & Garcia-Segura L.M.** (2011) Estradiol synthesis within the brain. *Neurosci.*, 191:139–147. URL http://www.ncbi.nlm.nih.gov/pubmed/21320576.

[325] **Gehm B.D., McAndrews J.M., Chien P.Y. & Jamesn J.L.** (1997) Resveratrol, a polyphenolic compound found in grapes and wine, is an agonist for the estrogen receptor. *PNAS*, 94:14138–14143. URL http://www.ncbi.nlm.nih.gov/pubmed/9391166.

[326] **Bowers J.L., Tyulmenkov V.V., Jernigan S.C. & Klinge C.M.** (2000) Resveratrol acts as a mixed agonist/antagonist for estrogen receptors alpha and beta. *Endocrinology*, 141:3657–3667. URL http://www.ncbi.nlm.nih.gov/pubmed/11014220.

[327] **Mitchell S.H., Zhu W. & Young C.Y.** (1999) Resveratrol inhibits the expresson and function of the androgen recetpor in LNCaP prostate cancer cells. *Cancer Res.*, 59:5892–5895. URL http://www.ncbi.nlm.nih.gov/pubmed/10606230.

[328] **Siddiqui I.A., Asim M., Hafeez B.B., Adhami V.M., Tarapore R.S. & Mukhtar H.** (2011) Green tea polyphenol EGCG blunts androgen receptor function in prostate cancer. *FASEB J.*, 25:1198–1207. URL http://www.ncbi.nlm.nih.gov/pubmed/21177307.

[329] **Bowers J.L., Tyulmenkov V.V., Jernigan S.C. & Klinge C.M.** (2000) Resveratrol acts as a mixed agonist/antagonist for estrogen receptors α and β. *Endocrinology*, 141:3657–3667. URL http://www.ncbi.nlm.nih.gov/pubmed/11014220.

[330] **Robb E.L. & Stuart J.A.** (2011) Resveratrol interacts with estrogen receptor-β to inhibit cell replicative growth and enhance stress resistance by upregulating mitochondrial superoxide dismutase. *Free Radic. Biol. Med.*, 50:821–831. URL http://www.ncbi.nlm.nih.gov/pubmed/21215799.

[331] **Yu H.P., Hwang T.L., Hsieh P.W. & Lau Y.T.** (2011) Role of estrogen receptor-dependent upregulation of P38 MAPK/heme oxygenase 1 in resveratrol-mediated attenuation of intestinal injury after trauma-hemorrhage. *Shock*, 35:517–523. URL http://www.ncbi.nlm.nih.gov/pubmed/21192278.

[332] **Lu A., Ran R.Q., Clark J., Reilly M., Nee A. & Sharp F.R.** (2002) 17-beta-estradiol induces heat shock proteins in brain arteries and potentiates ischemic heat shock protein induction in glia and neurons. *J. Cereb. Blood Flow Metab.*, 22:183–195. URL http://www.ncbi.nlm.nih.gov/pubmed/11823716.

[333] **Han Y.S., Bastianetto S., Dumont Y. & Quirion R.** (2006) Specific plasma membrane binding sites for polyphenols, including resveratrol, in the rat brain. *J. Pharmacol. Exp. Ther.*, 318:238–245. URL http://www.ncbi.nlm.nih.gov/pubmed/16574779.

[334] **Bastianetto S., Dumont Y., Duranton A., Vercauteren F., Breton L. & Quirion R.** (2010) Protective action of resveratrol in human skin: possible involvement of specific receptor binding sites. *PLosS One*, 5:e12935. URL http://www.ncbi.nlm.nih.gov/pubmed/20886076.

[335] **Femandez J.W., Rezai-Zadeh K., Obregon D. & Tan J.** (2010) ECGC functions through estrogen receptor-mediated activation of ADAM10 in the promotion of non-amyloidogenic processing of APP. *FEBS Lett.*, 584:4259–4267. URL http://www.ncbi.nlm.nih.gov/pubmed/20849853.

[336] **Valles S.L., Dolz-Gaiton P., Gambini J., Borras C., Lloret A., Pallardo F.V. & Viña J.** (2010) Estradiol or genistein prevent Alzheimer's disease-associated inflammation correlating with an increase PPAR gamma expression in cultured astrocytes. *Brain Res.*, 1312:138–144. URL http://www.ncbi.nlm.nih.gov/pubmed/19948157.

[337] **Vivani B., Corsini E., Binaglia M., Lucchi L., Galli C.L. & Marinovich M.** (2002) The anti-inflammatory activity of estrogen in glial cells is regulated by the PKC anchoring protein RACK-1. *J. Neurochem.*, 83:1180–1187. URL http://www.ncbi.nlm.nih.gov/pubmed/12437589.

[338] **Han Y.S., Zheng W.H., Bastianetto S., Chabot J.G. & Quirion R.** (2004) Neuroprotective effects of resveratrol against β-amyloid-induced neurotoxicity in rat hippocampal neurons: Involvement of protein kinase C. *Br. J. Pharmacol.*, 141:997–1005. URL http://www.ncbi.nlm.nih.gov/pubmed/15028639.

[339] **Levites Y., Amit T., Mandel S. & Youdim M.B.** (2003) Neuroprotection and neurorescue aginast abeta toxicity and PKC-dependent release of nonamyloidogenic soluble precursor protein by green tea polyphenol (-)-epigallocatechin-3-gallate. *FASEB J.*, 17:952–954. URL http://www.ncbi.nlm.nih.gov/pubmed/12670874.

[340] **Galluzzo P., Martini C., Bulzomi P., Leone S., Bolli A., Pallottini V. & Marino M.** (2009) Quercetin-induced apoptotic cascade in cancer cells: antioxidant versus estrogen receptor alpha-dependent mechanisms. *Mol. Nutr. Food Res.*, 53:699–708. URL http://www.ncbi.nlm.nih.gov/pubmed/19194971.

[341] **Banks W.A., Kastrin A.J., Huang W., Jaspan J.B. & Maness L.M.** (1996) Leptin enters the brain by a saturable system independent of insulin. *Peptides*, 17:305–311. URL http://www.ncbi.nlm.nih.gov/pubmed/8801538.

[342] **Garvcia-Segura L.M., Chowen J.A. & Naftolin F.** (1996) Endocrine glia: roles of glial cells in the brain actions of steroid and thyroid hormones and the regulation of hormone secreation. *Fontiers in Neuroendocrinology*, 17:180–211. URL http://www.ncbi.nlm.nih.gov/pubmed/8812295.

[343] **Faragher R.G., Burton D.G., Majecha P., Fong N.S., Davis T., Sheerin A. & Ostler E.L.** (2011) Resveratrol, but not dihydroresveratrol, induces premature senescence in primary human fibroblasts. *Age (Dordr)*, 33:555–564. URL http://www.ncbi.nlm.nih.gov/pubmed/21318333.

[344] **Watanabe C.M., Wolffram S., Ader P., Rimbach G., Packer L., Maguire J.J., Schultz P.G. & Gohil K.** (2001) The in vivo neuromodulatory effects of herbal medicine *Ginkgo biloba*. *PNAS*, 98:6577–6580. URL http://www.ncbi.nlm.nih.gov/pubmed/11381109.

[345] **Azcoitia I., Santos-Galindo M., Arevalo M.A. & Garcia-Segura L.M.** (2010) Roles of astroglia in the neuroplastic and neuroprotective actions of estradiol. *Eur. J. Neurosci.*, 32:1995–2002. URL http://www.ncbi.nlm.nih.gov/pubmed/21143654.

[346] **Morale M.C., Serra P.A., L'episcopo F., Tirolo C., Caniglia S., Testa N., Gennuso F., Giaquinta G., Rocchitta G. & Desole M.S.** (2006) Estrogen, neuroinflammation and neuroprotection in Parkinson's disease: glia dictates resistance versus vulnerability to neurodegeneration. *Neurosci.*, 138:869–878. URL http://www.ncbi.nlm.nih.gov/pubmed/16337092.

[347] **Stridh M.H., Correa F., Nodin C., Weber S.G., Blomstrand F., Nilsson M. & Sandberg M.** (2010) Enhanced glutathione efflux from astrocytes in culture by low extracellular Ca^{2+} and curcumin. *Neurochem. Res.*, 35:1231–1238. URL http://www.ncbi.nlm.nih.gov/pubmed/20437093.

[348] **Jahanshahi M., Sadeghi Y., Hosseini A., Naghdi N. & Marjani A.** (2008) The effect of spatial learning on the number of astrocytes in the CA3 subfield of the rat hippocampus. *Singapore Med. J.*, 49:388–391. URL http://www.ncbi.nlm.nih.gov/pubmed/18465048.

[349] **Quincozes-Santos A. & Gottfried C.** (2011) Resveratrol modulates astroglial functions: neuroprotective hypothesis. *Ann. N. Y. Acad. Sci.*, 1215:72–78. URL http://www.ncbi.nlm.nih.gov/pubmed/21261643.

[350] **de Almeida L.M., Piñeiro C.C., Leite M.C., Brolese G., Tramontina F., Feoli A.M., Gottfried C. & Gonçalves C.A.** (2007) Resveratrol increases glutamate uptake, glutathione content, and S100B secretion in cortical astrocyte cultures. *Cell Mol. Neurobiol.*, 27:661–668. URL http://www.ncbi.nlm.nih.gov/pubmed/17554623.

[351] **Webb S.J., Geoghegan T.E., Prough R.A. & Michael Miller K.K.** (2006) The biological actions of dehydroepiandrosterone involves multiple receptors. *Drug. Metab. Rev.*, 38:89–116. URL http://www.ncbi.nlm.nih.gov/pubmed/16684650.

[352] **Liu J.** (2005) Oleanolic acid and ursolic acid: research perspectives. *J. Ethnopharmacol.*, 100:92–94. URL http://www.ncbi.nlm.nih.gov/pubmed/15994040.

[353] **Neto C.C.** (2007) Cranberry and blueberry: evidence for protective effects against cancer and vascular diseases. *Mol. Nutr. Food Res.*, 51:652–664. URL http://www.ncbi.nlm.nih.gov/pubmed/17533651.

[354] **Radler F. & Hom D.H.S.** (1965) The composition of grape cuticle wax. *Aust. J. Chem.*, 18:1059–1069. URL http://www.publish.csiro.au/paper/CH9651059.

[355] **Shih Y.H., Chein Y.C., Wang J.Y. & Fu Y.S.** (2004) Ursolic acid protects hippocampal neurons against kainate-induced excitotoxicity in rats. *Neurosci. Lett.*, 362:136–140. URL http://www.ncbi.nlm.nih.gov/pubmed/15193771.

[356] **Matteucci A., Cammarota R., Paradisi S., Varano M., Balduzzi M., Leo L., Bellenchi G.C., De Nuccio C., Carnovale-Scalzo G., Scorcia G., Frank C., Mallozzi C., Di Stasi A.M., Visentin S. & Malchiodi-Albedi F.** (2011) Cucumin protects against NMDA-induced toxicity: a possible role for NR2A subunit. *Invest. Ophthalmol. Vis. Sci.*, 52:1070–1077. URL http://www.ncbi.nlm.nih.gov/pubmed/20861489.

[357] **Lee H., Bae J.H. & Lee S.R.** (2004) Protective effect of green tea polyphenol EGCG against neuronal damage and brain edema after unilateral cerebral ischemia in gerbils. *J. Neurosci. Res.*, 77:892–900. URL http://www.ncbi.nlm.nih.gov/pubmed/15334607.

[358] **Wang Q., Yu S., Simonyi A., Rottinghaus G., Sun G.Y. & Sun A.Y.** (2004) Resveratrol protects against neurotoxicity induced by kainic acid. *Neurochem. Res.*, 29:2105–2112. URL http://www.ncbi.nlm.nih.gov/pubmed/15662844.

[359] **Goldberg D.M., J. Y. & Soleas G.J.** (2003) Absorption of three wine-related polyphenols in three different matrices by healthy subjects. *Clin. Biochem.*, 36:79–87. URL http://www.ncbi.nlm.nih.gov/pubmed/12554065.

[360] **Del Rio D., Borges G. & Crozier A.** (2010) Berry flavonoids and phenolics: bioavailablity and evidence of protective effects. *Br. J. Nutr.*, 104 S3:S67–90. URL http://www.ncbi.nlm.nih.gov/pubmed/20955651.

[361] **Ghosh D. & Scheepens A.** (2009) Vascular action of polyphenols. *Mol. Nutr. Food Res.*, 53:322–331. URL http://www.ncbi.nlm.nih.gov/pubmed/19051188.

[362] **West S.G.** (2001) Effect of diet on vascular reactivity: an emerging marker for vascular risk. *Curr. Atheroscler. Rep.*, 3:446–455. URL http://www.ncbi.nlm.nih.gov/pubmed/11602064.

[363] **Cheng H.C., Chan C.M., Tsay H.S., Liang H.J., Liang Y.C. & Liu D.Z.** (2007) Improving effects of epigalocatechin-3-gallate on hemorheological abnormalities of aging guinea pigs. *Circ. J.*, 71:597–603. URL http://www.ncbi.nlm.nih.gov/pubmed/17384465.

[364] **Grassi D., Desideri G., Necozione S., Lippi C., Casale R., Properzi G., Blumberg J.B. & Ferri C.** (2008) Blood pressure is reduced and insulin sensitivity increased in glucose-intolerant, hypertensive subjects after 15 days of consuming high-polyphenol dark chocolate. *J. Nutr.*, 138:1671–1676. URL http://www.ncbi.nlm.nih.gov/pubmed/18716168.

[365] **Dohadwala M.M., Holbrook M., Hamburg N.M., Shenouda S.M., Chung W.B., Titas M., Kluge M.A., Wang N., Palmisano J., Milbury P.E., Blumberg J.B. & Vita J.A.** (2011) Effects of cranberry juice consumption on vascular function in patients with coronary artery disease. *Am. J. Clin. Nutr.*, 93:934–940. URL http://www.ncbi.nlm.nih.gov/pubmed/21411615.

[366] **Kalea A.Z., Clark K., Schuschke D.A. & Klimis-Zacas D.J.** (2009) Vascular reactivity is affected by dietary consumption of wild blueberries in the Sprague-Dawley rat. *J. Med. Food*, 12:21–28. URL http://www.ncbi.nlm.nih.gov/pubmed/19298192.

[367] **Kristo A.S., Kalea A.Z., Schuschke D.A. & Klimis-Zacas D.J.** (2010) A wild blueberry-enriched diet (*Vaccinium angustifolium*) improves vascular tone in the adult spontaneously hypertensive rat. *J. Agric. Food Chem.*, 58:11600–11605. URL http://www.ncbi.nlm.nih.gov/pubmed/20964405.

[368] **Schewe T., Steffen Y. & Sies H.** (2008) How do dietary flavanols improve vascular function? a position paper. *Arch. Biochem. Biophys.*, 476:102–106. URL http://www.ncbi.nlm.nih.gov/pubmed/18358827.

[369] **Reiter C.E., Kim J.A. & Quon M.J.** (2010) Green tea polyphenol epigallocatechin gallate reduces endothelin-1 expression and secretion in vascular endothelial cells: roles for AMP-activated protein kinase, Akt, and FOXO1. *Endocrinology*, 151:103–114. URL http://www.ncbi.nlm.nih.gov/pubmed/19887561.

[370] **Wood E.G., Carrier M.J. & Crozier A.** (2006) Red wine procyanidins and vascular health. *Nature*, 444:566. URL http://www.ncbi.nlm.nih.gov/pubmed/17136085.

[371] **Chan S.L., Capdeville-Atkinson C. & Atkinson J.** (2008) Red wine polyphenols improve endothelium-dependent dilation in rat cerebral arterioles. *J. Cardiovasc. Pharmacol.*, 51:553–558. URL http://www.ncbi.nlm.nih.gov/pubmed/18496148.

[372] **van Mierlo L.A., Zock P.L., van der Knaap H.C. & Draijer R.** (2010) Grape polyphenols do not affect vascular function in healthy men. *J. Nutr.*, 140:1769–1773. URL http://www.ncbi.nlm.nih.gov/pubmed/20702747.

[373] **Khan A.A., Dace D.S., Ryazanov A.G., Kelly J. & Apte R.S.** (2010) Resveratrol regulates pathologic angiogenesis by a eukaryotic elongation factor-2 kinase regulated pathway. *Am. J. Pathol.*, 177:481–492. URL http://www.ncbi.nlm.nih.gov/pubmed/20472894.

[374] **Willis L.M., Small B.J., Bickford P.C., Umphlet C.D., Moore A.B. & Granholm A.C.** (2008) Dietary blueberry supplementation affects growth but not vascularization of neural transplants. *J. Cereb. Blood Flow Metab.*, 28:1150–1164. URL http://www.ncbi.nlm.nih.gov/pubmed/18285804.

[375] **Xia L., Wang X.X., Hu X.S., Guo X.G., Shang Y.P., Chen H.J., Zeng C.L., Zhang F.R. & Chen J.Z.** (2008) Resveratrol reduces endothelial progenitor cells senescence through augmentation of telomerase activity by Akt-dependent mechanisms. *Br. J. Pharmacol.*, 155:387–394. URL http://www.ncbi.nlm.nih.gov/pubmed/18587418.

[376] **Pieper A.A., Xie S., Capota E., Estill S.J., Zhong J., Long J.M., Becker G.L., Huntington P., Goldman S.E., Shen C.H., Capota M., Britt J.K., Kotti T., Ure K., Brat D.J., Williams N.S., MacMillan K.S., Naidoo J., Melito L., Hsieh J., De Brabander J., Ready J.M. & McKnight S.L.** (2010) Discovery of a proneurogenic, neuroprotective chemical. *Cell*, **142**:39–51. URL http://www.ncbi.nlm.nih.gov/pubmed/20603013.

[377] **Rafalski V.A. & Brunet A.** (2011) Energy metabolism in adult neural stem cell fate. *Prog. Neurobiol.*, **93**:182–203. URL http://www.ncbi.nlm.nih.gov/pubmed/21056618.

[378] **Wu C.W., Chang Y.T., Yu L., Chen H.I., Jen C.J., Wu S.Y., Lo C.P. & Kuo Y.M.** (2008) Exercise enhances the proliferation of neural stem cells and neurite growth and survival of neuronal progenitor cells in dentate gyrus of middle-aged mice. *J. Appl. Physiol.*, **105**:1585–1594. URL http://www.ncbi.nlm.nih.gov/pubmed/18801961.

[379] **Barzilai N., Atzmon G., Schechter C., Schaefer E.J. & Cupples A.L.e.a.** (2003) Unique lipoprotein phenotype and genotype associated with exceptional longevity. *JAMA.*, **290**:2030–2040. URL http://www.ncbi.nlm.nih.gov/pubmed/14559957.

[380] **Atzmon G., Rincon M., Schechter C.B., Shuldiner A.R. & Lipton R.B.e.a.** (2006) Lipoprotein genotype and conserved pathway for exceptional longevity in humans. *PLoS Biol.*, **4**:e113. URL http://www.ncbi.nlm.nih.gov/pubmed/16602826.

[381] **Korolainen M.A., Auriola S., Nyman T.A., Alanfuzoff I. & Pirttilä T.** (2005) Proteomic analysis of glial fibrillary acidic protein in Alzheimer's disease and aging brain. *Neurobiol. Dis.*, **20**:858–870. URL http://www.ncbi.nlm.nih.gov/pubmed/15979880.

[382] **Genade T. & Lang D.M.** (2011) Antibody markers for studying neurodegeneration in the *Nothobranchius* central nervous system. *J. Cyto. & Histol.*, **2**:1000120. URL http://dx.doi.org/10.4172/2157-7099.1000120.

[383] **Chen L. & Zhou S.** (2010) "CRASH"ing with the worm: insights into L1CAM functions and mechanisms. *Develop. Dyn.*, **239**:1490–1501. URL http://www.ncbi.nlm.nih.gov/pubmed/20225255.

[384] **Lang D.M., Monson-Mayor M., del Mar Romero-Aleman M., Yanes C., Santos E. & Pesheva P.** (2008) Tenascin-R and axon growth promoting molecules are up regulated in the regenerating visual pathway of the lizard (*Gallotia galloti*). *Dev. Neurobiol.*, **68**:899–916. URL http://www.ncbi.nlm.nih.gov/pubmed/18361401.

[385] **Liao H., Bu W.Y., Wang T.H., Ahmed S. & Xiao Z.C.** (2005) Tenascin-R plays a role in neuroprotection via its distinct domains that coordinate to modulate the microglia function. *J. Biol. Chem.*, **280**:8316–8323. URL http://www.ncbi.nlm.nih.gov/pubmed/15615725.

[386] **He P. & Shen Y.** (2009) Interuption of β-catenin signaling reduces neurogenesis in Alzheimer's disease. *J. Neurosci.*, **29**:6545–6557. URL http://www.ncbi.nlm.nih.gov/pubmed/19458225.

[387] **Zhang F., Liu J. & Shi J.S.** (2010) Anti-inflammatory activities of resveratrol in the brain: role of resveratrol in microglial activation. *Eur. J. Pharmacol.*, **25**:1–7. URL http://www.ncbi.nlm.nih.gov/pubmed/20361959.

[388] **Genade T.** (2005) *Laboratory manual for culturing* N. furzeri.. *Nothobranchius* information center. URL http://www.nothobranchius.info.

[389] **Gallagher S.R.** (1995) One-dimensional SDS gell electrophoresis of proteins. *Curr. Protoc. Protein Sci.*, **10**:1.1–1.34. URL http://www.ncbi.nlm.nih.gov/pubmed/18265373.

[390] **Woodhead A.D. & Pond V.** (1984) Aging changes in the optic tectum of the guppy *Poecilia* (*Lebistes*) *reticulatus*. *Exp. Geront.*, **19**:305–311. URL http://www.ncbi.nlm.nih.gov/pubmed/6510475.

[391] **Bancroft J.D. & Gamble M.** (2007) *Theory and practice of histological techniques*. Churchill Livingstone, 5th edition.

[392] **Adams J.C.** (1981) Heavy metal intensification of DAB-based HRP reaction product. *J. Histochem. Cytochem*, **29**:775. URL http://www.ncbi.nlm.nih.gov/pubmed/7252134.

[393] **Sas E. & Maler L.** (1986) The optic tectum of gymnotiform teleosts Eigenmannia virescens and Apteronotus leptorhynchus: a Golgi study. *Neuroscience*, 18:215–246. URL http://www.ncbi.nlm.nih.gov/pubmed/2426630.

[394] **Schmidt J.T.** (1979) The laminar organization of optic nerves in the tectum of the goldfish. *Proc. R. Soc. Lond. B.*, 205:287–306. URL http://www.ncbi.nlm.nih.gov/pubmed/40252.

[395] **Lee V.M., Carden M.J., Schaepfer W.W. & Trojanowski J.Q.** (1987) Monoclonal antibodies distinguish several differentially phosphorylated states of the two largest rat neurofilament subunits (NF-H and NF-M) and demonstrate their existence in the normal nervous system of adult rats. *J. Neurosci.*, 7:3474–3488. URL http://www.ncbi.nlm.nih.gov/pubmed/3119789.

[396] **Shea T.B. & Chan W.K.** (2008) Regulation of neurofilament dynamics by phosphorylation. *Eur. J. Neurosci.*, 27:1893–1901. URL http://www.ncbi.nlm.nih.gov/pubmed/18412610.

[397] **Jin L.Q., Zhang G., Pennicooke B., Laramore C. & Selzer M.E.** (2011) Multiple neurofilament subunits are present in lamprey CNS. *Brain Res.*, 1370:16–33. URL http://www.ncbi.nlm.nih.gov/pubmed/21081119.

[398] **Weigum S.E., García D.M., Raabe T.D., Christodoulides N. & Koke J.R.** (2003) Discrete nuclear structures in actively growing neuroblastoma cells are revealed by antibodies raised against phosphorylated neurofilament proteins. *BMC Neurosci.*, 4:6. URL http://www.ncbi.nlm.nih.gov/pubmed/12697053.

[399] **Middledorp J., van der Berge S.A., Aronica E., Speijer D. & Hol E.M.** (2009) Specific human astrocyte subtype revealed by affinity purified GFAP^{+1} antibody; unpurified serum cross-reacts with neurofilament L in Alzheimer. *PLoS*, 4:e7663. URL http://www.ncbi.nlm.nih.gov/pubmed/19888461.

[400] **Froöjdö E., Westerlund J. & Isomaa B.** (2002) Culturing and characterisation of astocytes isolated from juvenile rainbow trout (*Oncorhynchus mykiss*). *Comp. Biochem. & Physiol. Part A.*, 133:17–28. URL http://www.ncbi.nlm.nih.gov/pubmed/12160869.

[401] **García D.M., Weigum S.E. & Koke J.R.** (2003) GFAP and nuclear lamins share an epitope recognized by monoclonal antibody J1-31. *Brain Res.*, 976:9–21. URL http://www.ncbi.nlm.nih.gov/pubmed/12763617.

[402] **Santa Cruz Biotechnology Inc** (2011) Gfap (GA-5): sc-58766. URL http://www.scbt.com/datasheet-58766-gfap-ga-5-antibody.html.

[403] **Franke F.E., Schachenmayr W., Osborn M. & Altmannsberger M.** (1991) Unexpected immunoreactivities of intermediate filament antibodies in human brain and brain tumors. *Am. J. Pathol.*, 139:67–79. URL http://www.ncbi.nlm.nih.gov/pubmed/1713022.

[404] **Schäfer M.K. & Altevogt P.** (2010) L1CAM malfunction in the nervous system and human carcinomas. *Cell Mol. Life Sci.*, 67:2425–2437. URL http://www.ncbi.nlm.nih.gov/pubmed/20237819.

[405] **Maness P.F. & Schachner M.** (2007) Neural recognition molecules of the immunoglobin superfamily: signalling transducers of axon guidance and neuronal migration. *Nat. Neurosci.*, 10:19–26. URL http://www.ncbi.nlm.nih.gov/pubmed/17189949.

[406] **Ankerhold R., Leppert C.A., Bastmeyer M. & Stuermer C.A.O.** (1998) E587 antigen is upregulated by goldfish oligodendrocytes after optic nerve lesion and supports retinal axon regeneration. *Glia*, 23:257–270. URL http://www.ncbi.nlm.nih.gov/pubmed/9633810.

[407] **Takeda Y., Asou H., Murakami Y., Miura M., Kobayashi M. & Uyemura K.** (1996) A non-neuronal isoform of cell adhesion molecule L1: tissue-specific expression and functional analysis. *J. Neurochem.*, 66:2338–2349. URL http://www.ncbi.nlm.nih.gov/pubmed/8632156.

[408] **Crawford M.A., Bazinet R.P. & Sinclair A.J.** (2009) Fat intake and cns functioning: ageing and disease. *Ann. Nutr. Metab.*, 55:202–228. URL http://www.ncbi.nlm.nih.gov/pubmed/19752543.

[409] **Hsia H.C. & Schwarzbauer J.E.** (2005) Meet the tenascins: Multifunctional and mysterious. *J. Biol. Chem.*, 280:26641–26644. URL http://www.ncbi.nlm.nih.gov/pubmed/15932878.

[410] **D'Angelo L., De Girolamo P., Cellerino A., Tozzini E.T., Varricchio E., Castaldo L. & Lucini C.** (2012) Immunolocalization of S100-like protein in the brain of an emerging model organism: Nothobranchius furzeri. *Microsc. Res. Tech.*, 75:441–447. URL http://www.ncbi.nlm.nih.gov/pubmed/22021149.

[411] **Bekku Y., Rauch U., Ninomiya Y. & Oohashi T.** (2009) Brevican distinctively assembles extracellular components at the large diameter nodes of Ranvier in the CNS. *J. Neurochem.*, 108:1266–1276. URL http://www.ncbi.nlm.nih.gov/pubmed/19141078.

[412] **Dours-Zimmermann M.T., Maurer K., Rauch U., Stoffel W., Fassler R. & Zimmermann D.R.** (2009) Versican V2 assembles the extracellular matrix surrounding the nodes of ranvier in the CNS. *J. Neurosci.*, 29:7731–7742. URL http://www.ncbi.nlm.nih.gov/pubmed/19535585.

[413] **Richard T., Pwlus A.D., Iglésias M.L., Pedrot E., Waffo-Teguo P., Mérillon J.M. & Monti J.P.** (2011) Neuroprotective properties of resveratrol and derivatives. *Ann. N. Y. Acad. Sci.*, 1215:103–108. URL http://www.ncbi.nlm.nih.gov/pubmed/21261647.

[414] **Espinosa A., Gil-Sanz C., Yanagawa Y. & Fairen A.** (2009) Two separate subtypes of early non-subplate projection neurons in the developing cerebral cortex of rodents. *Front Neuroanat*, 3:27. URL http://www.ncbi.nlm.nih.gov/pubmed/19949463.

[415] **Styren S.D., Miller P.D., Lagenaur C.F. & DeKosky S.T.** (1995) Alternate strategies in lesion-induced reactive synaptogenesis: differential expression of L1 in two populations of sprouting axons. *Exp. Neurol.*, 131:165–173. URL http://www.ncbi.nlm.nih.gov/pubmed/7895817.

[416] **Chen S., Mantei N., Dong L. & Schachner M.** (1999) Prevention of neuronal cell death by neural adhesion molecules L1 and CHL1. *J. Neurobiol.*, 38:428–439. URL http://www.ncbi.nlm.nih.gov/pubmed/10022583.

[417] **Cumming G., Fidler F. & Vaux D.L.** (2007) Error bars in experimental biology. *J. Cell Biol.*, 177:7–11. URL http://www.ncbi.nlm.nih.gov/pubmed/17420288.

[418] **Terzibasi Tozzini E., Baumgart M., Battistoni G. & Cellerino A.** (2011) Adult neurogenesis in the short-lived teleost *Nothobranchius furzeri*: localization of neurogenic niches, molecular characterization and effects of aging. *Aging Cell*. URL http://www.ncbi.nlm.nih.gov/pubmed/22171971.

[419] **Thelen K., Kedar V., Panicker A.K., Schmid R.S., Midkiff B. & Maness P.F.** (2002) The neural cell adhesion molecule L1 potentiates integrin-dependent cell migration to extracellular matrix proteins. *J. Neurosci.*, 22:4918–4931. URL http://www.ncbi.nlm.nih.gov/pubmed/12077189.

[420] **Webb D.J., Zhang H., Majumdar D. & Horwitz A.F.** (2009) $\beta 5$ integrin signaling regulates the formation of spines and synapses in hippocampal neurons. *J. Biol. Chem.*, 282:6929–6935. URL http://www.ncbi.nlm.nih.gov/pubmed/2750863.

[421] **Wu Y., Li X., Zhu J.X., Xie W., Le W., Fan Z., Jankovic J. & Pan T.** (2011) Resveratrol-activated AMPK/SIRT1/autophagy in cellular models of Parkinson's Disease. *Neurosignals*, 19:163–174. URL http://www.ncbi.nlm.nih.gov/pubmed/21778691.

[422] **Lee M.K., Kang S.J., Poncz M., Song K.J. & Park K.S.** (2007) Resveratrol protects SH-SY5Y neuroblastoma cells from apoptosis induced by dopamine. *Expr. & Mol. Med.*, 39:376–384. URL http://www.ncbi.nlm.nih.gov/pubmed/17603292.

[423] **Liu C., Shi Z., Fan L., Zhang C., Wang K. & Wang B.** (2011) Resveratrol improves neuron protection and functional recovery in rat model of spinal cord injury. *Brain Res.*, 1374:100–109. URL http://www.ncbi.nlm.nih.gov/pubmed/21111721.

[424] **Rose S.** (2006) *The future of the brain*. Oxford University Press, Inc., New York, New York, USA.

[425] **Giordano D.L., Murray M. & Cunningham T.J.** (1980) Naturally occuring neuron death in the optic layers of superior colliculus of the postnatal rat. *J. Neurocytology*, 9:603–614. URL http://www.ncbi.nlm.nih.gov/pubmed/7441305.

[426] **Gundersen H.J.G., Bagger P., Bentsen T.F., Evans S.M., Korbo L., Marcussen N., Mø ller A., Nielsen K., Nyengaard J.R., Pakkenberg B., Srensen F.B., Vesterby A. & West M.J.** (1988) The new stereological tools: disector, fractionator, nucleator and point sampled intercepts and their use in pathological research and diagnosis. *APMIS*, 96:857–881. URL http://www.ncbi.nlm.nih.gov/pubmed/3056461.

[427] **Bloss E.B., Janssen W.G., Ohm D.T., Yuk E.J., Wadsworth S., Saardi K.M., McEwen B.S. & Morrison J.H.** (2011) Evidence for reduced experience-dependent dendrtic spine plasticity in the aging prefrontal cortex. *J. Neurosci.*, 31:7831–7839. URL http://www.ncbi.nlm.nih.gov/pubmed/21613496.

[428] **Hagihara K., Miura R., Kosaki R., Berglund E., Ranscht B. & Yamaguchi Y.** (1999) Immunohistochemical evidence for the brevican-tenascin-R interaction: colocalization in perineuronal nets suggests a physiological role for the interaction in the adult rat brain. *J. Comp. Neurol.*, 410:256–264. URL http://www.ncbi.nlm.nih.gov/pubmed/10414531.

[429] **Carulli D., Pizzorusso T., Kwok J.C., Putignano E., Poli A., Forostyak S., Andrews M.R., Deepa S.S., Glant T.T. & Fawcett J.W.** (2010) Animals lacking link protein have attenuated perineuronal nets and persistent plasticity. *Brain*, 133:2331–2347. URL http://www.ncbi.nlm.nih.gov/pubmed/20566484.

[430] **Gogolla N., Caroni P., Luthi A. & Herry C.** (2009) Perineuronal nets protect fear memories from erasure. *Science*, 325:1258–1261. URL http://www.ncbi.nlm.nih.gov/pubmed/19729657.

[431] **Morales E., Fernandez E.R., Sinclair S., Molineux M.L., Mehaffey W.H. & Turner R.W.** (2004) Releasing the peri-neuronal net to patch-clamp neurons in adult CNS. *Pflugers Arch.*, 448:248–258. URL http://www.ncbi.nlm.nih.gov/pubmed/14985983.

[432] **McBride R.** (2006) *The expression and functional role of Tenascin-R during axon regeneration in the adult goldfish,* Carassius auratus.. Ph.D. thesis, University of Cape Town.

[433] **Manlow A. & Munoz D.G.** (1992) A non-toxic method for the demonstration of gliosis. *J. Neuropathol. Exp. Neurol.*, 51:298–302. URL http://www.ncbi.nlm.nih.gov/pubmed/1374794.

[434] **Walker J.M.**, editor (2009) *The protein protocols Handbook*. Humana Press, 3rd edition.

[435] **Stanley P.** (2004) Using ImageJ for densitometry. *Pamela Stanley Lab*. URL http://stanxterm.aecom.yu.edu/PamelaStanleylabwiki-UsingImageJ.pdf.

[436] **Aldridge G.M., Podrebarac D.M., Greenough W.T. & Weiler I.J.** (2008) The use of total protein stains as loading controls: an alternative to high-abundance single protein controls in semi-quantitative immunoblotting. *J. Neurosci. Methods*, 172:250–254. URL http://www.ncbi.nlm.nih.gov/pubmed/18571732.

[437] **Ike H., Tamada Y., Uemura M., Ishihara A., Suwa F. & Ibata Y.** (2004) Age-related changes in astrocytes and microvasculature in the median eminence of the rat. *Acta Histochemica et Cytochemica*, 37(2):129–138. URL http://www.jstage.jst.go.jp/article/ahc/37/2/37_129/_article.

[438] **Zoli M., Ferraguti F., Frasoldati A., Biagini G. & Agnati L.F.** (1995) Age-related alterations in tanycytes of the mediobasal hypothalamus of the male rat. *Neurobiol. Aging*, 16:77–83. URL http://www.ncbi.nlm.nih.gov/pubmed/7723939.

[439] **Liem R.K. & Messing A.** (2009) Dysfunctions of neuronal and glial intermediate filaments in disease. *J. Clin. Invest.*, 119:1814–1824. URL http://www.ncbi.nlm.nih.gov/pubmed/19587456.

[440] **Singh R., Nielsen A.L., Johansen M.G. & Jørgensen A.L.** (2003) Genetic polymorphism and sequence evolution of an alternatively spliced exon of the glial fibrillary acidic protein gene, GFAP. *Genomics*, 82:185–193. URL http://www.ncbi.nlm.nih.gov/pubmed/12837269.

[441] **Blechingberg J., Holm I.E., Nielsen K.B., Jensen T.H., Jørgensen A.L. & Nielsen A.L.** (2007) Identification and characterization of GFAPkappa, a novel glial fibrillary acidic protein isoform. *Glia*, 55:497–507. URL http://www.ncbi.nlm.nih.gov/pubmed/17203480.

[442] **Roelofs R.F., Fischer D.F., Houtman S.H., Sluijs J.A., Van Haren W., Van Leeuwen F.W. & Hol E.M.** (2005) Adult human subventricular, subgranular, and subpial zones contain astrocytes with a specialized intermediate filament cytoskeleton. *Glia*, 52:289–300. URL http://www.ncbi.nlm.nih.gov/pubmed/16001427.

[443] **Jung M., Pesheva P., Schachner M. & Trotter J.** (1993) Astrocytes and neurons regulate the expression of the neural recognition molecule Janusin by cultured oligodendrocytes. *Glia*, 9:163–175. URL http://www.ncbi.nlm.nih.gov/pubmed/8294147.

[444] **Wenker I.** (2010) An active role for astrocytes in synaptic plasticity? *J. Neurophysiol.*, 104:1216–1218. URL http://www.ncbi.nlm.nih.gov/pubmed/20610782.

[445] **Karetko-Sysa M., Skangiel-Kramska J. & Nowicka D.** (2011) Disturbance of perineuronal nets in the perilesional area after thrombosis is not associated with neuronal death. *Exp. Neurol.*, 231:113–126. URL http://www.ncbi.nlm.nih.gov/pubmed/21683696.

[446] **Herron L.R., Hill M., Davey F. & Gunn-Moore F.J.** (2009) The intracellular interactions of the L1 family of cell adhesion molecules. *Biochem. J.*, 419:519–531. URL http://www.ncbi.nlm.nih.gov/pubmed/19356150.

[447] **Wirths O., Breyhan H., Marcello A., Cotel M.C., Bruck W. & Bayer T.A.** (2010) Inflammatory changes are tightly associated with neurodegeneration in the brain and spinal cord of the APP/PS1KI mouse model of Alzheimer's disease. *Neurobiol. Aging*, 31:747–757. URL http://www.ncbi.nlm.nih.gov/pubmed/18657882.

[448] **Xu X., Warrington A.E., Bieber A.J. & Rodriguez M.** (2011) Enhancing CNS repair in neurological disease: challenges arising from neurodegeneration and rewiring of the network. *CNS Drugs*, 25:555–573. URL http://www.ncbi.nlm.nih.gov/pubmed/21699269.

[449] **L. A., Paris J., González B. & Castellano B.** (2002) Glial expression of small heat shock proteins following an excitotoxic lesion in the immature rat brain. *Glia*, 38:1–14. URL http://www.ncbi.nlm.nih.gov/pubmed/11921199.

[450] **Clarke G., Collins R.A., Leavitt B.R., Andrews D.F., Hayden M.R., Lumsden C.J. & McInnes R.R.** (2000) A one-hit model of cell death in inherited neuronal degenerations. *Nature*, 406:195–199. URL http://www.ncbi.nlm.nih.gov/pubmed/10910361.

[451] **Ribas V.T., Arruda-Carvalho M., Linden R. & Chiarini L.B.** (2011) Early c-jun N-terminal kinase-dependent phosphorylation of activating transcription factor-2 is associated with degeneration of retinal ganglion cells. *Neurosci.*, 180:64–74. URL http://www.ncbi.nlm.nih.gov/pubmed/21300140.

[452] **Marshall W.S., Ossum C.G. & Hoffmann E.K.** (2005) Hypotonic shock mediation by p38 MAPK, JNK, PKC, FAK, OSR1 and SPAK in osmosensing chloride secreting cells of killifish opercular epithelium. *J. Exp. Biol.*, 208:1063–1077. URL http://www.ncbi.nlm.nih.gov/pubmed/15767308.

[453] **Svoboda K.R., Linares A.E. & Ribera A.B.** (2001) Activity regulates programmed cell death of zebrafish Rohon-Beard neurons. *Development*, 128:3511–3520. URL http://www.ncbi.nlm.nih.gov/pubmed/11566856.

[454] **Hou Y., Aboukhatwa M.A., Lei D.L., Manaye K., Khan I. & Luo Y.** (2010) Anti-depressant natural flavonols modulate BDNF and beta amyloid in neurons and hippocampus of double TgAD mice. *Neuropharmacol.*, 58:911–920. URL http://www.ncbi.nlm.nih.gov/pubmed/19917299.

[455] **Rehvar M., Nikseresht M., Shafiee S.M., Naghibalhossaini E., Rasti M., Pankehshahin M.R. & Owji A.A.** (2011) Effect of oral resveratrol on the BDNF gene expression in the hippocampus of the rat brain. *Neurochem. Res.*, 36:761–765. URL http://www.ncbi.nlm.nih.gov/pubmed/21221775.

[456] **Espinoza M., de Silva R., Dickson D.W. & Davies P.** (2008) Differential incorporation of tau isoforms in Alzheimer's Disease. *J. Alzheimers Dis.*, **14**:1–16. URL http://www.ncbi.nlm.nih.gov/pubmed/18525123.

[457] **Smith C.J., Anderton B.H., Davis D.R. & Gallo J.M.** (1995) Tau isoform expression and phosphorylation state during differentiation of cultured neuronal cells. *FEBS Lett.*, **375**:243–248. URL http://www.ncbi.nlm.nih.gov/pubmed/7498509.

[458] **Tomasiewicz H.G. & Wood J.G.** (1999) Characterization of microtubule-associated proteins in teleosts. *Cell Motil. Cytoskeleton*, **44**:155–167. URL http://www.ncbi.nlm.nih.gov/pubmed/10542364.

[459] **Mantel C. & Broxmeyer H.E.** (2008) Sirtuin 1, stem cells, aging, and stem cell aging. *Curr. Opin. Hematol.*, **15**:326–331.

[460] **Tang X., Falls D.L., Li X., Lane T. & Luskin M.B.** (2007) Antigen-retrieval procedure for bromodeoxyuridine immunolabeling with concurrent labeling of nuclear DNA and antigens damaged by HCl pretreatment. *J. Neurosci.*, **27**:5837–5844. URL http://www.ncbi.nlm.nih.gov/pubmed/17537952.

[461] **Galtrey C.M., Kwok J.C., Carulli D., Rhodes K.E. & Fawcett J.W.** (2008) Distribution and synthesis of extracellular matrix proteoglycans, hyaluronan, link proteins and tenascin-R in the rat spinal cord. *Eur. J. Neurosci.*, **27**:1373–1390. URL http://www.ncbi.nlm.nih.gov/pubmed/18364019.

[462] **Arata N. & Nakayasu H.** (2003) A periaxonal net in the zebrafish central nervous system. *Brain Res.*, **961**:179–189. URL http://www.ncbi.nlm.nih.gov/pubmed/12531485.

[463] **Götz R., Raulf F. & Schartl M.** (1992) Brain-Derived Neurotrophic Factor is more highly conserved in structure and function than Nerve Growth Factor during vertebrate evolution. *J. Neuroschem.*, **59**:432–442. URL http://www.ncbi.nlm.nih.gov/pubmed/1629719.

There ain't no grave can hold my body down,
when I hear that trumpet sound,
I'm going to raise right out of the ground,
ain't no grave can hold my body down.

Ain't no grave, Johnny Cash.